



UNIVERSITAT DE
BARCELONA

Bacterial populations and functions driving the decontamination of polycyclic aromatic compounds polluted soils

Poblacions i funcions bacterianes implicades en la descontaminació de sòls contaminats amb CAPs

Margalida Tauler Ferrer

ADVERTIMENT. La consulta d'aquesta tesi queda condicionada a l'acceptació de les següents condicions d'ús: La difusió d'aquesta tesi per mitjà del servei TDX (www.tdx.cat) i a través del Dipòsit Digital de la UB (diposit.ub.edu) ha estat autoritzada pels titulars dels drets de propietat intel·lectual únicament per a usos privats emmarcats en activitats d'investigació i docència. No s'autoritza la seva reproducció amb finalitats de lucre ni la seva difusió i posada a disposició des d'un lloc aliè al servei TDX ni al Dipòsit Digital de la UB. No s'autoritza la presentació del seu contingut en una finestra o marc aliè a TDX o al Dipòsit Digital de la UB (framing). Aquesta reserva de drets afecta tant al resum de presentació de la tesi com als seus continguts. En la utilització o cita de parts de la tesi és obligat indicar el nom de la persona autora.

ADVERTENCIA. La consulta de esta tesis queda condicionada a la aceptación de las siguientes condiciones de uso: La difusión de esta tesis por medio del servicio TDR (www.tdx.cat) y a través del Repositorio Digital de la UB (diposit.ub.edu) ha sido autorizada por los titulares de los derechos de propiedad intelectual únicamente para usos privados enmarcados en actividades de investigación y docencia. No se autoriza su reproducción con finalidades de lucro ni su difusión y puesta a disposición desde un sitio ajeno al servicio TDR o al Repositorio Digital de la UB. No se autoriza la presentación de su contenido en una ventana o marco ajeno a TDR o al Repositorio Digital de la UB (framing). Esta reserva de derechos afecta tanto al resumen de presentación de la tesis como a sus contenidos. En la utilización o cita de partes de la tesis es obligado indicar el nombre de la persona autora.

WARNING. On having consulted this thesis you're accepting the following use conditions: Spreading this thesis by the TDX (www.tdx.cat) service and by the UB Digital Repository (diposit.ub.edu) has been authorized by the titular of the intellectual property rights only for private uses placed in investigation and teaching activities. Reproduction with lucrative aims is not authorized nor its spreading and availability from a site foreign to the TDX service or to the UB Digital Repository. Introducing its content in a window or frame foreign to the TDX service or to the UB Digital Repository is not authorized (framing). Those rights affect to the presentation summary of the thesis as well as to its contents. In the using or citation of parts of the thesis it's obliged to indicate the name of the author.



FACULTAT DE BIOLOGIA
DEPARTAMENT DE MICROBIOLOGIA

Bacterial populations and functions driving the decontamination of PAC polluted soils

Poblacions i funcions bacterianes implicades en la descontaminació de sòls contaminats amb CAPs

Memòria presentada per Margalida Tauler Ferrer per optar al Grau de Doctor per la Universitat de Barcelona

V. i P. de la directora

V. i P. de la tutora

Doctoranda

Dra. Magdalena Grifoll Ruiz

Dra. Magdalena Grifoll Ruiz

Margalida Tauler Ferrer

Programa de doctorat: Microbiologia Ambiental i Biotecnologia

Barcelona, juliol de 2015

This Thesis was financially supported by the Spanish Ministry of Economy and Competitiveness through the FPI program, and the CGL2010-22068-C02-02 and CGL2013-44554-R projects.

A sa meva família i a la M.D.S.B.

Acknowledgements

He d'admetre que fer es doctorat no ha estat un camí de roses. Has de fer es cap viu perquè hi ha moments d'estrès i frustració, situacions que te treuen d'es solc i dies que vas amb so cop-piu. Però tot això se veu més que compensat quan fas es balanç global. Després de veure s'evolució personal i professional i haver conegut a gent encantadora que m'ha acompanyat durant aquesta etapa, per res d'aquest món canviaria aquests anys de Tesi. Per això, dedicaré un parell (mallorquí) de paraules d'agraïment a totes aquestes persones, intentant no deixar-me ningú.

Primer de tot, vull donar ses gràcies a sa Dra. Magdalena Grifoll per haver-me donat s'oportunitat d'entrar dins es seu grup de recerca i haver-me concedit sa beca per fer sa Tesi. També li vull agrair que m'hagi transmès sa passió per sa biodegradació i bioremediació i m'hagi format des des criteri científic, s'exigència i des de fer ses coses ben fetes. En segon lloc, també vull donar ses gràcies a na Magda per sa seva humanitat, per sa confiança depositada en jo, per ensenyar-me a trivialitzar ses coses i pes gran suport que m'ha donat, sobretot durant sa darrera etapa d'escriptura. A n'es fons ets com una micobacteria: ets membres des teu gènere no sou molt abundants, però ses teves dioxigenasses s'expressen com ses que més i exerceixen una funció vital per aquesta societat. De veres, moltíssimes gràcies pes teu esforç. No podria haver tengut una directora millor.

També vull donar ses gràcies a n'en Quim per tot lo que ha fer per jo. A part d'haver-me ensenyat a fer feina de manera rigurosa, a gestionar un laboratori de recerca i a fer miracles sense recursos, és sa persona que més ha estat a n'es meu costat durant aquests 6 anys (tant en sentit figurat com literal). Gràcies per transmetre'm sa passió, motivació i il·lusió que tu tens per sa bioremediació. Hem compartit moments molt bons i no tant bons, però sense tu, *Juaquín*, això no hagués estat lo mateix. Crec que no hi ha paraules suficients per poder expressar sa meva gratitud.

Al Dr. José Julio Ortega le quiero agradecer el haber estado biodisponible siempre que le hemos necesitado y sobre todo por potenciar directamente mi accesibilidad *in situ* al suelo contaminado con creosota.

Gràcies també a n'es Dr. José María Nieto per haver-me donat suport amb s'anàlisis de seqüències, haver-me submergit dins es món des Bioedit i pes teus *Mantecados Manchegos*.

Merci beaucoup à Aurélie Cébron pour m'avoir accepté dans son laboratoire. J'ai beaucoup aimé les discussions scientifiques pendant des heures et avec lesquelles j'ai appris beaucoup. Merci pour ta disponibilité pour mes questions de 5 minutes avant 17h00 et pour la bienvenue que vous m'avez fait.

A més a més, moltes gràcies a tots ets companys des laboratoris 5. A n'és Solanas, Salva i Laia gràcies per haver-me donat exemple i haver contestat a tots ets meus dubtes. Salva, gràcies pes moments musicals de reggae i pes crits de 'FORT' que aixecaven sa moral a qualsevol. I tu Laia, no ets una *lerda*, ets una *campiona* i tots ho sabem. Aintz, tu també podries estar en es paràgraf des amics, però també m'has estat de gran ajuda a n'és laboratoris, així que gràcies per ses DGGE, per ses nits ludòpates i pes teu suport. Gràcies també a na Sara i en David, que no per ser es darrers en arribar sou menys importants, sinó tot lo contrari. Gràcies per animar-me i per aguantar tots ets moments de crisi. Sa veritat es que m'heu fet molt fàcil es darrer any de tesis. Gràcies pes vostro suport incondicional i incansable. Moltes gràcies David pes teu carisma i sa teva força de voluntat i a *ti* Sara per fer que ses coses sempre sigui una mica més boniques (*menos feas*). Ha estat un plaer ser es vostro bistec. Sense voltros segur que m'hagués quedat com un colom amb *muñones*.

Gràcies a n'és *Laboratorio Amigo* per fer ses coses tant fàcils i anar tots a una: Susana, Amanda, Cessarini, Arnau, Óscar... Gràcies també a tota sa gent que ha passat pes Departament de Microbiologia i que hem compartit hores de dinar, celebracions de tesis, biofestes, etc. No posaré noms perquè seguríssim que me deixaria qualcú i me sabia molt de greu.

Asun, a tu t'agraesc sa paciència que has tengut analitzant amb jo espectres i més espectres. Gràcies per sa teva amabilitat i dolçor. És un plaer treballar amb gent com tu. Gràcies també a n'en Joan Romanyà per deixar-mos sa màquina per tamisar es sòl i per fer ses coses fàcils. Marc Viñas, m'encanten ses teves dissertacions científiques i gràcies per ajudar-me en l'anàlisi de les dades de piroseqüenciació.

També vull agrair a sa gent de s'oficina de gestió departamental s'ajuda per fer paperassa i sa seva eficiència. Gràcies Susana, Macu, Bea, Rosario i Manolo.

Je me sentais vraiment chez moi parce que j'ai trouvé des personnes merveilleuses a Nancy. Marie, merci pour m'avoir ouvert chez toi et pour m'avoir montré un autre Nancy. Je voudrais répéter le tour sur le bateau gonflable, entendre à nouveau le bruit des cerfs et voir comme le soleil balaie les champs d'herbe. Je n'ai pas assez de mots de gratitude pour te remercier. Merci beaucoup à toi aussi, Amélia, pour faire mon stage au laboratoire si facile et pour ton spontanéité. Thierry, guapo, moltes gràcies també per obrir-me ses portes de casa teva, ensenyar-me que és es Mont d'or i per subministrar-me mitjà de transport, sa bici.

Ambientòlics, voltros ja fa més temps que m'aguantau i vos he de dir que sou molt especials. He passat ets millors anys de sa meva vida i que mai oblidaré amb voltros. Ruth, moltíssimes gràcies per millions de coses que som incapaç d'enumerar i que per totes elles tu formes part des meu jardí florit. Vilafonts, nucli dur, què faria jo sense vosaltres i els

nostres vídeos de gats? Aina i Pash, sense voltros una festa no és una festa. Gràcies de tot cor per haver-me donat suport i valorar el que faig.

Cati Bel, moltes gràcies per sa preciosa portada que m'has fet i per haver compartit amb jo aquesta etapa tan important de sa meva vida.

Si hi ha qualcú que ha estat imprescindible per muntar tot aquest *tinglado*, aquests són sa meva família. Gràcies papà i mamà per creure en jo, per valorar-me i per ajudar-me cada dia. Mil gràcies per donar-me suport per fer tot lo que he volgut, vos hagi o no agradat. Gràcies per donar-me ales i no retreure'm ses meves errades. Miquel, moltes gràcies per protegir-me i cuidar-me i per fer-me sentir especial. Ets un tros de pa encara que no ho vulguis aparentar. Tenc sa sort de tenir una família molt gran i unida capaç de fer coses enormes. Gràcies padrines i padrins, guitzes i guitzos per estar a n'es meu costat i fer telefonades que te fan fer una rialla fresca de tant en quant.

Diuen que es primers són es darrers i es darrers són es primers. Tu ets sa darrera, però no per això sa menys important, sinó tot lo contrari. No puc escriure aquest paràgraf sense que se m'humitegin ets ulls. Me sent afortunadíssima de poder compartir sa vida amb tu i que m'hagis acompanyat durant aquests anys, que segur que sense tu fossin estat infinitament més durs. Gràcies, Ana, per fer ses coses tan fàcils i estimar-me sense esperar res a canvi.

Table of contents

Acknowledgements	i
Abbreviation list	ix
1 Introduction	3
1.1 Soil Pollution.....	3
1.2 PAH polluted soils.....	7
1.3 Biodegradation of PAHs in terrestrial environments	11
1.4 Scope of this Thesis	16
2 Objectives.....	21
3 Experimental layout.....	25
4 Key HMW PAH-degrading bacteria in a soil consortium enriched using a biodegraded creosote residue in a sand-in-liquid culture system.....	29
4.1 Materials and methods	30
4.1.1 Chemicals.....	30
4.1.2 Creosote-HMW PAH residue.....	30
4.1.3 Enrichment of the HMW PAH-degrading microbial consortium UBHP	31
4.1.4 Enumeration of the PAH-degrading microbial populations by MPN.....	31
4.1.5 Biodegradation of the creosote HMW PAH mixture by consortium UBHP .	31
4.1.6 Chemical analyses of residual PAHs and accumulated metabolites.....	32
4.1.7 UBHP microbial community response to single PAHs.....	32
4.1.8 DNA extraction and PCR amplification	32
4.1.9 DGGE analysis	33
4.1.10 16S rRNA gene clone library analysis.....	33
4.1.11 Detection and phylogenetic analysis of PAH ring hydroxylating dioxygenases (RHD).....	34
4.1.12 Isolation of PAH-degrading bacteria	34
4.1.13 Statistical analysis	34
4.2 Results.....	34
4.2.1 Microbial Consortium UBHP	34
4.2.2 Biodegradation of the HMW PAH-residue by microbial consortium UBHP.	35

4.2.3	Microbial community structure of consortium UBHP	39
4.2.4	Functional screening of consortium UBHP by RHD gene amplification	41
4.2.5	Selective detection of actinobacterial populations in consortium UBHP	42
4.2.6	Microbial community shifts in response to exposure to single PAHs.....	42
4.2.7	Retrieval and characterization of the UBHP bacterial phylotypes as pure cultures	44
4.3	Discussion.....	46
5	PAH biodegradation and metabolite formation during a lab-scale bioestimulation of a creosote-polluted soil.....	53
5.1	Materials and methods	53
5.1.1	Chemicals.....	53
5.1.2	Soil.....	54
5.1.3	Experimental design	54
5.1.4	PACs and acidic metabolites analyses.....	55
5.1.5	Enumeration of PAH- and Oxy-PAC-degrading populations.....	56
5.1.6	DNA extraction and PCR amplification.....	56
5.1.7	DGGE analysis and sequencing	56
5.1.8	Statistical and multivariate analysis.....	57
5.2	Results.....	57
5.2.1	Soil.....	57
5.2.2	Effects of nutrient addition in PAH removal and PAH-degrading populations	58
5.2.3	PAH biodegradation kinetics in the nutrient treated soil.....	61
5.2.4	Evolution of oxy-PAHs during PAH degradation in the nutrient treated soil	63
5.2.5	Production and accumulation of acidic metabolites during the degradation of PAHs in the soil treated with nutrients	64
5.2.6	N-PAC biodegradation kinetics.....	67
5.2.7	Dynamics of the heterotrophic and PAC-degrading populations.....	68
5.3	Discussion.....	74
6	Structural and quantitative changes in the microbial community of the creosote polluted soil associated to enhanced PAH degradation.	83

6.1	Materials and methods	84
6.1.1	Soil and experimental layout	84
6.1.2	Nucleic acids extraction and reverse-transcription	84
6.1.3	qPCR amplification	84
6.1.4	Diversity of PAH-RHD by clone library analysis	85
6.1.5	Barcoded pyrosequencing	85
6.1.6	Statistical and multivariate analysis	85
6.2	Results	86
6.2.1	Evolution of total and active microbial populations during PAC degradation with or without nutrient limitation conditions.....	86
6.2.2	Abundance and expression levels of PAH-RHD genes in GN and GP bacteria	87
6.2.3	Phylogenetic analysis of the detected RHD gene transcripts.....	90
6.2.4	Role of <i>Mycobacterium</i> in the biodegradation of PAHs	92
6.2.5	Community structure dynamics of the total and active bacteria in the soil	93
6.3	Discussion.....	98
7	General discussion.....	105
8	Conclusions	115
9	References	119
10	Summary (Resum)	133
10.1	Introducció	133
10.2	Objectius.....	136
10.3	Resultats i discussió.....	137
10.4	Conclusions.....	151
11	Annex	155

Abbreviation list

ACN	Acenaphtene
ACNY	Acenaphtylene
ANT	Anthracene
BaA	Benz(<i>a</i>)anthracene
BaPY	Benzo(<i>a</i>)pyrene
BbFT	Benzo(<i>b</i>)fluoranthene
BePY	Benzo(<i>e</i>)pyrene
BkFT	Benzo(<i>k</i>)fluoranthene
BOE	Boletín Oficial del Estado
BP	Benzo(<i>g,h,i</i>)perylene
BTEX	Benzene, toluene, ethylbenzene and xylene
CA	Correspondence analysis
CCA	Canonical correspondence analysis
cDNA	Complementary deoxyribonucleic acid
CERCLA	Comprehensive Environmental Response, Compensation and Liability Act
CHY	Chrysene
DBANT	Dibenz(<i>a,h</i>)anthracene
DGGE	Denaturing gradient gel electrophoresis
DNA	Deoxyribonucleic acid
EEA	European Environment Agency
FAO	Food and Agriculture Organization of the United Nations
FL	Fluorene
FT	Fluoranthene
GC	Gas chromatography
GC-FID	Gas chromatography - flame ionization detector
GC-MS	Gas chromatography - mass spectrometry
GN	Gram-negative
GP	Gram-positive
GRL	General reference level
HMW PAH	High-molecular-weight polycyclic aromatic hydrocarbons
INDPY	Indeno(1,2,3- <i>c,d</i>)pyrene
IRNASE	Instituto de Recursos Naturales y Agrobiología de Sevilla
IYS	International Year of Soils
JRC	Joint Research Centre
LIEC	Laboratoire des Environnements Continentaux
LMW PAH	Low-molecular-weight polycyclic aromatic hydrocarbons
MPN	Most probable number
NAPH	Naphtalene
NAPL	Non-aqueous phase liquid
NGS	Next-generation sequencing
NIST	National Institute of Standards and Technology

N-PAC	Nitrogenated polycyclic aromatic compounds
OTU	Operational taxonomic unit
Oxy-PAHs	Oxygenated polycyclic aromatic hydrocarbons
PAH	Polycyclic aromatic hydrocarbons
PAH-RHD	Polycyclic aromatic hydrocarbon ring-hydroxylating dioxygenases
PHE	Phenanthrene
PY	Pyrene
RDP	Ribosomal Database Project
RNA	Ribonucleic acid
rRNA	Ribosomal ribonucleic acid
TPH	Total petroleum hydrocarbon
US-EPA	United States Environmental Protection Agency
WHC	Water holding capacity
WSD	World Soil Day

CHAPTER 1

Introduction

1 Introduction

1.1 Soil Pollution

SOIL AS A RESOURCE

Soil, generally defined as the top layer of the earth's crust, it is a very dynamic system, which performs vital functions for the survival of humankind and ecosystems. These functions include to provide a physical and cultural environment for human activities; to produce biomass (i. e. food) and raw materials; to filter and transform nutrients, a variety of chemical substances and water; to host biodiversity; to act as a global carbon sink (soil captures about 20% of the world's man-made carbon dioxide emissions) (The European Commission, 2007); to have a key role in the biogeochemical cycles; and to store the geological and archaeological heritage. Although soil appears to be an almost infinite resource because its ubiquitousness, it is considered as a nonrenewable resource due to the extremely slowness of its formation and regeneration processes. It takes centuries to create a mere centimeter of soil, but it can be quickly destroyed, therefore soils need to be protected against their degradation.

Soil contamination is one of the main causes for soil degradation. The last JRC reference report on contaminated sites (Liedekerke et al. 2014), identified 342,000 sites in Europe with polluted soil requiring remediation. Nevertheless, the same report estimated that up to 2.5 million sites might be potentially affected by dangerous pollutants. Thus, taking into account that only a 15% of the identified sites have been remediated, the problem is still growing.

Among all the soil remediation strategies, bioremediation, which exploits the natural microbial catabolic capabilities, is known as the most sustainable (economical and ecofriendly) technique to restore a polluted site. Despite its attractiveness in terms of bioeconomy, the primary driver for bioremediation application should be the regulatory compliance rather than the manufacturing profit (Gillespie & Philp, 2013). When compared to other remediation techniques, such as incineration, it is obvious that physico-chemical processes are more effective in terms of cleaning-up; however, they lead to soil destruction and to the irreversible loss of its key ecological functions. In the past decade, remediation of contaminated land has largely been based on prevention of unacceptable risks to human health and the environment, to ensure that a site is 'fit for use'. Determining the most appropriate course of action when faced with soil contamination requires the consideration of technologies or approaches that can feasibly reduce the contamination to the required target level within project-defined time and cost constraints. Recently, there has been an increasing interest in including sustainability as

a decision-making criterion (Bardos et al. 2011). Known as sustainable remediation, this concept refers to decision-making protocols that minimize the environmental footprint of soil remediation while meeting regulatory requirements and weighing community goals and costs. These decisions may influence actions and technologies at all phases of the cleanup and may relate to everything from management practices, to the very nature of the cleanup technology, to planning for the sustainable long-term use of the site. The Sustainable Remediation Forum (SURF) defines sustainable remediation as remediation that protects human health and the environment while maximizing the environmental, social, and economic benefits throughout the project life cycle (US-SURF, 2009).

One of the main drawbacks for the implementation of bioremediation is the global perception that this technology is less reliable than others are. It is true that it requires longer treatment times and that the endpoint concentrations of the pollutants are difficult to predict; however, all this disadvantages could be corrected by understanding the underlying biological processes, moving from the current “black box” application, to an actual environmental biotechnology.

LEGAL FRAMEWORKS

The lack of legislation and regulation regarding the application of (bio)remediation as a decontamination strategy is another of the causes for its low current incidence in restoration projects. In fact, nowadays, a specific legislation for soil protection does not even exist in the frame of the EU. References to soil protection can be found scattered throughout the European Community regulatory structure, with instruments and measures directly and indirectly related to soil contamination and/or remediation aspects being addressed by waste, water, chemical, impact assessment, environmental liability, and air quality policies (Table 1.1).

Concern about soil pollution has always been associated with the limitations or the suitability of a soil for a certain use and this is, at the same time, linked to the concept of soil quality. Soil quality is defined as the capacity of a soil to function with the ecosystem boundaries to sustain plant and animal productivity, maintain or enhance water and air quality and support human health and habitation (Rodrigues et al. 2009). The quality of soil is strongly dependent on the interactions taking place with the other components of the ecosystem such as biota, air, water quality and human health. Thus, the interest in soil quality increased after industries caused serious public health damages by chemical waste disposals under residential areas, such as Love Canal in the United States (1976) and Lekkerkerk in The Netherlands (1978). The first soil pollution legislation appeared in 1980 in the USA. CERCLA (Comprehensive Environmental Response, Compensation and Liability Act), commonly known as Superfund, started to regulate and to fund the cleanup of several hazardous waste sites. CERCLA set up a trust funded by taxes on the

chemical and petroleum industries, and provided federal authority to respond to releases or threatened releases of hazardous substances that may endanger public health or the environment. This program, mediated by the US-EPA, authorizes the short-term removal and long-term remediation of hazardous substances, includes wide information about polluted sites, and states the prohibitions and requirements in relation with polluted areas in the United States (<http://www.epa.gov/superfund/index.htm>).

Table 1.1. UE policy measures and instruments that directly or indirectly address aspects of soil contamination (Source: Rodrigues et al. 2009).

UE environmental policies		Diffuse soil contamination		Local soil contamination	
		Directly	Indirectly	Directly	Indirectly
Waste	Waste Framework Directive (2006/12/EC, codified version of Directive 75/442/EEC as amended)				✓
	Directive 91/689/EEC on Hazardous Waste, amended in 1994				✓
	Directive on the Disposal of Waste Oils (75/439/EEC amended in 2000)				✓
	Landfill Directive (1999/31/EC)				✓
	Sewage Sludge Directive (86/278/EEC)	✓			
	Directive 2006/21/EC on the management of waste from the extractive industries	✓		✓	
Water	Water Framework Directive (2000/60/EC)	✓			
	Nitrates Directive (91/676/EEC)	✓			
	Urban Wastewater Treatment Directive (91/271/EEC)		✓		
	Bathing Water Directive (2006/7/EC)		✓		
Air	Air Quality Framework Directive (96/62/EC) and its Daughter Directives		✓		
	Directive on National Emissions Ceilings (2001/81/EC)		✓		
	Directive on Integrated Pollution Prevention and Control (96/61/EC)	✓			
	Directive on Large Combustion Plants (LCPD) (2001/80/EC)		✓		
Chemicals	Thematic strategy on the sustainable use of pesticides	✓			
	Directive on Biocidal Products (98/8/EC)	✓			
	Directive 91/414/EEC on plant protection products	✓			
Impact assessment	Environmental Impact Assessment Directive (85/337/EEC amended in 1997 and 2003)	✓		✓	
	Strategic Environmental Assessment Directive (SEA) (2001/42/EC)	✓			

In Europe, in the 1980s the Norwegian government was the first to define provisions related to soil pollution by introducing the “Pollution Control Act”, based on the polluter-pays principle. The Netherlands was one of the pioneering EU Member States to establish specific legislation on soil protection because, while a housing project was under construction in Lekkerkerk, a large-scale soil contamination problem was discovered giving to this town a national notoriety. However, it was not until 1996 that the European Union established the 96/61/EC Council Directive, which contains general aspects

regarding the pollution prevention and control in air, water and soils. The application of this directive required the cooperation of the member states in the identification and localization of polluted sites, especially those used for industrial and military activities and waste dumpsites. Nevertheless, this law was not a specific regulation of the protections of soil.

The first time that the EU proposed a framework and common objectives to prevent soil degradation, to preserve soil functions and to remediate degraded soil was in 2002, when the *Thematic Strategy for Soil Protection* (2002, 2006, and 2012) was proposed. The strategy includes setting up a legislative framework for the protection and sustainable use of soil, integrating soil protection into national and EU policies, improving knowledge in this area and increasing public awareness. The proposal for a Directive (The European Commission, 2006) in 2006 was a key component of the strategy, enabling Member States to adopt measures tailored to their local needs and providing for measures to identify problems, prevent soil degradation and remediate polluted or degraded soil. The European Parliament adopted its first-reading opinion on the proposal for a Soil Framework Directive on November 2007, the Committee of the Regions and the Economic and Social Committee delivered their opinions on February and on April 2007, respectively. In Council, the proposal was repeatedly discussed but always ran into a blocking minority.

In October 2013 the Commission adopted the Communication on *Regulatory Fitness and Performance (REFIT): Results and Next Steps* in which it noted that the proposal for a Soil Framework Directive had been pending for eight years, resulting in no effective action during that period. Therefore, the Commission would examine carefully whether the objective of the proposal would be best served by maintaining the proposal or by withdrawing it, thus opening the way for an alternative initiative. A possible way forward on soil protection at EU level was briefly discussed during the Environment Council meeting on March 2014. The debate indicated that protecting soils remained an important objective for the Union, despite the fact that, in its present format, the proposal for a Soil Framework Directive could not be agreed by a qualified majority. In light of the above, on April 2014 the Commission took the decision to withdraw the proposal for a Soil Framework Directive. Differences in national contaminated land regimes and associated risk management approaches across Europe pose important challenges regarding the implementation of an EU regulatory framework and the development of a concerted approach to deal with common problems.

In Spain, the first action taken by the Government was in the period of 1990-1995, when a National Plan for the Remediation of Contaminated Soils was developed (BOE 172 of 20-7-1995) with the objective of identifying polluted sites, create a database, develop a risk assessment methodology, calculate the cost of the actions, propose a program of action,

evaluate the remediation costs and consider a legal framework. As a result, in 1998 the Law 10/1998 of 21st April on Waste was passed, including a definition for contaminated areas, the need for a list of potentially polluting activities and a subsequent inventory of polluted sites, the responsibilities associated, and the standards for allowable levels of contamination for soils depending on their future uses. The next step was the Royal Decree 9/2005, which established the general reference levels (GRL) for specific pollutants such as the tolerable levels of total petroleum hydrocarbons (TPH, 50 ppm), polychlorinated biphenyls (PCBs), PAHs or BTEX among others. Finally, Law 22/2011 of 28th July was enforced, refining certain concepts such as determination of the responsible subjects of the pollution, as well as the reporting obligations for both the legal responsible of potentially polluting activities and the owners of contaminated soils.

Under suggestion of FAO's Global Soil Partnership and with the support of the EU, in December 2013 the General Assembly of the United Nations proclaimed 2015 as the *International Year of Soils* (IYS) and 5 December of each year as the 'World Soil Day' (WSD) (United Nations, 2013).

1.2 PAH polluted soils

PAHs are a class of organic compounds containing two or more fused benzene rings in linear, angular, or cluster structural arrangements (Bamforth & Singleton, 2005). They can also present alkylated forms that can be even more abundant than the non-substituted, especially in petrogenic products. By definition, PAHs only contain C and H atoms. However, N, S and O atoms may readily substitute one of the carbons of the benzene ring to form heterocyclic aromatic compounds, commonly found as co-occurring contaminants with PAHs (e.g. in creosote, see below) (Wilson & Jones, 1993). PAHs with 2 or 3 aromatic rings are generally classified as low molecular weight (LMW) PAHs, while those containing 4 or more aromatic rings are known as high molecular weight (HMW) PAHs.

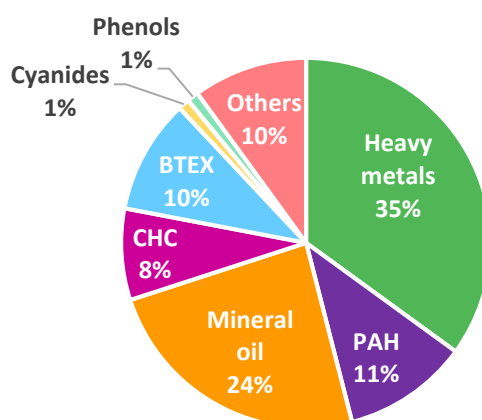


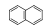
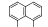
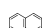

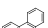
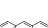
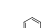

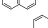

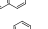


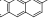
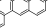

Figure 1.1. Overview of contaminants affecting soil in Europe in 2011. Source: Progress in the management of Contaminated Sites in Europe 2014.

PAHs are part of the fossil fuels but are also originated during their combustion, by waste incineration, coal gasification, and petroleum refining, and by natural phenomena such as volcanic eruptions and forest fires. Consequently, PAHs are ubiquitous in natural environments, including air, water, soil and sediment. Due to their low water solubility, high hydrophobicity, and complex chemical structure (Table 1.2), PAHs tend to accumulate in soils and sediments and present limited availability to biodegradation. However, microbial degradation is still a major environmental process affecting the fate of PAHs in terrestrial ecosystems.

In Europe, about 11% of the point source polluted sites have PAHs as the major contaminants (Figure 1.1). This does not include a number of mineral oil and BTEX polluted sites that present variable amounts of alkyl PAHs that often are not quantified as PAHs (see below). Those sites pose a major health and environmental concern because PAHs present toxicity to a variety of organisms, some are mutagenic, with the consequent carcinogenic potentials to humans, and have capacity to accumulate through the food chain (Mrozik et al. 2003). In 1979 the U.S. Environmental Protection Agency included the “16 EPA PAHs” in the Consent Decree Priority Pollutant list (Keith & Telliard, 1979). Since then, this list has been frequently adopted by regulatory authorities to identify site contamination and to specify monitoring parameters. The list of 16 EPA PAHs has, in general terms, become the standard set of compounds involved in many environmental studies of PAHs and has constituted a milestone in the environmental chemistry, since it presents several advantages. For example, the EPA priority list involves acceptable costs due to its limited analytical complexity and the commercial availability of the compounds and standards, and, since it has been used all over the world during almost 4 decades, it offers good comparability.

Nowadays, though, the validity of the 16 EPA PAHs as the only parameter in risk assessment for PAH polluted sites is being questioned for a number of reasons (Andersson & Achten, 2015). The advances in analytical chemistry and ecotoxicology research have revealed the presence of PAHs of considerably higher toxicity than those included in the priority list in different environmental samples. In addition, as previously stated, in petrogenic products the alkylated PAHs are substantially more abundant than their parental-PAHs. Moreover, as explained below, other polycyclic aromatic compounds (PACs) such as oxygenated (oxy)- PAHs and nitrogen containing (N-)PACs, are also present in polluted soils, being more bioavailable, mobile, and sometimes more toxic than their PAH analogs. In fact, some of them are found at similar concentrations than EPA PAHs (Lundstedt et al. 2007).

Table 1.2. Physic-chemical and toxicological properties of the 16 EPA PAHs, including molecular structure, chemical formula, molecular weight (MW), boiling point (B_p), vapor pressure (P_v), aqueous solubility (S), octanol-water partitioning coefficient (K_{ow}), mutagenicity (Mut.) and carcinogenicity to humans (Carc.). T=25°C unless denoted differently. Sources: Sims and Overcash 1983; Mueller et al. 1996; van Agteren et al. 1998; Pothuluri and Cerniglia 1998; IARC 1987; van Brummelen et al. 1998; Kästner 2000.

PAHs	Molecular structure	Chemical formula	MW (g/mol)	Bp (°C)	Pv (mm Hg)	S (mg/l)	K _{ow}	Mut.	Carc.
Naphtalene		C ₁₀ H ₈	128	218	4.92·10 ⁻²	31	3.37	-	
Acenaphtylene		C ₁₂ H ₈	152	265	2.9·10 ⁻²	3.93	4.07		
Acenaphtene		C ₁₂ H ₁₀	154	278	2.0·10 ⁻²	3.8	4.33	+	
Fluorene		C ₁₃ H ₁₀	166	295	1.3·10 ⁻²	1.9	4.18		U
Phenanthrene		C ₁₄ H ₁₀	178	339	6.80·10 ⁻⁴	1.1	4.57	-	U
Anthracene		C ₁₄ H ₁₀	178	340	1.96·10 ⁻⁴	4.5·10 ⁻²	4.54	-	U
Fluoranthene		C ₁₆ H ₁₀	202	375	6.0·10 ⁻⁶	0.26	5.22	+	U*
Pyrene		C ₁₆ H ₁₀	202	360	6.85·10 ⁻⁷	0.132	5.18	±	U
Benzo(a)anthracene		C ₁₈ H ₁₂	228	435	5.0·10 ⁻⁹	1.1·10 ⁻²	5.91	+	A
Chrysene		C ₁₈ H ₂₂	228	448	6.3·10 ⁻⁷	2·10 ⁻³	5.75	+	U*
Benzo(b)fluoranthene		C ₂₀ H ₁₂	252		5.0·10 ⁻⁷	1.2·10 ⁻³	6.57		B
Benzo(k)fluoranthene		C ₂₀ H ₁₂	252	480	5.0·10 ⁻⁷	5.5·10 ⁻⁴	6.84		B
Benzo(a)pyrene		C ₂₀ H ₁₂	252	495	5.0·10 ⁻⁷	3.8·10 ⁻³	6.04	+	A
Dibenzo(a,h)anthracene		C ₂₂ H ₁₄	278	524	1.0·10 ⁻¹⁰	6·10 ⁻⁴	6.75	+	A
Benzo(g,h,i)perylene		C ₂₂ H ₁₂	276		1.0·10 ⁻¹⁰	2.6·10 ⁻⁴	7.23		U
Indeno(1,2,3-c,d)pyrene		C ₂₂ H ₁₂	276		1.0·10 ⁻¹⁰	6.2·10 ⁻²	7.66		B

+:positive Ames assay; -:negative Ames assay. A: probably carcinogenic; B: possibly carcinogenic; U: unclassifiable as to carcinogenicity to humans, *classified as weak carcinogens in Pothuluri and Cerniglia 1998.

OXY PAHs AND N-CAPs

Oxy-PAHs are abundant but often neglected co-occurring contaminants in PAH polluted soils. These compounds are defined as PAHs derivatives with one or more carbonylic oxygen(s) attached to the aromatic ring structure, and in some cases, they also contain other chemical groups, such as alkyl and hydroxyl groups (Figure 1.2). Oxy-PAHs present a relative persistence in the environment but, due to their higher aqueous solubility, they are more mobile than PAHs (Table 1.3). This property promote their tendency to spread in contaminated sites, which could become an important ecotoxicological issue, since oxy-PAHs also pose a risk for human and ecosystem health (Bleeker et al., 1999).

OXY-PAHs are part of the polar fraction of fossil fuel and derivatives, but they can be readily formed *in situ* by photochemical, chemical, and microbial oxidation of the parent PAHs, thus, their concentration could increase with time in polluted sites (Lundstedt et al. 2007; Wilcke et al. 2014).

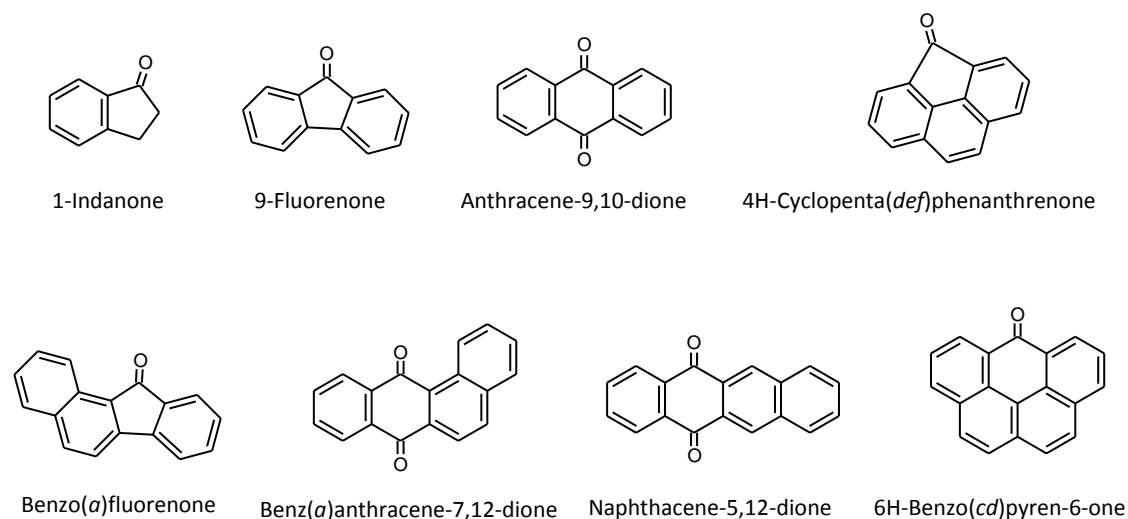


Figure 1.2. Chemical structure of the most studied oxy-PAHs.

Table 1.3 Physic-chemical properties of the most studied oxy-PAHs and N-PACs, including chemical formula, molecular weight (MW), boiling point (B_p), vapor pressure (P_v), aqueous solubility (S) and octanol-water partitioning coefficient (K_{ow}). T=25°C unless denoted differently. Source: Lundstedt et al. 2007.

	Chemical formula	MW (g/mol)	Bp (°C)	Pv (mm Hg)	S (mg/L)	K _{ow}
oxy-PAHs						
9-Fluorenone	C ₁₃ H ₈ O	180	342	5.7·10 ⁻⁵	3.7	3.58
Anthracene-9,10-dione	C ₁₄ H ₈ O ₂	208	377	3.8·10 ⁻⁸	1.4	3.39
Benz(<i>a</i>)anthracene-7,12-dione	C ₁₈ H ₁₀ O ₂	258	434	3.9·10 ⁻⁸	0.29	4.40
1-Indanone	C ₉ H ₈ O	132	243	2.7·10 ⁻²	1427	2.11
4H-Cyclopenta(<i>def</i>)phenanthrenone	C ₁₅ H ₈ O	204	375	2.7·10 ⁻⁶	0.94	4.14
Benzo(<i>a</i>)fluorenone	C ₁₇ H ₁₀ O	230	403	3.9·10 ⁻⁷	0.22	4.73
Naphthacene-5,12-dione	C ₁₈ H ₁₀ O ₂	258	434	3.5·10 ⁻⁸	0.23	4.52
6H-benzo(<i>cd</i>)pyren-6-one	C ₁₉ H ₁₀ O	254	447	1.5·10 ⁻⁸	0.05	5.31
N-PACs						
Quinoline	C ₉ H ₇ N	129	240	5.4·10 ⁻²	1711	2.03
Benzo(<i>h</i>)quinoline	C ₁₃ H ₉ N	179	339	1.4·10 ⁻⁴	5.08	3.43
Carbazole	C ₁₂ H ₉ N	167	315	1.8·10 ⁻⁴	21.1	3.29
Acridine	C ₁₃ H ₉ N	179	345	2.6·10 ⁻⁵	5.38	3.40

Azaarenes (N- PACs) are composed by fused aromatic rings harboring one nitrogen in one of the ring positions (Figure 1.3). They are also found as polar constituents of fossil fuels and have been identified in PAH polluted sites. Even though the effects on organisms are less well studied than those of PAHs, N-PACs have a large range of ecotoxicological effects such as cytotoxicity, mutagenicity, carcinogenicity and reproductive toxicity (Bleeker et al., 1999). In fact, in an early study of the group these compounds were associated to the most mutagenic fractions of organic extracts from sediments (Fernandez et al. 1992).

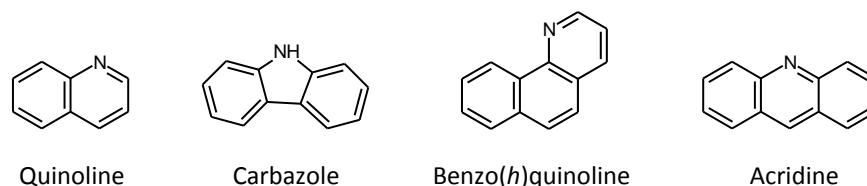


Figure 1.3. Chemical structure of the most abundant N-PACs in creosote polluted soils.

CREOSOTE

Creosote is a brown colored oil obtained from the distillation of coal tar that was traditionally used as preservative of outdoors wood and as antiseptic. Spillage during its massive application, for example on railway ties, resulted in a number of polluted sites in Europe and the USA that need to be decontaminated. Commercial creosote contains an 85% of PAHs, 10% of phenolic compounds, and 5% of N-CAPs, and all these components persist in contaminated soils. Due to its carcinogenic potential, the European Union banned the commercialization of creosote in 2003.

Creosote major components can be easily identified and quantified, since it is a relatively low complex mixture. In this Thesis a creosote polluted soil is used as a model to investigate the microbial routes and populations that determine the environmental fate and eventual removal of PAHs, oxy-PAHs and N-CAPs from the soil.

1.3 Biodegradation of PAHs in terrestrial environments

Once organic pollutants enter the complex matrix that constitutes soil they may undergo a variety of non-excluding environmental processes. They may experience volatilization, leaching, chemical oxidation, photo-oxidation, biodegradation, sorption to soil particles, accumulation inside soil pores, and bioaccumulation, among others.

Nevertheless, the biological degradation carried out by soil microorganisms is the only process that conducts to their complete removal, without causing a mere change in the distribution of the contaminant between the different ecological compartments. In fact, as mentioned before, bioremediation technologies exploit these natural microbial metabolic

capabilities to mitigate organic contaminants and restore the ecological functions of polluted soils, resulting in a cost-effective and sustainable cleaning technology (Gillespie & Philp, 2013). However, its application is still constrained by factors related to the unpredictable endpoint PAH-concentrations, mainly containing HMW compounds, the lack of adequate monitoring tools to guarantee the occurrence of active biodegradation processes, and the not entirely accurate risk assessment policies, specially related with the formation and fate of oxy- and N-PACs. The unraveling of the complex metabolic networks determining the fate of PAHs *in situ* is fundamental to optimize the available technologies (Vila et al. 2015).

The biodegradation of PAHs in soils is mainly driven by aerobic reactions carried out by bacteria or fungi. Many microorganisms are capable of oxidizing PACs to yield carbon and energy for growth. This process can culminate the complete degradation of the substrate into carbon dioxide and water (mineralization) or in a partial oxidation to give the so-called dead-end metabolites (partial degradation). Otherwise, the PACs may undergo unspecific oxidation reactions at the expenses of compounds supporting microbial growth (cometabolism), which will also produce partially oxidized products.

BIOCHEMISTRY OF THE MICROBIAL ATTACK TO PAHs

The first step of the aerobic biodegradation of polyaromatic compounds is catalyzed by the ring hydroxylating dioxygenases (RHD). These enzymes introduce two oxygen atoms in vicinal carbons of the aromatic ring forming *cis*-dihydrodiols, whose further dehydrogenation leaves the molecule ready for a second dioxygenase attack that cleaves the ring (Figure 1.4) introducing oxygen in *ortho* or *meta* positions. Subsequent rearrangements, releases of 2-3 carbon fragments that enter the central metabolism, and new dioxygenation cycles leads to the progressive degradation of the different rings producing biomass and energy for microbial growth. PAHs can be also attacked by bacterial monooxygenases, especially P450 monooxygenases, to form *trans*-dihydrodiols, but this activity is generally lower than the dioxygenase activity in the same organism.

RHD are multi-component enzymes formed by large α and small β subunits. The α subunit contains two conserved regions: the [Fe2-S2] Rieske center and the mononuclear iron-containing catalytic domain. RHD are classified into five clusters according to substrate preference and phylogenetic comparison of their α -subunit amino acid sequences (Kweon et al., 2008). Most PCR-mediated functional studies target the α -subunits of the two clusters specifically linked to PAH-degradation in Gram-negative and Gram-positive bacteria (Iwai et al. 2011). Quantitative analyses using qPCR demonstrated changes in PAH catabolic potential of soil communities during natural attenuation (Debruyne & Saylor, 2009) and in response to rhizosphere or root exudates (Cébron et al., 2009, 2011).

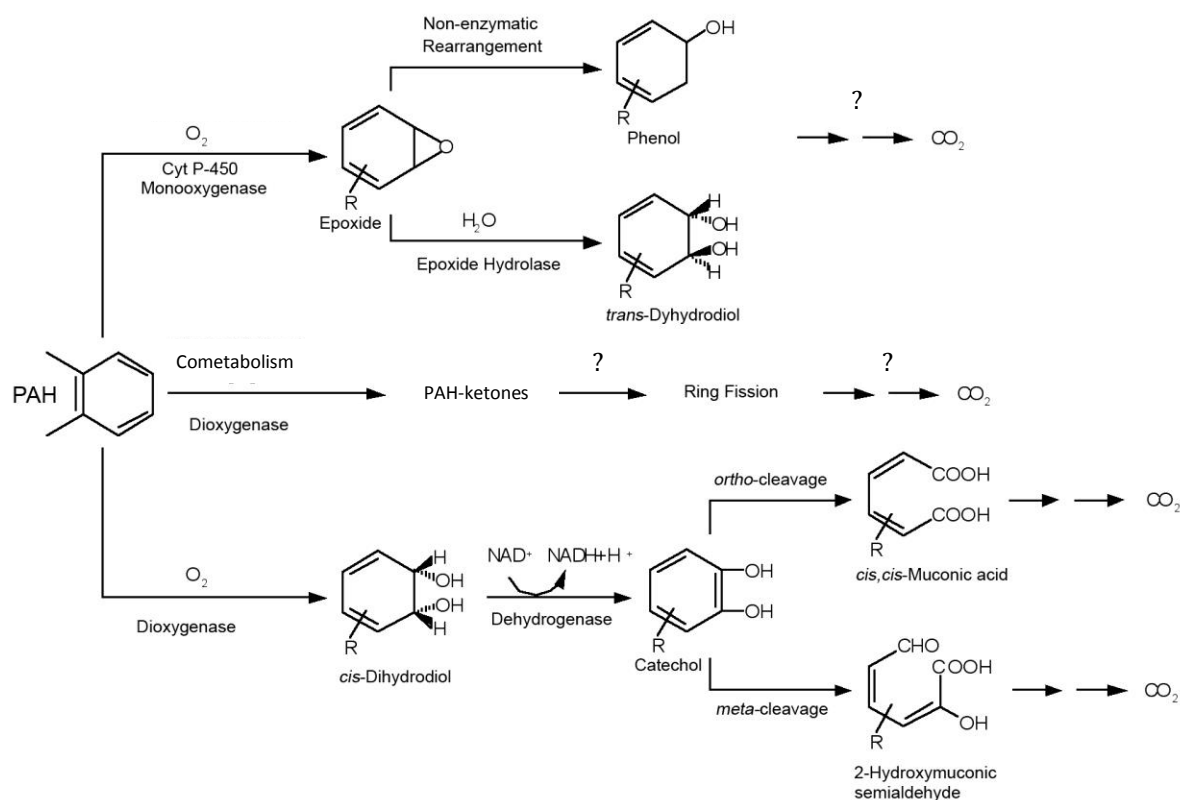


Figure 1.4. General pathway of the aerobic biodegradation of PAHs. Source: Kästner 2000.

It is known that RHD are versatile enzymes with a broad substrate specificity, easily accommodating a variety of structural analogues to give the corresponding diols whose further degradation will depend of the capability of the subsequent enzymes to recognize them as substrates. This explains the partial degradation and accumulation of dead-end products. Conversely, it has been demonstrated that dioxygenases may catalyze a fortuitous and ready monooxygenation of some reactive carbons, such methylenic or methylic groups of naphthenic or alkyl PAHs, respectively. The result is the production of ketones/quinones (oxy PAHs) and aromatic carboxylic acids that may accumulate as dead-end cometabolic products (Grifoll et al. 1994).

PAH METABOLIC PATHWAYS IN ISOLATED BACTERIAL STRAINS

There exist a vast number of known PAH-degrading bacteria. The classical approach to study PAH metabolism has been the reconstruction of pathways from the incubation of pure cultures with single PAHs (Kanaly and Harayama 2010; Mallick et al. 2011). Apart from the well-known PAH-degrading genus *Pseudomonas* (Kazunga et al. 2001; Stringfellow & Aitken, 1995), the most recent metabolic studies focus on sphingomonads and actinobacteria, especially in their ability to attack HMW compounds.

Sphingomonads show a great versatility that relies on both, the possession of several different and up-regulated ring-hydroxylating dioxygenases (RHD) and the relaxed specificity of those enzymes. For example, *Sphingobium* sp. KK22 grew on phenanthrene and transformed the HMW PAHs fluoranthene, benz(a)anthracene and benzo(k)fluoranthene, initiating their oxidation in different positions (Kunihiro et al. 2013; Maeda et al. 2014). Similarly, *Sphingobium* sp. PNB dihydroxylated phenanthrene on carbons 1,2; 3,4 or 9,10 (Roy et al. 2012). In fact, a recent and illustrative work shows that strain PNB, capable of acting on a wide range of mono- and polyaromatic substrates, harbors seven sets of ring hydroxylating oxygenases (RHO) with a variety of substrate specificities that share a sole set of electron transport proteins (Khara et al. 2014). Similar genetic arrangements, usually involving plasmids or mobile genetic elements, were found in *Sphingobium yanoikuyae* B1, *Sphingobium* sp. P2, *Novosphingobium aromaticivorans* F199 or *Sphingomonas* sp. LH128, indicating their widespread distribution and horizontal transfer within sphingomonads (Stolz, 2014). This plasticity in their catabolic networks and their short duplication times confer sphingomonads a pronounced selective advantage (r-strategists) towards a wide range of aromatic pollutants, contributing to their fast response to sudden PAH-pollution and nutrient supply (Vila et al. 2015).

In contrast, *Actinobacteria*, with their ability to adhere to hydrophobic surfaces and slow growth rates, are highly adapted to the low bioavailable HMW substrates (k-strategists) (Kanaly & Harayama, 2010). In a recent study, Kweon *et al.* (2010) demonstrated that the RHDs NidAB and NidA3B3 from the pyrene-degrading strain *Mycobacterium vanbaalenii* PYR-1, despite their relaxed specificity towards aromatic compounds, presented the highest conversion rates for pyrene and fluoranthene, respectively. These enzymes had evolved to specifically accommodate HMW PAHs in the large substrate-binding pockets of their active sites, thus satisfying spatial requirements for their efficient and regiospecific dihydroxylation. In the most exhaustive metabolic characterization of a PAH-degrading strain (PYR-1) performed so far, these authors reconstructed a comprehensive and hierarchical metabolic network (183 intermediates, 224 chemical reactions) in funnel organized modules, with a diversity of ring-cleavage and side chain processes that progressively narrow down to central metabolism; thus providing a systems-wide perspective on the biodegradation of PAHs (Kweon et al., 2011).

ACTIONS OF SINGLE ISOLATES IN COMPLEX MIXTURES

Knowledge gathered from the actions of pure cultures or enzymes towards single substrates is a first and fundamental step in the progressive approach for comprehending the ecosystem networks that determine the fate of PAHs. However, in the environment PAHs are found as complex mixtures and degrading populations will simultaneously act on different components. The type of initial attack and extent of oxidation of one substrate will be conditioned by the presence and abundance of others, thus determining if it is

channeled through productive pathways and mineralized, or partially oxidized. Dead-end products for one strain may be substrates for others. Hence, the accommodation of single cell metabolic networks to the degradation of PAH-mixtures is a key issue that has been seldom addressed. In one of these studies López et al. (2008) incubated the pyrene-degrading strain *Mycobacterium* sp. AP1 with a creosote-PAH-mixture. This strain acted on three- and four-ring components, causing the simultaneous depletion of 25% of the total PAHs in 30 days. During the incubation, a number of acidic metabolites indicative of distinctive reactions only described for HMW PAH degrading mycobacteria accumulated in the medium.

Oxy-PAHs and carboxylic acids produced by the relaxed specificity of the PAH-degradation enzymes from certain microorganisms, may accumulate or act as nodules in complex food webs. In fact, an interesting approach to assess *in situ* PAH degradation that would provide robust evidence for the occurrence of compound specific transformation pathways is the detection of signature metabolites. Recently, Lundstedt et al. (2014) published the first intercomparison study of analytical methods for the simultaneous detection of PAH and oxy-PAHs, but acidic PAH metabolites were not included. In this thesis, we investigate the kinetics of degradation of the most abundant creosote components (PAHs, oxy-PAHs, and N-PACs) in a stimulated creosote polluted soil, together with the formation and accumulation of acidic metabolites (results are shown in Chapter 5).

PAH-DEGRADING MICROBIAL COMMUNITIES

As well as PACs are not present as single compounds in the environment, single microorganisms do not live isolated from others. Actually, they are part of organized communities with complex interactions. Culture-based studies underestimate the actual diversity of natural communities and neglect the potential interactions between their components. In fact, it has been estimated that only a 0.3% of the soil diversity can be recovered as pure cultures (Amann et al. 1995). Thus, culture-independent methods have been increasingly applied to identify key microbial groups associated to PAH degradation without the need to recover them as pure cultures. Most widely used approaches include community structure analysis based on 16S rRNA gene-PCR amplification followed by fingerprinting (*i.e.* DGGE), clone libraries or tag-encoded pyrosequencing. These tools have been applied to the characterization of enriched microbial consortia (Dastgheib et al., 2012; Lafortune et al., 2009; Sun et al. 2010) as well as to assess structural changes in natural communities in response to PAH-pollution and bioremediation processes (Alonso-Gutiérrez et al. 2009; Coulon et al. 2012; Lladó et al. 2009; Niepceron et al. 2010; Singleton et al. 2013; Singleton et al. 2011).

The reduced complexity of microbial consortia enriched from natural communities facilitates the correlation between specific populations and functions. However, even though this provides the taxonomical composition of the microbial community, the actual role of the identified phylotypes is presumptively assigned based on phylogenetic affiliation to previously described hydrocarbon-degrading representatives. Therefore, the function of an often substantial proportion of yet unculturable members that persist in selective enrichments or dilution-to-extinction experiments is difficult to infer. In these cases, directed-isolation (i.e. custom-made media) of target phylotypes followed by thorough characterization of the new isolates could produce valuable results (Singleton et al. 2009). Chapter 4 of this thesis, describes the obtaining of a HMW PAH-degrading soil microbial consortium using an *ad hoc* designed enrichment methodology. The structure of this simplified community and its changes after single PAH exposure are analyzed by molecular techniques, and a key component of the community is directly isolated.

Recent studies on the identification of PAH-degrading phylotypes are based on DNA-Stable Isotope Probing (SIP) (Jones et al. 2011; Martin et al. 2012). SIP-based molecular analysis overcome the necessity of isolation to identify active players in specific substrate assimilation, representing a further decisive step in linking microbial populations to functions (Dumont & Murrell, 2005).

Another alternative that would facilitate the linking of the disappearance of certain compounds to the action of specific microbial populations would be the utilization of transcriptomics. Some studies (Di Gennaro et al., 2009; Niepceon et al., 2010) had identified particular functions in the metabolically active populations by analyzing the retrotranscribed RNA (cDNA) with denaturing gradient gel electrophoresis (DGGE). In Chapter 6 of this Thesis, an exhaustive study of the active community structure by barcoded pyrosequencing and the expression of functional genes (PAH-RHD) are correlated with the disappearance of PAH during a lab-scale bioremediation of a real creosote polluted soil.

1.4 Scope of this Thesis

This PhD Thesis has been developed in the frame of two research projects focused on PAH biodegradation in polluted soils: “Identification, evaluation and exploitation of the rhizosphere catabolic functions for the restoration of the PAH polluted soils” (CGL2010-22068-C02-02), and “Functional synergies between microorganisms and plants in sustainable remediation of soils contaminated by PAHs” (CGL2013-44554-R). Both projects were funded by the Spanish Government, and were conducted in cooperation with the research group of Dr. José Julio Ortega-Calvo (IRNASE, Seville), specialized in pollutant bioavailability. Dr. Magdalena Grifoll leads the research group at the University of Barcelona and has wide experience in bacterial metabolism and community analysis.

Part of the community analyses of the Chapter 6 of this thesis was carried out in the Laboratoire Interdisciplinaire des Environnements Continentaux (Nancy, France) during a visit of 3 months.

During the formation period, the PhD candidate had the opportunity to collaborate in the technological transfer to bioremediation companies, which culminated with the publication of an informative article (see Annex II). Meanwhile, the PhD student also participated in the writing of a review about the state of the art of bacterial PAH biodegradation which was recently published in Current Opinion in Biotechnology (see Annex II).

CHAPTER 2

Objectives

2 Objectives

The general goal of this Thesis is to contribute to the elucidation of the microbial processes occurring during active PAH biodegradation in polluted soils. This will permit to identify key microbial taxa, functions and possible new target analytes, with the ultimate aim of improving current bioremediation technologies and their monitoring and risk assessment protocols. To achieve this goal, a creosote-polluted soil from a site in the south of Spain was chosen as a model soil because its high PAH concentration levels and the long pollution history suggested the existence of a well-established and highly adapted PAH-degrading community. Special emphasis is made on HMW PAHs, as they are the main constituents of the residual endpoint concentrations endangering the success of bioremediation approaches, and the formation and fate of generally neglected oxy- and N-PACs.

Within this global aim, the specific objectives to be developed in this Thesis are:

- To select and characterize the HMW PAH-degrading communities by enrichment of a low diversity consortium using a novel sand-in-liquid biphasic system and a biologically weathered creosote NAPL. Key players within the community will be identified on the basis of substrate-specific responses; phylogenetic, functional and metabolomic profiles; and their recovery as pure cultures.
- To comprehensively assess the microbial processes driving the *in situ* removal of PAHs during the incubation of the model creosote-polluted soil in enhanced biodegradation conditions. The dynamics of PAHs, oxy-PAHs and N-PACs biodegradation, together with the potential formation and fate of oxidation products, will be correlated with specific key phylotypes and community changes. A real time insight into community dynamics will be obtained from the combined analysis of changes in the global (genes) and active (transcripts) microbial communities, both at the phylogenetic (16S rRNA gene) and functional (RHD genes) levels.

CHAPTER 3

Experimental layout

3 Experimental layout

The overall experimental layout used in this Thesis is summarized in Figure 3.1. A sample of about 100 kg of creosote polluted soil was collected from a historical contaminated site in the South of Spain. The soil was dried, sieved and homogenized using a Soil Deagglomerator Pulverisette 8 machine (Fritsch GmbH). A subsample of the soil was used to inoculate a long time enrichment procedure to obtain a simplified and stable HMW

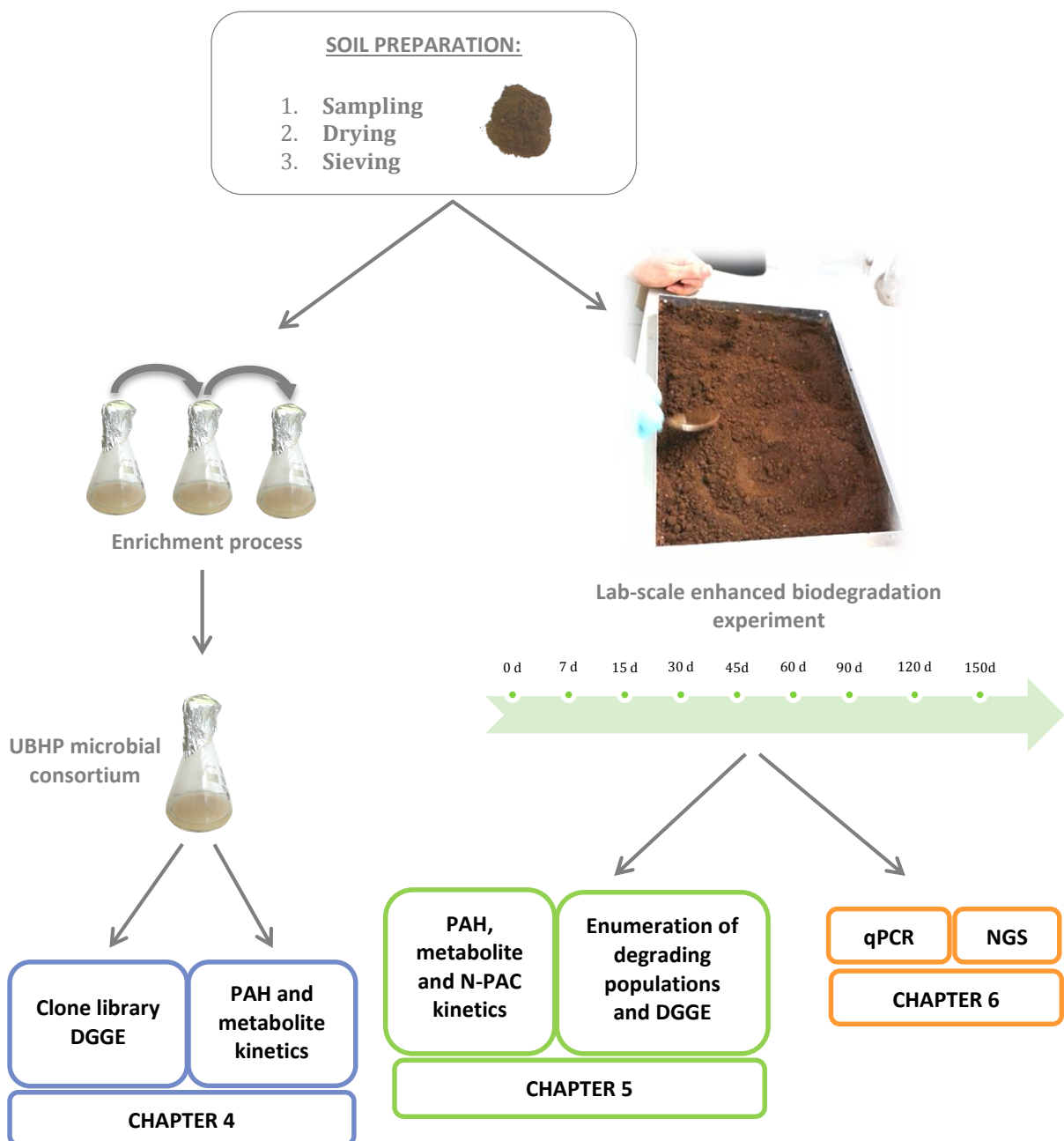


Figure 3.1. Global experimental layout of the thesis

PAH-degrading soil community: the bacterial consortium UBHP. A larger part of the soil was used to set up a lab-scale experiment in solid state where the biodegradation of the PACs present in the soil was enhanced by means of two different aerobic treatments: i) water content adjustment, and ii) water content adjustment and nutrient addition (N and P).

Microbial consortium UBHP was selected by serial transfers using a sand-in-liquid microcosm system that consisted in Erlenmeyer flasks containing sand coated with a weathered creosote-HMW PAH residue and mineral medium. The initial culture was inoculated with a small sample of the creosote-polluted soil, and the cultures were transferred every 4 weeks during 2 years. Chapter 4 summarizes the characterization of the catabolic potential of the UBHP consortium, the analysis of its microbial community structure, and the isolation of key bacteria.

For the lab-scale enhanced biodegradation experiment the original soil, with a high concentration of PAHs (about 30,000 ppm), was combined with an agricultural soil (1:2, polluted soil: agricultural soil) by using a tumble mixer. The resulting soil was distributed in trays (2.5 kg) and incubated during 5 months. Two different treatments were carried out in triplicate (three trays per treatment): i) manual aeration and water content adjustment (40% of WHC), and ii) manual aeration, water content adjustment (40% of WHC) and nutrient addition (C:N:P, 300:10:1). Triplicates of non-treated dry soil were also incubated as controls. At 0, 7, 15, 30, 45, 60, 90, 120 and 150 days samples were collected from each tray for MPN counts (5 g), chemical (20 g) and molecular microbial ecology (5 g) analyses. The MPN counts were performed directly after sampling, while samples for chemical and molecular analysis were stored at -20 and -80°C, respectively.

The chemical analyses at each data point included the identification and quantification of PAHs, N-PACs, oxy-PAHs and acidic metabolites. PAHs-, oxy-PAH- and N-PAC-degrading bacteria and the total heterotrophic populations were counted by a miniaturized MPN method. The community able to grow in the most diluted wells for each substrate was identified by PCR-DGGE and sequencing of the excised bands. Results are described in Chapter 5.

Total nucleic acids were extracted from the samples stored at -80°C. The community dynamics associated to PAC-removal were assessed by structural (pyrosequencing of 16S rRNA genes) and quantitative (qPCR) changes in the bacterial (16S rRNA genes), fungal (18S rRNA genes), mycobacterial (*Mycobacterium* specific 16S rRNA genes) and PAH-degrading (PAH-RHD genes) communities, both at the gene (DNA) and transcript (cDNA or RNA) levels. The results are included in Chapter 6.

CHAPTER 4

Key HMW PAH-degrading bacteria in a soil consortium enriched using a biodegraded creosote residue in a sand-in-liquid culture system

4 Key HMW PAH-degrading bacteria in a soil consortium enriched using a biodegraded creosote residue in a sand-in-liquid culture system

Stimulation of microbial degradation is the most sustainable approach to decontaminate PAH polluted soils, while restoring/preserving their natural functions (Gillespie & Philp, 2013). However, the viability of biological treatments for PAH decontamination is constrained by the frequently high end point concentrations reached, due to the formation of a persistent residue enriched in HMW PAHs with 4 or more aromatic rings. A first step in the necessary understanding of the *in situ* microbial processes leading to HMW PAH removal is the identification of the key microorganisms involved and their function within the degrading communities.

A number of soil bacterial strains isolated for their capacity to grow on 4-ring HMW PAHs are able to completely mineralize them (Kanaly & Harayama 2010; Vila et al. 2001; Vila et al. 2015). Most pyrene-degrading isolates are actinobacteria also able to degrade or cometabolize a variety of 3-5 ring PAHs both as single compounds or in NAPL mixtures (López et al. 2008; Vila & Grifoll 2009; Vila et al. 2001). Fluoranthene (FT) degradation has been largely associated to versatile sphingomonads harboring several sets of dioxygenases that attack a variety of aromatic compounds (Stolz, 2009). Other less documented HMW PAH-oxydizing strains include members of the *Alpha*- and *Gammaproteobacteria*, i.e the PY-degrading *Stenotrophomonas maltophilia* strain VUN 10,003 (Juhász & Naidu, 2000) or the chrysene (CHY)-degrading *Pseudomonas fluorescens* strain P2A (Caldini et al. 1995). Many of those strains also degrade or cometabolize other 4- and 5-ring PAHs, simultaneously attacking them when exposed to environmental mixtures, and producing more available oxydated (oxy)-PAHs and aromatic dicarboxylic acids that will require the action of other members of the community to be removed. This is especially important for 5-ring PAHs such as benzo(*a*)pyrene (BaPY), whose degradation has only been demonstrated by the cooperation of various bacteria initiated by cometabolic attacks (Jones et al. 2014; Kanaly et al. 2000; Kanaly & Harayama 2010). Studies with single strains are fundamental, but do not inform on the *in situ* cooperative catabolic microbial interactions, the overall relevance of the described bacteria in soils or the potential role of the non-yet cultured bacteria. High throughput molecular approaches offer an exhaustive analysis of the natural communities, but the association of the key phylotypes to specific functions can often only be indirectly inferred on the basis of previous knowledge gathered from pure cultures (Vila et al., 2015). DNA-SIP analysis has greatly contributed to identify key degraders of specific PAH substrates, highlighting them within the complex *in situ* communities. However, the analysis of cometabolic interactions requires to obtain representative model consortia, whose reduced-

complexity permits a thorough analysis of the individual microbial components and their interactions.

The HMW PAH-degrading microbial consortia described until now have been generally enriched using single substrates (Dastgheib et al. 2012; Sun et al. 2010) or synthetic mixtures with a limited number of compounds (Bouchez et al. 2000; Lafortune et al. 2009). It is known that PAHs degradation is strongly conditioned by their inclusion in natural NAPL mixtures (Efroymsen & Alexander 1994; Ortega-Calvo et al. 1995), thus some authors have used synthetic biphasic systems with PAHs supplied in a predominant organic matrix (Lafortune et al., 2009). It is known that the uptake of highly hydrophobic HMW PAHs is favored by adhesion and biofilm formation on polluted solid matrices (Edwards et al. 2013).

Here we present the establishment of a specialized HMW PAH-degrading soil consortium by enrichment of the natural microbial community present in a creosote polluted soil using a sand-in-liquid culture system in which the sand particles are coated with a HMW PAH residue obtained by previous biodegradation of commercial creosote (Grifoll et al., 1995). The simplified HMW PAH-degrading microbial consortium is thoroughly characterized by a combination of culture dependent and independent methods in an attempt to identify key phylotypes, recover them as single isolates, and associate them to specific catabolic roles.

4.1 Materials and methods

4.1.1 Chemicals

Phenanthrene (PHE, 98% purity), fluoranthene (FT, >97%), pyrene (PY, 98%), benz(*a*)anthracene [BaA, 99%], chrysene (CHY, 98%) and benzo(*a*)pyrene [BaPY, ≥ 96%] were purchased from Sigma-Aldrich Chemie (Steinheim, Germany). The 16-PAH standard solution was purchased from Dr. Ehrenstorfer (PAH-mix 9, Augsburg, Germany). Solvents (organic residue analysis grade) were obtained from J.T. Baker (Deventer, The Netherlands).

4.1.2 Creosote-HMW PAH residue

To obtain the creosote-HMW PAH mixture used as carbon source for enrichment cultures, the total PAHs present in a commercial creosote (West Chester, PA) were purified by column chromatography (Grifoll et al., 1995) and supplied as carbon source (1 g·L⁻¹) to 400-mL cultures of the fluorene-degrading strain *Bulkholderia cepacia* F297 in mineral medium (MM) as described previously (Grifoll et al., 1995). After one month of incubation most of the low molecular weight (LMW) PAHs had been degraded and the residual HMW PAHs were recovered by solvent extraction with dichloromethane and further

purification in alumina columns. Typically, 2.5 g of commercial creosote gave 2.15 g of PAHs (86%) and incubation of 400 mg of this mixture with the strain F297 resulted in 144 mg of a clean HMW PAH oily residue (36% of PAHs).

4.1.3 Enrichment of the HMW PAH-degrading microbial consortium UBHP

The HMW PAH-degrading microbial populations present in a historically creosote polluted soil from the south of Spain were enriched using an especially designed sand-in-liquid culture system which consisted in 100-ml Erlenmeyer flasks containing liquid mineral medium (20 mL) and washed sea sand (10 g, thin grain, Panreac, Barcelona) coated with the creosote-HMW PAH residue ($1 \text{ g}\cdot\text{L}^{-1}$). The sand, treated at 400°C overnight to remove organic residues, was added to the sterile empty flasks and spiked with the HMW PAH residue in dichloromethane solution. After evaporating the solvent by gentle rotation overnight the flasks received the sterile mineral medium. The initial sand-in-liquid culture was inoculated using 5g of the polluted soil, incubated under aerobic conditions (rotary shaker, 80 rpm), and transferred (0.5 mL of liquid phase and sand) monthly. Routine DGGE analyses (see below) were performed before each transfer to check culture stability. At the time this work was carried out consortium UBHP had been transferred for 2 years, and all the experiments presented here were inoculated using 30 days sand-in-liquid cultures.

4.1.4 Enumeration of the PAH-degrading microbial populations by MPN

Bacterial counts of consortium UBHP were performed using the miniaturized most probable (MPN) method (Wrenn & Venosa, 1996). Total heterotrophs were counted in diluted Luria Bertani medium (LB 1/10). PAH degraders were counted in mineral medium containing individual hydrocarbons at $0.5 \text{ g}\cdot\text{L}^{-1}$ (PHE, FT, PY, BaA or CHY).

4.1.5 Biodegradation of the creosote HMW PAH mixture by consortium UBHP

Series of triplicate sand-in-liquid cultures inoculated with 0.5 ml of consortium UBHP were incubated during 0, 3, 6 or 12 weeks. Identical uninoculated flasks were included as abiotic controls. At each incubation time, a set of control and culture flasks was removed and their liquid and solid phases were separated by filtration (Whatman No. 1, GE Healthcare, United Kingdom). The solid phase was extracted with dichloromethane:acetone (2:1) (5 x 50 mL) in an ultrasonic bath. The aqueous phase was extracted with dichloromethane (5 x 20 mL), acidified to pH 2 and extracted again using ethyl acetate. All the extracts were dried using Na_2SO_4 and concentrated under vacuum to 1 mL previous to GC or GC-MS analysis.

4.1.6 Chemical analyses of residual PAHs and accumulated metabolites

GC analyses were performed on a TRACE GC2000 (Thermo, USA) gas chromatograph (GC-FID) or on an Agilent Technologies 6890N gas chromatograph coupled to a 5975 inert mass spectrometer (GC-MS), as described elsewhere (López et al. 2008). Prior to analysis, the acidic extracts were derivatized with diazomethane and the metabolites were identified by comparison with authentic standards, our in-house analytic database, or the NIST library. The concentration of each of the PAHs was quantified using five point standard calibration curves. To plot their degradation kinetics, the percentage of remaining PAHs was calculated from their normalized concentration using benzo(*g,h,i*)perylene (BP) as internal standard (considered as not biodegraded), as shown in the following equation: $C_t/C_0 = [(C_t/BP_t)/(C_0/BP_0)]$, where C_t and BP_t are the concentrations of the target analyte (PAH) and BP, respectively, at time t and C_0 and BP_0 are the concentrations of those compounds at the beginning of the experiment. BP was chosen because it is a highly stable condensed 6-ring PAH, whose degradation has never been reported. Therefore, its utilization here as internal standard is analogous to that of the hopanes used to normalize the concentration of single components in degraded crude oils.

4.1.7 UBHP microbial community response to single PAHs

Consortium UBHP was used to inoculate triplicate sand-in-liquid cultures in which the sand was coated with one of the following single PAHs ($0.2 \text{ g}\cdot\text{L}^{-1}$): PHE, FT, PY, BaA, CHY and BaPY. Abiotic controls were also included. After 6 weeks of incubation controls and cultures were extracted as described above to quantify residual PAHs and possible metabolites. Separate triplicate cultures were incubated in parallel to determine microbial growth and changes in microbial community structure. Growth was demonstrated by a significant (T-Student, $p < 0.05$) increment in protein content in respect to the corresponding time zero cultures determined as in Vila et al. (2001); while changes in microbial community structure were analyzed by PCR-DGGE.

4.1.8 DNA extraction and PCR amplification

Total DNA from sand-in-liquid UBHP cultures was obtained from 0.4 mL samples, containing both liquid medium and sand, and the Power Soil DNA isolation kit (Mobio, Carlsbad, USA). DNA from bacterial isolates was purified using InstaGene Matrix (Bio-rad, Hercules, CA). 16S rRNA and PAH ring hydroxylating dioxygenase (RHD) gene fragments were amplified using pureTaq™Ready-To-Go™ PCR bead tubes (GE healthcare, United Kingdom). 1 μL of DNA extract was used as the template for 25 μL reactions containing 25 pmol of each primer (Sigma-Aldrich, Steinheim, Germany). All the PCR amplifications were performed on an Eppendorf Mastercycler as described below.

4.1.9 DGGE analysis

Partial 16S rRNA gene fragments from the total DNA extracts of UBHP cultures were amplified using primers GC40-63F and 518R (El Fantroussi et al. 1999), quantified with a Nanodrop spectrophotometer, and used in equal concentrations for DGGE analysis on 6% polyacrylamide gels with denaturing gradients ranging from 45% to 70% (100% denaturant contains 7 M urea and 40% formamide) in the conditions described in Gallego et al. 2013. DGGE bands were processed and quantified using Image Lab Version 4.0.1 build 6 image analysis software (Bio-Rad Laboratories) and further used to perform a correspondence analysis (CA). When indicated, the main bands of each lane were excised and sequenced.

The actinobacterial diversity present in consortium UBHP was analyzed by a nested-PCR approach using primers F243 and R1378 for the first amplification and F984GC and R1378 for the second PCR, as described by Heuer et al. (1997). PCR products were analyzed by DGGE on 8% polyacrylamide gels with denaturing gradients ranging from 30% to 60%. Electrophoresis was performed at a constant voltage of 150 V for 9 h in 1x TAE buffer at 60°C.

4.1.10 16S rRNA gene clone library analysis

A DNA extract from consortium UBHP was amplified using universal bacterial primers 27F and 1492R (Weisburg et al. 1991) as indicated above. PCR products were purified using the Wizard®SV Gel and PCR Clean-Up system (Promega, Madison, USA) and cloned using the pGEM®-T Easy Vector System (Promega, Madison, USA). Transformants were selected by PCR amplification using vector primers. PCR products were purified, and complete sequences of the inserts were obtained using the ABI Prism BigDye Terminator cycle-sequencing reaction kit (version 3.1) with the amplification primers. The sequencing reactions were analyzed on an ABI prism 3700 Applied Biosystems automated sequencer at the Scientific and Technological Centers of the University of Barcelona. DNA sequencing runs were assembled, aligned and manually adjusted using BioEdit Software. Detection of chimeras was performed with the DECIPHER's Find Chimeras web tool (Wright et al. 2012). The resulting DNA sequences were examined and compared with the BLAST alignment tool (<http://blast.ncbi.nlm.nih.gov/Blast.cgi>) and the classifier and tree builder tools of the Ribosomal Database Project II (Wang et al. 2007). Clones with more than 99% of sequence similarity were considered as a single OTU. According to this, the diversity coverage of the library was estimated with the following equation: $C = (1 - n/N) \times 100$, where C (%) is the coverage; n, the number of OTUs, and N, the total number of positive clones (Buckley et al. 1998). DNA sequences from each phylotype are available in GenBank under the following accessions numbers: KP398522-KP398553.

4.1.11 Detection and phylogenetic analysis of PAH ring hydroxylating dioxygenases (RHD)

Genes encoding for RHDs present in consortium UBHP or in the recovered bacterial isolates (see below) were PCR amplified using the PAH-RHD primer sets for Gram-positive (GP) and Gram-negative (GN) bacteria designed by Cébron et al. (2008). For microbial consortium UBHP, amplification was also attempted with the primer sets Ac596R (reverse complemented) and NAPH2R, and NidA-forward and pdo1-r, as recommended by Iwai et al. (2011). *Bulkholderia cepacia* strain F297 (Grifoll et al., 1995) and the pyrene-degrading strain *Mycobacterium gilvum* AP1 (Vila et al. 2001) served as positive controls, and three different annealing temperatures (35, 40 and 45°C) were assayed with the PCR conditions described above. PCR products amplified from consortium UBHP DNA were used to construct clone libraries with pGEM-T Easy vector and sequenced as described above. DNA sequences from PAH RHD are available in GenBank under the following accessions numbers: KP398515-KP398521 and KP398554-KP398561.

4.1.12 Isolation of PAH-degrading bacteria

Serial dilutions of consortium UBHP were inoculated into four different series of solid media: i) mineral medium with single PAHs [FT, PY, BaA and CHY, 0.1 g·L⁻¹ final concentration] or creosote-HMW PAH mixture; ii) soil extract agar medium (Hamaki et al. 2005); iii) soil extract medium combined with the above PAHs and HMW PAH mixture; and iv) diluted LB (1/100). Colonies showing different morphologies from each medium were selected, purified on 1/10 LB agar plates and identified according to their 16S rRNA gene sequence. For the specific recovery of sphingomonads we used mineral medium with PHE (0.1g·L⁻¹) supplemented with streptomycin (0.2g·L⁻¹) according to Vanbroekhoven et al. (2004).

4.1.13 Statistical analysis

T-test and analysis of variance (ANOVA) followed by Tuckey pot-hoc test were performed using IBM SPSS Statistics 20 with mean differences significant at the 0.05 level. The same software was used to perform a Correspondence Analysis (CA) based on band intensity data of the different DGGE profiles.

4.2 Results

4.2.1 Microbial Consortium UBHP

The designed sand-in-liquid enrichment system, using a degraded creosote-PAH residue as carbon source (84% of 4-, 5- and 6-ring PAHs), allowed establishing a HMW PAH

degrading microbial consortium (UBHP) from creosote polluted soil. Consortium UBHP was maintained by monthly transfers and routine 16S rRNA PCR-DGGE analysis showed that at the time of the study the community structure of the sequential cultures had become highly stable (data not shown). Bacterial counts indicated a total heterotrophic population of $5.7 \cdot 10^9$ MPN·ml⁻¹, while FT and PY-degrading populations were at $1.8 \cdot 10^7$ and $7.9 \cdot 10^6$ MPN·ml⁻¹, respectively.

4.2.2 Biodegradation of the HMW PAH-residue by microbial consortium UBHP

The capability of consortium UBHP to attack the HMW PAHs in the supplied residue was determined in triplicate sand-in-liquid cultures incubated during 3, 6 and 12 weeks. At the end of incubation all the 4- and 5-ring PAHs as well as their methyl derivatives had been significantly ($p < 0.05$) and extensively attacked (Figure 4.1, Figure 4.2 and Figure 4.3). These included methyl- (C1-PY, 80%) and dimethylpyrenes (C2-PY, 66%), BaA (66%), CHY (59%), methylchrysenes (C1-CHY, 55%), benzo(*b+k*)fluoranthene [*Bb+k*FT, 58%], BaPY (40%), benzo(*e*)pyrene [BePY, 7%], and dibenzo(*a,h*)anthracene [DBANT, 39%]. The 6-ring PAH indene(1,2,3-*cd*)pyrene (INDPY) was also significantly depleted (7%). All the compounds were attacked simultaneously, but the preference in the degradation (rates and extension) was consistent with their water solubility and number

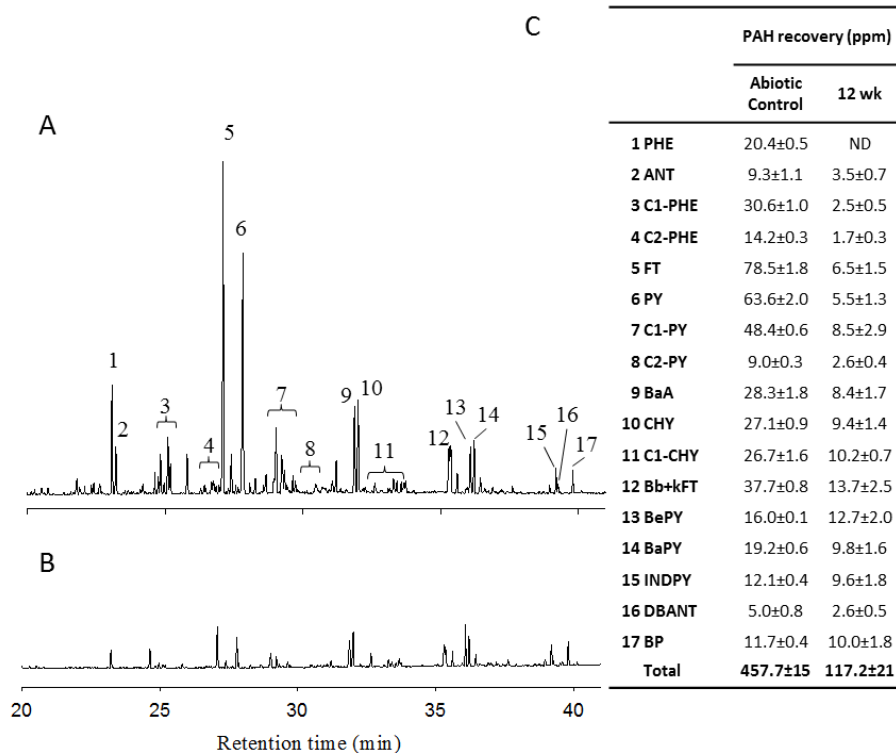


Figure 4.1. GC-FID profiles from the neutral extracts of an abiotic control (A), showing the composition of the creosote-HMW PAH residue used as a carbon source, and from a representative culture of consortium UBHP after 12 weeks of incubation (B). C shows the average concentrations of each PAH from triplicate controls and cultures at the end of incubation. Abbreviations are spelled in the text.

of alkyl substituents: PHE > FT/PY/C1-PHE > C2-PHE > BaA > CHY > C1-PY > C2-PY > C1-CHY > DBANT > Bb+kFT > BaPY > BePY/INDPY. Anthracene (ANT) was an exception, presenting lower degradation rates than 4-ring PAHs with considerably lower water solubilities. Leaving aside the methyl derivatives, PHE, FT and PY showed very similar kinetics, with highest degradation rates during the first 3 weeks (e.g. at least $57 \text{ nmol}\cdot\text{h}^{-1}\cdot\text{ml}^{-1}$ for FT and $41 \text{ nmol}\cdot\text{h}^{-1}\cdot\text{ml}^{-1}$ for PY) that strongly attenuated thereafter. BaA and CHY were degraded in parallel, with linear kinetics and maximum rates between 0-6 weeks (7 and $6 \text{ nmol}\cdot\text{h}^{-1}\cdot\text{ml}^{-1}$, respectively) that dramatically decreased thereafter. Conversely, the five ring compounds Bb+kFT and BaPY were mainly degraded after the third week, with linear kinetics until the end of incubation ($4 \text{ nmol}\cdot\text{h}^{-1}\cdot\text{ml}^{-1}$, and $2 \text{ nmol}\cdot\text{h}^{-1}\cdot\text{ml}^{-1}$, respectively), suggesting that a longer incubation period could result in a more extended degradation.

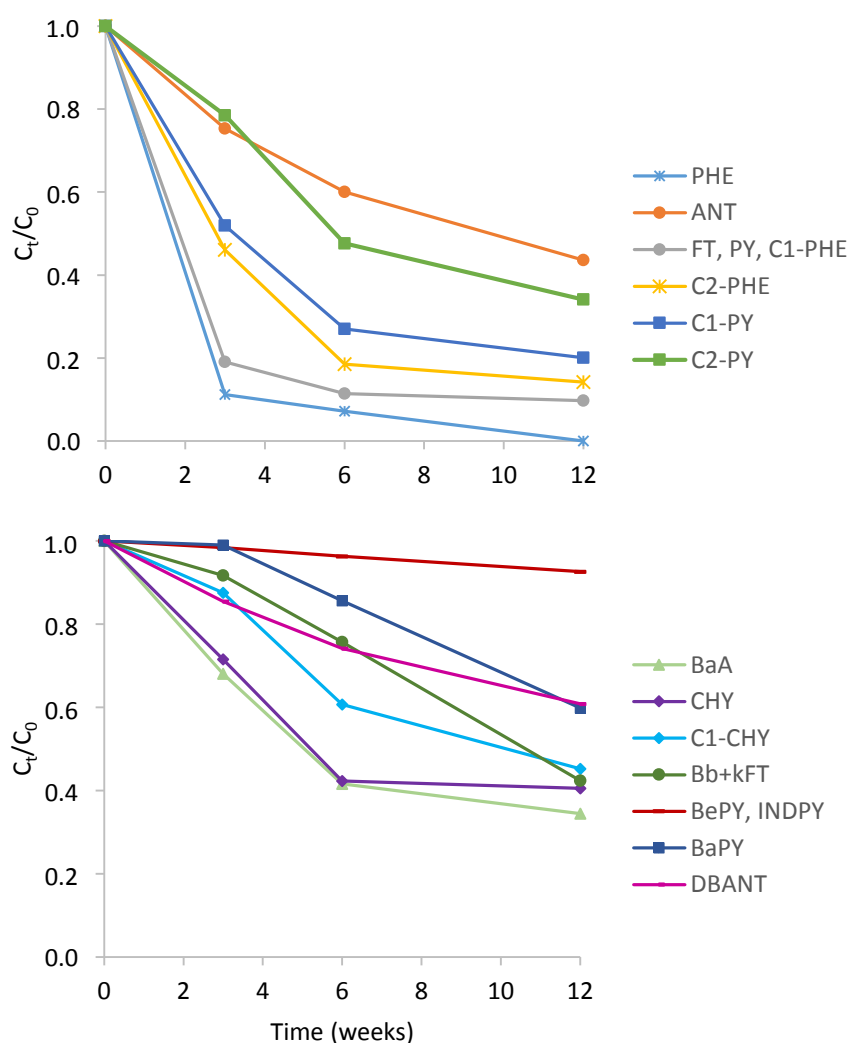


Figure 4.2. Depletion of individual PAHs in cultures of consortium UBHP in mineral medium and the creosote-HMW PAH mixture as carbon source. Each data point corresponds to the average of triplicates. Error bars showing the standard deviation have been omitted for clarity. Kinetics of FT, PY and C1-PHE, and of BePY and INDPY were grouped in the same plots because their values at each data point were not significantly different

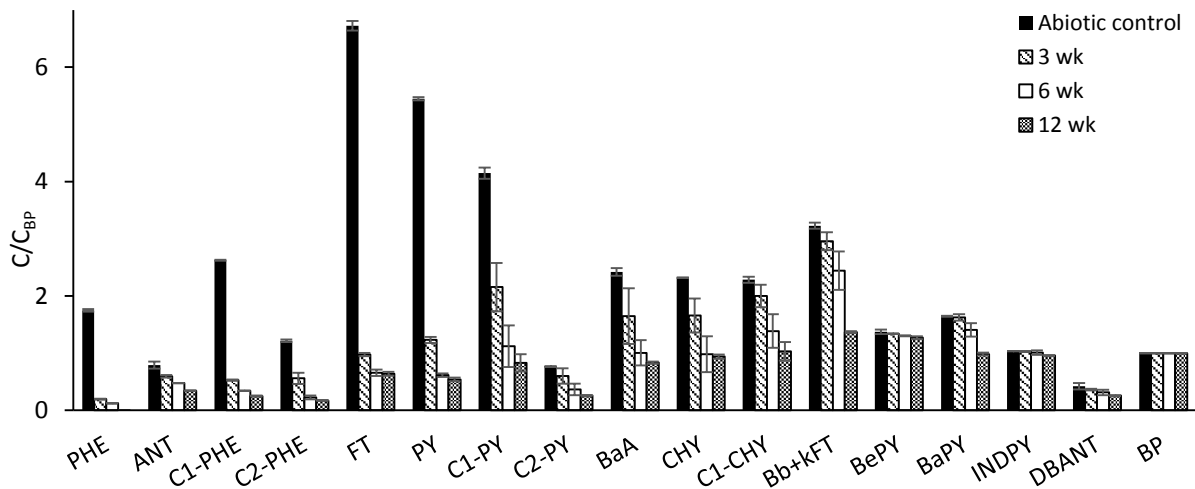


Figure 4.3. PAH concentrations respect to the concentration of BP in the abiotic control and at 3, 6 and 12 weeks of incubation.

Throughout the incubation five major PAH metabolites accumulated in the culture fluids (Table 4.1, Figure 4.4). Three of them, phenanthrene 4,5-dicarboxylic acid (II), 6,6'-dihydroxy-2,2'-biphenyl dicarboxylic acid (V), and product III, with a mass spectrum indicative of an aromatic dicarboxylic acid [methylated derivative with m/z 296 (M^+), 265 ($M^+ - OCH_3$), 237 ($M^+ - COOCH_3$), 222 ($M^+ - COOCH_3 - CH_3$), 206 ($M^+ - COOCH_3 - OCH_3$), 179 ($M^+ - COOCH_3 - COOCH_3 + H^+$)], have been routinely identified as metabolites from the degradation of pyrene by mycobacteria (Kanaly & Harayama 2010; Vila et al. 2001 and non-published results). Metabolite IV, Z-9-(methoxycarbovinyl)-9H-fluorene-1-carboxylic acid is a typical metabolite of fluoranthene also in mycobacteria (López et al. 2006). The last of the major compounds, metabolite I, presented a mass spectrum consistent with a naphthalene dicarboxylic acid whose retention time ruled out both the 1,6- and the 1,8- isomers. Interestingly, most of these metabolites reached maximum concentrations at 3 or 6 weeks that progressively decreased thereafter, indicating their possible reutilization. This included metabolite V, accumulated as a dead end product in the degradation of pyrene by axenic cultures (Vila et al. 2001). By contrast, the concentration of metabolite IV increased until the end of the incubation, as observed during the degradation of fluoranthene by single strains (López et al. 2006). These kinetics indicate that the degradation of the PY and FT molecules, the PAHs with higher concentrations in the creosote HMW PAH mixture (31%), continued long after the fast initial depletion of the parent compounds.

Table 4.1. GC-MS characteristics of the major acidic metabolites identified in the cultures of consortium UBHP with the creosote-HMW PAH mixture. The relative abundances shown correspond to the analysis of the cultures after 3 weeks (3 replicates). The substrate column indicates the PAH from which the metabolite originated, as determined from the cultures of consortium UBHP in mineral medium and individual PAHs as sole carbon sources.

Product no.	R _t (min)	m/z of fragment ions (% relative intensity)	Abundance ^a (%)	Substrate
I	25.5	244(M ⁺ , 36), 213(100), 198(1), 185(4), 170(4), 154(6), 127(29), 126(15), 114(6)	4.4 ± 2.2	BaA
II	30.5	294(M ⁺ , 4), 263(1), 235(100), 220(49), 204(4), 192(8), 178(8), 163(13), 150(3)	5.5 ± 6.3	PY
III	30.7	296(M ⁺ , 63), 265(100), 237(42), 222(30), 206(5), 194(6), 179(7), 166(10), 151(20), 138(13)	10.3 ± 1.1	PY
IV	31.3	308(M ⁺ , 24), 276(36), 249(5), 245(5), 232(36), 217(100), 205(13), 189(74), 176(14), 163(10), 151(6), 138(3), 124(6), 108(3), 94(12)	3.3 ± 2.6	FT
V	31.5	302(M ⁺ , 4), 300(59), 270(7), 269(40), 241(100), 226(58), 210(8), 198(12), 184(2), 183(3), 182(8), 170(9)	7.8 ± 1.7	PY

^a Relative abundances in the biodegradation experiments of consortium UBHP with the creosote-HMW PAH mixture after 3 weeks of incubation.

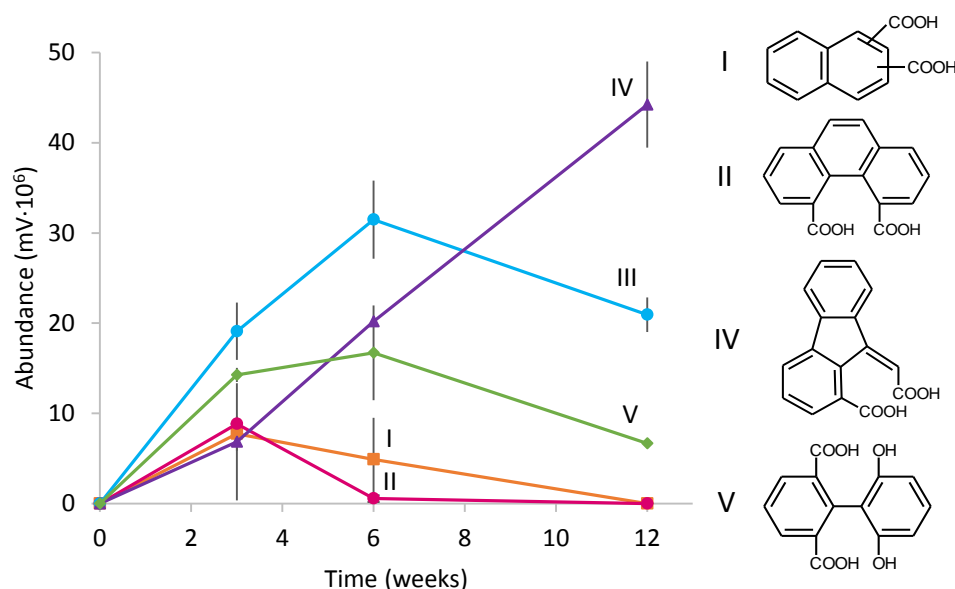


Figure 4.4. Time course accumulation of the most abundant metabolites identified in the acidic extracts of cultures of the consortium UBHP in mineral medium and the creosote-HMW PAH residue as sole carbon source. The abundance values shown correspond to the average areas of GC-MS peaks from three replicate cultures. Error bars show the standard deviation. Injection volume was 1 μ l from a total of 1 ml after derivatization with diazomethane. Metabolite I, naphthalene 1,2- or 2,3- dicarboxylic acid; II, phenanthrene 4,5-dicarboxylic acid; III, non-identified aromatic dicarboxylic acid previously observed during the degradation of pyrene by mycobacteria; IV, Z-9-(methoxycarbonyl)-9H-fluorene-1-carboxylic acid; V, 6,6'- dihydroxy-2,2'-biphenyl dicarboxylic acid.

4.2.3 Microbial community structure of consortium UBHP

The analysis of the 16S rRNA gene clone library produced a total of 70 sequences that grouped in 20 different OTUs at less than 1% sequence divergence (diversity coverage of 71%, Figure 4.5), most of them belonging to phylum *Proteobacteria* (81%) (Table 4.2). About 32% were *Alphaproteobacteria* that affiliated within the genera *Sphingomonas* (1%, phylotype S1), *Sphingobium* (22%; S2, S3), *Azospirillum* (5%; S4, S5), *Bradyrhizobium* (1%; S6) and *Rhodoplanes* (1%; S7); a smaller portion (4%) were classified within the betaproteobacterial genus *Achromobacter* (4%, S8); and the remaining 45% fell into *Gammaproteobacteria*. Although a few phylotypes within this class were properly affiliated to *Pseudomonadaceae* (4%, S9-S11), *Xanthomonadaceae* (5%, S12-S14), and *Steroidobacter* (*Sinobacteraceae*, 2%, S15, S16), most of the OTUs were only distantly related to cultured bacteria and could not be affiliated within any known taxon (32%; S17-S20). The analysis of the reference sequences for those OTUs, which were highly similar to each other (>96%), revealed that they were closely related to members of an uncultured group of soil γ -*Proteobacteria* that have been associated with pyrene degradation in DNA-SIP studies and designated as pyrene group 2 (Figure 4.6). Apart from *Proteobacteria*, only members of the phylum *CFB* were detected, accounting for 19% of the total community, and being represented by a single phylotype (S21) that belonged to the genus *Terrimonas*.

In general, the sequences of the most abundant clones coincided with those found for major bands in the 16S rDNA DGGE profiles of consortium UBHP (Figure 4.7A, lane UBHP). One exception was the clone identified as *Terrimonas* (S21), which could not be assigned to any band because when analyzed by DGGE produced a smear instead of a defined band in polyacrylamide gels. Scarcely represented components, such as the members of *Pseudoxanthomonadaceae* (S12-S14), also escaped to DGGE detection. Interestingly, at this point, none of the clones or the DGGE bands that could be sequenced directly from the consortium UBHP profile corresponded to *Actinobacteria*, a phylum traditionally related to HMW PAH degradation (Kanaly & Harayama, 2010).

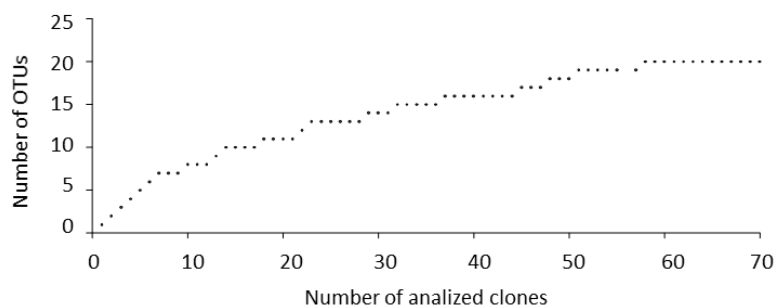


Figure 4.5. Rarefaction curve of the library clone of the consortium 16S rRNA gene.

Table 4.2. Analysis of the 16S rRNA gene sequences detected in the clone library analysis (C) and/or as bands in DGGE profiles (B). Phylotypes in bold were later recovered as isolates (I). Sequences obtained from clones, bands or isolates were grouped as single phylotype when presented 100% similarity.

Phylotype	Detected as	Freq (%)	Length (bp)	Prob (%) ^a	RDP classification ^b
S1	C,B,I	1	1278	99	<i>Sphingomonas</i> (α) (<i>Sphingomonadaceae</i>, 100%)
S2	C,B	13	1313	100	<i>Sphingobium</i> (α)
S3	C,B,I	9	1319	100	<i>Sphingobium</i> (α)
S4	C,B,I	4	1314	100	<i>Azospirillum</i> (α)
S5	C	1	1302	100	<i>Azospirillum</i> (α)
S6	C,I	1	1317	100	<i>Bradyrhizobium</i> (α)
S7	C	1	1317	100	<i>Rhodoplanes</i> (α)
S8	C,B,I	4	1387	100	<i>Achromobacter</i> (β)
S9	C,B,I	3	1407	100	<i>Pseudomonas</i> (γ)
S10	B		385	87	<i>Pseudomonas</i> (γ) (<i>Pseudomonadaceae</i> , 100%)
S11	C	1	1322	67	<i>Pseudomonas</i> (γ) (<i>Pseudomonadaceae</i> , 100%)
S12	C	3	1375	100	<i>Pseudoxanthomonas</i> (γ)
S13	C	1	1235	100	<i>Pseudoxanthomonas</i> (γ)
S14	C	1	1431	93	<i>Pseudoxanthomonas</i> (γ) (<i>Xanthomonadaceae</i> , 100%)
S15	C	1	1417	100	<i>Steroidobacter</i> (γ)
S16	C	1	961	100	<i>Steroidobacter</i> (γ)
S17	C,B	9	1360	37	<i>Thiohalobacter</i> (γ) (<i>Gammaproteobacteria</i> , 100%)
S18	C,B	14	1374	36	<i>Thiohalobacter</i> (γ) (<i>Gammaproteobacteria</i> , 100%)
S19	C	6	1360	47	<i>Thiohalobacter</i> (γ) (<i>Gammaproteobacteria</i> , 100%)
S20	C	3	1350	46	<i>Thiopfundum</i> (γ) (<i>Gammaproteobacteria</i> , 100%)
S21	C,I	19	1348	100	<i>Terrimonas</i> (CFB)
S22	B,I		1331	100	<i>Mycobacterium</i> (<i>Actinobacteria</i>)
S23	B,I		1335	100	<i>Mycobacterium</i> (<i>Actinobacteria</i>)

^a Probability calculated according to Wang et al 2007.

^b When genus assignment has a probability lower than 100%, the immediate higher taxon with a 100% probability is shown in brackets.

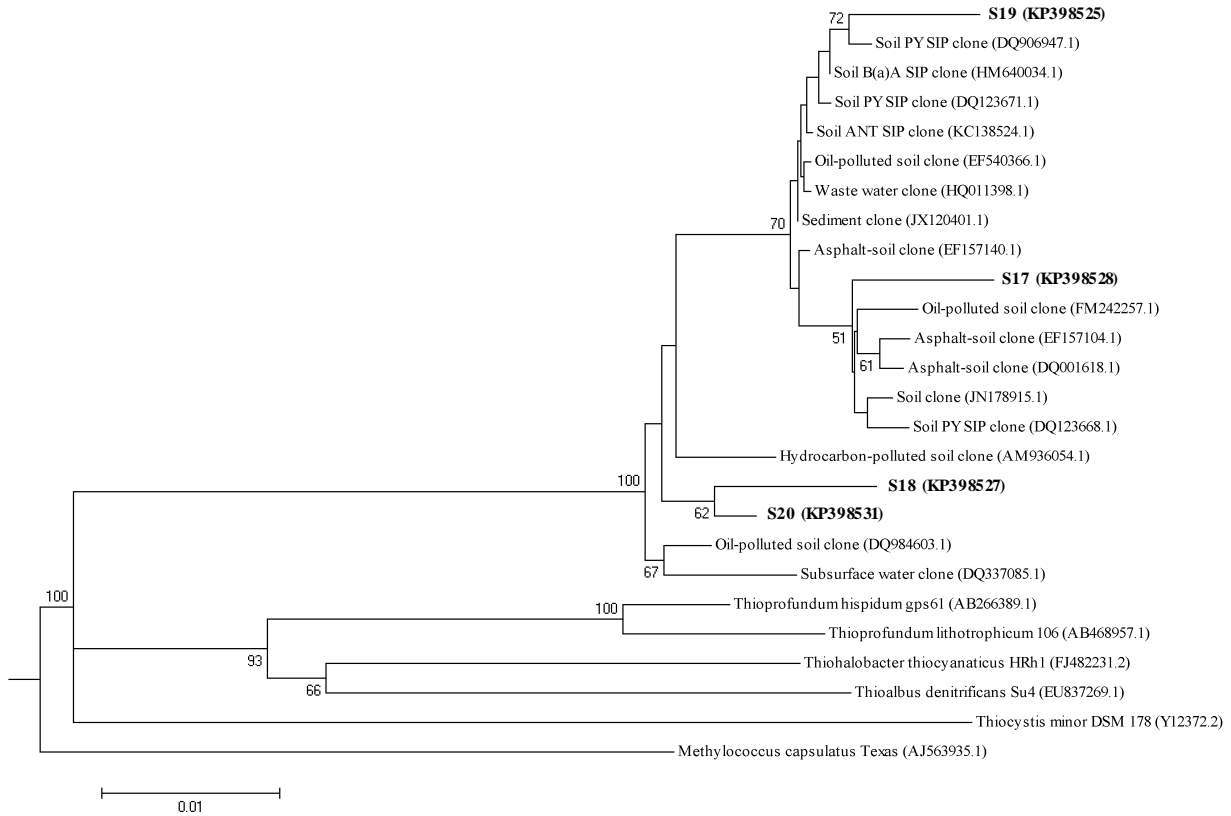


Figure 4.6. Phylogenetic tree of representative partial 16S rRNA gene sequences from OTUs corresponding to the unclassified Gammaproteobacteria detected in the microbial consortium UBHP (S17, S18, S19 and S20) and selected reference sequences. The included reference sequences correspond to the most closely related 5 unclassified bacteria and 5 bacterial type strains in the RDP database. The position of the phylotypes detected in this work and their corresponding GeneBank accession numbers, in brackets, are shown in bold. Bootstrap values >50% are shown in nodes.

4.2.4 Functional screening of consortium UBHP by RHD gene amplification

A PAH-RHD gene-targeted PCR amplification of the total DNA from consortium UBHP using the primer sets described by Cébron et al. (2008), produced positive amplifications for both, GN and GP RHDs. Sequence analysis of the corresponding clone libraries revealed five different unique sequences (100% identity) for each gene. The five GN RHD sequences detected presented a 95-99% sequence similarity to each other, and were closely related (94.4-97.6%) to the *nahAc* gene encoding for the naphthalene dioxygenase iron sulfur domain of *Pseudomonas balearica* LS401 (AF306420) and *Pseudomonas stutzeri* AN11 (AF306419), that cluster within the *Pseudomonas stutzeri* AN10 subgroup (Ferrero et al. 2002). The five distinct GP RHD sequences also presented a high similarity

(96.6-99.6%) and clustered with the *NidA3* gene of a number of well-known pyrene-degrading strains (DeBruyn et al. 2012; Vila et al. 2001), including that of *Mycobacterium vanbaalenii* PYR-1 (DQ028634.1) (97.5-99.6% sequence similarity) that, despite its relaxed specificity towards aromatic compounds, presents the highest conversion rates for FT (Kweon et al. 2010). Therefore, although these primer pairs have been designed to target a number of GN (e.g. *phnAc*, *nagAc*, *ndoB*, *pahA3* or *bphAc*) and GP RHD gene families (e.g. *narAa*, *phdA/pdoA2*, *nidA/pdoA1*, *nidA3/fadA1*) (Cébron et al., 2008), only one type of gene was detected from each amplification.

In an attempt to increase the coverage, an additional RHD gene screening was performed using the primer sets recommended by Iwai et al. (2011), however, in spite of the variety of conditions tested, all the amplifications resulted unproductive.

4.2.5 Selective detection of actinobacterial populations in consortium UBHP

Although the microbial community analysis had revealed a predominance of *Proteobacteria* and *CFB*, the metabolomic profiles, with a major presence of mycobacterial PY and FT metabolites, together with the detection of the *NidA3* RHD genes in the functional screening, suggested that actinobacteria might play a key role in PAH biodegradation. A nested 16S rRNA gene PCR amplification followed by DGGE analysis using *Actinobacteria* specific primers produced two bands with sequences corresponding to two different *Mycobacterium* phlotypes (S22, S23). Additional quantitative evidence was obtained from the 16S rRNA gene PCR-DGGE analysis of the most diluted wells with positive growth of the MPN counts for FT and PY degraders in consortium UBHP. The *Mycobacterium* phlotypes S22 and S23, were present in all cases, thus indicating that the members of this genus were within the most abundant FT and PY degrading bacteria in the consortium ($> 10^7$ MPN·mL⁻¹) (results not shown).

4.2.6 Microbial community shifts in response to exposure to single PAHs

To link the detected phlotypes with specific PAH biodegradation capabilities, consortium UBHP was incubated in mineral medium with each of the major components of the HMW PAH-mixture supplied as single substrates. All of these cultures, except those with BaPY, showed significant ($p < 0.05$) biodegradation in respect to uninoculated controls: PHE 96.4±0.2%, FT 94.0±1.4%, PY 91.7±1.7%, BaA 72.4±1.0% and CHY 28.1±3.7%. However, significant growth was only confirmed for PHE, FT, PY, and BaA, with a cell protein increase of at least 3 folds in respect to controls without carbon source in all cases (results not shown). The different subcultures showed distinctive DGGE profiles when compared with those of consortium UBHP growing on the HMW PAH residue (Figure 4.7A). Correspondence analysis (CA) of the DGGE fingerprints indicated that the banding patterns of the cultures with FT and PY were the most divergent in respect to that of UBHP (Figure 4.7B). In the presence of FT, the increase in the intensity of bands corresponding

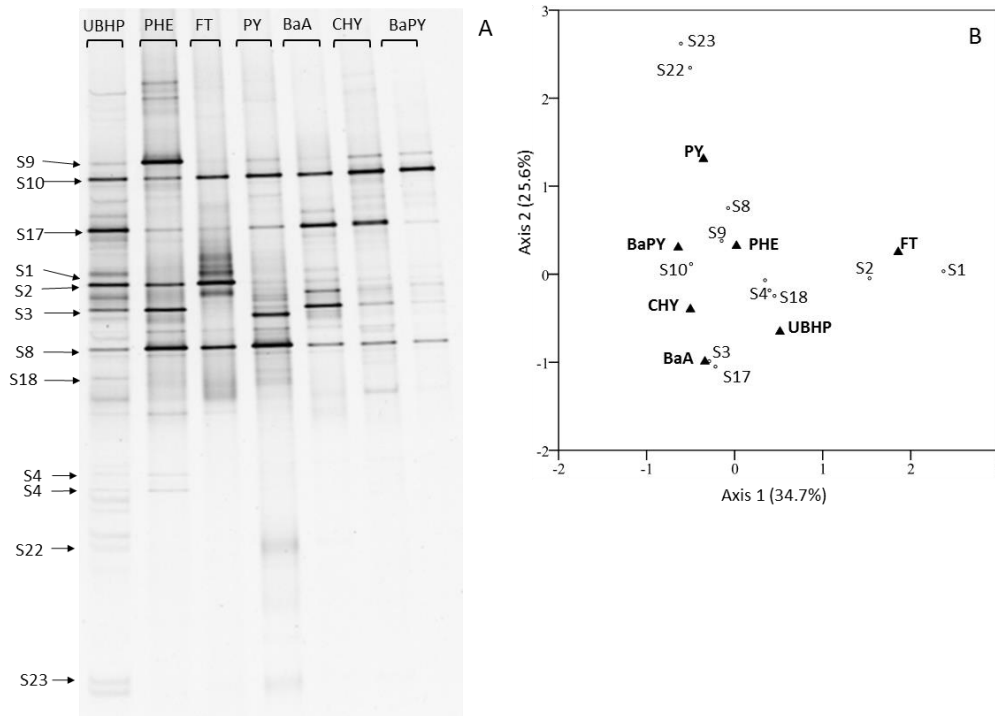


Figure 4.7. DGGE profiles of PCR-amplified 16S rRNA gene fragments from the incubation of the consortium UBHP in mineral medium with single PAHs as sole carbon source (A). Major bands were excised, sequenced and, with a few exceptions, assigned to previously observed phylotypes (100% sequence similarity). Previously, their intensity at each lane was quantified for further correspondence analysis (B). The first two axes of the corresponding biplot explained 60.3% of the overall variance observed. Dark triangles depict the distribution of the UBHP microbial consortium used as inoculum (UBHP) and of the cultures with each of the single PAHs (PHE, FT, PY, BaA, CHY and BaPY). Open circles indicate the distribution of the 12 bands identified.

to members of sphingomonads (*Sphingobium*, phylotype S2; and *Sphingomonas*, S1), suggested their main role in FT biodegradation. Conversely, sphingomonads did not seem to positively respond to exposure to PY, where an increased intensity of phylotype S8 (*Achromobacter*), and the appearance of two bands related to *Mycobacterium* (S22 and S23) were observed. In fact, those new bands comigrated with two minor bands in the total UBHP community profiles that had escaped the initial band sequencing.

In cultures with PHE the major bands detected were those of *Sphingobium* (S3, 9%), *Achromobacter* (S8, 16%), and *Pseudomonas* (S9, 23%). In fact, *Pseudomonas* S9, the predominant band in this profile, showed a low intensity in the rest of the cultures (2-7%), which clearly linked this phylotype with the utilization of PHE. Lastly, in the BaA cultures the distribution in the CA was associated with that of phylotypes S17 (an uncultured Gammaproteobacteria related with pyrene group 2), *Sphingobium* (S3), and *Pseudomonas* (S10). Interestingly, a highly similar profile was observed in the cultures with CHY that, as previously shown, was removed from the HMW PAH mixture with almost identical biodegradation kinetics and extension than BaA.

The analysis of culture fluids definitively associated the metabolites previously identified during the biodegradation of the HMW PAH residue by consortium UBHP with their parent substrates. PY cultures accumulated the typical mycobacterial metabolites II, III, and V; fluoranthene cultures accumulated metabolite IV; and cultures with BaA accumulated metabolite I, thus indicating that this naphthalene dicarboxylic acid, corresponded to a non-previously identified metabolite from the degradation of this PAH. According with the chemical structure of BaA and the general pathways for PAH biodegradation, this compound could be either naphthalene 1,2-dicarboxylic or naphthalene 2,3-dicarboxylic acid.

4.2.7 Retrieval and characterization of the UBHP bacterial phylotypes as pure cultures

An extensive isolation approach using 12 different combinations of mineral and soil extract agar media with a series of PAH substrates produced a total of 129 isolates that grouped in 40 different colony morphologies. The 16S rRNA gene sequencing revealed 17 different sequences from which one representative isolate was selected for further work (Table 4.3). The MM with PAHs was far more efficient in diversity recovery than LB 1/100, and, in general, presented higher efficiency than soil extract with PAHs. The only exception was phylotype S21, *Terrimonas*, only recovered in soil extract medium with CHY.

Some of the most abundant phylotypes detected by molecular analysis, including *Sphingobium* S2 and S3, and the not-yet cultured *Gammaproteobacteria* S17, S18, and S19, were not retrieved in those media. In a molecular-directed attempt to selectively recover the members of *Sphingobium*, we supplemented PHE solid mineral medium with streptomycin, which produced an isolate with 16S rRNA gene sequence identical to phylotype S3, which had been related with PHE, BaA and CHY utilization. With S3, a total of 9 of the phylotypes identified in the molecular analysis were retrieved as pure cultures, 7 presented 16S rRNA gene sequences identical to clones S1, S3, S4, S6, S8, S9 and S21 (42% of the total abundance in the clone library), and two corresponded to members of *Mycobacterium*. The analysis of the almost complete 16S rRNA gene sequence of the latter unequivocally associated them to the mycobacteria detected first in the *Actinobacteria*-specific analysis and then in the DGGE fingerprint of the PY cultures (S22, S23). These mycobacterial isolates presented high 16S rRNA gene sequence similarity (99%) to two pyrene-degrading *Mycobacterium gilvum* strains, CP1 and CP2, isolated in a previous work from a near site (López et al. 2005), and to *Mycobacterium gilvum* strain AP1 (Vila et al. 2001).

Incubation of each isolate with the creosote-HMW PAH residue using the sand-in-liquid system developed for consortium UBHP, revealed the capacity of *Sphingobium* sp. strain

Table 4.3. Identification of the bacterial strains recovered from consortium UBHP and their action as pure cultures on the components of the creosote-HMW PAH residue in mineral medium. Isolates were assigned to phylotypes previously detected in the molecular analysis only when presented a 100% sequence similarity (in bold).

Phylotype /Strain	Length (bp)	Prob (%) ^a	RDP classification ^b	Isolation medium ^c	PAH removal ^d
S1	1278	99	<i>Sphingomonas</i> (α) (<i>Sphingomonadaceae</i>)	CHY MM	-
S3	1319	100	<i>Sphingobium</i> (α)	PHE ^{Str} MM	PHE, ant, FT, PY, chy
S4	1314	100	<i>Azospirillum</i> (α)	PY MM	phe, ant, ft, py
S6	1317	100	<i>Bradyrhizobium</i> (α)	HMW SEM	phe, ft
S24	1287	100	<i>Mesorhizobium</i> (α)	FT MM	-
S25	1261	100	<i>Bosea</i> (α)	FT SEM	phe, ft, chy
S26	1314	100	<i>Methylobacterium</i> (α)	PY MM	phe, ant
S27	1311	100	<i>Chelatococcus</i> (α)	B(a)A MM	ant
S28	1314	52	<i>Rhodoplanes</i> (α)	CHY SEM	ant, ft py
S29	1304	100	<i>Pseudolabrys</i> (α)	B(a)A MM	phe, ant, ft py
S8	1387	100	<i>Achromobacter</i> (β)	PY SEM	PHE, ant, FT, PY, chy
S9	1407	100	<i>Pseudomonas</i> (γ)	CHY MM	ant, ft, py
S30	1302	100	<i>Luteimonas</i> (γ)	PY SEM	phe, ant, ft, py
S21	1348	100	<i>Terrimonas</i> (CFB)	CHY SEM	-
S31	1305	100	<i>Olivibacter</i> (CFB)	HMW MM	-
S22	1331	100	<i>Mycobacterium</i> (<i>Actinobacteria</i>)	PY MM	PHE, ant, FT, PY, cry
S23	1335	100	<i>Mycobacterium</i> (<i>Actinobacteria</i>)	FT MM	PHE, ant, FT, PY, cry

^a Probability calculated according to Wang et al 2007.

^b When genus assignation has a probability lower than 100%, the immediate higher taxon with a 100% probability is shown in brackets.

^c MM, mineral medium, SEM, soil extract, HMW SE or MM medium with creosote-HMW PAH residue as carbon source, MM PHE^{Str} mineral medium with phenanthrene and streptomycin.

^d Listed PAHs were significantly removed in respect to uninoculated controls, capital letters indicate more than 50% removal, lower case letters indicate less than 50%.

S3, *Achromobacter* sp. strain S8, and *Mycobacterium* sp. strains S22 and S23 to extensively attack PHE (93-100%), fluoranthene (91-95%, except for S3 that was 51%) and PY (90-95%), and, in a minor extent other PAHs, in respect to uninoculated controls (Table 4.3). Other strains, including the representatives of phylotypes S4, S6, and S9 had a moderate activity in the HMW PAH mixture, while *Sphingomonas* sp. strain S1 and the abundant *Terrimonas* sp. strain S21, did not show activity towards PAHs in those conditions. It is important to notice that, given the size of the inocula used in these biodegradation assays, this does not necessarily imply the capacity of these strains to grow on the HMW PAHs as pure cultures.

Amplification of total DNA from each isolate with the RHD primers for GP and GN bacteria only produced positive results with the two *Mycobacterium* strains. Sequence analysis of the respective clone libraries obtained from amplification products of strains S22 and 23

identified 2 and 4 unique RHD-GP gene sequences in each isolate. Interestingly, the two most abundant sequences from each library (7/8 and 4/8, respectively) had identical sequences to that of two RHD-GP genes detected in the microbial consortium DNA extracts, unequivocally linking those genes with the recovered phylotypes, and providing evidences of their functional role within the community. As mentioned during the functional screening of the consortium, both sequences presented their maximum similarity (100 and 98%, respectively) with *NidA3* genes from different *Mycobacterium* strains. Apart from those, additional RHD gene sequences were detected in both strains. Phylotype S23 presented two additional copies of RHD genes closely related to *NidA3* of *Mycobacterium*, with similarities between the paralogs ranging from 99 to 99.5%. The last sequences from each library, showed the higher similarities (99 and 93%, respectively) to *PdoA2* genes of *Mycobacterium* strains such as PYR-GK, 6PY1, SPyr or CH1. A recent study using a mutant strain of *Mycobacterium vanbaalenii* PYR-1 defective in *PdoA2* genes, revealed the substrate preference of this dioxygenase for LMW PAHs (Kweon et al., 2014).

4.3 Discussion

Knowledge on bacterial metabolism of PAHs is mostly based on the actions of pure isolates on single compounds (Kanaly & Harayama, 2010) or environmental mixtures (López et al. 2008; Vila & Grifoll 2009). Now, molecular based studies offer a systems biology approach to unravel the complex biodegradation networks that drive PAH removal in the environment (Vila et al., 2015). These studies have confirmed the environmental role of some taxa previously described and extensively characterized in pure cultures (Leys et al. 2004; Leys et al. 2005a; Leys et al. 2005b), but have also suggested the involvement of a higher diversity of microorganisms whose specific function is only indirectly inferred (Kostka et al., 2011; Lladó et al. 2013; Viñas et al. 2005). The enrichment system presented here, inoculated with soil from a historical creosote polluted site, served to obtain a simplified microbial community that extensively degraded 3-, 4- and 5-ring PAHs in conditions that mimic those found in the environment, where those compounds are part of a weathered NAPL adsorbed to a solid phase that is attacked by complexly interacting populations. The composition of this community has been determined through a combined culture dependent/independent approach, making available as pure cultures some of the most relevant components for further fundamental studies and biotechnological applications. Moreover, the actual relevance of the identified taxa in soil PAH removal has been confirmed by their selective assessment in the original creosote polluted soil and in the same soil after a stimulated PAH biodegradation process.

Consortium UBHP also degraded PHE, FT, PY and BaA when supplied as single substrates (72-96%), growing at their expense. CHY was significantly depleted (22%) but did not produce significant growth, while benzo(a)pyrene was not attacked. This suggests that the degradation of these two PAHs depends on the presence of the other components

either acting as cosubstrates (Jones et al. 2014; Kanaly et al. 2000; Moody et al. 2004) or as a NAPL increasing their bioavailability.

The thorough molecular analysis of consortium UBHP, the shifts in community structure in response to exposure to single PAHs, and the further isolation and strain characterization results, unequivocally linked five genera to the removal of several HMW PAHs by consortium UBHP. Those genera, accounting for one third of the community according to clone library analysis, encompassed 10 different phlotypes, classified as: *Sphingobium* and *Sphingomonas* (23%, *Alphaproteobacteria*), *Achromobacter* (4%, *Betaproteobacteria*), *Pseudomonas* (4%, *Gammaproteobacteria*) and *Mycobacterium* (less than 1.5%, *Actinobacteria*). A second third corresponded to a closely related group of not-yet cultured *Gammaproteobacteria* (32%) that was indirectly associated to PY and BaA degradation. Lastly, a single phlotype of the CFB genus *Terrimonas* (19%) presented identical 16S rRNA gene sequence to an isolate that did not show PAH degradation capabilities.

PHE, FT and PY were the fastest PAHs to be removed showing highly similar kinetics. The notable increase in relative abundance of phlotypes *Sphingobium* S1 and S2 in response to FT and that of *Sphingobium* S3 in the presence of PHE and BaA indicates their gaining of carbon at the expense of those compounds. In addition, the molecular-directed isolation of sphingomonads using PHE-mineral agar with streptomycine, permitted to recover one member of *Sphingobium* with 16S rRNA gene sequence identical to phlotype S3, which unequivocally proved its capability to remove PHE, FT and PY from the HMW PAH residue. All these results are consistent with members of the genus *Sphingobium* playing a main role in the simultaneous oxidation of PHE, FT and PY, the latter possibly by cometabolism, and also cooperating in the later degradation of BaA. This would be in agreement with previous observations describing *Sphingomonadaceae* as a highly versatile group of xenobiotic degraders (Stolz, 2009), including a number of isolates with proven capacity to attack HMW PAHs (Kunihiro et al., 2013; Mueller et al. 1990; Schuler et al. 2009; Sohn et al. 2004). Those isolates have been mainly recovered from PAH polluted soils by their ability to use phenanthrene (Kunihiro et al. 2013; Roy et al. 2012; Schuler et al. 2009) or fluoranthene (Mueller et al., 1990), but not pyrene. In fact, phlotypes S2 (13%) and S3 (9%), are closely related to *Sphingobium* sp. strain PNB (99%), with capacity to degrade monoaromatic hydrocarbons, biphenyl and several PAHs, and to *Sphingobium* sp. strain KK22 (98%), that grows on phenanthrene and transforms benzo(a)anthracene (Khara et al., 2014; Kunihiro et al., 2013).

The only betaproteobacterial phlotype (S8), identified as *Achromobacter* was detected in all the DGGE fingerprints from the single-PAH subcultures, but its relative abundance only increased in response to PHE, FT and PY. In fact, the isolate with identical 16S rRNA gene sequence, extensively removed these three PAHs from the HMW PAH mixture, thus

confirming its collaboration with sphingomonads in the degradation of these three most abundant constituents. Its detection and active contribution to PAH biodegradation is in agreement with recent direct observations from soils using stable isotope probing, where different betaproteobacterial phylotypes have been associated with PAH turnover (Jones et al. 2011), especially during the initial stages of biodegradation (Martin et al. 2012). Members of *Achromobacter* have been related to PAH biodegradation under nutrient stimulated conditions in a creosote polluted soil (Viñas et al., 2005); however, the isolation of PAH-degrading strains belonging to this genus has been scarce (Weissenfels et al. 1990) and their catabolic pathways have been scantily documented (Kohlmeier et al., 2005), even when we consider the emended description of previous members of *Alcaligenes* as members of *Achromobacter* (Yabuuchi et al. 1998). Our isolate shows very slow growth in PAH mineral medium that is strongly enhanced in the presence of yeast extract. This could indicate that its degradation depends on carbon or growth factors supplied by other members of the consortium.

The most abundant class within the UBHP microbial community corresponded to members of *Gammaproteobacteria* (43%), mainly encompassing a number of not-yet cultured phylotypes. A minor phylotype of this class that clearly responded to phenanthrene, S9 (3% in the clone library), presented identical 16S rRNA gene sequence to isolate *Pseudomonas* sp. S9. The moderate attack of this isolate to PHE, ANT, FT, PY and CHY when incubated with the HMW PAH mixture, suggests its role as primary degrader of 3-ring PAHs and the potential cometabolic oxidation of 4-ring compounds. This is consistent with its absence or low prevalence in the remaining single-substrate incubations. *Pseudomonaceae* have been largely associated to LMW PAH degradation, and their metabolic pathways and enzyme systems for NAPH and PHE degradation are widely documented (Peng et al. 2008).

The main gammaproteobacterial phylotypes (S17 and S18), were distantly related from any previously cultured member of this class. Their specific role could not be unequivocally assigned at this time, but S17 was clearly associated to BaA and CHY degradation in single-PAH incubations. Interestingly, this phylotype presented >99% 16S rRNA gene sequence similarity with members of the still uncultured pyrene group 2 of gammaproteobacteria described during a DNA-SIP study of a bioreactor treating PAH-polluted soil from a manufactured gas plant in North Carolina (Singleton et al. 2006). Further SIP experiments demonstrated that members of this group were also the major constituents in the BaA-degrading community in that soil (Jones et al. 2011).

Two actinobacterial phylotypes (S22, S23) not detected in the clone library analysis, were identified as active contributors to PAH biodegradation by consortium UBHP, based on the identification of actinobacterial PY (Vila et al. 2001) and FT (López et al. 2006) signature metabolites, the detection of *NidA* genes closely related to those of the *NidA3B3*

gene cluster of *Mycobacterium vanbaalenii* PYR-1 (Kweon et al. 2011), and the presence of the corresponding DGGE bands in the incubations of consortium UBHP with PY. Furthermore, the molecular analysis of PY- and FT-grown MPN wells demonstrated that those phylotypes were within the most abundant populations able to grow on PY- and FT- as single substrates ($>10^7$ MPN·ml⁻¹). Once again, the detected phylotypes were isolated and their catabolic capacities corroborated. Therefore, it is concluded that mycobacteria are key HMW PAH degraders but when faced to PAH mixtures and mixed natural populations they may be outnumbered by faster growing bacteria probably favored by cometabolic and cooperative interactions in which mycobacteria could also play a role (i.e. either supplying growth factors, partially oxidized PAH metabolites or enhancing substrate bioavailability). Because of their biology they could gain importance in case of bioavailability, nutrient and/or oxygen restrictions. Their low relative abundance compared with members of *Proteobacteria* is consistent with the microbial community composition commonly found in PAH polluted soils (Lladó et al., 2015; Mukherjee et al., 2014). However, it might not correspond to their overall activity in the removal of 4-5 ring components, especially of those showing the slowest kinetics (CHY, Bb+kFT and BaPY), that according to our results, are degraded by the cometabolic cooperation between the different members of the community.

Despite being the most abundant component in the clone library (19%), phylotype S21, identified as *Terrimonas* (*Cytophaga-Flavobacterium-Bacteroides*), could not be associated to PAH degradation. The corresponding isolate, with identical almost complete 16S rRNA gene sequence, did not attack any of the components of the creosote HMW PAH mixture. This suggests that a large population of secondary degraders grazing on carbon made available by true PAH degraders, accompany and possibly favor their actions in nature.

Regarding functional screening for dioxygenase genes, it is important to notice that all the isolates were negative for the RHD screening with the different sets of primers proposed by (Iwai et al., 2011), and only mycobacteria gave positive amplification with those proposed by Cébron et al. (2008). The limited results obtained with the proven PAH degraders and in general, with consortium UBHP cultures, indicate that the available primers are only partially effective in covering the whole PAH RHD diversity, especially those of gram negatives. In fact, the potential great diversity of sequences in nature may preclude the detection of wide groups of RHD by one single analysis. More research is needed to complete and cure the available dioxygenase gene databases and for the design of new specific primers.

CHAPTER 5

PAH biodegradation and metabolite formation during a lab-scale bioremediation of a creosote polluted soil

5 PAH biodegradation and metabolite formation during a lab-scale bioestimulation of a creosote-polluted soil

As previously explained (Chapter 1), creosote is composed by an 85% of PAHs and a 15% of heterocyclic and phenolic compounds. The microbial metabolic pathways and the degrading populations for PAHs degradation have been extensively studied. However, the major part of this research has been addressed with pure cultures (López et al. 2006; Vila & Grifoll 2009) or simplified communities (consortia) (Lafortune et al. 2009; Sun et al. 2010) in batch experiments. Nowadays, the challenge is to apply all the knowledge accumulated from those works to investigate what processes are actually taking place *in situ*, considering the microbial communities as a whole and the interactions between populations and with the environmental complex matrixes.

Polar compounds such as oxy-PAHs and N-PACs, neglected for a long time, have now become a matter of concern. Oxy-PAHs have been found at relatively high concentrations in PAH polluted soils (Lundstedt et al. 2014), they present higher mobility than PAHs (higher water solubility) and possess a demonstrated toxicity. It is also known that oxy-PAHs can be produced *in situ* by photo-, chemical, or microbial oxidation of PAHs (Wilcke et al. 2014). Most of the available works on N-PACs focused on polluted aquifers (Blum et al., 2011), but significant azaarene concentrations have also been found in urban soils and road dust (Bandowe et al. 2014; Wei et al. 2015). The most studied heterocyclic compound is carbazole, which is also the most abundant azaarene in creosote and other coal derivatives (Pasternak et al. 2012; Salam et al. 2014; Singh et al. 2011). Considering the increasing evidences pointing out to their environmental relevance and risk, more research is needed to identify the microorganisms and the processes involved in the potential removal of oxy-PAHs and N-PACs from polluted sites. The gathered knowledge will then permit to incorporate them in risk assessment evaluations and provide the tools to stimulate their biodegradation during the biological treatment of polluted soils.

In this chapter we study in detail the degradation kinetics of the individual components of creosote (PAHs, oxy-PAHs and N-PACs) and the potential accumulation/disappearance of the corresponding metabolites in a real polluted soil incubated in aerobic conditions with or without nutrient addition. Moreover, we monitor the compound specific degrading populations and identify the most abundant in each case.

5.1 Materials and methods

5.1.1 Chemicals

Solvents (organic residue analysis grade) were obtained from J.T. Baker (Deventer, The Netherlands). The 16 EPA PAH standard solution was purchased from Dr. Ehrenstorfer

(PAH-mix 9, Augsburg, Germany). The oxy-PAH/N-PAC reference standard mixture contained the following compounds according to Lundstedt et al. (2014): 1-indanone, 9-fluorenone, anthracene-9,10-dione, 4H-cyclopenta(*def*)phenanthrenone, 2-methylanthracene-9,10-dione, benzo(*a*)fluorenone, 7H-benz(*de*)anthracen-7-one, benz(*a*)anthracene-7,12-dione, naphthacene-5,12-dione, 6H-benzo(*cd*)pyren-6-one, quinoline, benzo(*h*)quinoline, acridine and carbazole. All of them were purchased from Sigma-Aldrich Chemie (Steinheim, Germany) with a purity > 97%.

5.1.2 Soil

The creosote polluted soil used in this study was obtained by combining a heavily polluted soil (silty clay loam) from a historical wood treating facility in southern Spain with a soil (sandy loam) from the Agricultural Experiment Station of the University of Barcelona. Before combining them, both soils were air dried and sieved (2mm mesh). The agricultural soil was then distributed in 1L bottles and subjected to three cycles of autoclave each of 45 min at 121°C in 24 h intervals. The effectiveness of this treatment to eliminate viable microorganisms was corroborated by MPN counts of heterotrophic and PAH-degrading populations (see below). 20 kg of the agricultural soil were combined with 10 kg of soil from the creosote site (2:1 w/w) and the mixture was homogenized in a tumbler mixer for 24 h. The resulting experimental creosote polluted soil (from now on the creosote polluted soil) was thoroughly characterized before using it in the lab-scale bioremediation experiment. Soil texture was determined by Coulter LS 230; total organic carbon (TOC) and nitrogen were measured by organic elemental analysis (OEA); while PO_4^{3-} , NO_3^- , NO_2^- and NH_4^+ content were analyzed by ion exchange HPLC at the Scientific and Technological Center of the University of Barcelona. The PAH, N-PAC and oxy-PAH content was also determined as explained below.

5.1.3 Experimental design

The creosote polluted soil was distributed in three series of triplicate aluminum trays (2.5 kg of soil per tray in a total of 9 trays) to simulate a bioremediation treatment by dynamic biopiles during 5 months. In the first series (treatment **-N**) the water content of the soil was adjusted and maintained at 40% of its WHC. The second series (nutrient treatment, **+N**) was amended with urea and K_2HPO_4 to reach a C:N:P ratio of 300:10:1, taking in to account the C content of the total PAHs and the N and P present as NO_3^- , NO_2^- , NH_4^+ and PO_4^{3-} , and the water content was adjusted in the same manner. The water content was readjusted once a week and then the soil was aerated by manual mixing during 10 minutes. The third series of trays was not treated (control, **CTL**) and was incubated as dry soil. All the trays were covered with aluminum foil and incubated in darkness at room temperature. At 0, 7, 15, 30, 45, 60, 90, 120 and 150 days a 30 g composite sample was taken from each tray. After homogenization, 20 g of the soil sample were stored at -20°C

for chemical analysis, 5 g were placed at -80°C for molecular microbial ecology analyses, and the remaining 5 g were used immediately to inoculate 96-well plates for the MPN counts (see below).

5.1.4 PACs and acidic metabolites analyses

5 g of each sample stored at -20°C were mixed with 5 g of Na₂SO₄ and extracted in a Soxhlet apparatus (dichloromethane:acetone, 2:1) for 6h. The organic extracts were then concentrated and loaded to silica columns to separate two fractions. The first (F1) was eluted with 13 ml of hexane:dichloromethane (80:20) plus 2 ml of pure dichloromethane and contained the PAHs, that were analyzed and quantified by gas chromatography (GC-FID). The second (F2) was eluted with 1 ml of dichloromethane followed by 6 ml of methanol and contained the oxy-PAHs and N-PACs, that were identified by gas chromatography coupled to mass spectrometry (GC-MS).

10 g of soil from the same sample were mixed with 50 ml of water to obtain a soil leachate containing the water-soluble PACs. After shaking for 30 min (200 rpm), the suspended solid phase was removed by filtration (Whatman filters, 125 mm diameter, Maidstone, England). The aqueous phase, containing the acidic metabolites, was then acidified (HCl 5M) to pH 2 and extracted using 10 ml of ethyl acetate for 5 times. All the extracts were dried with Na₂SO₄, concentrated under vacuum to 1 mL, and derivatized with diazomethane previous to GC-MS analysis.

GC analyses were performed on a TRACE GC2000 (Thermo, USA) gas chromatograph (GC-FID) or on an Agilent Technologies 6890N gas chromatograph coupled to a 5975 inert mass spectrometer (GC-MS), as described elsewhere (López et al. 2008). The 16 EPA PAHs were quantified using five point standard calibration curves. BePY was identified by comparison with the NIST database and was quantified using BaPY as standard. In the results section, the concentration of the total PAHs is referred to as \sum 17 PAHs and includes the sum of the concentrations of the 16 EPA PAHs plus that of BePY. Oxy-PAHs and N-PACs were identified by comparison with the reference mixture and quantified selecting their diagnostic ions (molecular ions) from the EI chromatograms in the samples and the oxy-PAH/N-PAC reference standard mixture. Methyl derivatives of the identified N-PACs (methyl-quinolines, dimethyl-quinolines, methyl-acridines/methyl-phenanthridines and methyl-carbazoles) were identified by their molecular ion and quantified using their non-methylated counterparts from the same reference standards. The total concentration of oxy-PAHs and N-PACs (\sum 10 Oxy-PAHs and \sum 7 N-PACs) was calculated as the sum of the concentrations of the individual compounds identified and quantified based on the reference mixture. Other N-PACs and acidic compounds were identified by comparing their spectra to those available at the NIST (match >90%) or our in house databases.

5.1.5 Enumeration of PAH- and Oxy-PAC-degrading populations

Bacterial counts from each of the triplicate soil samples were performed using a miniaturized most probable number (MPN) method in 96-well microtiter plates with 4 replicate wells per dilution (Wrenn & Venosa, 1996). Total heterotrophs were counted in Triptone Soy Broth (TSB) while PAH- and metabolite-degraders were counted in mineral medium (Grifoll et al., 1995) containing the corresponding single substrate at a final concentration of $0.5 \text{ g}\cdot\text{L}^{-1}$. The selected substrates included the PAHs FL, PHE, ANT, FT, PY and BaA ; the Oxy-PAHs 9-fluorenone, anthracene-9,10-dione, and benz(*a*)anthracene-7,12-dione; the acidic metabolites phthalic acid, diphenic acid, and naphthalic anhydride (in equilibrium with its acid 1,8-naphthalene carboxylic acid); and the N-PACs carbazole and acridine. These carbon sources were added to the empty wells dissolved in different organic solvents, and the sterile medium (180 μl) was added after solvent evaporation. MPN plates were incubated at room temperature and darkness during two months and, after recording the positive wells (based on turbidity and/or observable coloration), 100 μl of three of the most diluted positive wells for each carbon source and triplicate were stored at -20°C for molecular analysis.

5.1.6 DNA extraction and PCR amplification

The DNA from the most diluted wells of the MPN counts from the soil with the nutrients treatment was extracted using Power Soil DNA isolation kit (Mobio, Carlsbad, USA). The 16S rRNA gene fragments from those DNA extracts were amplified using pureTaq Ready-To-Go PCR bead tubes (GE healthcare, United Kingdom). 1 μL of DNA extract was used as the template for 25 μL reactions containing 25 pmol of each primer (Sigma-Aldrich, Steinheim, Germany). All the PCR amplifications were performed on an Eppendorf Mastercycler using primers GC40-63F and 518R (El Fantroussi et al., 1999).

5.1.7 DGGE analysis and sequencing

PCR products were run on 6% polyacrylamide gels with denaturing gradients ranging from 45% to 70% (100% denaturant contains 7 M urea and 40% formamide) in the conditions described in Gallego et al. (2013). DGGE bands were processed using Image Lab Version 4.0.1 build 6 image analysis software (Bio-Rad Laboratories). The major bands of each lane were excised and sent to the MacroGen Europe sequencing service (The Netherlands). The resulting DNA sequences were edited and manually aligned using BioEdit (version 7.2.5) and compared with the BLAST alignment tool (<http://blast.ncbi.nlm.nih.gov/Blast.cgi>) and the classifier and tree builder tools of the Ribosomal Database Project II (Wang et al., 2007).

5.1.8 Statistical and multivariate analysis

PAH and N-PAC concentrations and MPN data were analyzed by ANOVA (IBM SPSS statistics 20 software) using a Tukey test at $P < 0.05$.

5.2 Results

5.2.1 Soil

The creosote polluted soil used in this study was a loamy soil (24.8% clay, 36.3% silt, 11.2% very thin sand, 9.2% thin-grained sand, 10.2% medium sand and 8.3% coarse-grained sand) with pH 8.06. Its total carbon content was 7.06%, while organic carbon (TOC) was 5.23%. The total nitrogen was 0.16%, with $105 \text{ mg}\cdot\text{kg}^{-1}$ of NO_3^- and $15 \text{ mg}\cdot\text{kg}^{-1}$ of NH_4^+ . The water holding capacity (WHC) was $0.365 \text{ ml H}_2\text{O}\cdot\text{g}^{-1}$ of dry soil, and the water content after the homogenization was 3.36%.

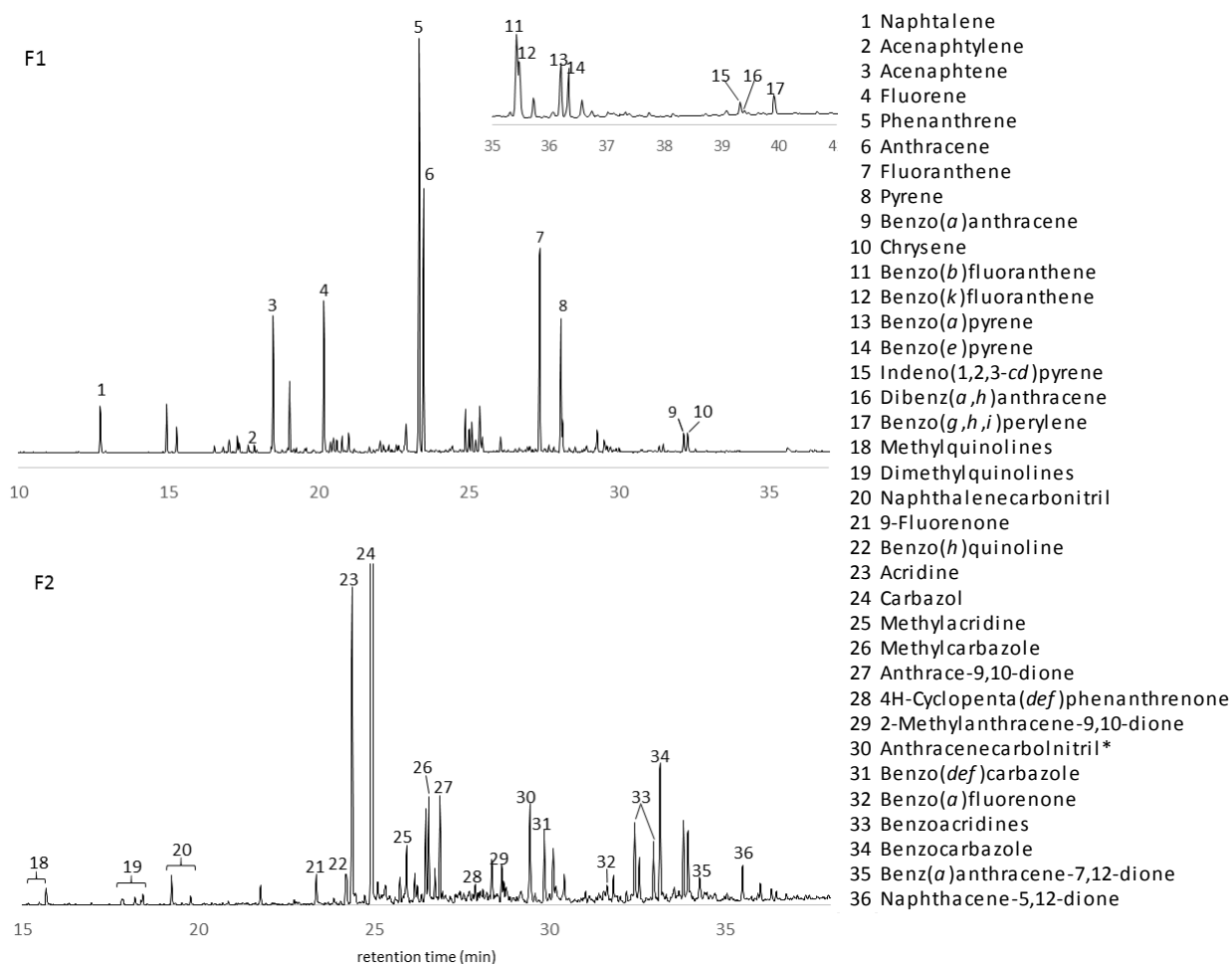


Figure 5.1. GC-FID profile of the PAH fraction (F1) and TIC chromatogram (GC-MS) of the Oxy-PAH/N-PACs fraction (F2) at time 0 days showing the compounds identified and quantified. *Product 30 presented equal match (90%) with anthracenecarbolnitrile, acenaphtopyridine and indenoisoquinoline.

The total PAH content of the soil (Σ 17 PAHs) was of $8,597 \pm 704$ ppm, with PHE ($2,622 \pm 180$ ppm), ANT ($1,387 \pm 356$ ppm) and FT ($1,228 \pm 82$ ppm) as the most abundant compounds (Figure 5.1). N-PACs were found at one lower order of magnitude, with a Σ 7 N-PACs concentration of 856 ± 122 ppm, maintaining a proportion towards PAHs similar to that in commercial creosote. As observed for PAHs, the major N-PACs at the beginning of the experiment were those with 3 rings: carbazole (613 ± 134 ppm) and acridine (113 ± 10 ppm). The Σ 10 Oxy-PAHs was at a concentration of 93 ± 3 ppm, with anthracene-9,10-dione (41 ± 0 ppm) representing almost a half of the total oxy-PAH concentration, followed by naphthalene-5,12-dione (15 ± 1 ppm) and 9-fluorenone (14 ± 0 ppm).

5.2.2 Effects of nutrient addition in PAH removal and PAH-degrading populations

The GC-FID analysis of fraction F1 from the soil organic extracts showed an extensive PAH biodegradation in both, the soil treated with only water content adjustment (-N) and that with nutrient addition (+N) (Figure 5.2, Figure 5.3). The dry control did not show significant changes in PAHs concentration. At the end of the incubation, the treatment without nutrients had caused a reduction of 69% of the Σ 17 PAHs in respect to the control, while the stimulation with nutrients increased this percentage to 93%. A more detailed analysis of the data, grouping the PAHs into LMW (up to 3-rings) and HMW (4 or more rings) indicated that the differences between treatments were mainly associated with the degradation of the HMW compounds. In fact, the comparison of the LMW PAH

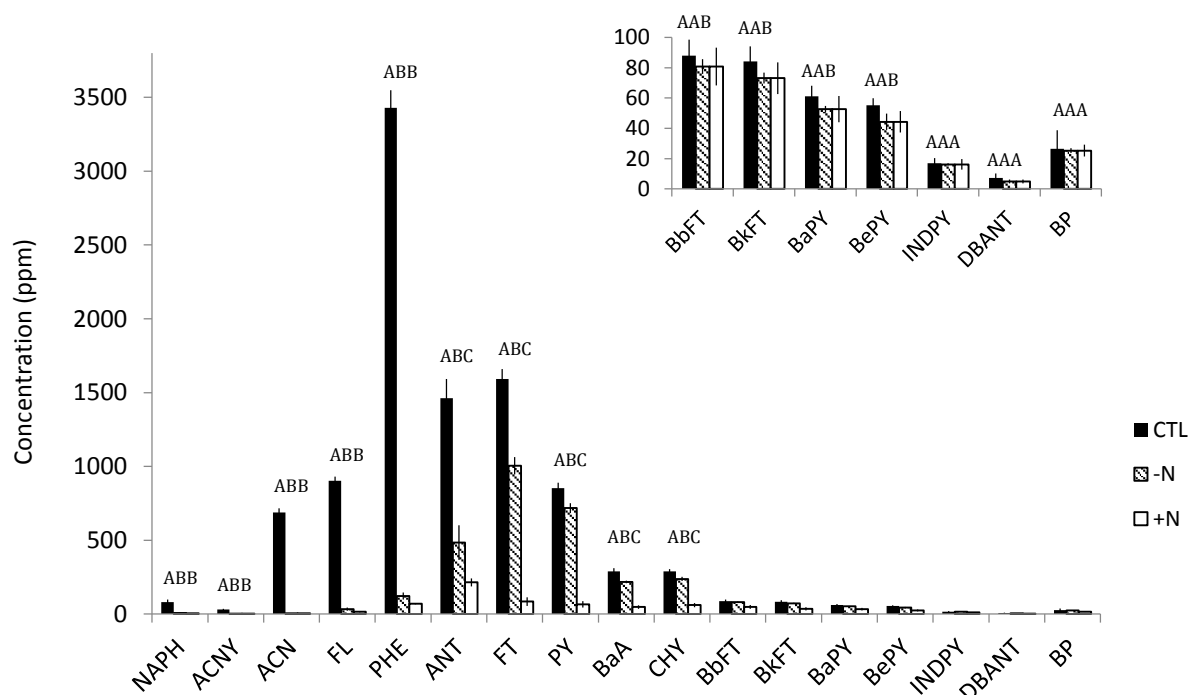


Figure 5.2. End point concentrations of PAHs in the soil after the different treatments (150 days of incubation). Different letters on the top of the bars indicate significant differences between treatments.

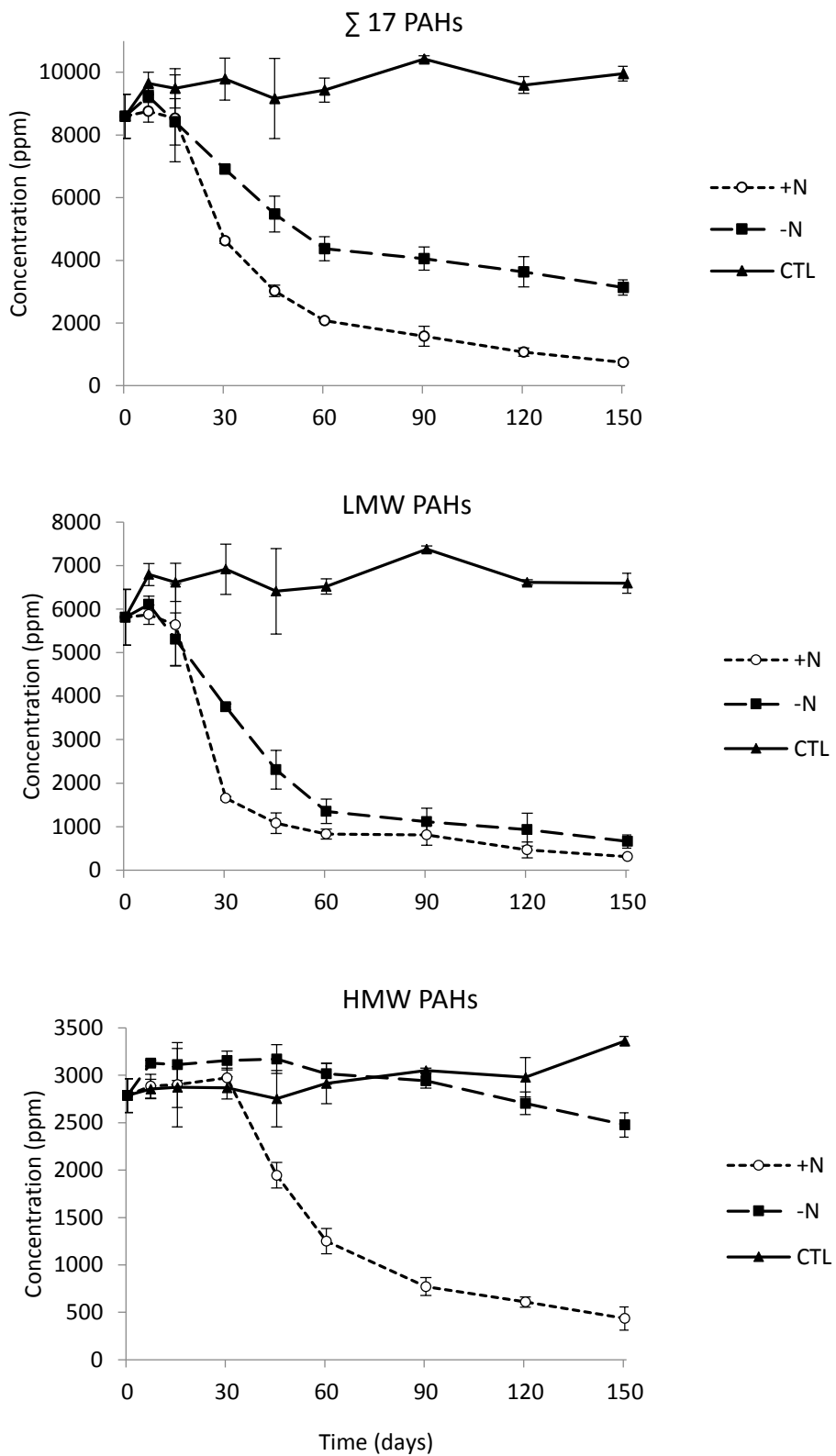


Figure 5.3. Time course biodegradation of Σ 17 PAHs, LMW PAHs and HMW PAHs with (+N) or without (-N) nutrient addition, and in the dry control (CTL).

concentrations throughout the incubation did not show significant differences, with a 95% of final degradation for the nutrient amended soil and a 90% for the soil without nutrients. However, whereas the treatment without nutrients produced a low biodegradation (16-37%) of the 4-ring PAHs and no significant depletion of the 5-ring PAHs, the addition of nutrients resulted in an important attack to both, the 4- (79-95%) and the 5-ring PAHs (44-57%). Neither of the treatments caused a significant disappearance of the 6-ring PAHs indeno(1,2,3-*cd*)pyrene, dibenz(*a,h*)anthracene and benzo(*g,h,i*)perilene. Unexpectedly, the final PAH residue of the soil stimulated with nitrogen and phosphorous was rich in anthracene (215±28 ppm), while in that without nutrients the predominant compounds were fluoranthene (1,004±59 ppm) and pyrene (718±33 ppm).

In both conditions, a clear succession in the removal of LMW PAHs and HMW PAHs was observed (Figure 5.3). With nutrient addition, the biodegradation rates for LMW PAHs reached their maxima between 15 and 30 days (265 mg·kg⁻¹·day⁻¹), while the HMW PAHs were mainly degraded (68 mg·kg⁻¹·day⁻¹) during the second month. Despite achieving similar degradation extents, without nutrient addition the biodegradation rates for LMW PAHs were slower, with maximum rates (104 mg·kg⁻¹·day⁻¹) being observed between 7

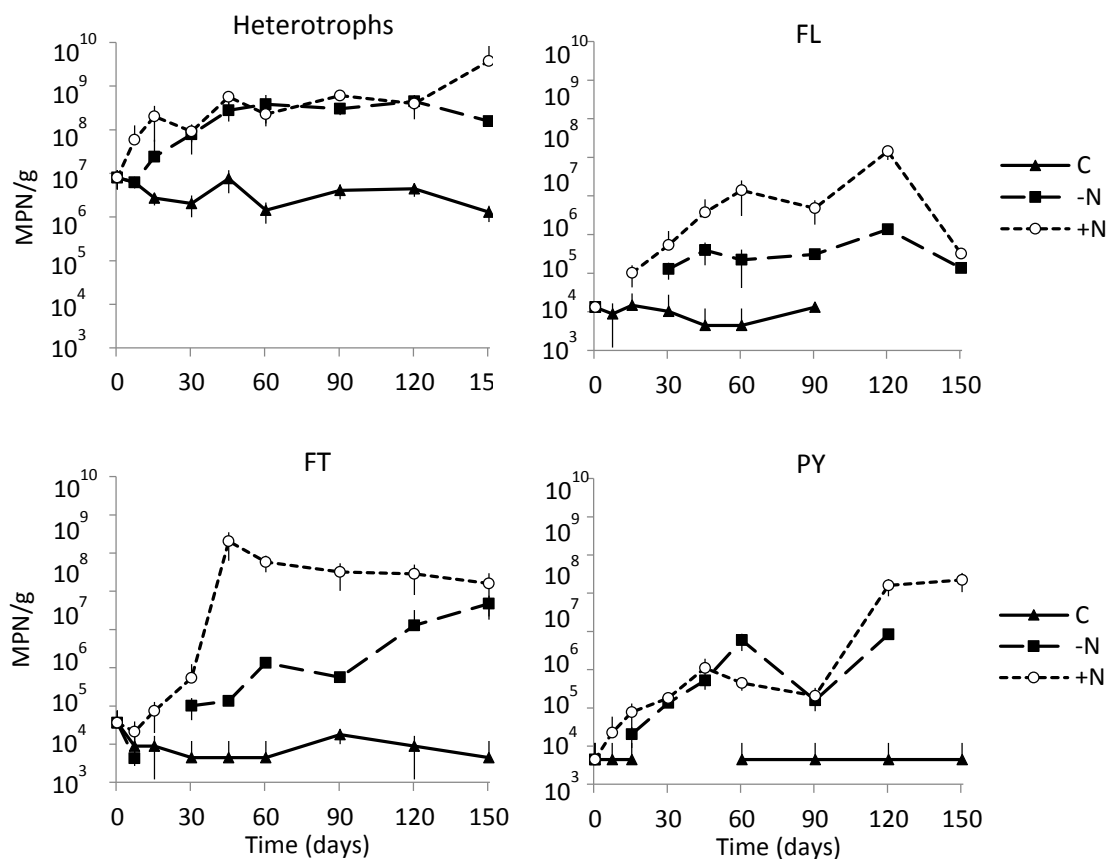


Figure 5.4. Enumeration of heterotrophic and the individual PAH-degrading populations that showed significantly different counts in both treatments (-N and +N) during the incubation time (i.e. FL, FT, and PY degraders).

and 45 days. The HMW PAH degradation started thereafter, presenting linear and very slow decrease kinetics from day 45 until the end of incubation ($8 \text{ mg}\cdot\text{kg}^{-1}\cdot\text{day}^{-1}$).

The results of the enumeration of the heterotrophic and PAH-degrading populations were consistent with those of the PAHs removal. In both treatments there was an important and significant increment of the total heterotrophic populations ($1.6\cdot 10^8$ - $3.7\cdot 10^9 \text{ MPN}\cdot\text{g}^{-1}$ at 150 days) in respect to the control dry soil ($1.3\cdot 10^6 \text{ MPN}\cdot\text{g}^{-1}$ at the end of the incubation). The addition of nutrients increased slightly but significantly the growth of heterotrophs (Figure 5.4) in respect to the soil without nutrients. The counts of PHE, ANT, and BaA degraders increased in both conditions, with no significant differences in terms of the $\text{MPN}\cdot\text{g}^{-1}$, which coincides with an also similar removal of PHE and ANT. In contrast, the populations growing on FL, FT and PY exhibited significant higher concentrations in the nutrient amended soil (Figure 5.4), in accordance to the higher HMW PAH degradation in the nutrients treatment.

5.2.3 PAH biodegradation kinetics in the nutrient treated soil

Once confirmed that the soil treated with nutrients (+N) presented the widest and most extensive attack of the creosote PAHs, we chose this soil to further investigate the kinetics of individual PAH, oxy-PAH and N-PAC degradation and metabolite formation.

As shown in Figure 5.5, there was a sequential biodegradation of the individual PAHs, with depletion rates decreasing with the increase in number of rings. The different PAHs fall into discrete groups with highly similar kinetics. As expected, NAPH was the first to be attacked, with highest depletion rates during the first week ($198 \text{ nmol}\cdot\text{kg}^{-1}\cdot\text{day}^{-1}$) and being almost completely removed at day 15. During the third and fourth week, there was a dramatic removal of the 3-ring PAHs ACNY ($8 \text{ nmol}\cdot\text{kg}^{-1}\cdot\text{day}^{-1}$), ACN ($226 \text{ nmol}\cdot\text{kg}^{-1}\cdot\text{day}^{-1}$), FL ($305 \text{ nmol}\cdot\text{kg}^{-1}\cdot\text{day}^{-1}$) and PHE ($919 \text{ nmol}\cdot\text{kg}^{-1}\cdot\text{day}^{-1}$). At 30 days, when the degradation of the LMW PAHs had attenuated, the removal of the 4-ring PAHs initiated, reaching maximum rates between 30 and 60 days and gradually attenuating thereafter. PY and FT were removed faster (maximum rates at 30-60 days of $239 \text{ nmol}\cdot\text{kg}^{-1}\cdot\text{day}^{-1}$ and $78 \text{ nmol}\cdot\text{kg}^{-1}\cdot\text{day}^{-1}$, respectively), but were closely followed by BaA and CHY, with a softer slope ($28 \text{ nmol}\cdot\text{kg}^{-1}\cdot\text{day}^{-1}$ and $33 \text{ nmol}\cdot\text{kg}^{-1}\cdot\text{day}^{-1}$). Finally, the five ring PAHs BbFT, BkFT, BaP and BeP presented almost identical curves, with a slow but progressive degradation from day 30 to the end of incubation.

Interestingly, ANT exhibited a unique bimodal kinetics, with linear maximum rates between 0-60days ($76 \text{ nmol}\cdot\text{kg}^{-1}\cdot\text{day}^{-1}$), a plateau during the following month, and another linear degradation phase from then until the end of incubation.

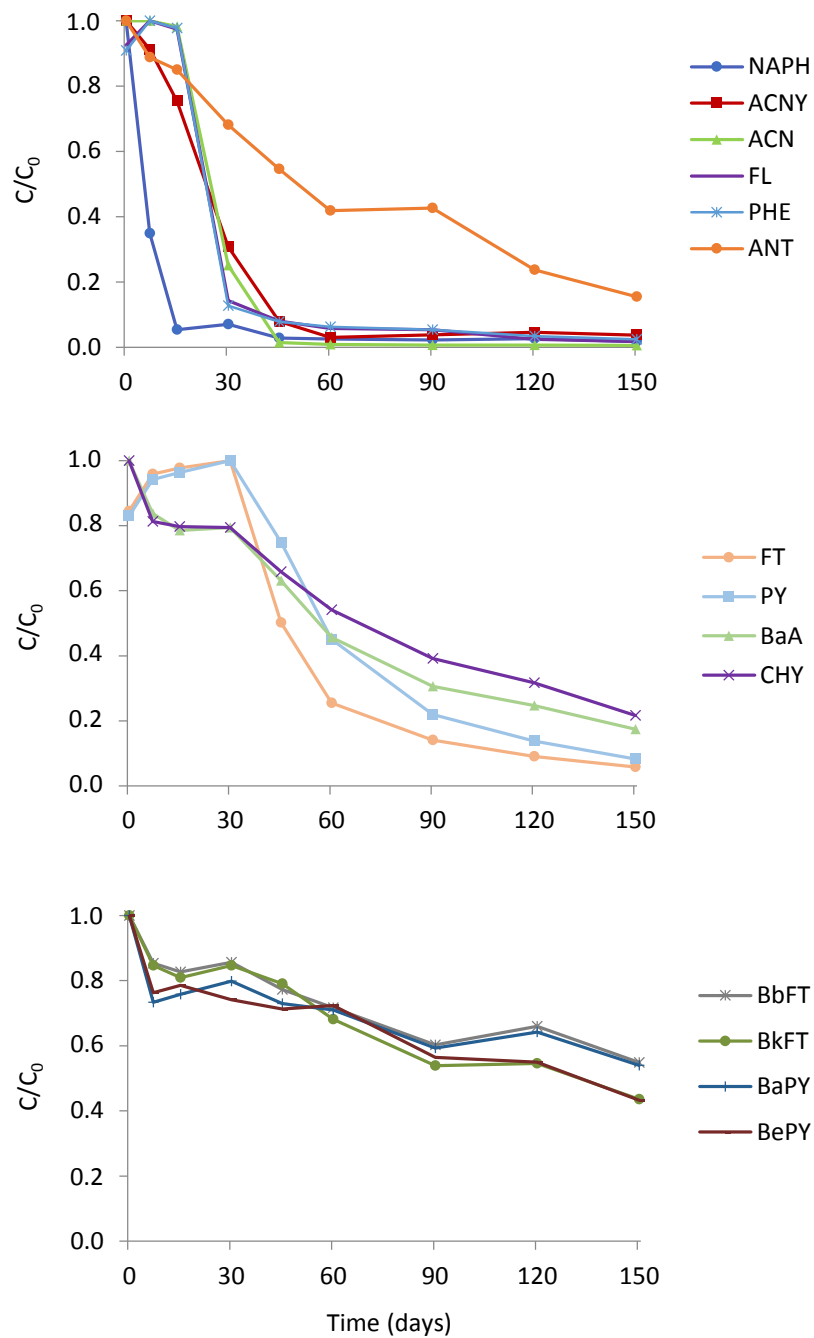


Figure 5.5. Biodegradation kinetics of the PAHs significantly removed in the soil treated with nutrients (+N). Error bars are not represented for clarity. Average absolute concentration and standard deviation values are shown in Table S1 (Annex I).

5.2.4 Evolution of oxy-PAHs during PAH degradation in the nutrient treated soil

As mentioned, creosote contains oxy-PAHs in its commercial formulation, especially aromatic ketones, but these compounds can also be formed in the soil as a result of partial chemical or biological oxidations (Lundstedt et al., 2007). In order to investigate the fate of oxy-PAHs in soils undergoing PAH degradation and the role of the microbial activity in their possible formation and/or degradation, we studied the evolution of the oxy-PAHs in the nutrient treated soil in comparison to that in the dry control.

The GC-MS analysis of fraction F2 from the organic extracts showed that in the initial soil the concentration of the \sum 10 oxy-PAHs (93 ± 3 ppm) was in a proportion of around 1:100 in respect to that of the \sum 17 PAHs. Unexpectedly, in the dry control, that concentration slowly increased along the incubation (491 ± 23 ppm at day 150) to reach a ratio of 1:20 respect the PAHs at the end of the experiment. The 3-ring aromatic ketones 9-fluorenone and 9,10-anthraquinone were the products that experienced higher increases, with final concentrations of 158 ± 7 ppm and 162 ± 7 ppm, respectively, but also 4H-cyclopenta(*def*)phenanthrenone and benzo(*a*)fluorenone underwent substantial linear increments (to 50 ± 2.5 and 63 ± 3.3 ppm, respectively) (Figure 5.6).

The initial evolution of the oxy-PAHs in the nutrients treated soil was similar to that in the control, however after a certain incubation period that varied for each compound, the kinetics diverged. In general, the treated soil showed a transient accumulation of the oxy PAHs that were later degraded.

9-Fluorenone and benzo(*a*)fluorenone were rapidly attacked reaching basal levels at day 30 that remained until the end of the incubation. Anthracene-9,10-dione started to decrease at day 30 until almost disappear at day 60. By contrast, 4H-cyclopenta(*def*)phenanthrenone experienced a fast increase from day 15 to reach a maximum at 45 days with a concentration about 5 times higher (129 ± 5 ppm) than that of the control, this coinciding with the maximum degradation rates for the 3-ring PAHs, FT and PY. Other less abundant oxy-PAHs presented similar evolutions, with a transient peak at some point of the incubation. For example, 2-methylanthracenedione also had a maximum at 30 days to later disappear.

It is interesting to note that the kinetics of 9-fluorenone removal was parallel to that of its parent PAH fluorene, its concentration starting to decrease at day 7 (15 ± 1 ppm) and reaching the asymptotic phase at day 30 (4 ± 0 ppm).

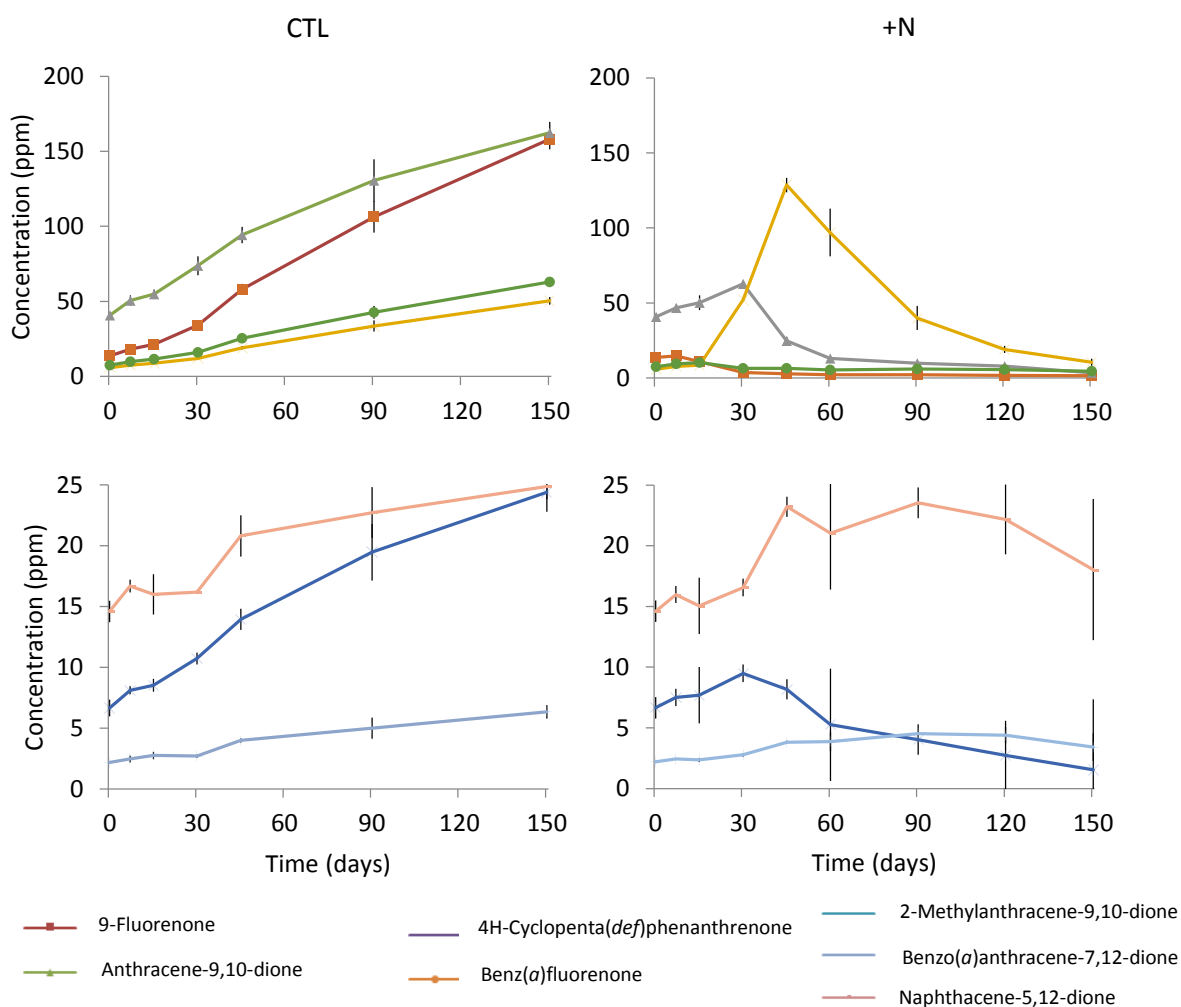


Figure 5.6. Accumulation of oxy-PAHs during the incubation of the control dry soil and the soil treated with nutrients.

5.2.5 Production and accumulation of acidic metabolites during the degradation of PAHs in the soil treated with nutrients

The GC-MS analysis of the acidic extracts from leachates obtained from the nutrient treated soil at the different incubation times revealed the successive and transient accumulation of a number of phenolic and carboxylic aromatic compounds. Figure 5.7 shows typical chromatographic profiles from days 15 and 45, while the identified peaks are listed in Table 5.1. Two major acidic compounds were identified as dehydroabiatic acid (product 49) and 7-oxodehydroabiatic acid (product 52), which are secondary metabolites of plants usually found in soils and are not attributable to PAH degradation.

A first group of acidic metabolites presenting maximum accumulation at 7-15 days (Figure 5.8) were identified as early oxidation products from the LMW PAHs ACN (acenaphthenol, 1,8-naphthalic anhydride/1,8-naphthalene dicarboxylic acid), FL (9-

Table 5.1. Retention times in GC and spectral properties (EI) of the major acidic compounds identified in leachates of the soil treated with nutrients throughout the incubation time. Products were analyzed as methyl ester derivatives.

Product number	Retention time (min)	Product	Fragmentation (m/z)
37	12,9	Salicylic acid ME*	152 ,136,123,121, <u>120</u> ,107,95,92
38	17,9	Phthalic acid DME	194 ,180, <u>163</u> ,148,133,120,104,92,77
39	19,1	1-Naphtenol	145 , <u>144</u> ,116,115,89,72,63
40	21,0	Naphtalenecarboxylic acid (ism1) ME	186 ,182,169,162, <u>155</u> ,127,115,101,77
41	21,3	Naphtalenecarboxylic acid (ism2) ME	186 ,182,167,161, <u>155</u> ,127,115,101,77
42	21,7	1-Acenaphtenol	170 , <u>169</u> ,152,141,115,74,63
43	23,0	9H-Fluoren-9-ol	183 , <u>181</u> ,165,152,126,91,76
44	23,5	3-Hydroxy-2-Naphtalenecarboxylic acid ME	202 ,171, <u>170</u> ,142,114,88,71
45	26,8	1,8-Naphtalenedicarboxylic acid DME ^b	244 ,229, <u>213</u> ,185,170,154
46	27,4	1,8-Naphtalic anhydride	198 , <u>154</u> ,126,87,74,62
47	28,7	<i>cis</i> -4-(2-Hydroxynaphth-3-yl)-2-oxobut-3-enoic DME ^a	270 ,223, <u>211</u> ,180,168,152,139,76
48	30,0	9-Phenanthroic acid ME	237 , <u>236</u> ,205,177,151,88
49	31,0	Dehydroabiestic acid ME	314 ,299,240, <u>239</u> ,197,173,141,129
50	32,8	Z-9-Carboxymethylene-fluorene-1-carboxylic acid DME ^b	308 ,275,232, <u>217</u> ,205,189
51	33,0	6,6'-Dihydroxy-2,2'-biphenyldicarboxylic acid DME ^b	300 ,269, <u>241</u> ,226
52	33,8	7-Oxodehydroabiestic acid ME	328 ,313,296,281,269, <u>253</u> ,213,187

^a Temptatively identified by comparison to literature data

^b Identified by comparison to inhouse database

* ME, methyl ester, DME, dimethylester

fluorenol) and methyl NAPH (naphthalene carboxylic acid isomers). Interestingly, all these products are formed by the monooxygenation of methylenic and methylic groups, a reaction that has been demonstrated for ring hydroxylating dioxygenases acting fortuitously (Grifoll et al. 1994). At this early stage, we also detected small amounts of the common intermediates in PAH degradation salicylic acid and phthalic acid (Figure 5.8). The second group was mainly detected at day 30, including a product resulting from the degradation of one of the rings of ANT (3-hydroxy-2-naphthalene carboxylic acid), a carboxylic acid from the oxidation of either 1-, 2-, 3- or 9-methyl PHE (phenanthrene carboxylic acid), and a phenolic derivative of NAPH (naphthenol). Two characteristic ring-cleavage metabolites from the 4-ring PAHs PY (6,6'-dihydroxy-2,2'-biphenyl dicarboxylic acid, 51) and FT (Z-9-carboxymethylene-fluorene-1-carboxylic acid, 50) accumulated between 30 and 90 days. Notably, those acids have only been identified as metabolites in the degradation of those PAHs by pure cultures of mycobacteria, and their further degradation has not been demonstrated in the studied strains (López et al. 2006). Finally, there is one acidic metabolite that accumulates over a long period of time (15-90 days) and, based on literature data (Van Herwijnen et al., 2003) and previous results from our group, has been presumptively identified as a *meta*-cleavage product of anthracene.

It is important to note that at later incubation times the presence of unknown products with higher molecular weights increased. In fact, at the end of the incubation there was a group of HMW unidentified compounds (data not shown), probably originated from the biodegradation of 5- and 6-ring PAHs.

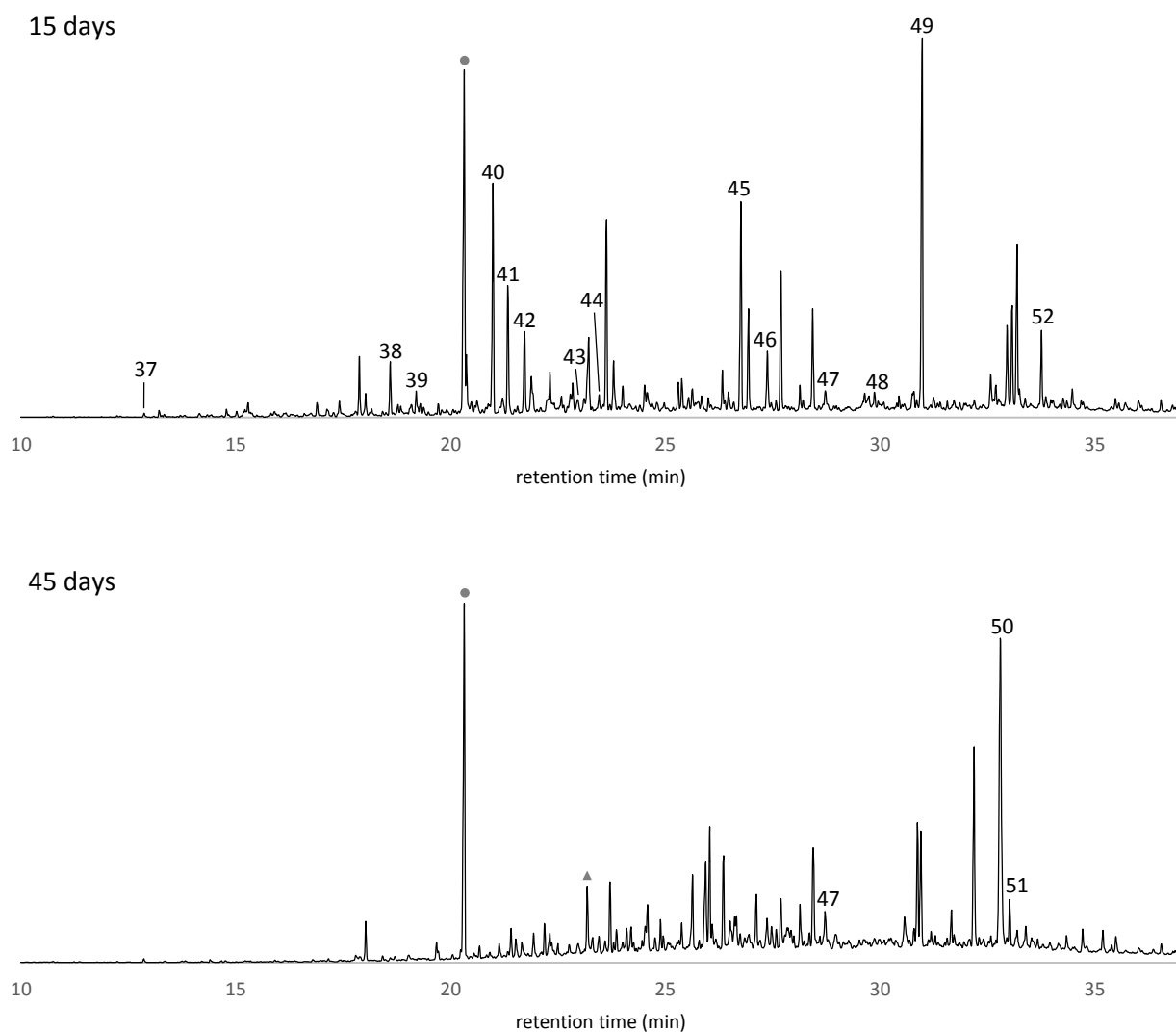


Figure 5.7. GC-MS chromatograms of the methylated acidic extracts from one of the triplicate samples at day 15 and day 45. The identity of the peaks is indicated in Table 5.1. Circles indicate dimethyl phthalate and triangle, parental compound.

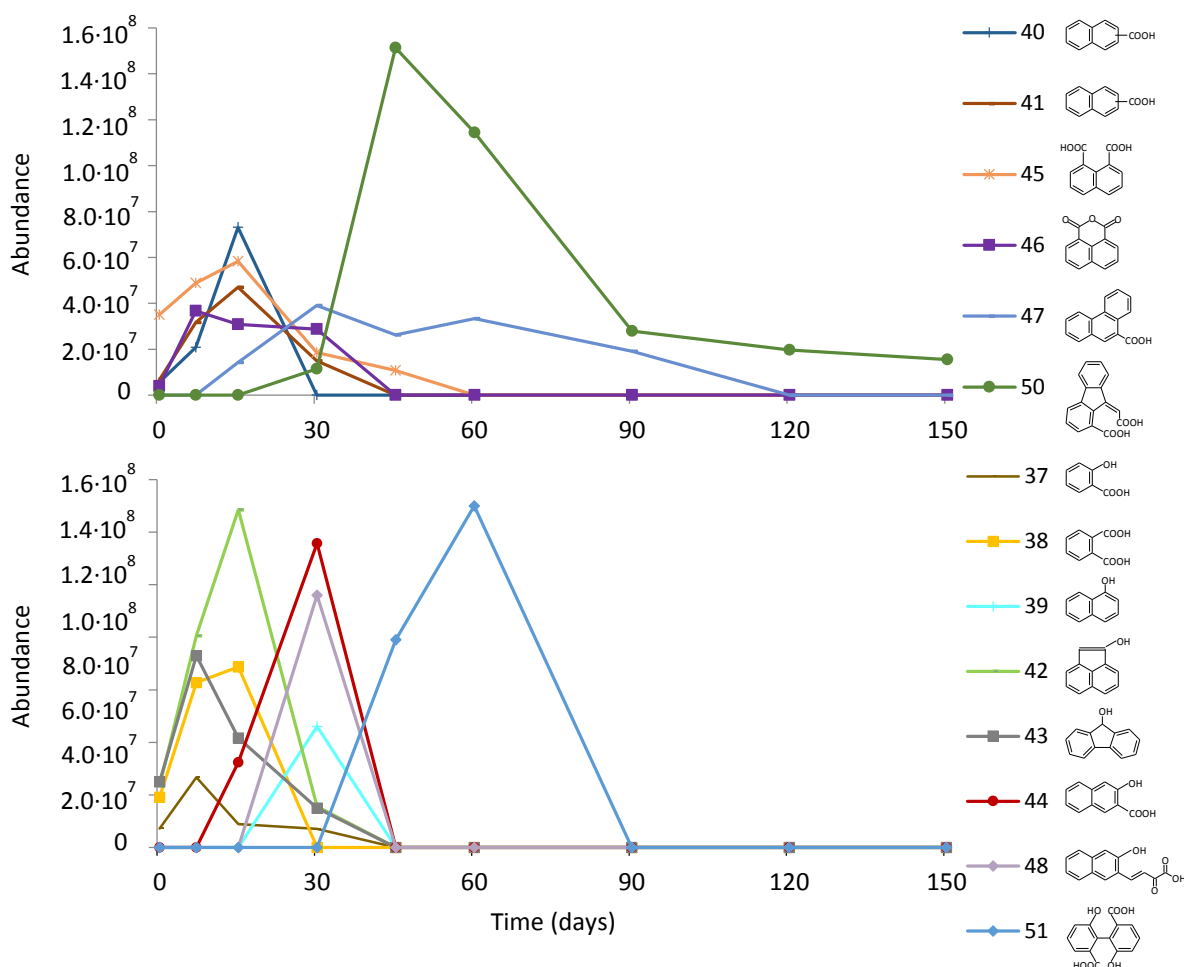


Figure 5.8. Time course evolution of the identified acidic metabolites along the incubation. Abundance is shown as GC-MS peak areas. The chemical structure for each metabolite is provided, and their identity and spectral characteristics are shown in Table 5.1.

5.2.6 N-PAC biodegradation kinetics

As expected, the azaarenes were recovered in fraction F2 of the organic extracts (together with the oxy-PAHs) and some of them presented concentrations in the same order of magnitude than the PAHs (Figure 5.1). The overall concentration of the $\Sigma 7$ N-PACs was of 856 ± 122 ppm, about ten times lower than that of the $\Sigma 17$ PAHs, with the most concentrated components being carbazole (613 ± 137 ppm) and acridine (113 ± 10 ppm). The stimulation with nutrients resulted in an 85% degradation of the $\Sigma 7$ N-PACs at the end of incubation (Figure 5.9), a percentage slightly lower than that obtained for the $\Sigma 17$ PAHs (93%). Thus, the end-point residue was enriched N-PACs if compared with the starting soil. In the dry control there was no significant decrease in the concentration.

Figure 5.10 shows the kinetics of degradation for each of the 7 quantified N-PACs. In all cases, the methyl and dimethyl derivatives were removed simultaneously with their non-alkylated analogues. Carbazole, with the heteroatom in a center five-membered ring, presented bimodal degradation kinetics, with a rapid disappearance phase during the first 15 days ($142 \text{ nmol}\cdot\text{kg}^{-1}\cdot\text{day}^{-1}$ the first week) to reach about 50% of degradation, that strongly attenuated thereafter and came to a stop between 60-90 days. However, after this time, the degradation of this compound resumed progressing until the end of the incubation (until 85% of degradation). Methylcarbazole followed a similar kinetics ($21 \text{ nmol}\cdot\text{kg}^{-1}\cdot\text{day}^{-1}$ the first week). The degradation of the rest of the heterocycles, containing the N atom in one of the aromatic rings, followed a succession consistent with their increasing number of rings and/or methyl groups. The 2-ring N-PAC monomethylquinoline presented maximum degradation rates during the first month ($3 \text{ nmol}\cdot\text{kg}^{-1}\cdot\text{day}^{-1}$), dimethylquinolines between 15 and 45 days ($3 \text{ nmol}\cdot\text{kg}^{-1}\cdot\text{day}^{-1}$), while acridine and methylacridine were not attacked until day 45 ($21 \text{ nmol}\cdot\text{kg}^{-1}\cdot\text{day}^{-1}$ and $5 \text{ nmol}\cdot\text{kg}^{-1}\cdot\text{day}^{-1}$ 45-60 days, respectively). The degradation of benzo(*h*)quinoline presented a high variability between replicates.

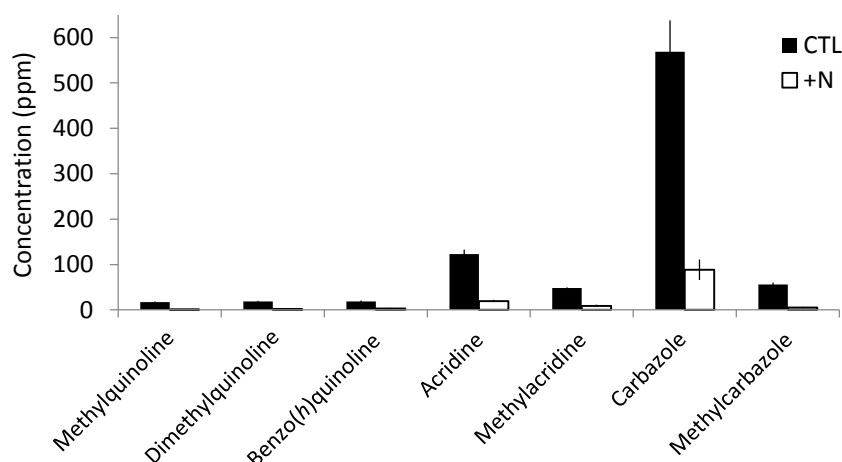


Figure 5.9. Azaarene concentrations at the end of incubation for the dry control and the +N treatment.

5.2.7 Dynamics of the heterotrophic and PAC-degrading populations

As shown in section 5.2.2, the total heterotrophic populations of the nutrients treated soil experienced a substantial growth during the first 15 days of incubation (from $8\cdot 10^6$ to $2\cdot 10^8$ MPN/g) to remain approximately stable from then until day 120. Surprisingly, during the last month, they incremented their number again to reach a final concentration of $4\cdot 10^9$ MPN $\cdot\text{g}^{-1}$ at day 150 (Figure 5.4).

The counts of PAH- and metabolite-degrading bacteria exhibited different trends (Figure 5.11). Almost all of them (except FL- and PY-degraders) increased between 3 and 6 orders of magnitude during the first 45 days. This is consistent with the rapid removal of the LMW PAHs during the first 30 days and the subsequent maximum degradation rates observed for HMW PAHs (30-45 days) (Figure 5.5). In the initial soil, the microorganisms able to grow on PHE were at numbers two orders of magnitude higher than the populations using any of the other PAHs. Between 45-90 days they were still the largest of the single PAH-degrading populations together with the FT degraders, then followed by the ANT and BaA degraders, and finally the FL and PY-degrading populations. The exponential increase of these single PAH-degrading populations attenuated after day 45

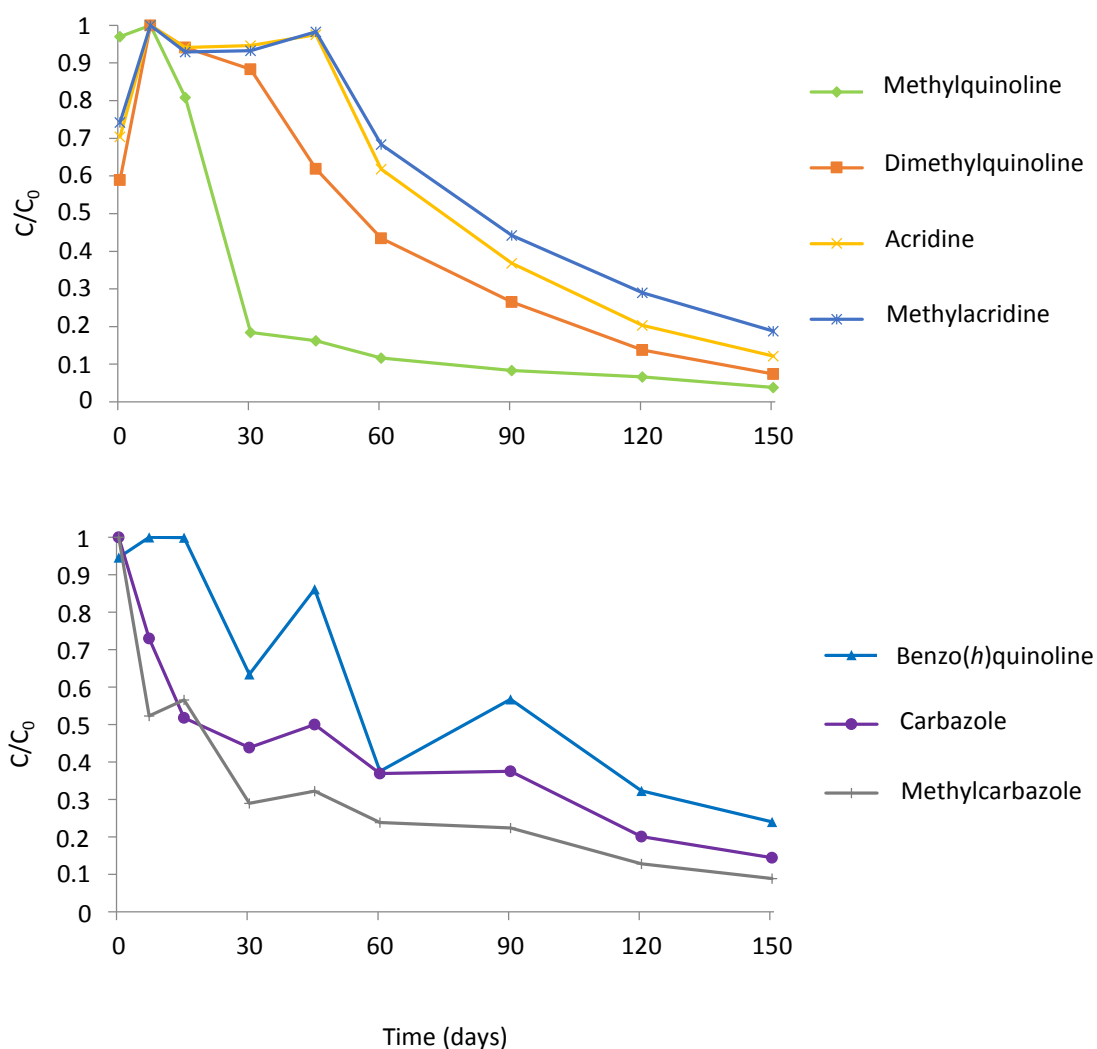


Figure 5.10. Kinetics of biodegradation of the identified and quantified N-PACs. Error bars are not shown for clarity in the interpretation of the results. Average absolute concentration and standard deviation values are shown in Table S3 (Annex I).

reaching a plateau phase until the end of incubation. In contrast, the FL- and PY-degrading microorganisms, after a first phase of exponential growth between 0-45 or 0-60 days, respectively, also showed a plateau phase until day 90, when, surprisingly, experienced a second phase of rapid growth to reach similar counts than the rest of the PAH-degrading populations at day 120 (around 10^7 MPN·g⁻¹). This increment between 90 and 120 days coincided with an increase in the biodegradation rates for anthracene, the most abundant PAH during this period.

To identify the PAH- and metabolite-degrading bacteria we extracted the DNA from three of the most diluted MPN wells for each carbon source at two data points. The extracts were analyzed by 16S rRNA PCR-DGGE and the major bands were excised and sequenced. The chosen data points were the incubation times flanking the period of maximum degradation rate for the corresponding PAH. For the oxy-PAHs the analyzed data points were the same analyzed for their parent PAHs to be able to compare both populations. Sequence analysis of the bands recovered from all the DGGE profiles identified 27 unique sequences (B1-B27) (Figure S1-S7, Annex I). The phylogenetic affiliation of the most relevant ones is summarized in Table 5.2.

Most of the identified sequences fell into a reduced number of genera belonging to the *Alpha-*, *Beta-* and *Gammaproteobacteria*, and only one genus (*Olivibacter*) affiliated to the phylum *Bacteroidetes*. However, it is interesting to note that within each genus there were a variety of sequences that were associated with different PAHs.

The increase in the phenanthrene degraders during the first 15 days of incubation, when only NAPH was degraded, suggested that these populations were actually growing on NAPH. The most abundant genera within this group of bacteria were *Pseudomonas* (B18, B19, B15) and *Pseudoxanthomonas* (B21). At 30 days, after the most important depletion of PHE, those microorganisms still predominated in the most diluted MPN wells, but in almost all of them, members of *Sphingobium* (B25, B27) and *Achromobacter* (B7) were also detected. Notice that the fact that these populations are two orders of magnitude higher than any other of the PAH-degrading populations indicate that their most abundant members could not utilize the other assayed PAHs for growth.

Between 15 and 30 days, concurring with the depletion of the 3-ring compounds, there was also an increase of the populations able to grow on ANT and BaA. These ANT and BaA degraders could not degrade FT, PY or FL. The analysis of the ANT degraders was performed at 30 and 45 days, and the identified phylotypes included members of *Pseudomonas* (B16, B19, B13), *Olivibacter* (B9), and *Achromobacter* (B1). Unfortunately, other relevant bands in the DGGE profiles could not be assigned because of the poor quality of the reads. The BaA degraders were analyzed in later data points (60-90 days), when maximum degradation rates were observed for this PAH.

Coinciding with the maximum depletion rates for fluoranthene (30 and 45 days), there was a fast and dramatic increment of the fluoranthene-degrading populations, which became the predominant among the analyzed PAH-degraders. The most abundant bacterial components included members of *Sphingobium* (B25, B26) that, according with the results, were not capable of growth on PY or FL.

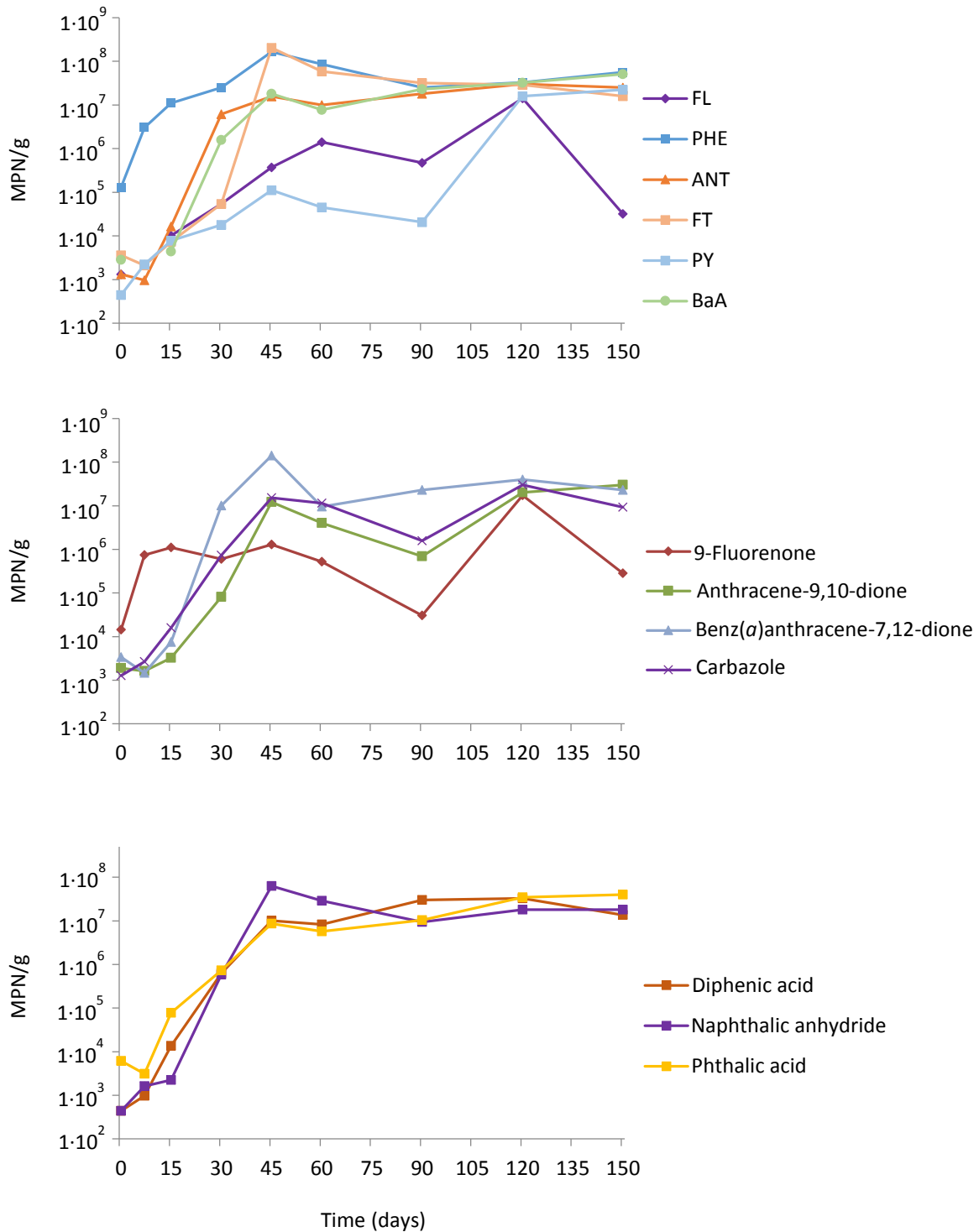


Figure 5.11. Enumeration of PAH- and metabolite-degrading populations over the incubation time. Error bars are not shown for clarity. The actual values for the means standard deviations obtained from the MPN counts are shown in the Table S4 (Annex I).

Table 5.2. Identified phylotypes within the most abundant populations detected with the different PACs as the sole carbon source for growth. Data correspond to selected unique sequences with a length of 341-440 bp. Taxonomic affiliations were assigned based on the RDP classifier considering bootstrap confidence scores > 97%.

Substrate	Incubation time (days)	Microbial counts (MPN·g ⁻¹)	Phylotypes
Fluorene	15	1.0·10 ⁴	<i>Achromobacter</i> B2, B3
	30	5.4·10 ⁴	<i>Ralstonia</i> B22
Phenanthrene	15	1.0·10 ⁷	<i>Alcaligenaceae</i> B7 <i>Pseudomonadaceae</i> B15
	30	2.5·10 ⁷	<i>Pseudomonas</i> B18, B19
Anthracene	30	6.2·10 ⁶	<i>Achromobacter</i> B1 <i>Pseudomonas</i> B16
	45	1.2·10 ⁷	<i>Olivibacter</i> B9
Fluoranthene	30	5.4·10 ⁴	<i>Sphingobium</i> B25, B26
	45	5.9·10 ⁷	
Pyrene	60	4.5·10 ⁴	<i>Achromobacter</i> B1, B5 <i>Pseudomonas</i> B19
	120	1.6·10 ⁷	Non-identified band
Benz(a)anthracene	60	7.7·10 ⁶	<i>Achromobacter</i> B1 <i>Bradyrhizobiaceae</i> B8 <i>Olivibacter</i> B12
	90	2.3·10 ⁷	<i>Pseudomonas</i> B18
Carbazole	15	1.6·10 ⁴	<i>Pseudomonas</i> B16 <i>Pseudomonadaceae</i> B13
	30	7.3·10 ⁵	<i>Achromobacter</i> B1
Acridine	120	1.2·10 ⁵	<i>Pseudomonas</i> B19 <i>Achromobacter</i> B1
9-Fluorenone	15	1.1·10 ⁶	<i>Achromobacter</i> B3 <i>Olivibacter</i> B9 <i>Pseudomonas</i> B17
	30	6.0·10 ⁵	<i>Ralstonia</i> B22
Anthracene-9,10-dione	30	8.1·10 ⁴	<i>Achromobacter</i> B1 <i>Pseudomonas</i> B19
	45	1.2·10 ⁷	<i>Sphingobium</i> B24
Benz(a)anthracene-7,12-dione	60	9.6·10 ⁶	<i>Achromobacter</i> B1 <i>Bradyrhizobiaceae</i> B8
	90	2.3·10 ⁷	<i>Olivibacter</i> B12
Diphenic acid	15	1.4·10 ⁴	<i>Achromobacter</i> B1 <i>Pseudomonas</i> B18, B19
	30	6.3·10 ⁵	<i>Pseudoxanthomonas</i> B21
Phthalic acid	30	7.3·10 ⁵	<i>Achromobacter</i> B1 <i>Pseudomonadaceae</i> B13
	60	5.7·10 ⁶	<i>Pseudomonas</i> B16, B20 <i>Olivibacter</i> B11
Naphthalic anhydride	30	5.8·10 ⁵	<i>Achromobacter</i> B1
	30, 60	2.9·10 ⁷	<i>Pseudomonas</i> B19

PY-degrading populations presented a slow increment between 0-45 days to start a slow decrease thereafter. However, this dynamics was not consistent with the kinetics of PY depletion, suggesting that the detected PY degraders were feeding on other products. In fact, PY mainly disappeared between 30 and 90 days. At 60 days in the PY-degrading populations predominated members of *Pseudomonas* (B19), *Achromobacter* (B1) and a non-identified phylotype. Between 90 and 120 days the PY-degraders exhibit a second increment and the DGGE profiles revealed a shift in their composition, with the most abundant members being *Achromobacter* (B1, B5) and the non-identified phylotype.

Similarly to PY degraders, the evolution of the populations able to grow on FL did not follow the dynamics of the depletion of this PAH, showing also two separated rising periods, the first from 0-60 days and a second one from 90 to 120 days. The most intense bands detected at 15-30 days corresponded to *Pseudomonas* (B16, B18), *Pseudoxanthomonas* (B21), *Achromobacter* (B1, B2 and B3) and *Ralstonia* B22. Since at these same times B16, B1, B21, and B18 had been identified as degraders of other PAHs at several orders of magnitude higher, their presence here may be residual. Therefore, those attacking FL in the MPN plates would mainly be two members of *Achromobacter* (B2, B3) and a member of *Ralstonia* (B22). Unfortunately we did not analyze the FL-degrading populations at time 120d.

The BaA degrading populations were analyzed at the beginning and the end of maximum degradation for this PAH (60 and 90 days), giving similar profiles that included phylotypes of *Pseudomonas* (B18), *Achromobacter* (B1), *Bradyrhizobium* (B8) and *Olivibacter* (B12).

As mentioned before, the analysis of the specific communities able to grow on single compounds was performed not only with PAHs but also with some relevant oxy-PAHs. The aim was to find out if the populations driving the degradation of the parent PAHs coincided with those involved in the final fate of the ketone and quinones resulting from their cometabolic oxidation.

The 9-fluorenone degraders increased during the first week to reach values more than 2 orders of magnitude above those of the FL-degraders. The analysis of the most diluted MPN wells at day 15 revealed the presence of several microorganisms already detected as PHE degraders at higher concentrations: *Pseudomonas* (B16 and B18) and *Pseudoxanthomonas* (B21). The only bacteria exclusively detected in the 9-fluorenone profiles were *Pseudomonas* (B17) and *Ralstonia* (B22). The latter was also found in the fluorene wells at much lower concentrations, indicating that grew in the fluorenone produced by other microorganisms. At day 30 the same microorganisms remained, but other groups appeared: *Olivibacter* (B9), detected as ANT degrader at similar concentrations, and *Achromobacter* (B3), identified as FL degrader. In any case, FL and 9-fluorenone degraders followed different kinetics until day 90, when, as observed for other

compounds, the 9-fluorenone degraders experienced a second increase achieving their maximum at 120 with concentrations coinciding with the rest of degraders.

The dynamics of the 9,10-anthraquinone degraders followed that of the anthracene degraders with some delay, being consistent with the rapid depletion of the accumulated anthraquinone between 30 and 45 days. The most abundant 9,10-anthraquinone degrading microorganism not detected in higher concentrations in any other substrate was a member of *Sphingobium* (B24).

Within the azaarenes, only the degrading populations for carbazole and acridine were assessed. Carbazole degraders increased from 0-45 days, coinciding with its maximum removal rates. Community analysis identified *Pseudomonas* (B16), present in all the wells analyzed, *Pseudomonas* (B13) and *Achromobacter* (B1) as the most abundant components within the carbazole degraders. Finally, despite of its significant depletion, the counts for acridine degraders did not produce positive wells until day 120, with $1,2 \cdot 10^5$ MPN·g⁻¹. Curiously, the most diluted wells presented a low diversity, with clear bands for *Pseudomonas* (B19) and *Achromobacter* (B1).

The degrading populations of the metabolites diphenic acid, phtalic acid and naphthalic anhydride were also monitored during the soil treatment. All of them presented similar dynamics with a fast growth between 7 and 45 days reaching maxima of $8.6 \cdot 10^6$ - $6.3 \cdot 10^7$ and coinciding with the maximum PAH degradation rates and following the transient accumulation of acidic compounds in the soil. The most diluted MPN wells did not show specific phlotypes for the degradation of these metabolites.

5.3 Discussion

The available literature on microbially-mediated PAH transformation includes a great number of works based on batch experiments using liquid mineral media with single or discrete mixtures of PAHs (Haritash & Kaushik, 2009; Kanaly & Harayama, 2010; Vila et al., 2015). Little is known about the actual processes taking place during the biodegradation of PAHs in real polluted soils, and even less for the more polar and co-occurring oxy-PAHs and N-PACs. The aim of this Chapter was to elucidate the *in situ* kinetics of PAC degradation/accumulation and the associated dynamics of the compound specific degrading populations using a creosote polluted soil as a model. Two treatments (-N and +N) were tested to find the appropriate conditions for the biodegradation of both LMW and HMW PAHs, since it has been proven that the addition of nutrients not always benefits the HMW PAH removal (Viñas et al. 2005). Both conditions showed high LMW PAH depletion percentages (90-95%), nonetheless the addition of nutrients gave the major extent of 4- and 5-ring PAHs biodegradation (87% in front of 26% without nutrients). Hence, this treatment was chosen to investigate the kinetics of removal or accumulation of 17 PAHs, 7 N-PACs, 10 oxy-PAHs and 14 acidic aromatic metabolites.

In the nutrient amended soil, the PAHs were removed according to their water solubility (Table 1.2), forming groups with clear similar kinetics. NAPH, presenting the higher water solubility ($31 \text{ mg}\cdot\text{L}^{-1}$), was removed during the first week of incubation, followed by the 3-ring PAHs depleted between 15 and 30 days. ANT was the exception, since with his similar solubility to the 4-ring PAH BaA (Table 1.2), was removed alongside the whole incubation with an almost linear kinetics. Then, the HMW PAHs were removed grouped in pairs, also according to their solubility in water ($0.26\text{-}0.0038 \text{ mg}\cdot\text{L}^{-1}$). The pair FT and PY exhibited a fast decrease between 30-90 days, while BaA and CHY disappeared at a constant pace from day 30 until the end of incubation. The concentration of the 5-ring PAHs decreased with a slow linear kinetics until day 90, when they split into two groups: BbFT and BkFT continued being reduced with similar rates, while the degradation of BePY and BaPY slowed down. The analogous degradation kinetics could indicate that the PAH grouped in pairs are attacked by the same bacterial populations. Of course, these kinetics are very different from those reported in the literature for liquid cultures (Lafortune et al. 2009; López et al. 2008).

To the best of our knowledge, the biodegradation dynamics of N-PACs in a real creosote polluted soil has never been addressed before. The presence of the heteroatom in azaarenes confers these compounds highly distinctive chemical properties compared to their PAH counterparts (Table 1.2). As a consequence differences in their degradation kinetics were expected. In the nutrient amended soil carbazole and their alkyl-derivatives presented a higher biodegradability than the family of the acridines, which is consistent with fluorene being faster removed than anthracene. However, if we compare the degradation rates within each pair of analog compounds, it is clear that the degradation of N-PACs (carbazole and acridine), despite their higher water solubility, was slower than that of the corresponding PAHs (FL and ANT, respectively). Therefore, the presence of the heteroatom seems to have a strong impact on determining the microbial processes dealing with their environmental fate.

Recent works demonstrated that oxy-PAHs are produced in soil by microbial activity (Wilcke et al., 2014). Here, in the dry control, where the MPN counts of PAH-degrading bacteria did not increase and PAH degradation was not detected, the concentration of oxy-PAHs present in the original soil incremented linearly until the end of incubation. An explanation for this phenomenon could be that the weekly aeration favored the chemical oxidation of PAHs into oxy-PAHs. However, in the treated soil, without nutrient limitation and optimal oxygen conditions, the initial oxy-PAHs concentrations were either rapidly reduced (i.e. 9-fluorenone) or transiently incremented to higher values than in the control, to be later progressively degraded. Thus, here we demonstrated that even though the polyaromatic ketones and quinones are formed by microbial attack, if there is an appropriate stimulation of the degrading microorganisms, these potentially carcinogenic compounds will not be accumulated in the soil.

On the other hand, PAH degradation was accompanied by the production of detectable amounts of water-soluble acidic metabolites, but suitable stimulation also favored their elimination. Two of the most abundant were the mycobacterial metabolites 6,6'-dihydroxy-2,2'-biphenyl dicarboxylic acid and *Z*-9-carboxymethylene-fluorene-1-carboxylic acid, two products that typically accumulate in pure cultures of degrading mycobacteria with pyrene and fluoranthene, respectively (López et al., 2006; Vila et al. 2001), and that had been considered for a long time as dead end products of non-productive routes. This together with other results (see below) supports the idea that in the environment, microbial populations are interconnected by complex metabolic networks, where secondary metabolites produced by certain populations can be utilized by other populations (secondary degraders) (Vila et al. 2015).

In previous works, our group detected the accumulation of these and other key acidic metabolites during the degradation of PAH mixtures (i.e. creosote and fuel oil) in liquid cultures (López et al. 2008; Vila & Grifoll 2009; Vila et al. 2001) and also, punctually, in groundwater from an aquifer contaminated with creosote (Soares et al. 2008). Their detection in soils reinforce our hypothesis that these acidic compounds could be useful tools as indicators of active biodegradation during bioattenuation of enhanced bioremediation strategies. On the other hand, the presence of ketones and quinones would indicate

With the aim to understand the role of each population in the removal of the individual PAHs and identify the microbial key players, we analyzed together the kinetics of the depletion/accumulation of single PAHs and their metabolites, and the dynamics (MPN enumeration) and composition (PCR-DGGE analysis and identification of phylotypes) of their specific degrading populations.

During the first two weeks of incubation, the disappearance of NAPH co-occurred with a first rapid increment of the PHE degraders, which most abundant numbers corresponded to members of *Pseudomonas* and *Pseudoxanthomonas*. As there was no removal of PHE or other PAHs, it is reasonable to assume that these populations grew on NAPH. In fact, these two genus of *Gammaproteobacteria* are well-known NAPH-degrading bacteria, particularly *Pseudomonas*, that presents the capability to oxidize a wide range of LMW substrates (Haritash & Kaushik, 2009; Li et al. 2011; Pathak, Kantharia et al. 2009) and the capacity to attack both naphthalene and phenanthrene is frequent in Gram negatives. Moreover, products such as phthalic acid and salicylic acid, which are intermediates of the biodegradation pathway of NAPH, showed their maxima accumulation during this period.

The almost exhaustion of NAPH at day 15 triggered the biodegradation of the 3-ring PAHs, the most abundant being PHE, ANT and FL. All of them, with the exception of ANT exhibited their maximum degradation rates from 15 to 30 days.

Along this time the growth of the populations able to grow on PHE attenuated but their numbers kept high, with the previously found representatives of *Pseudomonas* and *Pseudoxanthomonas* as the most abundant phylotypes, together with the newly detected members of *Sphingobium* and *Achromobacter*. By contrast, the ANT and BaA degraders experimented a fast increment, *Achromobacter* and *Olivibacter* being the most abundant phylotypes. It seems plausible that all these populations participate in the removal of the 3-ring PAH.

Throughout the almost complete depletion of FL, only an initial increment of its degraders (less than one order of magnitude) was detected (Figure 5.12). This suggests that this PAH could be mainly transformed by the unspecific action of bacteria that do not grow well at its expense. Fluorene is readily cometabolized to 9-fluorenone by the unspecific action of naphthalene-type RHD (Selifonov et al. 1996). Even some 3-ring PAH degraders, including FL-degrading strains obtaining carbon from fluorene by an alternative dioxygenasic pathway, accumulate 9-fluorenone as a side product that they could not further utilize (Grifoll et al. 1992). In fact, there is a study demonstrating the cooperative mineralization of fluorene by one of these strains, *Arthrobacter* sp. F101, producing 9-fluorenone that is then further oxidized by a *Pseudomonas* strain that is not able to attack FL (Casellas et al. 1998). The fact that 9-fluorenone degraders are in a higher concentration than those of FL during the disappearance of this PAH, strongly supports that an important part of FL is channeled through its ketone by cometabolism, and then further degraded by secondary populations present in the soil. This is also consistent with the fast reduction of the initial 9-fluorenone concentrations. Within the specific populations that degrade this ketone a member of *Ralstonia* (*Bulkholderiaceae*) stands up. The importance of the cometabolic reactions is also supported by the transient accumulation of several oxy-PAHs deriving of the monooxydation of the methylenic groups of acenaphthene, and the carboxylic metabolites of methyl phenantrene and methyl naphthalene.

The C-9 and C-10 carbons in the central ring of anthracene have analog reactive properties than the C-9 of fluorene, thus they are readily oxidized to give first 9-anthracenone, and then 9,10-anthraquinone. We have observed the formation and accumulation of the quinone as a result of the exposure of anthracene to different PAH-degraders (Grifoll et al., 1995, 1994; López et al., 2008; Vila et al., 2001). Therefore, the high concentration of naphthalene-type RHD during the first month would also account for the transient accumulation of anthraquinone in the soil (Figure 5.12). At its peak of abundance at day 30, this oxy-PAH represented the 5% of the total depleted ANT, but based on the subsequent rise in more than two orders of magnitude of the anthraquinone degraders a much greater part of anthracene seems to be oxidized *via* its quinone. Then, specific populations mostly unable to degrade anthracene, would remove this oxy-PAH. This was confirmed by the different DGGE profiles obtained for the most abundant populations of each case. Within the ANT degraders the preeminent populations

corresponded to *Pseudomonas*, *Achromobacter* and specially a member of *Olivibacter*, while in the case of 9,10-anthraquinone a specific member of *Sphingobium* stand up.

The rapid diminution of FT coincides with a fast growth of the FT-degrading populations between 30 and 45 days of incubation. Thus, it is clear that members of *Sphingobium*, found in the most diluted FT wells at 45 days, drive the biodegradation of this 4-ring PAH. Taking into account that PY depletion follows kinetics highly similar to that of FT, and that the PY degraders remain at low concentrations, it is reasonable to assume that to the rapid decrease of the pyrene concentration contributed the fluoranthene degraders (i.e. *Sphingobium* between others) that do not use it as a carbon source. Of course, the identification of the signature FT and PY acidic metabolites (peaks at 45 and 60 days) indicates that actinobacteria, although in lower concentrations, also play a key role in the oxidation of those compounds.

As mentioned, the initial rapid increment of microorganisms able to degrade BaA did not correlate with its its slow degradation, suggesting that, as already described elsewhere, some BaA degraders were also able to utilize 3-ring compounds (Koukkou & Vandera, 2011). The analysis of the populations was done between 60-90 days and the DGGE profiles showed as preeminent BaA degraders members of *Olivibacter*, *Achromobacter*, and especially a representative of *Bradyrhizobiaceae* not found in other substrates. Part of BaA was monooxdated to its quinone, but in this case its degrading populations are similar to those of the PAH.

Unfortunately, chrysene degraders were not followed over the experiment, but, according to the similarity between its kinetics and that of BaA we could hypothesize that they were probably oxidized by the similar bacterial populations.

The overall PAC removal kinetics reveals two distinct cycles of biodegradation during the treatment of the soil. The first cycle (0-60 days) corresponds to a rapid depletion of the major 3-4 ring compounds, and is accompanied by a fast growth of their degrading populations. Between 60 and 90 days, when the other 3-ring PAHs had been almost completely removed, there is a standstill in the degradation of ANT and carbazole, still at relatively high concentrations, that coincides with a plateau phase or a decrease of in all the degrading populations. Then, at 90 days, another cycle seems to start, with an important increment of the less abundant degrading populations (those of FL, PY, carbazole, 9-fluorenone and 9,10-anthraquinone) to converge in number (about $3 \cdot 10^7$ MPN·g⁻¹) with all the other degraders at time 120 days. This change is concomitant with a new rise in the taxes of degradation of ANT, carbazole and, subsequently, the 5-ring PAHs. This evolution of the microbial counts and degradation rates is consistent with a shift in the degrading microbial community structure. Unfortunately, at 120 days we only analyzed the PY degraders, where a non-identified preeminent phylotype appeared that could have played a key role in this new degradation stage. A possible explanation to this

bimodal degradation kinetics would be that the exhaustion of the easily degradable fraction of the PACs at around 90 days, the initial degraders are outcompeted by a slower growing community, that attack the low available residue more efficiently resuming the degradation of the remaining ANT, carbazole and, subsequently, the 5-ring PAHs.

Finally, a few phylotypes belonging to *Achromobacter* and *Pseudomonas* were found as the most abundant members in the counts with all the substrates. We hypothesized that, independently of their possible degradative capabilities, these fast growing and oligotrophic bacteria can efficiently feed in the carbon fragments made available by other groups, thus reaching high concentrations.

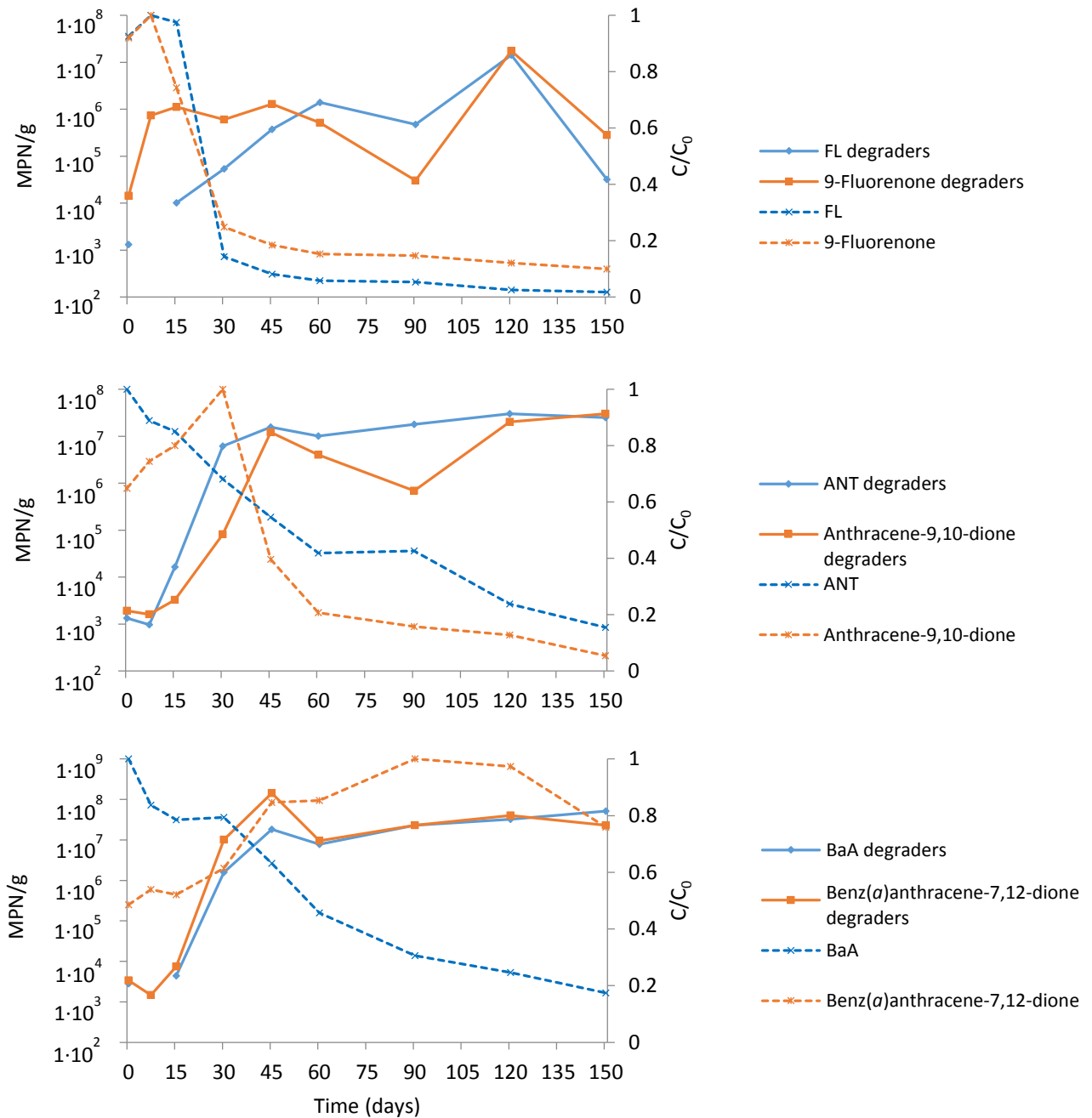


Figure 5.12. Kinetics of fluorene, anthracene, benz(a)anthracene and their corresponding oxy-PAH together with the MPN enumerations of their degrading populations.

CHAPTER 6

Structural and quantitative changes in the microbial community of the creosote polluted soil associated to enhanced PAH degradation

6 Structural and quantitative changes in the microbial community of the creosote polluted soil associated to enhanced PAH degradation.

During the last decade, molecular microbial ecology methods for the study of community composition have rapidly evolved due to the development of next generation sequencing (NGS) technologies. Pyrosequencing of tag encoded 16S rRNA gene libraries has become the most cost-efficient and high throughput method to elucidate the community structure present in environmental samples. A few examples of the application of NGS population studies to PAH biodegradation already exist, and have been applied to ascertain microbial community shifts during soil bioremediation in bioreactors (Singleton et al. 2013; 2011) or lab-scale biopiles (Lladó et al., 2015). These analyses, based on total genomic DNA extracts, provide an overview on the most abundant components of the microbial community, but may encompass dead, dormant and inactive microorganisms. Pyrosequencing of the 16S rRNA amplicons from the reverse-transcribed RNA (cDNA) is better suited to gain insight into the bacteria actually carrying out a particular function in a specific time, thus allowing estimating the current *in situ* activity of the different taxa present in an ecosystem. In biodegradation experiments, pyrosequencing and also quantification of transcripts become powerful tools to target active bacteria when specific processes are produced, such as PAH removal or metabolite formation, since rRNA concentration is generally well correlated with growth rate and activity (Poulsen et al. 1993). Transcriptomic assessment studies of active soil microbial communities in the field of PAH biodegradation are scarce. To our knowledge only two works are available and are based on the DGGE profiling of 16S rRNA transcript libraries (Di Gennaro et al. 2009; Niepceon et al. 2010), a method with a lower resolution than NGS. Barcoded 16S rRNA pyrosequencing of cDNA has not yet been applied to study the PAH degrading microbial communities of polluted sites.

The main goal of this chapter is to identify the microbial populations actually attacking the PAHs in the creosote polluted soil experiment, by tracking their quantitative (qPCR) and structural (tag encoded pyrosequencing) changes at the genomic and transcriptomic levels. The combined analysis of both DNA and cDNA will not only permit to elucidate the structure of the total community but also to reveal the active populations at each data point. In addition to 16S rRNA, the presence and expression levels of RHD genes for GN and GP bacteria will be monitored as an estimate of the abundance and activity of PAH-degrading communities.

6.1 Materials and methods

6.1.1 Soil and experimental layout

The characterization of the creosote polluted soil, the layout of the experiment and the kinetics of degradation of PAHs have been described in detail the previous chapter (5.1.1, 5.1.2 and 5.2.1).

6.1.2 Nucleic acids extraction and reverse-transcription

Total DNA and RNA were extracted, following the manufacturer's instructions, from two separate aliquots (0.5 g) of soil samples using FastDNA™ Spin kit for soil and FastRNA® Pro Soil-Direct Kit (MP biomedical, USA), respectively. RNA was treated with DNase I RNase-free (Thermo Scientific, USA) and purified using RNAeasy mini Kit (Qiagen, Germany) before reverse-transcription with Superscript™ III first strand synthesis system for RT-PCR (Invitrogen, USA) using random hexamers, and following manufacturer's instructions.

6.1.3 qPCR amplification

Prior to qPCR amplification, the concentration of DNA extracts and cDNA was estimated by UV absorbance measurement using a UV1800 (Shimadzu, Japan) spectrophotometer equipped with a Traycell adapter (Hellma, Germany); and adjusted to equal concentrations ($10 \text{ ng}\cdot\mu\text{L}^{-1}$). Real-time PCR (qPCR) was conducted in CFX96 Real-Time PCR detection system (Bio-Rad, USA) to quantify 16S rRNA, 18S rRNA, and PAH-RHD genes and transcripts copy numbers as described in Cébron et al. (2008) and Thion et al. (2012). *Mycobacterium* populations were also tracked by using the genus specific primers described by Leys et al. (2005). The primer pairs and conditions used for each determination are described in Table 6.1. Data from qPCR were expressed as gene copy number per g of dry soil, or as ratios: transcript copies relative to the corresponding gene

Table 6.1. Characteristics of PCR primer sets used in this study.

Primer	Sequence (5'-3')	Annealing temperature	Reference
968R	AACGCGAAGAACCTTAC	56	Felske et al. 1998
1401F	CGGTGTGTACAAGACCC		
Fung5F	GTAAAAGTCCTGGTTCCCC	50	Lueders et al. 2004
FF390R	CGATAACGAACGAGACCT		
MYCO66F	CATGCAAGTCGAACGGAAA	50	Leys et al. 2005
MYCO600R	TGTGAGTTTTACGAACA		
PAH-RHD α GNF	GAGATGCATACCACGTKGGTTGGA	57	Cébron et al. 2008
PAH-RHD α GNR	AGCTGTTGTTCCGGGAAGAYWGTGCMGTT		
PAH-RHD α GPF	CGGCGCCGACAAYTTYGTNGG	54	Cébron et al. 2008
PAH-RHD α GPR	GGGGAACACGGTGCCRTGDATRAA		

copies, one specific gene copies relative to 16S rRNA gene copies, and functional gene transcript copies relative to 16S rRNA transcript copies.

6.1.4 Diversity of PAH-RHD by clone library analysis

The diversity of transcripts of PAH-RHD in the soil treated with nutrients (+N) was assessed by clone library analysis of the qPCR amplicons obtained at their peak of expression (T15 for GN and T120 for GP). At the corresponding data point, the cDNA qPCR amplicons were combined to give two composite qPCR products that were then purified using EZNA Cycle Pure Kit (Omega Bio-tek, USA) and cloned using pGEM[®]-T Easy Vector System (Promega, USA). 20 transformants from each library were selected and the presence of inserts of the appropriate size was confirmed by PCR amplification using vector M13 primers. PCR products were purified and sent to a sequencing service (Eurofins Genomics, Germany). DNA sequencing runs were aligned and manually adjusted using BioEdit 7.0.5.3 Software. The resulting DNA sequences were examined and compared with databases using the BLAST alignment tool (<http://blast.ncbi.nlm.nih.gov/Blast.cgi>).

6.1.5 Barcoded pyrosequencing

DNA and cDNA from triplicate samples of each data point of the nutrients treated soil were sequenced using Roche 454 FLX titanium equipment and reagents at Molecular Research DNA (Shallowater, Texas). Data were processed using Mothur 1.35.1 (Schloss et al., 2009) following the 454 standard operating procedure (SOP) described by Schloss and col (2011). In brief, the pyrosequencing *.sff file was demultiplexed with the barcode mismatch tolerance of one base for the 8 bp Molecular Identifier (MID) tags. After trimming barcodes and primers, raw reads were subjected to a quality filtering including the removal of reads that were smaller than 250 bp, contained homopolymers of eight or more bases, or ambiguous base calls. Sequences were aligned using SILVA v119 reference files and grouped into operational taxonomic units (OTUs) with a distance criterion of 0.03. Taxonomic affiliation was assigned according to RDP database v10. Rarefaction curves and diversity indexes were also estimated using Mothur 1.35.1 normalizing the number of reads/sample to that of the least represented sample (1,550 reads). The 454 pyrosequencing libraries produced a total of 391,798 good sequences with an average of $7,390 \pm 3,184$ reads per sample.

6.1.6 Statistical and multivariate analysis

PAHs concentration and qPCR data were analyzed by ANOVA (IBM SPSS statistics 20 software) using the Tukey posthoc test at $P < 0.05$. The pyrosequencing data were analyzed by Canonical Correspondence Analysis (CCA) using R-3.2.0 and including the

biodegradation percentages for LMW and HMW PAHs as explanatory environmental variables.

6.2 Results

6.2.1 Evolution of total and active microbial populations during PAC degradation with or without nutrient limitation conditions

The abundance of total bacterial and fungal populations, expressed as gene copies \cdot g of dry soil⁻¹, was estimated based on the qPCR amplification of the 16S and 18S rRNA genes, respectively. This quantification, and that of RHD genes (Chapter 6.2.3) was performed in the +N and -N treatments but not in the CTL. This decision was sustained on the absence of significant PAH biodegradation and the low numbers retrieved during the enumeration of heterotrophic and PAH-degrading bacteria (see Chapter 5) in the controls.

At the beginning of the experiment, the creosote polluted soil presented a concentration of total bacteria of $2.8 \cdot 10^8$ 16S rRNA gene copies \cdot g of dry soil⁻¹ and these values did not

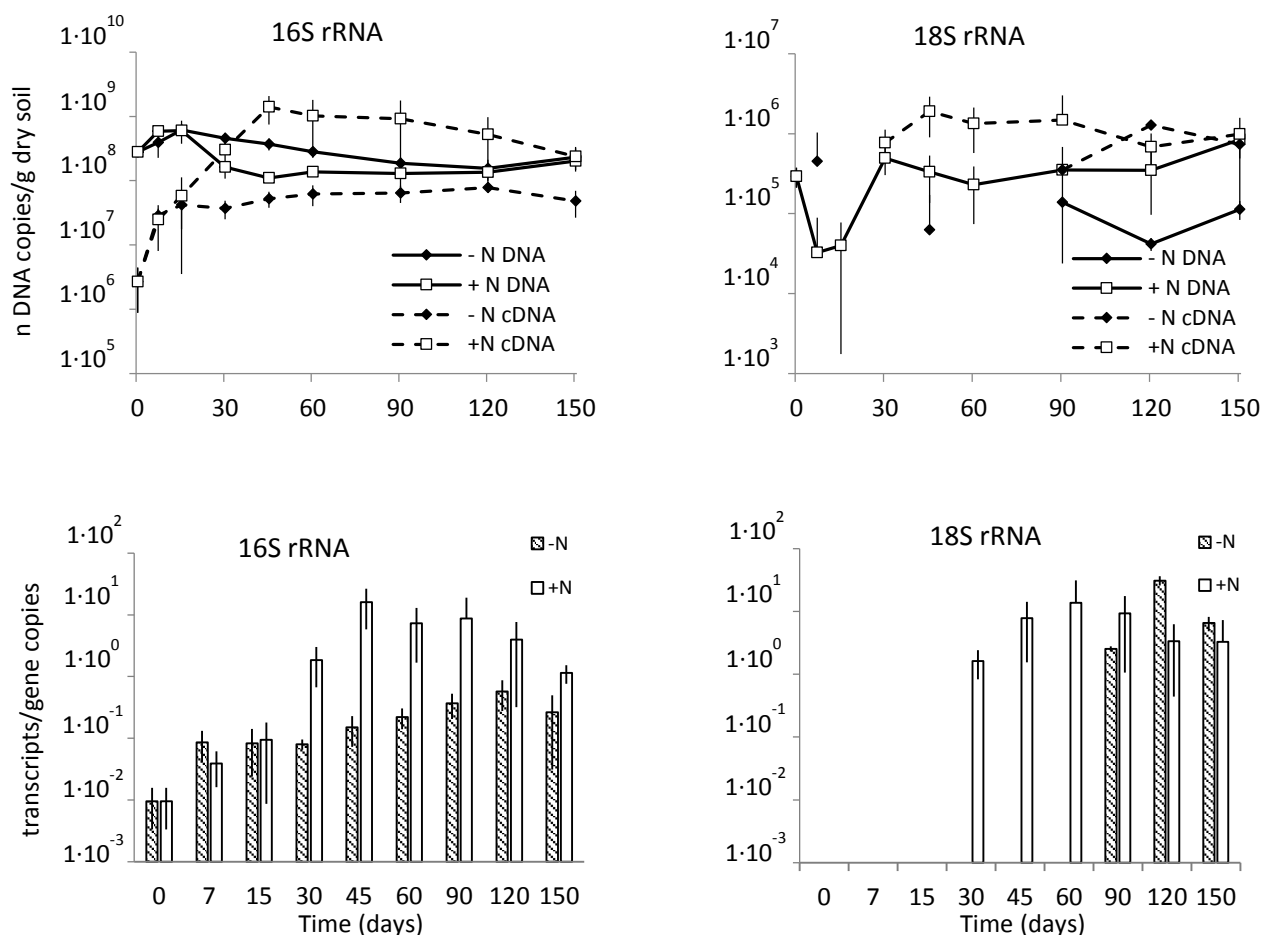


Figure 6.1. On the top, quantification by qPCR of 16S rRNA and 18S rRNA gene copies (DNA) and their transcripts (cDNA) throughout both treatments (-N and +N). At the bottom, the ratios of the transcripts/gene copies for 16S rRNA and 18S rRNA, respectively. Missing points in the 18S plot correspond to values below the detection limit ($4.6 \cdot 10^3$ transcripts \cdot g⁻¹ and $2 \cdot 10^3$ gene copies \cdot g⁻¹).

experience substantial changes over the 5 months of incubation in any of the two treatments (ranging between $1.1 \cdot 10^8$ and $6.0 \cdot 10^8$ 16S rRNA gene copies \cdot g of dry soil⁻¹, Figure 6.1). Conversely, important differences were observed in the gene expression levels. The addition of nutrients resulted in a substantial increase in the expression of the 16S rRNA gene (from $2.67 \cdot 10^6$ 16S rRNA transcripts \cdot g of dry soil⁻¹ at time 0, to a maximum of $1.41 \cdot 10^9$ 16S rRNA transcripts \cdot g of dry soil⁻¹ at 45 days), while the treatment without nutrients induced an increment of only 1 order of magnitude during the first week to remain approximately constant ($5.16 \cdot 10^7$ 16S rRNA transcripts \cdot g of dry soil⁻¹) thereafter. This difference of two orders of magnitude in the 16S rRNA expression levels between the two treatments was consistent with the faster PAH degradation in the +N treatment observed during the first two months of incubation. These increased expression levels observed in the presence of nutrients were clearly visualized from the comparison of the evolution of the cDNA/DNA ratios for the 16S rRNA gene (Figure 6.1). The treatment with nutrients exhibited values of 16S rRNA gene transcripts 10 folds higher than those of gene copy numbers during the second and third months, with a maximum cDNA/DNA ratio of 16 at 45 days, indicating the high degree of activity within the bacterial community. In contrast, in the absence of nutrients those values remained below 1 throughout all the incubation, showing a moderate but constant increase until 120 days, when the maximum ratio of 0.6 was reached.

The abundance of the fungal community expressed as 18S rRNA gene copies was significantly lower than that of the bacterial community expressed as 16S rRNA gene copies, with ratios 18S/16S rDNA between $7.6 \cdot 10^{-4}$ and $3.9 \cdot 10^{-3}$ during the entire incubation period. Interestingly, 18S rRNA gene copy numbers remained under the limit of detection ($4.7 \cdot 10^3$ transcripts \cdot g⁻¹) during the first month. After that, the fungal populations became active in the presence of nutrients, reaching a maximum of expression of the 18S rRNA genes at 60 days with a cDNA/DNA ratio of about 10. In the -N treatment 18S rRNA transcripts were not detected until 90 days, with a ratio of 2.5 (Figure 6.1). Its maximum took place at 120 days of incubations with a ratio transcripts/gene copies of 31.

6.2.2 Abundance and expression levels of PAH-RHD genes in GN and GP bacteria

The number and expression levels of PAH-RHD genes from GN and GP bacteria were used in this study as indicators of the abundance and activity of the PAH-degrading populations, discriminating between LMW and HMW degrading conditions over time. In both treatments, the proportion of GN degraders in front of the total population (gene copies of RHD/16S rRNA) ranged from $3.4 \cdot 10^{-2}$ to $1.5 \cdot 10^{-1}$, while GP degraders were always in a lower proportion, $7.5 \cdot 10^{-5}$ – $1.6 \cdot 10^{-2}$ (Figure 6.2). Despite this approach should be considered with caution, due to the limitations derived from the distinct gene copy

numbers within a cell and the potential misdetection of RHD, this ratio suggests that GN degraders could represent up to 15% of the global community, while GP degraders would be in all cases below 2%.

As previously observed with the 16S rDNA, the PAH-RHD GN gene copy numbers did not undergo substantial changes throughout the incubation period in any of the treatments. Although the copy numbers of this gene were between 1 and 2 orders of magnitude lower than those of the 16S rDNA gene, this result suggests a parallel evolution of the GN PAH-degrading populations and the whole bacterial community. In contrast, the RHD gene expression analysis revealed significant differences between treatments and throughout the incubation time. The ratio of PAH-RHD GN transcripts relative to the number of the gene copies (Figure 6.2) drastically increased in both treatments during the first 15 days of incubation (e.g. from $3.95 \cdot 10^{-5}$ to $1.7 \cdot 10^{-3}$ in +N). Thereafter, in the absence of nutrients the gene expression decreased to reach initial values after 45 days, and becoming negligible during the last month. Conversely, in the presence of nutrients this ratio remained constant until day 90, and slowly decreased thereafter, suggesting that the PAH-

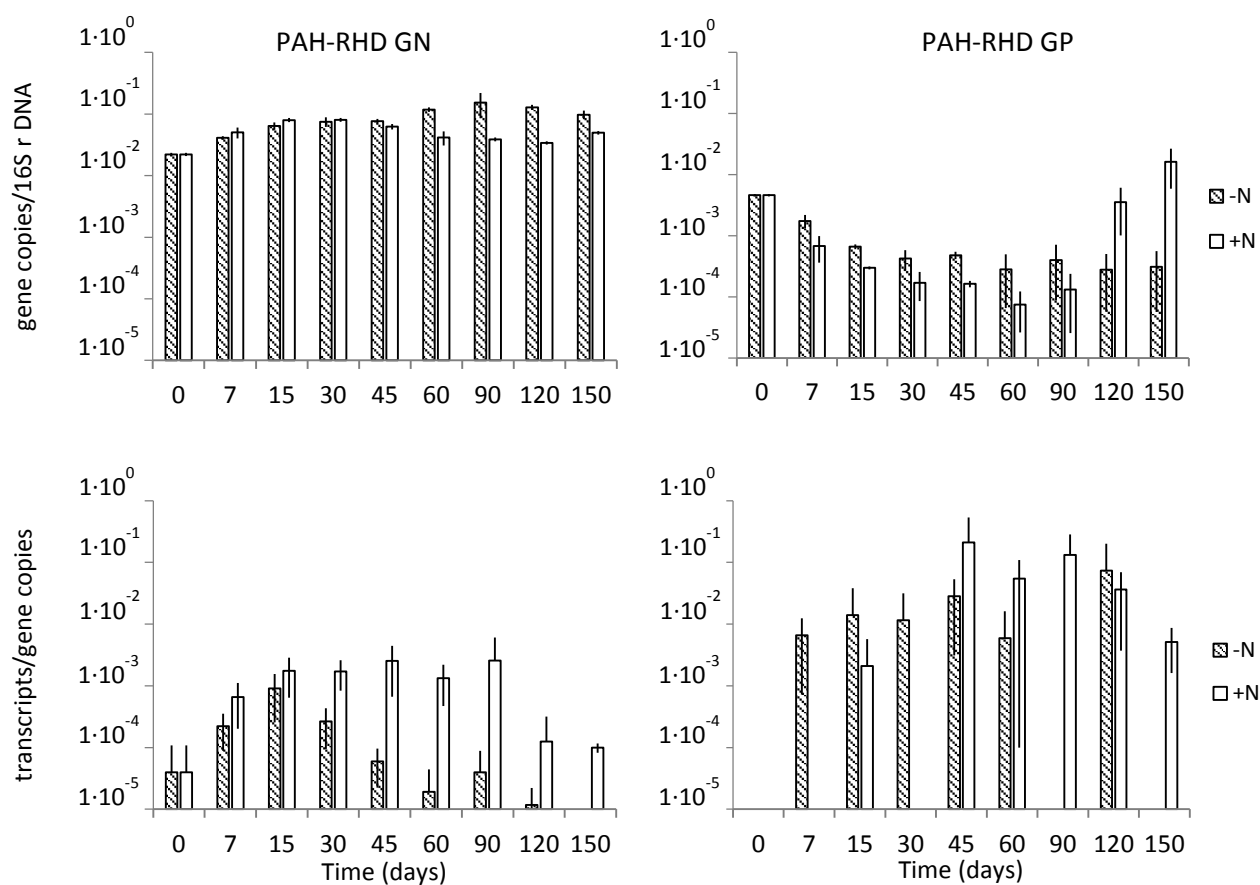


Figure 6.2. Evolution of the ratios PAH-RHD/16S rDNA for GN and GP bacteria in both treatments (-N and +N), on the top. On the bottom, the abundance of transcripts of GN and GP PAH-RHD represented respect to their gene copies for both conditions.

degrading activity catalyzed by Gram-negative bacteria was limited by nutrient bioavailability.

The ratio of PAH-RHD GP gene copies to 16S rDNA showed a similar initial evolution in both treatments, decreasing from day 0 to day 90 (e.g. from $4.63 \cdot 10^{-3}$ to $7.45 \cdot 10^{-5}$ with nutrient addition). However, at 120 days this ratio clearly increased with nutrient addition ($1.62 \cdot 10^{-2}$), reaching a maximum at the end of incubation, while remaining approximately constant in the soil without nutrients. The ratio of PAH-RHD GP gene transcripts to 16S rDNA did not follow a clear dynamics, but in the presence of nutrients, the levels of expression tended to increase at the latter phases of incubation. It is also interesting to note that at their respective stages of maximum activity, the expression levels of RHD (shown as their cDNA/DNA ratios, bottom of Figure 6.2) were between 1 or 2 orders of magnitude higher for GP bacteria ($2.1 \cdot 10^{-1}$) compared to GN ($2.6 \cdot 10^{-3}$). This result suggests that despite their reduced absolute numbers, GP bacteria could have a significant contribution to the overall PAH-biodegradation due to their increased relative activity.

If we focus now on the results obtained for the soil treated with nutrients (+N), the succession of the GN and GP PAH degraders coincides with the sequential elimination of LMW PAHs and HMW PAHs (Figure 6.3). While the relative abundance of GN degraders respect to the total population remained constant (0.02–0.08), the GP degraders decreased from time 0 ($4.6 \cdot 10^{-3}$) to day 60 ($7.5 \cdot 10^{-5}$), to increase thereafter in more than two orders of magnitude ($1.6 \cdot 10^{-2}$). If we plot the ratio number of transcripts of PAH-RHD/16S rRNA (Figure 6.3, right), it is even clearer that during the first 45 days of incubation GN PAH-degrading bacteria were the main drivers of LMW PAH biodegradation. On the other hand, GP degraders and also fungi, gain relevance during the latter phases, when LMW PAH biodegradation has already stopped, thus clearly linking their activity to the removal of the PAHs with more than three rings.

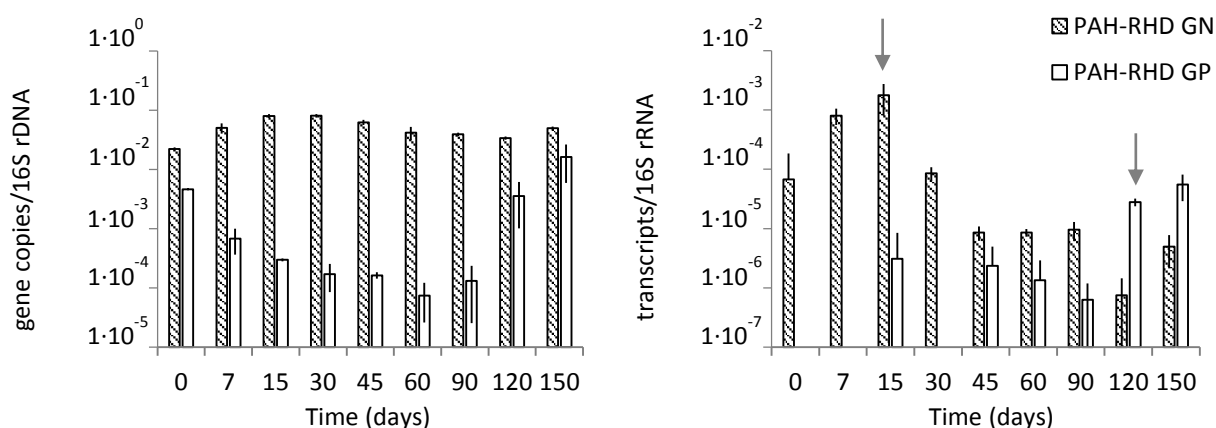


Figure 6.3. Proportion between PAH-RHD GN and GP genes copies related to 16S gene copies alongside the incubation time for the nutrients treatment (left) and active PAH-RHD GN and GP relative to 16S rRNA transcripts (right) in the nutrients treatment. Arrows point at the qPCR amplicons used to perform the clone libraries.

6.2.3 Phylogenetic analysis of the detected RHD gene transcripts

The phylogenetic assignment of the PAH-RHD GN and GP transcripts was investigated by clone library analysis of the amplicons obtained at their peaks of expression in the soil treated with nutrients, 15 and 120 days, respectively. For each set of primers, 20 clones were randomly selected and their respective inserts were sequenced. The analysis resulted in 19 quality reads from each library.

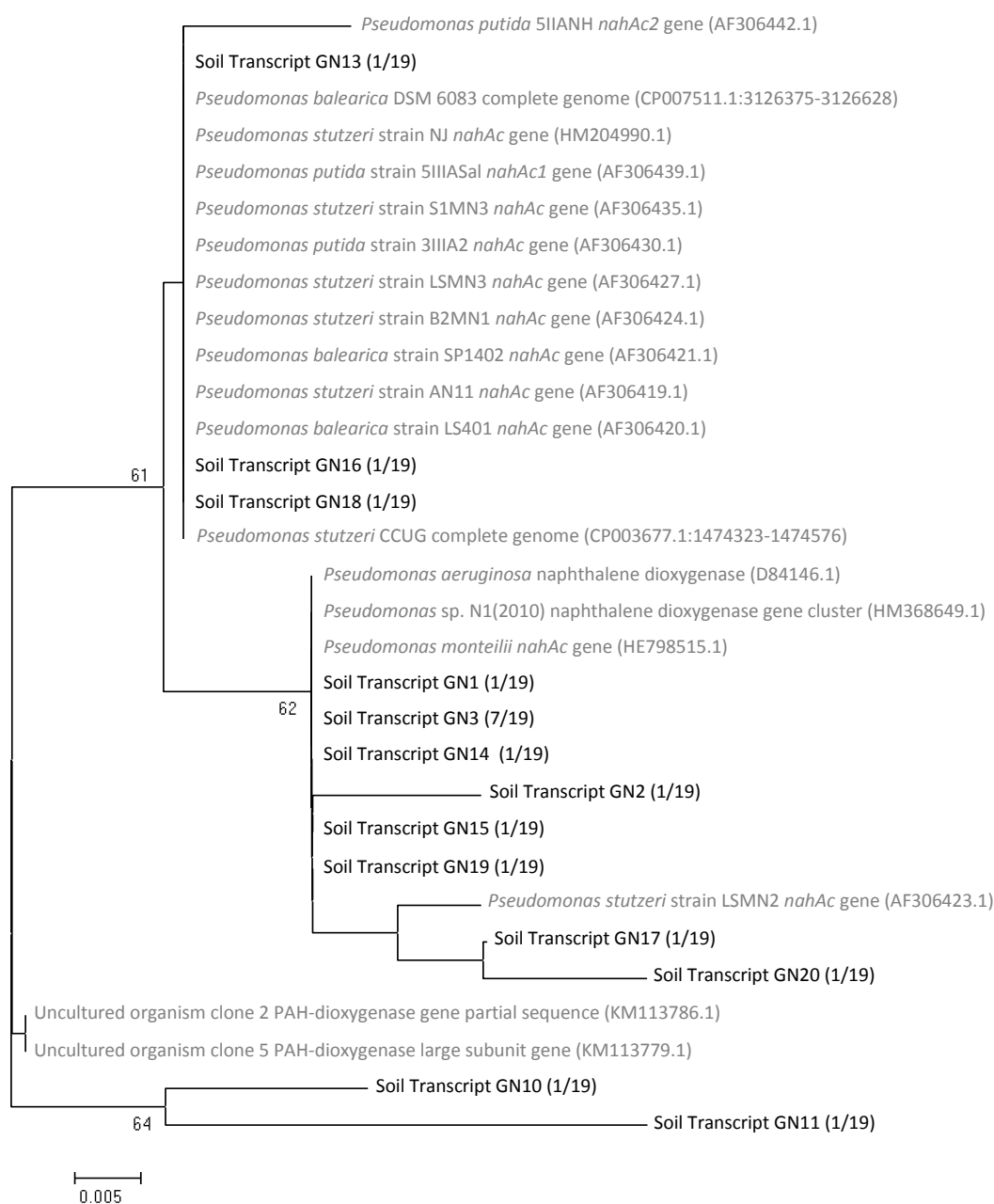


Figure 6.4. Phylogenetic reconstruction using the neighbor joining method of the deduced amino acid sequences from the clone libraries of the cDNA of PAH-RHD GN genes at the time of maximum expression (day 15) in the nutrients treatment. Reference sequences corresponding to the closest RHD GN gene sequences are also shown.

The sequence analysis of the clone library from the PAH-RHD GN gene produced 13 highly similar (94.2-99.6%) unique sequences. All clones presented a frequency of 1/19, except for GN3 (7/19), its predominance indicating the higher expression levels of this gene. When compared with the GeneBank database, all of them presented their highest similarity (98.8-100%) to *nahAc* genes from different *Pseudomonas* strains (Figure 6.4).

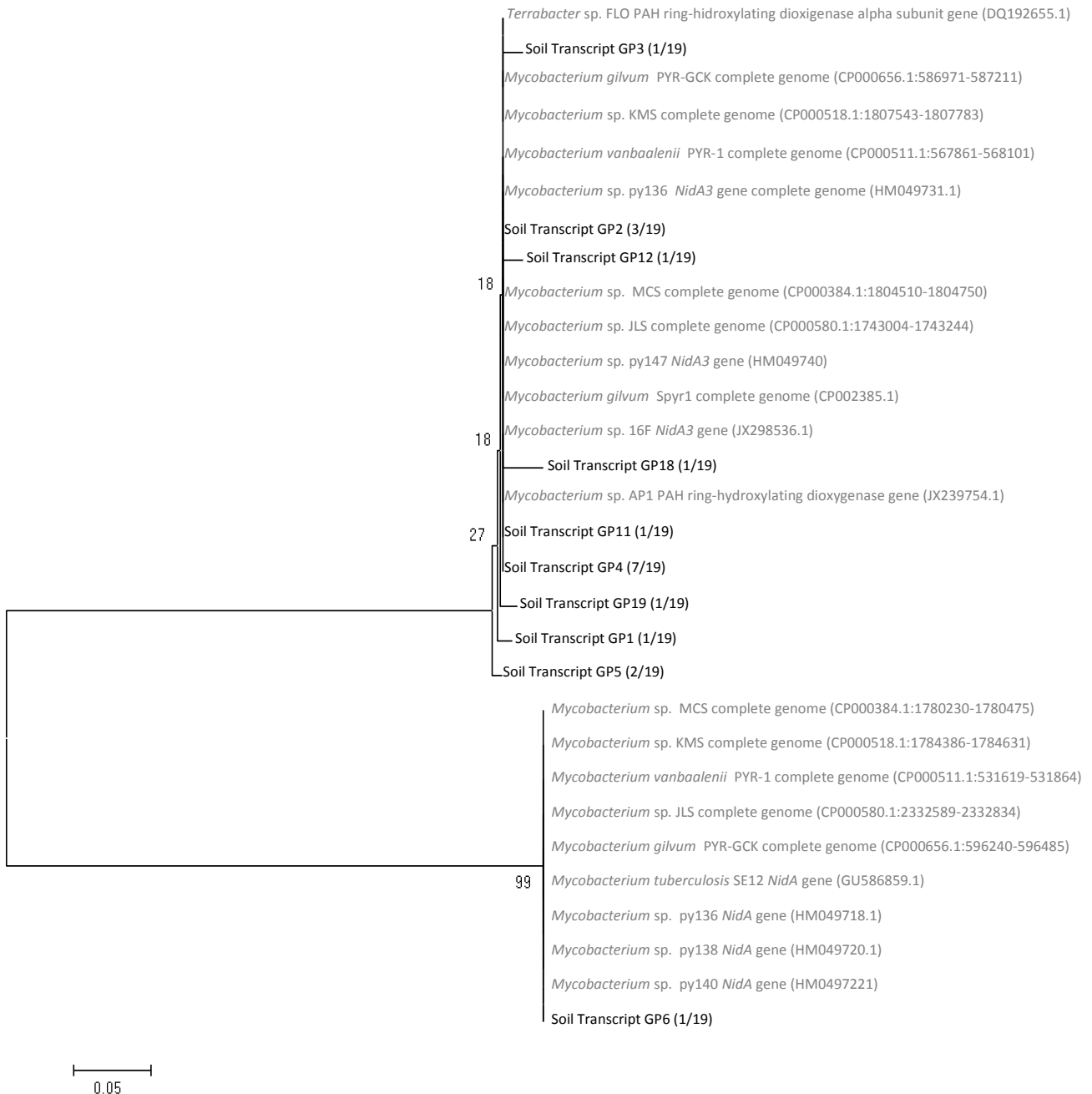


Figure 6.5. Phylogenetic reconstruction using the neighbor joining method of the deduced amino acid sequences from the clone libraries of the cDNA of PAH-RHD GP genes at the time of maximum expression (day 120) during the stimulation with nutrients. Reference sequences corresponding to the closest RHD GP gene sequences available in the Genebank database are also shown.

The sequence analysis of the RHD GP gene clone library resulted in 10 unique sequences. Their phylogenetic analysis demonstrated that the majority of the transcripts (18/19) corresponded to 9 highly similar (97.8-99.6%) sequences that were closely related (99.1-100%) to the *NidA3* genes of different *Mycobacterium* and *Terrabacter* strains (Figure 6.5). The remaining clone, GP6 (1/19), presented a completely distinct sequence, forming an independent branch within the phylogenetic tree. Comparison with sequences in databases identified GP6 as a *NidA* gene, with identical sequence to that of homologous genes from a number of *Mycobacterium* strains (Figure 6.5).

The relatively large number of different mRNA transcripts detected for each gene type (13 and 10, respectively) suggested the simultaneous expression of a number of homolog genes for RHD of GN and GP bacteria. This result illustrates that the observed PAH-degradation processes occurring in the soil would be probably the result of the synergistic cooperation of a number of different PAH-degrading strains, or enzyme activities, rather than from the action of a single main degrader.

6.2.4 Role of *Mycobacterium* in the biodegradation of PAHs

Considering the well-known capacity of *Mycobacterium* strains as HMW PAH-degrading bacteria (Kanaly and Harayama 2010; Vila et al. 2015), but also the evidences collected here indicating an increase of mRNA transcripts of PAH-RHD GP genes closely related to those described for mycobacteria coinciding with the phase of HMW PAH degradation, as well as the identification of signature mycobacterial FT and PY metabolites in the nutrient treated soil (Chapter 5), the presence, abundance and activity of members of *Mycobacterium* was tracked by qPCR using genus specific 16S rDNA primers (N. M. Leys, Ryngaert, et al., 2005b). The data obtained (Figure 6.6) showed a decrease in the

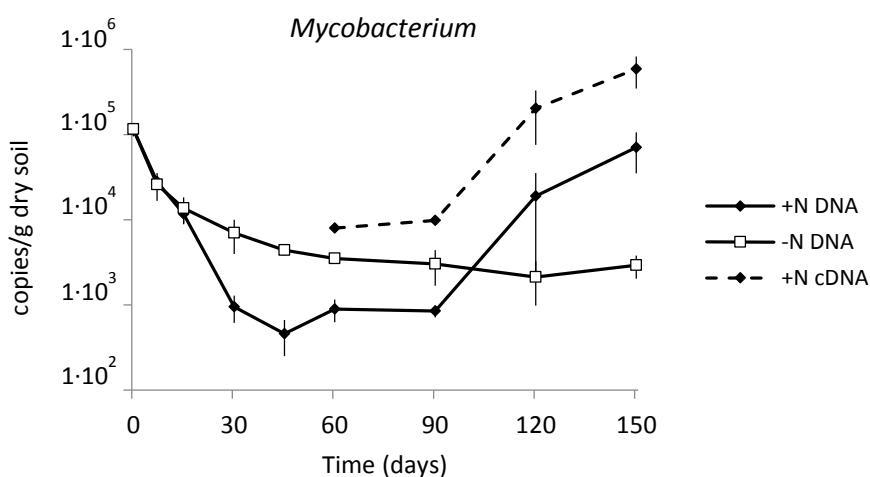


Figure 6.6. Quantification of the *Mycobacterium* specific 16S rRNA gene copies (DNA) and transcripts (cDNA) over the bioremediation process in both treatments (-N and +N). Missing points in the plot correspond to values below the detection limit. In the -N treatment, transcripts were not detected in any data point.

prevalence of the total mycobacterial populations for both treatments during the first 45 days, but from then on, in the nutrients treated soil the number of gene copies increased in more than 2 orders of magnitude. Consistently, without nutrients, mycobacterial 16S rRNA gene expression kept under the detection limit throughout the whole treatment, while the addition of nitrogen and phosphorous triggered the appearance of transcripts from day 60, and thereafter increased in parallel with the DNA copies, always 2 logarithms above, to reach a concentration of $5.88 \cdot 10^5$ 16S rRNA gene transcripts \cdot g dry soil⁻¹ at the end of incubation.

6.2.5 Community structure dynamics of the total and active bacteria in the soil

The quantitative differences observed between the 16S rRNA genes and their transcripts throughout the different phases of PAH biodegradation, raised the question of how different was the diversity and composition of the active populations in relation to the total bacterial community. Thus, the DNA and cDNA from the nutrient treated soil were analyzed by DGGE, revealing highly distinct banding profiles (data not shown). According to this, a pyrosequencing analysis of both DNA and cDNA was carried out for the treatment that involved both LMW and HMW PAH biodegradation, i.e. nutrient addition.

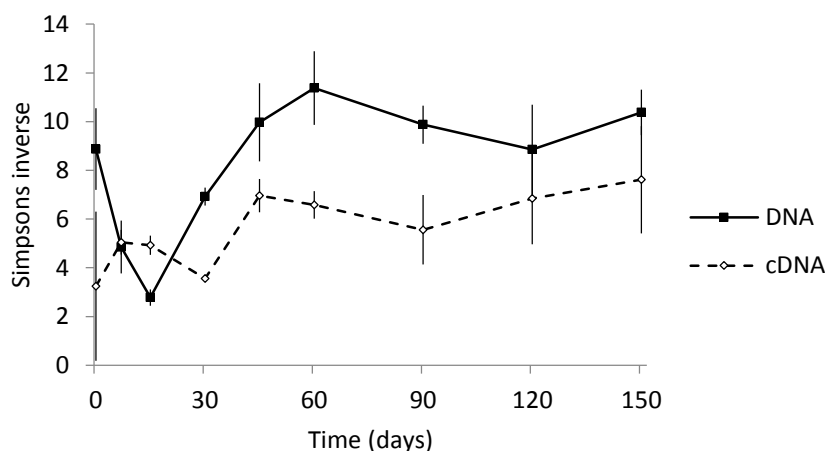


Figure 6.7. Alpha diversity estimated by the Simpsons' inverse index of the total (DNA) and active (cDNA) bacterial community throughout the incubation of the creosote polluted soil treated with nutrients.

The alpha diversity analysis of the 16S rDNA libraries expressed as the Simpsons' inverse index revealed differences between the total and active populations. In general, the diversity observed in the cDNA was always lower than that of the DNA extracts during almost all the incubation, revealing significant differences in composition between the total and active bacterial communities (Figure 6.7). This difference in the Simpsons' inverse index was even more pronounced during the peaks of activity (45 and 60 days), which coincided with the maximum degradation rates. This results suggest that only a

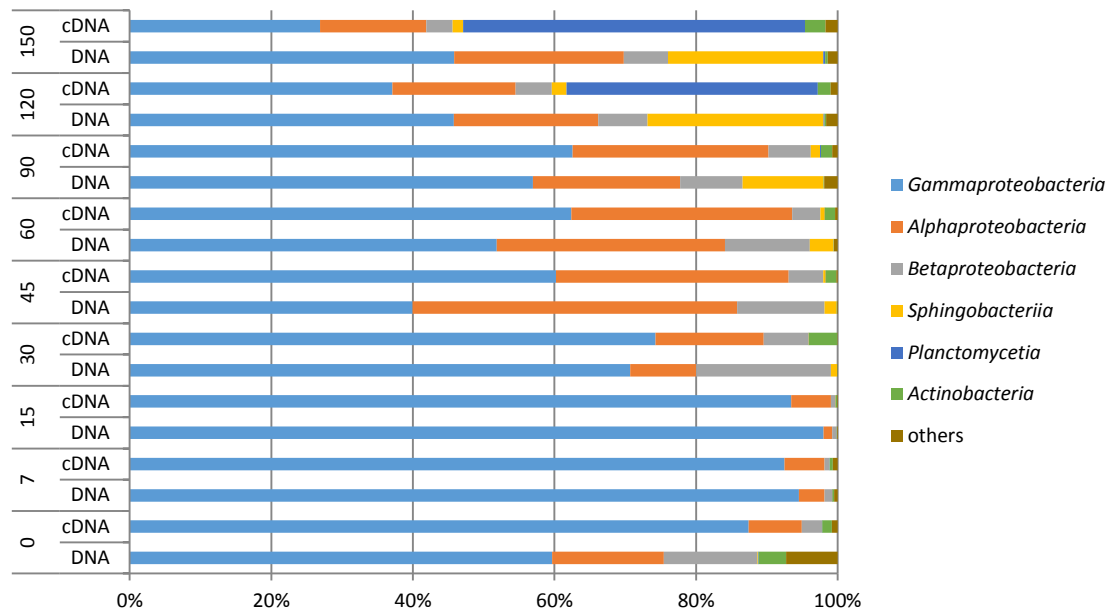


Figure 6.8. Relative abundance of the different classes that are part of the total (DNA) or the active populations (cDNA) in the soil during the incubation time. Others encompass the classes below the 0.5% of relative abundance and the unclassified sequences.

reduced fraction of the global community was actively contributing to PAH biodegradation.

The most abundant represented phylum in the soil throughout the experiment was *Proteobacteria* (47-99%, depending on the incubation time). Within this phylum there was a succession of the different classes. *Gammaproteobacteria* largely predominated during the first 90 days of incubation in both, the total (52-98%) and the active populations (60-93%), except for day 45 (Figure 6.8), when *Alphaproteobacteria* reached similar abundance in the DNA libraries but *Gammaproteobacteria* was still the major class in the active community (60%). *Alphaproteobacteria* was the second class in relative abundance, increasing after day 30 to reach a maximum at 45 days (46% of the total and active populations). *Betaproteobacteria* (initially 13%) remained almost undetectable during the first two weeks, but at 30 days suddenly incremented its relative abundance, reaching a maximum within the total (19%) and the active populations (6%) and experimenting little changes thereafter. *Sphingobacteriia*, widely the most abundant class within the *Bacteroidetes* in this soil (1% at T0), slowly gained importance after day 45 (2% in DNA and 0.3% in RNA) to reach its maximum at 120 days with a 25% of the total population and a 2% of the active bacteria. Surprisingly, *Planctomycetia*, a class within the phylum *Planctomycetes*, with very low abundance throughout the experiment (less than 0.2%) experienced a dramatic increase in relative abundance within the active populations (16S rRNA) at day 120 (36%). At 150 days, this unexpected class represented almost a half of the active population (48%). Lastly, *Actinobacteria* was unperceived when

we analyzed the total community, but was important in the active populations achieving maxima at 30 days (4%) and keeping at similar levels until the end of the treatment (150 days, 3%).

To correlate changes in the active microbial communities with PAH biodegradation, a Constrained Canonical Correspondence Analysis (CCA) was performed based on the distribution of the major active OTUs (>0.5%), accounting for 89 to 98% of the total relative abundances, throughout the nutrient treatment (Figure 6.9). The contribution of the LMW and HMW PAH biodegradation is represented in the plot with black arrows. The distribution of samples corresponding to time 0 until day 30 draw an imaginary line with similar direction and slope to those depicted by the vector illustrating the gradient of LMW PAH biodegradation. The most highly correlated active OTUs belong all to the phylum *Proteobacteria*, including members of the *Alpha* [*Haemobacter* (OTU20), *Skermanella* (OTU26), *Roseomonas* (OTU45) and *Bradyrhizobium* (OTU49)], *Beta* [*Acidovorax* (OTU29) and *Extensimonas* (OTU34)], and *Gamma* [*Pseudomonadaceae* (OTU1), *Pseudomonas* (OTU3, 4 and 17), *Pseudoxanthomonas* (OTU6), *Enterobacteriaceae* (OTU19) and *Nevskia* (OTU12)] subclasses. Some of these genera include well-known degrading strains or that have been previously related with PAH biodegradation, especially with 2 and 3 rings. The line drawn by the data points corresponding to the distribution of samples from time 45 days to the end of incubation completely change its direction, to correlate to that of the arrow representing the gradient of HMW PAH biodegradation. From 45 to 90 days the major active OTUs were still members of *Proteobacteria* but they fell into different genera. There was a clear predominance of members of the orders *Sphingomonadales*, including OTUs related to *Sphingobium* (10, 11, 14 and 16) and to uncultured representatives (18, 25, 32), and *Bulholderiales* (fam. *Alcaligenaceae*), including a single OTU affiliated to *Achromobacter* (7) and uncultured members of the order (21, 27). Other relevant *Proteobacteria* in this period were members of *Nevskia* (OTU12), *Pseudomonas* (OTU32), *Starkeya* (OTU46), *Acetobacteriaceae* (OTU39), *Roseomonas* (OTU48), *Rhizobiaceae* (OTU15) and *Methylocystaceae* (OTU35). However, from day 90 until the end of the experiment there was a dramatic shift in the structure of the active community, with the family *Planctomycetaceae*, including non-classified representatives (OTUs 23, 57 and 81) and members of the genus *Singulisphaera* (OTUs 13, 28, 33, 41, 42 and 67), becoming largely predominant. *Actinomycetales* (OTU66), including members of *Mycobacterium* (OTU70), were also active in these latter steps. One *Sphingobacteriia*, identified as *Olivibacter* (OTU9), and one *Sphingomonadaceae* (OTU68), belonging to *Alphaproteobacteria*, were also notably active between the 3rd and the 4th month of treatment.

The dynamics of the most active OTUs, showing relative abundances above the 5% in any of the cDNA libraries, were investigated in detail (Figure 6.10). At the beginning of the experiment, the active community was predominantly composed by one single OTU

affiliated to *Nevskia* (OTU12, 78%). Concomitantly with the global increase in bacterial activity within the community, this OTU was rapidly replaced by OTUs 4 (*Pseudomonadaceae*) and 6 (*Pseudoxanthomonas*) after the first week of incubation. One week later (15 days), the relative activity of two members of *Pseudomonadaceae* (OTU3, 28%; and OTU1, 17%) increased, the latter becoming the most active member of the community at day 30 (51%). Less active, but also with its peak of maximum relative expression at the same time, *Achromobacter* OTU7 appeared after one month (5%) of incubation to remain above the 2% of the total active community over the following two

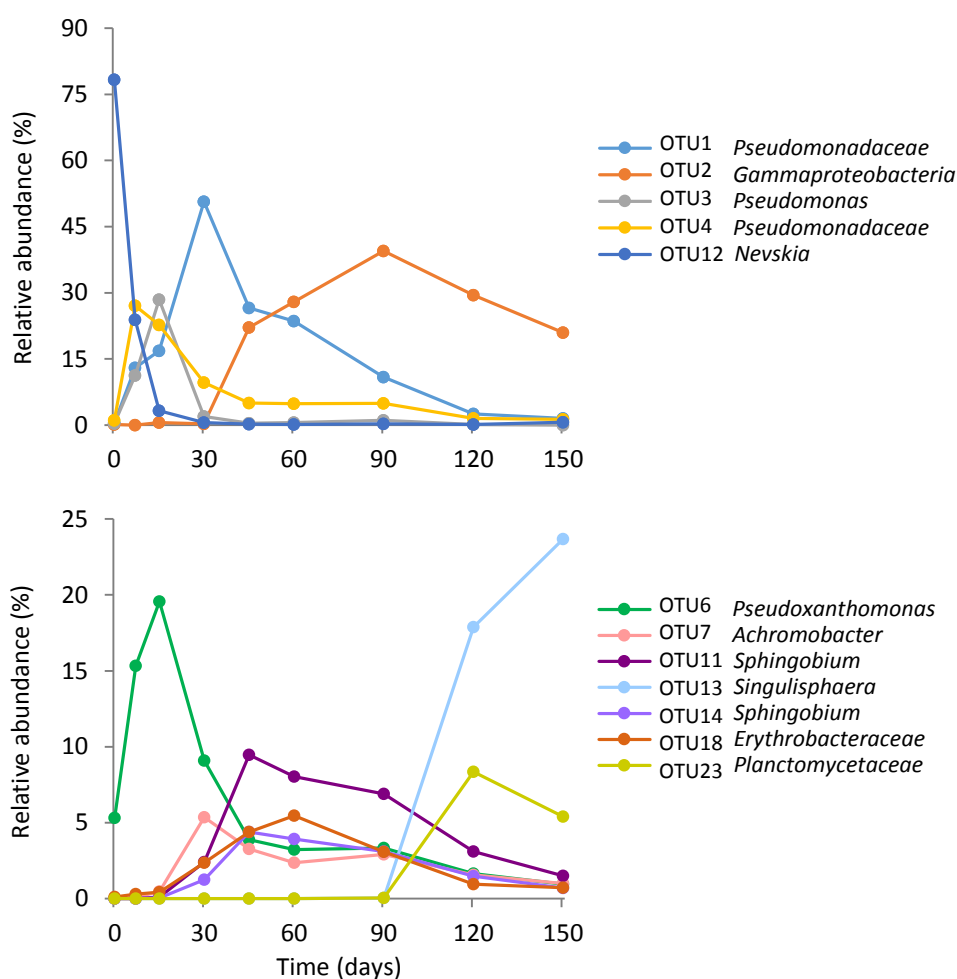


Figure 6.10. Relative abundance alongside the experiment of the most abundant OTUs in the cDNA (>20% on the top and >5% at the bottom). Error bars are not shown to improve the data interpretation.

months. At 45 days, coinciding with maximum depletion rates for HMW PAHs, three OTUs prevailed in the active community, one of the members of *Pseudomonadaceae* (OTU1, 27%), an unclassified Gammaproteobacteria (OTU2, 22%) and a member of *Sphingobium* (OTU11, 10%). These three OTUs were still the most active members of the community at 60 days, when a representative of *Erythrobacteraceae* (OTU18, 6%) became notably active. After three months of incubation, OTU2 (uncultured

Gammaproteobacteria) became from large (40%) the most active component. Finally, at 120 and 150 days the relative activity the members of *Plantomycetaceae* (OTUs 13 and 23) rose rapidly, which was consistent with that found in the CCA.

6.3 Discussion

Stimulation of the naturally occurring microbial communities by adjusting the soil water content with or without nutrients addition had proved to effectively stimulate PAH removal (93 and 69%, respectively) in the historically creosote polluted soil under study. These results demonstrated the existence of highly specialized autochthonous PAH-degrading populations, originating from the adaptive process to the long lasting contamination episode. Both treatments were carried out in parallel to ensure the necessary conditions for the PAHs to be degraded. Previous studies had indicated that full availability of nutrients might not always benefit PAH disappearance, as nitrogen and phosphorous could promote the growth of heterotrophic bacteria using carbon sources different from PAHs (Viñas et al., 2005). In our study, nutrient addition resulted in a higher rates and extension of PAH degradation, demonstrating their stimulatory effect on bacterial groups responsible for the degradation of all the PAHs, and being critical for the removal of HMW PAHs. Thus, the nutrient treatment was chosen to deepen in the study of the microbial community dynamics.

Quantitative and phylogenetic analysis of structural (16S rRNA) and functional (PAH-RHD) genes were performed both on DNA and RNA extracts. The observed quantitative and qualitative differences demonstrated the suitability of this combined methodological approach, provided the better accuracy of the RNA determinations to link functions to specific populations through time. DNA determinations might be biased by the presence of cells with a wide range of different levels of activity, including non-viable cells or free DNA, giving a distorted image of who is actually responsible of a given metabolic action in the soil at a specific moment.

The availability of nutrients did not have an effect on the total bacterial community (16S rDNA) concentration, that did not experience substantial changes during the incubation in any of the treatments. Bacterial activity (16S rRNA) increased during the first 15 days in both treatments, however, thereafter the increment with nutrient addition was dramatically higher indicating that it was limited in initial nutrient concentration conditions. This results are consistent with the occurrence of HMW PAH degradation only when nitrogen and phosphorous were added.

qPCR quantification of 18S rRNA genes indicated a minor abundance of fungal populations in terms of gene copies $\cdot g^{-1}$ of soil, showing values between 2 and 3 orders of magnitude lower than those of bacteria when incubated with nutrient addition. However, in this conditions, fungal populations became active after one month of incubation and

kept approximately constant thereafter. Thus, fungi could play a role on the biodegradation of HMW PAHs possibly in synergic collaboration with certain bacterial taxa. Considering that, a further analysis of the fungal community alongside the incubation could be of interest, and samples were stored to carry out these analysis in the near future.

The bacterial community was also analyzed from a functional point of view to specifically quantify the GN and GP PAH-degrading communities based on the abundance of genes encoding for RHDs. When nutrients were not limitant, high percentages (2-8%) of RHD-PAH GN respect to 16S rDNA were found. Those values were one or two orders of magnitude above those previously reported for other sites, for exemple Cébron et al. (2008) reported ratios between 0.02 and 0.6% for a former coking plant soil. However, the same authors described percertanges of RHD-PAH GP (0.05–0.92%) in the same range than those found here (0.01-1.62%). This relatively high abundance of the PAH degrading communities give additional support to the previous observation on the high degree of specialization of the authohtonous microbial community present in the soil under study. It is important to highlight that, although the PAH-RHD of GP presented lower gene copy numbers than those of GN during the whole incubation with nutrients, the GP RHDs exhibited substantially higher gene expression levels than those of GN, with transcript to gene copy ratios of 20%, in front of the 2% observed for GN.

Traditionally, Gram negative bacteria have been associated to the degradation of 2- and 3-ring PAHs, while HMW PAH depletion has been related to the metabolic action of Gram positives. In fact, if we only take into account the quantitative data from the analysis of the PAH-RHD transcripts our results would be consistent with this appreciation. The peak of RHD GN gene expression, between day 15 and and day 30, coincided with the highest LMW PAHs biodegradation. Interestingly, the most abundant phylotypes during that period were members of *Pseudomandaceae* and *Pseudoxanthomonas*, which is also consistent with the phylogenetic analysis of the RHD GN gene transcripts, showing their maximum similarity with *nahAc* genes of members of *Pseudomonas*. This genus is a well-known LMW PAH degrader and there are many publications supporting this capability (Haritash & Kaushik, 2009; Wilson & Jones 1993), one of the most recent reporting *Pseudomonas* sp. strain USTB-RU, isolated from a petroleum contaminated soil, and able to degrade phenanthrene through the protocatechuate pathway (Masakorala et al. 2013).

The presence of members of *Pseudoxanthomonas* has been commonly reported in community analysis during PAH degradation (Louvel et al. 2011; Singleton et al. 2011; Viñas et al. 2005), but only a few isolates of this genus have been proved to degrade PAHs. One *Pseudoxanthomonas* sp. DMVP2 recently isolated from a canal sediment in India degraded phenanthrene via the phthalic acid-protocatechuate acid pathway. Other studies reported the isolation of members of this genus for their ability to oxidize HMW PAHs, such as pyrene (Nopcharoenkul et al. 2011) and chrysene (Nayak et al. 2011), some

of them also being able to grow on phenanthrene. If we analyze our qPCR results of 16S rRNA transcripts together with the pyrosequencing data, *Pseudoxanthomonas* remained within the major active taxa until day 90, which could indicate its potential role also in the degradation of HMW PAHs.

Culture-independent methods have been increasingly applied to identify key microbial groups associated to PAH degradation, and this has permitted to bring to light a number of previously unknown taxa with PAH degrading capabilities (Vila et al. 2015), specially regarding HMW compounds. Culture dependent techniques easily produced 2- and 3-ring PAHs degrading isolates, more often GN, that grew on those compounds using lineal metabolic pathways (Mallick et al. 2011). Fluorathene degrading strains are both GN and GP (mycobacteria), while pyrene mineral media usually leded to the isolation of *Mycobacterium* (Kanaly & Harayama, 2010). On the other hand, it has been assumed that compounds with more than 4-rings are only degraded cometabolically (Jones et al. 2014; Kanaly et al. 2000). Nevertheless, recent studies on PAH degrading community dynamics often link GN bacteria to HMW disappearance and novel GN isolates have been reported to act on chrysene and pyrene (Vila et al., 2015). Thus, the perception that only GP bacteria were responsible for the removal of HMW PAH is changing. One possible explanation to the low succes on isolating HMW PAH-degrading bacteria other than mycobacteria, is that the degradation of those compounds would be driven by complex metabolic networks resulting from the cooperative interaction of various populations. Here, a number of GN phylotypes closely related to *Sphingobium*, *Achromobacter*, *Olivibacter*, *Starkeya*, *Acetobacteriaceae*, *Roseomonas*, *Rhizobiaceae* and *Methylocystaceae* were associated to 4- and 5-ring PAH removal. The majority of them have been previously related with the degradation of a variety of organic pollutants (Chen et al. 2013; Dashti et al. 2015; Viñas et al. 2005), but particularly, the first two are widely known PAH degraders (Deng et al. 2014; Ghevariya et al. 2011; Kunihiro et al. 2013; Maeda et al. 2014).

Despite their preference for LMW PAHs, some sphingomonads have been proven to also attack HMW compounds. This capability to oxidize a wide range of substrates relies on the possession of a number of diverse degradative enzymes and their relaxed substrate specificity (Kanaly & Harayama, 2010; Stolz, 2009; Vila et al., 2015). The existence of degradative plasmids containing a large number of genes encoding for xenobiotic-oxidating enzymes that can be only horizontally transferred between sphingomonads, provides this taxa with a powerful tool to rapidly adapt to new carbon sources (Stolz, 2014). *Sphingobium* sp. KK22 (Kunihiro et al., 2013; Maeda et al., 2014), that grows on PHE and also attacks FT, BaA and BkFT, and *Sphingobium* sp. PNB (Khara et al., 2014), that metabolizes some monoaromatic and polyaromatic compounds, are good examples of the metabolic plasticity of sphingomonads in front of PAHs.

Although some works describe the PAH-degrading capabilities of members of *Achromobacter*, this genus has not attracted as much attention as pseudomonads and sphingomonads. This could be attributed to its highly oligotrophic behaviour, that converts the members of *Achromobacter* as easy-to-isolate bacteria, but it is also difficult to demonstrate their growth at the expense of a single carbon source, since they can grow with trace concentrations of substrates. This genus is often found in saline environments such as polluted estuaries and seawater. In works from Ghevariya et al. (2011) and Dave et al. (2014) the chrysene biodegradation rate of an halotolerant *Achromobacter xylosoxidans* was greatly improved by regulating the pH and using Triton X-100, β -cyclodextrin and glucose as cosubstrate. This suggests that *Achromobacter* could need an extra carbon source to cometabolize HMW PAHs.

Olivibacter is a relatively new genus which was first isolated from olive-oil mill wastes (Ntougias et al. 2007). In that work, *Olivibacter* was also described as degrader of protochatechuate, a common monoaromatic intermediate in different PAH metabolic pathways. Thus, it would not surprise if this genus played a role as a secondary degrader, feeding on metabolites produced by other bacteria. More recently, this genus has been related to hydrocarbon biodegradation (Dashti et al. 2015; Szabó et al. 2011) and DDT pollution (Chen et al. 2013). Curiously, here the members of *Olivibacter* always presented higher proportions in the total community than in the active community. For example, at 120 days, when its peak of relative abundance occurred, this genus of *Sphingobacteriia* accounted for a 25% of the total community, but only a 2% of the active community.

Finally, the most studied HMW PAH-degrading class, *Actinobacteria*, also seem to play an important role in the removal of those compounds. The results obtained from the quantification of PAH-RHD GP transcripts indicated an activation of the GP degrading bacteria from day 45 until the end of incubation, reaching a maximum at 120 days. Simultaneously, during this period the concentration of HMW PAHs diminished. Knowing that the used primers basically targeted *Mycobacterium* dioxygenases, there could be a little delay in the activation of GP degraders and this may be in agreement with their slow growth rates (they are often considered as k-strategists). The peak of *Mycobacterium* specific 16S rRNA transcripts took place at the end of the experiment, and this could explain that the HMW PAH kinetics did not reach the asymptotic phase described by the "hockey stick" model. During this period, between 90 and 150 days, *Actinobacteria* now without competence from the faster growing members of the community, could have been able to degrade the low available residual HMW PAHs compounds enhancing their bioavailability with their known ability to adhere to hydrophobic surfaces. Actually, this strategy could have favored this taxon during the last two months, when the activity of all the other bacterial groups decreased (except *Singulisphaera*).

Singulisphaera, a genus within the *Plancomycetales* that has never been related to polluted environments, dramatically increased its activity between 90–120 days. At the end of incubation, it accounted for almost a 50% of the active community. Conversely, if we only had observed the 16S rDNA results, this bacterial group would have remained unnoticed, because it only represented the 0.27% of the whole community. Definitely, it could be of great interest to investigate its ecological function in the soil, which could be related with the restoration of natural soil conditions, and act as indicator of quality improvement of the soil. In fact, it has been proved that *Planctomycetes* abundance increases in abandoned soils or in soils without previous human activity, in respect to human impacted environments (Buckley et al. 2006).

To summarize, the most important conclusion of this chapter is that a mere analysis of the total community structure (DNA) could produce an important bias, that might be overcome by the complementary identification of their actually active components (cDNA).

CHAPTER 7

General discussion

7 General discussion

PACs in the environment are always encountered in the form of mixtures formed by a vast variety of compounds. Thus, it is to be expected that the natural cycling processes carried out by soil microbial communities would be the result of the interaction of different populations building complex metabolic networks. Understanding these processes is fundamental from a basic research point of view, but also to optimize current bioremediation strategies in terms of PAC-removal efficiency, monitoring and risk assessment. To unravel the functions carried out by specific populations it is necessary to use multidisciplinary approaches encompassing analytical chemistry, classical microbiology and molecular microbial ecology methods. In this Thesis the aim of linking functions to specific bacterial populations was addressed by applying such methods to selected low diversity microbial communities, pure cultures, and a real creosote polluted soil. The integration of the obtained results allowed a further insight into the key bacterial processes involved in the biodegradation of PACs in polluted soils.

It is well known that one of the main drawbacks for the implementation of bioremediation is the unpredictable endpoint concentrations of the technology, leading to the accumulation of a residual fraction of the contaminant enriched in HMW compounds (Ortega-Calvo et al. 2013). Here, we designed an *ad hoc* enrichment method to select a HMW PAH-degrading community from a polluted soil using a sand-in-liquid system containing sand coated with a biologically weathered creosote NAPL. After several transfers we obtained a stable microbial consortium designed UBHP. This less complex community became a model to study the microbial populations and processes involved in HMW PAH removal in PAH polluted soils by mimicking, in a more realistic manner than previous studies (Lafortune et al. 2009; Sun et al. 2010), the actual processes taking place *in situ*, facilitating at the same time the isolation of key players.

On the other hand, the aerobic stimulation of the microbial populations present in a real creosote polluted with and without nutrients addition, permitted to find the suitable conditions for the extensive biodegradation of both LMW and HMW PAHs. Nutrient addition highly increased HMW-PAH removal (up to 87%), and allowed, for the first time, to monitor the simultaneous N-PAC biodegradation and the formation and fate of oxy-PAHs. To identify the microbial communities involved, the kinetics of PAC biodegradation were compared with the substrate specific community dynamics analyzed with a combined culture-dependent (MPN enumeration) and independent (16S rDNA PCR-DGGE and sequencing) approach. Since the difference between treatments resided in the biodegradation of HMW PAHs in the nutrient amended soil, the soil treated with nutrients

was used to investigate the microbial communities and functional genes present (DNA) and actively contributing (RNA) to the depletion of 4- and 5-ring PAHs.

In both, the batch cultures of consortium UBHP and the lab scale enhanced natural attenuation experiment using real polluted soil the removal of PAHs was sequential. The LMW PAHs disappeared first and this triggered the depletion of the 4-ring PAHs, which degradation kinetics grouped in highly similar pairs (FT+PY and BaA+CHY) possibly indicating that they were attacked by the same microbial populations. ANT, despite the great difference in the initial concentration in the two studies, represented the exception of the 3-ring PAH degradation kinetics, showing a linear depletion along the incubation in both systems. The 5-ring PAHs are also degraded in similar extend in the UBHP cultures (42%) and in the amended soil (50%).

When we thoroughly examined all the analyzed parameters in the different stages of this sequential PAH diminution, we also observed many similarities between the bacterial populations and functions present in both communities (UBHP consortium and nutrient stimulated soil). During the first 2 weeks of incubation of the nutrient amended soil, naphthalene rapidly diminished to almost completely disappear. In this period also 9-fluorenone, carbazole and methylcarbazole exhibited a fast depletion. In addition, day 15 represents one of the peaks of accumulation of acidic metabolites, when well-known intermediates of LMW-PAH degradation, such as salicylic acid and phthalic acid, but also products of the cometabolic action of RDH dioxygenases on those compounds (i.e. naphthalene carboxylic acid, 1,8-naphthalic anhydride or 1,8-naphthalenedicarboxylic acid), were produced. Evidences indicate that the microbial populations responsible for the transformation of those PACs are members of *Pseudomonas* and *Pseudoxanthomonas*. On one hand, during the first 15 days, PHE and 9-fluorenone degraders increased in two orders of magnitude and the most abundant populations in the MPN wells belonged to those genera. On the other hand, the maximum of acidic metabolite accumulation co-occurred with the peak of expression of the PAH-RHD GN genes, with the subsequent phylogenetic analysis of the formed mRNAs associating them to *nahAc* genes of various *Pseudomonas* strains. Moreover, the great activity of these taxa during this specific period was also corroborated by the pyrosequencing analysis of 16S rRNA gene transcripts, since the families *Pseudomonadaceae* and *Xanthomonadaceae*, both represented basically by the previously named genera, accounted for 68 and 20%, respectively, of the total active community at time 15 days.

The disappearance of the 2-ring PAH NAPH was followed by a fast removal of the 3-ring PAHs and methylquinoline, all of them reaching more than a 70% of degradation between 15 and 30 days, with the exception of anthracene. This high transformation rates also resulted in a transient accumulation of oxidation products and intermediates of LMW PAH degradation pathways. For example, the mentioned 1,8-naphthalenedicarboxylic acid,

resulting from an unspecific attack by oxygenases on acenaphthene (Selifonov et al. 1996), maintained its maximum of accumulation after one month. Other products detected were the ANT degradation intermediate *cis*-4-(2-hydroxynaphth-3-yl)-2-oxobut-3-enoic acid and its cometabolic product 9,10-anthraquinone. 9-Phenanthroic acid resulting from the monooxidation of the methyl group of 9-methylphenanthrene, also accumulated, demonstrating the depletion of alkyl PAHs together with their non-methylated counterparts, as occurred during the batch incubations of consortium UBHP. As mentioned before, these cometabolic products could be attributed to a fortuitous attack of the PAH-RHD GN that remained highly active throughout this period.

During the fast removal of the 3-ring PAHs, PHE degraders remained as the most abundant degrading populations, but a new group of bacteria able to grow on ANT and BaA drastically increased feeding on the 3-ring compounds. In these populations the preeminent bacteria were members of *Achromobacter* and *Olivibacter*, thus representing, together with the phylotypes of *Pseudomonas* and *Pseudoxanthomonas*, the major actors in 3-ring PAH degradation. This is consistent with the detection by pyrosequencing of a dramatic increase within the active soil community of members of the genus *Achromobacter* (Figure 7.1). Another phylotype related to *Sphingobium* also presented a great increment in activity, but remained unperceived by the MPN-DGGE approach. This could be due to the presence of the representatives of *Pseudomonas* and *Pseudoxanthomonas* that were still the most abundant in that moment, and could have precluded the detection of *Sphingobium* in the most diluted PHE wells. Indeed, the community analysis of consortium UBHP revealed that members of *Sphingobium* and *Achromobacter* positively responded to exposure to PHE, and the isolates *Sphingobium* S3 and *Achromobacter* S8 were able to eliminate PHE from the sand-in-liquid system, confirming the actual key role of these taxa in the removal of PHE in the creosote polluted soil.

Following with the sequential degradation of PAHs, the depletion of the LMW PAHs triggered the removal of the 4-ring PAHs, grouped in pairs of highly similar kinetics (FT-PY and BaA-CRY), and that of the N-PACs acridine, methylacridine and dimethylquinolines. As observed for the dimethyl derivatives of PAHs in the cultures of consortium UBHP, in the soil the dimethylquinolines were removed later than the monomethylquinolines, suggesting that the preference of degradation for N-PACs followed patterns compatible with those for PAHs. At 30 days, an activation of the fungal community was observed reaching a maximum of 18S rRNA gene transcripts at 45 days. This also concurred with the peak of expression of the bacterial populations (16S rRNA transcripts) and the activation of PAH-degrading GP bacteria (estimated as RHD-GP gene transcripts).

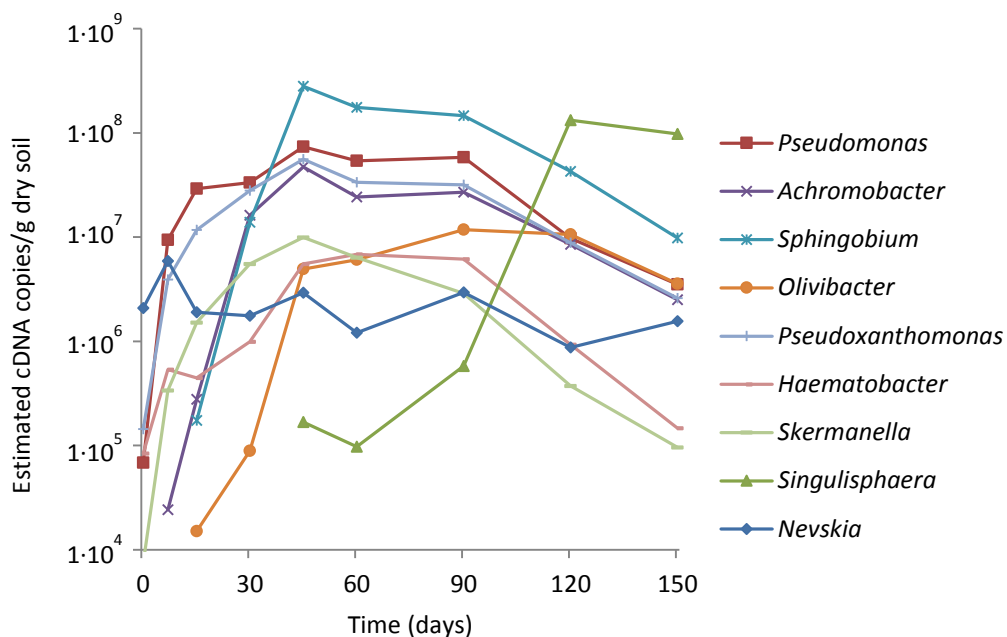


Figure 7.1. Estimated relative distribution of the 16S rRNA gene transcripts/g of dry soil for the most active genera. Estimation was based on qPCR data of 16S rRNA gene transcripts and the relative distribution of the different genera in the 16S rRNA pyrosequencing libraries of cDNA. Only those genera accounting for >2% in at least one library were considered.

The first HMW PAHs to be attacked was the pair FT/PY, their degradation being clearly correlated with the rapid increase of FT degraders that were mainly represented by members of *Sphingobium*. The substantial increase of the members of this genus within the active soil community (Figure 7.1), and their response to the exposure of consortium UBHP to FT, provided additional evidences of their key role in the removal of this PAH. In fact, when the isolate *Sphingobium* sp. S3 was incubated with the creosote PAH mixture, FT was drastically depleted, this giving a direct proof of the implication of this genus in FT removal in the soil. The fact that PY was also removed during the incubation of this strain with the weathered creosote, together with the low concentration of PY degraders in the soil in the initial phases of pyrene degradation, and the similar kinetics observed for FT and PY could indicate that *Sphingobium* oxidized pyrene without using it as a carbon source. Actually, Kunihiro et al. (2013) and Maeda et al. (2014) described the metabolic versatility of *Sphingobium* strain KK22 that grows on PHE and also oxidizes FT, BaA and BkFT.

The levels of gene expression of PAH-RHD GP at time 60 days, and the amplification of 16S rRNA gene transcripts using *Mycobacterium* specific primers from that point to the end of incubation, suggests that mycobacteria could also play a role in FT and PY degradation. Moreover, at day 60, signature metabolites of the degradation of FT [Z-9-(carboxymethylene)-9H-fluorene-1-carboxylic acid, (López et al. 2006)] and PY [6,6'-dihydroxy-2,2'-biphenildicarboxylic acid, (Vila et al. 2001)] by members of this genus reached their peak of maximum accumulation. Therefore, members of *Mycobacterium*,

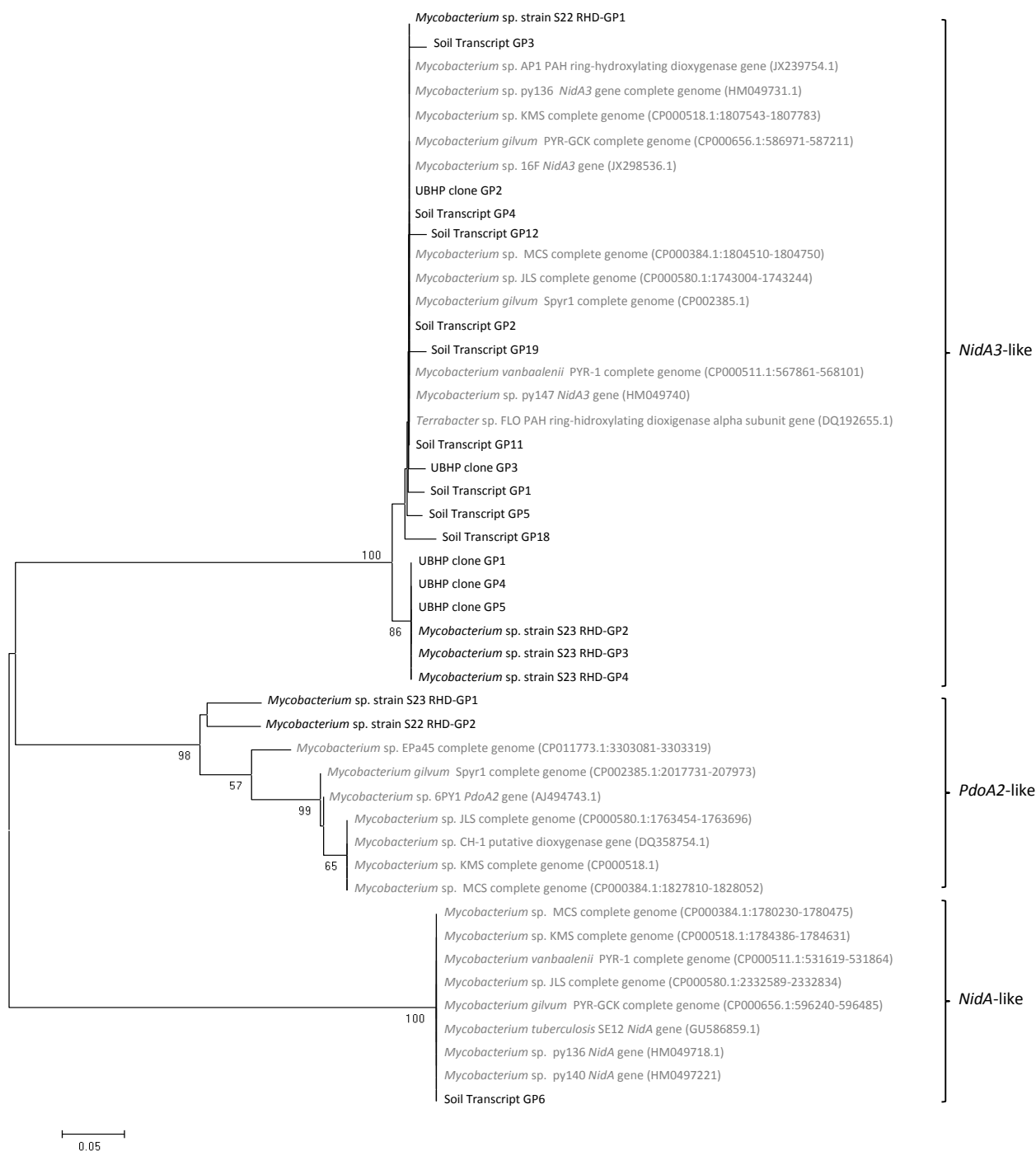


Figure 7.2. Phylogenetic reconstruction using the neighbor joining method of the deduced amino acid sequences from the clone libraries of the cDNA of PAH-RHD GP genes at the time of maximum expression (day 120) during the stimulation with nutrients, the clones from the consortium UBHP and the *Mycobacterium* strains S22 and S23. Reference sequences corresponding to the closest RHD GP gene sequences available in the Genbank database are also shown.

despite their low abundance within the global community, contributed to the degradation of PY and FT probably using them as a growth substrate. Of course, this statement is strongly supported by the results obtained with the isolated *Mycobacterium* strains (S22

and S23) acting on creosote, as well as by the analysis of the GP RHD in the UBHP consortium, in the isolates and in the nutrient treated soil.

The ratio of PAH-RHD GP transcripts/gene copies in the soil, with sequences closely related to genes of *Mycobacterium* strains, demonstrates their high activity, being 100 fold higher than those of GN at their respective peaks of maximum expression. Figure 7.2 shows the phylogenetic reconstruction of all the PAH-RHD GP sequences of both assays, including those detected in the consortium UBHP, in the *Mycobacterium* strains isolated from UBHP and the transcripts cloned from the biostimulated soil. All the sequences are distributed in three different clusters, corresponding to *NidA3*-, *NidA*- and *PdoA2*-like genes. Curiously, most of the GP RHD genes amplified clustered with *NidA3*-like sequences, and of special relevance is one of the RHDs of strain *Mycobacterium* sp. strain S22 (RHD-GP1) that was detected as a major RHD in the microbial consortium UBHP (UBHP clone GP2) but also as an active player within the soil community (soil transcript GP2).

The next PAH pair to be depleted, although with lower biodegradation rates, was BaA and CHY. Unfortunately, we did not follow the CHY degraders over the incubation of the stimulated soil. However, the highly consistent kinetics observed for both BaA and CHY, suggest that they might have been attacked by the same populations. In fact, when consortium UBHP was exposed to BaA and CHY supplied as single substrates, the community DGGE profiles from both incubations were highly similar, indicating that the same taxa, namely *Pseudomonas*, *Sphingobium*, *Achromobacter* and an unclassified *Gammaproteobacteria* were involved in their removal. A similar trend was observed during the degradation of a heavy fuel oil by an enriched marine microbial consortium; BaA and CHY presented identical biodegradation kinetics within the mixture, and presented highly consistent community profiles after exposure to both substrates independently (Vila et al., 2010).

Surprisingly, despite the removal of HMW PAHs without nutrients was scarce, there were no significant differences in the counts of BaA-degrading microorganisms between the soils treated with or without nutrients. These results are consistent with the increment of those populations in the nutrient amended soil during the fast removal of 3-ring PAHs, and further confirm that they were actually feeding on LMW PAHs. This is also in accordance with both the degradation kinetics and the degrading population dynamics (MPN) of ANT and BaA being alike. Assuming that they were attacked by the same microbial populations, the early grow of the BaA degraders before the depletion of that PAH is explained. According to the DGGE excised bands, these populations encompass members of *Achromobacter*, *Olivibacter* and *Bradyrhizobium*.

Otherwise, during the degradation of the pair BaA/CHY in the nutrient treated soil, there was an increment of the activity of an unclassified *Gammaproteobacteria* (Figure 7.1). It has not yet been elucidated if this phylotype corresponds to phylotypes S17-S20 detected in consortium UBHP. However work will be done to figure out if this highly relevant soil phylotype (OTU 2) is also related to the previously described Pyrene-Group 2 (Singleton et al., 2006), which has also been associated to BaA degradation by SIP analysis of a PAH-polluted soil (Jones et al. 2011).

Finally, the 5-ring PAHs were depleted following linear kinetics during almost all the incubation time of the nutrient amended soil, not presenting correlation to the specific grow of any of the assessed phylotypes. In fact, when the consortium UBHP was incubated with BaPY as a sole carbon source, there was neither a significant depletion of this PAH nor growth of the microbial community. This suggests that, as generally assumed, the biodegradation of these highly recalcitrant compounds needs the presence of more biodegradable cosubstrates that trigger the enzymatic induction, and thus, the cometabolic oxidation of these compounds. In fact, the major strains described as 5-ring PAH-degrading bacteria were cultured or induced with other substrates. For example, the above-mentioned strain *Sphingobium* KK22 is able to transform BkFT when cells are induced with PHE (Maeda et al. 2014), and members of this genus were very active in our soil experiment during almost all the treatment (Figure 7.1). *Sphingomonas yanoikuyae* JAR02 growing on salicylic acid was capable to cooxidize BaPY, while *Novosphingobium pentaromativorans* US6-1 incubated with a mixture of several HMW PAHs and 2-hydroxypropyl β -cyclodextrin acted on BbFT plus BaPY (Rentz et al. 2008; Sohn et al. 2004). As well, the well-known strain *Mycobacterium vanbaalenii* PYR-1 is able to cometabolically attack the highly carcinogenic PAH BaPY (Moody et al. 2004).

Overall, when analyzing the overall PAH degradation kinetics and the microbial community dynamics in the soil, two sequential cycles are observed. The first cycle (days 0-60) corresponds to the almost removal of the 3-ring PAHs, except anthracene, and maximum rates for fluoranthene and pyrene degradation. Then, it seems that there is a shift in the microbial populations (days 60-90 days) that is followed by another cycle (days 90-120) in which the degradation of anthracene is resumed and followed later on by a faster depletion of the 4- and 5- rings PAHs. If we analyze in detail the evolution of the populations, results from chapter 5 indicate that the second cycle includes a rise in the fluorene, pyrene, anthraquinone and diphenic acid degraders. Besides the specific results on mycobacteria and their RHDs discussed above, the information that we have about the possible shift in populations after 90 days are the DGGE analysis of the MPN wells from pyrene indicating the presence of unidentified new phylotypes, and subsequent dramatic increase of the genus *Singulisphaera* and another unclassified group of planctomycetes. The available literature information on *Singulisphaera* is scarce and

there is no association of the *Planctomycetes* with PAH degradation. With these data, it seems that mycobacteria play a key role in the removal of the residual PAHs between 90-120 days. We hypothesize during the first degradation cycle these slow growing bacteria are outcompeted by the faster growing Gram-negatives that grow on the readily available fraction of the PAHs. When this fraction is exhausted those bacterial groups become inactive, and the low growing mycobacteria, with their higher hydrophobicity and capacity to attach to NAPLs, start to efficiently degrade the residual less available fraction of anthracene, and 4- and 5- ring PAHs, maybe making available carbon that could be use by other bacterial groups.

CHAPTER 8

Conclusions

8 Conclusions

- The developed sand-in liquid enrichment system with the creosote HMW PAH-mixture as carbon source was a suitable method to obtain a representative microbial consortium that efficiently reproduced the processes for the *in situ* biodegradation of those PAHs in polluted soils.
- Consortium UBHP caused an extensive degradation of 4- and 5- ring PAHs. The thorough analysis of its community structure and functions provided insight into the interactions between populations and facilitated the recovery of relevant isolates with capacity to degrade PAHs.
- The natural microbial communities from the soil responded to the biostimulation treatment by extensively removing the bulk of PAHs (69% and 93%, in the absence or presence of nutrients, respectively). Nutrient addition resulted particularly effective in promoting the biodegradation of HMW PAHs (4- and 5-rings), N-PACs and Oxy-PAHs.
- The initial fast and almost complete removal of the 2- and 3-ring PAHs in the nutrient amended soil was attributed to the high activity of members of the genera *Pseudomonas*, *Pseudoxanthomonas*, *Achromobacter* and *Olivibacter*. Accordingly, the functional analysis of the community confirmed the expression of a number of *nahAc* genes mainly related to pseudomonads, which also seemed to act cometabolically on other substrates.
- The individual PAC degradation kinetics, molecular analyses and metabolomic profiles indicate that some PAHs are partially cometabolized in the initial phases of degradation, producing oxy-PAHs, especially ketones and quinones, which require the participation of alternative populations for their further removal. In non-limiting conditions the autochthonous populations effectively eliminate the transiently accumulated compounds also compensating for their chemical formation. This suggests that the oxy-PAHs could act as nodes in complex metabolic networks, where subproducts from one population maybe reutilized by another.
- The subsequent degradation of the 4-ring PAHs fluoranthene and pyrene is mainly associated to members of *Sphingobium*, which apparently cause a cometabolic non-productive degradation of the latter.

- The key role of the members of *Mycobacterium* in the degradation of HMW PAHs in soils is confirmed, outcompeting the LMW PAH degraders in the utilization of the low bioavailable residue during the late degradation phase. This group possibly cooperates with other bacterial taxa, such as a group of non-classified *Gammaproteobacteria*, and fungal populations.
- The transient accumulation of acidic metabolites during the PAH biodegradation and their further disappearance indicates that those products could be used as indicators of active biodegradation in natural attenuation technologies and to monitor the progress of a bioremediation processes.
- The total and active bacterial communities presented clearly distinct profiles along the incubation. The analysis of the dynamics of the active community provided a more accurate insight in the actual processes taking place *in situ* on a real-time basis, thus allowing a more precise linking between the communities and their function.
- The detection of functional genes and their expression levels proved to be useful in attributing functions to bacterial populations, especially pointing out the differential expression of GN (*nahAc*) and GP (mainly *NidA3*) dioxygenases in the initial and later phases of incubation, respectively. However, the information gathered from this analysis is still limited by the availability of primers that cover a wider diversity of dioxygenases.

CHAPTER 9

References

9 References

- Alonso-Gutiérrez, J., Figueras, A., Albaigés, J., Jiménez, N., Viñas, M., Solanas, A. M., & Novoa, B. (2009). Bacterial communities from shoreline environments (costa da morte, northwestern Spain) affected by the prestige oil spill. *Applied and Environmental Microbiology*, *75*(11), 3407–18.
- Amann, R. I., Ludwig, W., Schleifer, K. H., Amann, R. I., & Ludwig, W. (1995). Phylogenetic identification and in situ detection of individual microbial cells without cultivation . Phylogenetic Identification and In Situ Detection of Individual Microbial Cells without Cultivation, *59*(1), 143–169.
- Andersson, J. T., & Achten, C. (2015). Time to Say Goodbye to the 16 EPA PAHs? Toward an Up-to-Date Use of PACs for Environmental Purposes. *Polycyclic Aromatic Compounds*, 1–25.
- Bamforth, S. M., & Singleton, I. (2005). Bioremediation of polycyclic aromatic hydrocarbons: current knowledge and future directions. *Journal of Chemical Technology & Biotechnology*, *80*(7), 723–736.
- Bandowe, B. a M., Lueso, M. G., & Wilcke, W. (2014). Oxygenated polycyclic aromatic hydrocarbons and azaarenes in urban soils: A comparison of a tropical city (Bangkok) with two temperate cities (Bratislava and Gothenburg). *Chemosphere*, *107*, 407–414.
- Bardos, P., Bone, B., Boyle, R., Ellis, D., Frank, E., Harries, N. D., & Smith, J. W. N. (2011). Applying sustainable development principles to contaminated land management using the SuRF-UK framework. *Remediation Journal*, *21*(3), 81–87.
- Bleeker, E. A. J., Van Der Geest, H. G., Klamer, H. J. C., De Voogt, P., Wind, E., & Kraak, M. H. S. (1999). Toxic and genotoxic effects of azaarenes: Isomers and metabolites. *Polycyclic Aromatic Compounds*, *13*(2), 191–203.
- Blum, P., Sagner, A., Tiehm, A., Martus, P., Wendel, T., & Grathwohl, P. (2011). Importance of heterocyclic aromatic compounds in monitored natural attenuation for coal tar contaminated aquifers: A review. *Journal of Contaminant Hydrology*, *126*(3-4), 181–194.
- Bouchez, M., Blanchet, D., & Haeseler, F. (2000). Efficiency of defined strains and of soil consortia in the biodegradation of polycyclic aromatic hydrocarbon (PAH) mixtures, 429–435.
- Buckley, D. H., Graber, J. R., & Schmidt, T. M. (1998). Phylogenetic analysis of nonthermophilic members of the kingdom Crenarchaeota and their diversity and abundance in soils. *Applied and Environmental Microbiology*, *64*(11), 4333–4339.
- Buckley, D. H., Huangyutham, V., Nelson, T. a., Rumberger, A., & Thies, J. E. (2006). Diversity of Planctomycetes in soil in relation to soil history and environmental heterogeneity. *Applied and Environmental Microbiology*, *72*(7), 4522–4531.
- Caldini, G., Cenci, G., Manenti, R., & Morozzi, G. (1995). The ability of an environmental isolate of *Pseudomonas fluorescens* to utilize chrysene and other four-ring polynuclear aromatic hydrocarbons. *Applied Microbiology and Biotechnology*, *44*(1-2), 225–229.

- Casellas, M., Grifoll, M., Sabaté, J., & Solanas, A. M. (1998). Isolation and characterization of a 9-fluorenone-degrading bacterial strain and its role in synergistic degradation of fluorene by a consortium. *Canadian Journal of Microbiology*, 44(8), 734–742.
- Cébron, A., Beguiristain, T., Faure, P., Norini, M.-P., Masfaraud, J.-F., & Leyval, C. (2009). Influence of vegetation on the in situ bacterial community and polycyclic aromatic hydrocarbon (PAH) degraders in aged PAH-contaminated or thermal-desorption-treated soil. *Applied and Environmental Microbiology*, 75(19), 6322–30.
- Cébron, A., Cortet, J., Criquet, S., Biaz, A., Calvert, V., Caupert, C., Leyval, C. (2011). Biological functioning of PAH-polluted and thermal desorption-treated soils assessed by fauna and microbial bioindicators. *Research in Microbiology*, 162(9), 896–907.
- Cébron, A., Norini, M.-P., Beguiristain, T., & Leyval, C. (2008). Real-Time PCR quantification of PAH-ring hydroxylating dioxygenase (PAH-RHD α) genes from Gram positive and Gram negative bacteria in soil and sediment samples. *Journal of Microbiological Methods*, 73(2), 148–59.
- Chen, K., Tang, S.-K., Wang, G.-L., Nie, G.-X., Li, Q.-F., Zhang, J.-D., Li, S.-P. (2013). *Olivibacter jilunii* sp. nov., isolated from DDT-contaminated soil. *International Journal of Systematic and Evolutionary Microbiology*, 63(Pt 3), 1083–8.
- Coulon, F., Chronopoulou, P.-M., Fahy, A., Païssé, S., Goñi-Urriza, M., Peperzak, L., McGenity, T. J. (2012). Central role of dynamic tidal biofilms dominated by aerobic hydrocarbonoclastic bacteria and diatoms in the biodegradation of hydrocarbons in coastal mudflats. *Applied and Environmental Microbiology*, 78(10), 3638–48.
- Dashti, N., Ali, N., Khanafer, M., Al-Awadhi, H., Sorkhoh, N., & Radwan, S. (2015). Olive-pomace harbors bacteria with the potential for hydrocarbon-biodegradation, nitrogen-fixation and mercury-resistance: promising material for waste-oil-bioremediation. *Journal of Environmental Management*, 155, 49–57.
- Dastgheib, S. M. M., Amoozegar, M. A., Khajeh, K., Shavandi, M., & Ventosa, A. (2012). Biodegradation of polycyclic aromatic hydrocarbons by a halophilic microbial consortium. *Applied Microbiology and Biotechnology*, 95(3), 789–98.
- Dave, B. P., Ghevariya, C. M., Bhatt, J. K., Dudhagara, D. R., & Rajpara, R. K. (2014). Enhanced biodegradation of total polycyclic aromatic hydrocarbons (TPAHs) by marine halotolerant *Achromobacter xylosoxidans* using Triton X-100 and β -cyclodextrin--a microcosm approach. *Marine Pollution Bulletin*, 79(1-2), 123–9.
- DeBruyn, J. M., Mead, T. J., & Sayler, G. S. (2012). Horizontal transfer of PAH catabolism genes in *Mycobacterium*: evidence from comparative genomics and isolated pyrene-degrading bacteria. *Environmental Science & Technology*, 46(1), 99–106.
- Debruyn, J. M., & Sayler, G. S. (2009). Microbial community structure and biodegradation activity of particle-associated bacteria in a coal tar contaminated creek. *Environmental Science & Technology*, 43(9), 3047–53.
- Deng, M.-C., Li, J., Liang, F.-R., Yi, M., Xu, X.-M., Yuan, J.-P., Peng, J., Wu, C. F., Wang, J.-H. (2014). Isolation and characterization of a novel hydrocarbon-degrading bacterium *Achromobacter* sp. HZ01 from the crude oil-contaminated seawater at the Daya Bay, southern China. *Marine Pollution Bulletin* 83(1), 79-86.

- Di Gennaro, P., Moreno, B., Annoni, E., García-Rodríguez, S., Bestetti, G., & Benitez, E. (2009). Dynamic changes in bacterial community structure and in naphthalene dioxygenase expression in vermicompost-amended PAH-contaminated soils. *Journal of Hazardous Materials*, *172*(2-3), 1464–1469.
- Dumont, M. G., & Murrell, J. C. (2005). Stable isotope probing - linking microbial identity to function. *Nature Reviews. Microbiology*, *3*(6), 499–504.
- Edwards, S. J., & Kjellerup, B. V. (2013). Applications of biofilms in bioremediation and biotransformation of persistent organic pollutants, pharmaceuticals/personal care products, and heavy metals. *Applied Microbiology and Biotechnology*, *97*(23), 9909–21.
- Efroymsen, R. A., & Alexander, M. (1994). Biodegradation in soil of hydrophobic pollutants in nonaqueous-phase liquids (NAPLs). *Environmental Toxicology and Chemistry*, *13*(3), 405–411.
- El Fantroussi, S., Verschuere, L., Verstraete, W., & Top, E. M. (1999). Effect of phenylurea herbicides on soil microbial communities estimated by analysis of 16S rRNA gene fingerprints and community-level physiological profiles. *Applied and Environmental Microbiology*, *65*(3), 982–988.
- Fernandez, P., Grifoll, M., Solanas, M., Bayona, J. M., & Aibaigés, J. (1992). Bioassay-Directed Chemical Analysis of Genotoxic Components in Coastal Sediments. *Environmental Science & Technology*, *26*(4), 817–829.
- Ferrero, M., Llobet-Brossa, E., Lalucat, J., Garcia-Valdes, E., Rossello-Mora, R., & Bosch, R. (2002). Coexistence of Two Distinct Copies of Naphthalene Degradation Genes in Pseudomonas Strains Isolated from the Western Mediterranean Region. *Applied and Environmental Microbiology*, *68*(2), 957–962.
- Gallego, S., Vila, J., Tauler, M., Nieto, J. M., Breugelmans, P., Springael, D., & Grifoll, M. (2013). Community structure and PAH ring-hydroxylating dioxygenase genes of a marine pyrene-degrading microbial consortium. *Biodegradation*, 1–14.
- Ghevariya, C. M., Bhatt, J. K., & Dave, B. P. (2011). Enhanced chrysene degradation by halotolerant *Achromobacter xylosoxidans* using Response Surface Methodology. *Bioresource Technology*, *102*(20), 9668–74.
- Gillespie, I. M. M., & Philp, J. C. (2013). Bioremediation, an environmental remediation technology for the bioeconomy. *Trends in Biotechnology*, *31*(6), 329–32.
- Grifoll, M., Casellas, M., Bayona, J. M., & Solanas, a. M. (1992). Isolation and characterization of a fluorene-degrading bacterium: Identification of ring oxidation and ring fission products. *Applied and Environmental Microbiology*, *58*(9), 2910–2917.
- Grifoll, M., Selifonov, S. a., Gatlin, C. V., & Chapman, P. J. (1995). Actions of a versatile fluorene-degrading bacterial isolate on polycyclic aromatic compounds. *Applied and Environmental Microbiology*, *61*(10), 3711–23.
- Grifoll, M., Selifonov, S. a., & Chapman, P. J. (1994). Evidence for a novel pathway in the degradation of fluorene by *Pseudomonas* sp. strain F274. *Applied and Environmental Microbiology*, *60*(7), 2438–2449.

- Hamaki, T., Suzuki, M., Fudou, R., Jojima, Y., Kajiura, T., Tabuchi, A., ... Shibai, H. (2005). Isolation of novel bacteria and actinomycetes using soil-extract agar medium. *Journal of Bioscience and Bioengineering*, 99(5), 485–92.
- Haritash, A. K., & Kaushik, C. P. (2009). Biodegradation aspects of polycyclic aromatic hydrocarbons (PAHs): a review. *Journal of Hazardous Materials*, 169(1-3), 1–15.
- Heuer, H., Krsek, M., Baker, P., Smalla, K., & Wellington, E. M. (1997). Analysis of actinomycete communities by specific amplification of genes encoding 16S rRNA and gel-electrophoretic separation in denaturing gradients. *Applied and Environmental Microbiology*, 63(8), 3233–41.
- IARC (1987). Monographs on the evaluation of the carcinogenic risk of chemicals to humans, vol. 32, suppl. 7; International Agency for Research on Cancer. Lyon, France.
- Iwai, S., Johnson, T. a, Chai, B., Hashsham, S. a, & Tiedje, J. M. (2011). Comparison of the specificities and efficacies of primers for aromatic dioxygenase gene analysis of environmental samples. *Applied and Environmental Microbiology*, 77(11), 3551–7.
- Jones, M. D., Crandell, D. W., Singleton, D. R., & Aitken, M. D. (2011). Stable-isotope probing of the polycyclic aromatic hydrocarbon-degrading bacterial guild in a contaminated soil. *Environmental Microbiology*, 13(10), 2623–32.
- Jones, M. D., Rodgers-Vieira, E. a., Hu, J., & Aitken, M. D. (2014). Association of Growth Substrates and Bacterial Genera with Benzo[a]pyrene Mineralization in Contaminated Soil. *Environmental Engineering Science*, 31(12), 689–697.
- Jones, M. D., Singleton, D. R., Sun, W., & Aitken, M. D. (2011). Multiple DNA extractions coupled with stable-isotope probing of anthracene-degrading bacteria in contaminated soil. *Applied and Environmental Microbiology*, 77(9), 2984–91.
- Juhasz, A. L., & Naidu, R. (2000). Bioremediation of high molecular weight polycyclic aromatic hydrocarbons: a review of the microbial degradation of benzo[a]pyrene. *International Biodeterioration & Biodegradation*, 45(1-2), 57–88.
- Kanaly, R. a, & Harayama, S. (2010). Advances in the field of high-molecular-weight polycyclic aromatic hydrocarbon biodegradation by bacteria. *Microbial Biotechnology*, 3(2), 136–64.
- Kanaly, R. a., Bartha, R., Watanabe, K., & Harayama, S. (2000). Rapid Mineralization of Benzo[a]pyrene by a Microbial Consortium Growing on Diesel Fuel. *Applied and Environmental Microbiology*, 66(10), 4205–4211.
- Kästner, M. (2000). Degradation of aromatic and polyaromatic compounds. In *Biotechnology* (Second edi., pp. 211–239). Weinheim, Germany: Wiley-VCH Verlag GmbH.
- Kazunga, C., Aitken, M. D., Gold, A., & Sangaiah, R. (2001). Fluoranthene-2,3- and -1,5-diones Are Novel Products from the Bacterial Transformation of Fluoranthene. *Environmental Science & Technology*, 35(5), 917–922.
- Keith, L. H., & Telliard, W. A. (1979). Priority pollutants. I. A perspective view. *Environmental Science and Technology*.

- Khara, P., Roy, M., Chakraborty, J., Ghosal, D., & Dutta, T. K. (2014). Functional characterization of diverse ring-hydroxylating oxygenases and induction of complex aromatic catabolic gene clusters in *Sphingobium* sp. PNB. *FEBS Open Bio*, 4, 290–300.
- Kohlmeier, S., Smits, T. H. M., Ford, R. M., Keel, C., Harms, H., & Wick, L. Y. (2005). Taking the Fungal Highway: Mobilization of Pollutant-Degrading Bacteria by Fungi. *Environmental Science & Technology*, 39(12), 4640–4646.
- Kostka, J. E., Prakash, O., Overholt, W. a, Green, S. J., Freyer, G., Canion, A., ... Huettel, M. (2011). Hydrocarbon-degrading bacteria and the bacterial community response in gulf of Mexico beach sands impacted by the deepwater horizon oil spill. *Applied and Environmental Microbiology*, 77(22), 7962–74.
- Koukoku, A.-I., & Vandera, E. (2011). Microbial Bioremediation of Non-metals. In A.-I. Koukou (Ed.), *Hydrocarbon-degrading soil bacteria: Current research*. Caister Academic Press, Norfolk, UK.
- Kunihiro, M., Ozeki, Y., Nogi, Y., Hamamura, N., & Kanaly, R. A. (2013). Benz[a]anthracene biotransformation and production of ring fission products by *Sphingobium* sp. strain KK22. *Applied and Environmental Microbiology*, 79(14), 4410–20.
- Kweon, O., Kim, S.-J., Baek, S., Chae, J.-C., Adjei, M. D., Baek, D.-H., Kim Y.-C., & Cerniglia, C. E. (2008). A new classification system for bacterial Rieske non-heme iron aromatic ring-hydroxylating oxygenases. *BMC Biochemistry*, 9(1), 11.
- Kweon, O., Kim, S.-J., Freeman, J. P., Song, J., Baek, S., & Cerniglia, C. E. (2010). Substrate specificity and structural characteristics of the novel Rieske nonheme iron aromatic ring-hydroxylating oxygenases NidAB and NidA3B3 from *Mycobacterium vanbaalenii* PYR-1. *mBio*, 1(2).
- Kweon, O., Kim, S.-J., Holland, R. D., Chen, H., Kim, D.-W., Gao, Y., Yu. L. R., Baek, L., Bael D. H., Ahn H. & Cerniglia, C. E. (2011). Polycyclic aromatic hydrocarbon metabolic network in *Mycobacterium vanbaalenii* PYR-1. *Journal of Bacteriology*, 193(17), 4326–37.
- Kweon, O., Kim, S.-J., Kim, D.-W., Kim, J. M., Kim, H., Ahn, Y., Cerniglia, C. E. (2014). Pleiotropic and epistatic behavior of a ring-hydroxylating oxygenase system in the polycyclic aromatic hydrocarbon metabolic network from *Mycobacterium vanbaalenii* PYR-1. *Journal of Bacteriology*, 196(19), 3503–15.
- Lafortune, I., Juteau, P., Déziel, E., Lépine, F., Beaudet, R., & Villemur, R. (2009). Bacterial diversity of a consortium degrading high-molecular-weight polycyclic aromatic hydrocarbons in a two-liquid phase biosystem. *Microbial Ecology*, 57(3), 455–68.
- Leys, N. M., Bastiaens, L., Verstraete, W., & Springael, D. (2005a). Influence of the carbon/nitrogen/phosphorus ratio on polycyclic aromatic hydrocarbon degradation by *Mycobacterium* and *Sphingomonas* in soil. *Applied Microbiology and Biotechnology*, 66(6), 726–36.
- Leys, N. M. E. J., Ryngaert, A., Bastiaens, L., Verstraete, W., Top, E. M., & Springael, D. (2004). Occurrence and Phylogenetic Diversity of *Sphingomonas* Strains in Soils Contaminated with Polycyclic Aromatic Hydrocarbons. *Applied and Environmental Microbiology*, 70(4), 1944–1955.

- Leys, N. M., Ryngaert, A., Bastiaens, L., Wattiau, P., Top, E. M., Verstraete, W., & Springael, D. (2005b). Occurrence and community composition of fast-growing *Mycobacterium* in soils contaminated with polycyclic aromatic hydrocarbons. *FEMS Microbiology Ecology*, *51*(3), 375–88.
- Li, S., Li, X., Zhao, H., & Cai, B. (2011). Physiological role of the novel salicylaldehyde dehydrogenase NahV in mineralization of naphthalene by *Pseudomonas putida* ND6. *Microbiological Research*, *166*(8), 643–53.
- Liedekerke, M. Van, Prokop, G., Rabl-berger, S., & Kibblewhite, M. (2014). *Progress in the management of Contaminated Sites in Europe*. doi:10.2788/4658
- Lladó, S., Covino, S., Solanas, a. M., Petruccioli, M., D'annibale, a., & Viñas, M. (2015). Pyrosequencing reveals the effect of mobilizing agents and lignocellulosic substrate amendment on microbial community composition in a real industrial PAH-polluted soil. *Journal of Hazardous Materials*, *283*, 35–43.
- Lladó, S., Gràcia, E., Solanas, A. M., & Viñas, M. (2013). Fungal and bacterial microbial community assessment during bioremediation assays in an aged creosote-polluted soil. *Soil Biology and Biochemistry*, *67*, 114–123.
- Lladó, S., Jiménez, N., Viñas, M., & Solanas, A. M. (2009). Microbial populations related to PAH biodegradation in an aged biostimulated creosote-contaminated soil. *Biodegradation*, *20*(5), 593–601.
- López, Z., Vila, J., & Grifoll, M. (2005). Metabolism of fluoranthene by mycobacterial strains isolated by their ability to grow in fluoranthene or pyrene. *Journal of Industrial Microbiology & Biotechnology*, *32*(10), 455–64.
- López, Z., Vila, J., Minguillón, C., & Grifoll, M. (2006). Metabolism of fluoranthene by *Mycobacterium* sp. strain AP1. *Applied Microbiology and Biotechnology*, *70*(6), 747–56.
- López, Z., Vila, J., Ortega-Calvo, J.-J., & Grifoll, M. (2008). Simultaneous biodegradation of creosote-polycyclic aromatic hydrocarbons by a pyrene-degrading *Mycobacterium*. *Applied Microbiology and Biotechnology*, *78*(4), 739–739. d
- Louvel, B., Cébron, A., & Leyval, C. (2011). Root exudates affect phenanthrene biodegradation, bacterial community and functional gene expression in sand microcosms. *International Biodeterioration & Biodegradation*, *65*(7), 947–953.
- Lundstedt, S., Bandowe, B. A. M., Wilcke, W., Boll, E., Christensen, J. H., Vila, J., Ricci, M. (2014). First intercomparison study on the analysis of oxygenated polycyclic aromatic hydrocarbons (oxy-PAHs) and nitrogen heterocyclic polycyclic aromatic compounds (N-PACs) in contaminated soil. *TrAC Trends in Analytical Chemistry*, *57*, 83–92.
- Lundstedt, S., White, P. a, Lemieux, C. L., Lynes, K. D., Lambert, I. B., Oberg, L., Tysklind, M. (2007). Sources, fate, and toxic hazards of oxygenated polycyclic aromatic hydrocarbons (PAHs) at PAH-contaminated sites. *Ambio*, *36*(6), 475–85.
- Maeda, A. H., Nishi, S., Hatada, Y., Ozeki, Y., & Kanaly, R. A. (2014). Biotransformation of the high-molecular weight polycyclic aromatic hydrocarbon (PAH) benzo[k]fluoranthene by *Sphingobium* sp. strain KK22 and identification of new products of non-alternant PAH

- biodegradation by liquid chromatography electrospray ionization. *Microbial Biotechnology*, 7(2), 114–29.
- Mallick, S., Chakraborty, J., & Dutta, T. K. (2011). Role of oxygenases in guiding diverse metabolic pathways in the bacterial degradation of low-molecular-weight polycyclic aromatic hydrocarbons: a review. *Critical Reviews in Microbiology*, 37(1), 64–90.
- Martin, F., Torelli, S., Le Paslier, D., Barbance, A., Martin-Laurent, F., Bru, D., ... Jouanneau, Y. (2012). Betaproteobacteria dominance and diversity shifts in the bacterial community of a PAH-contaminated soil exposed to phenanthrene. *Environmental Pollution (Barking, Essex : 1987)*, 162, 345–53.
- Masakorala, K., Yao, J., Cai, M., Chandankere, R., Yuan, H., & Chen, H. (2013). Isolation and characterization of a novel phenanthrene (PHE) degrading strain *Pseudomonas* sp. USTB-RU from petroleum contaminated soil. *Journal of Hazardous Materials*, 263 Pt 2, 493–500.
- Moody, J. D., Freeman, J. P., Fu, P. P., & Cerniglia, C. E. (2004). Degradation of Benzo[a]pyrene by *Mycobacterium vanbaalenii* PYR-1. *Applied and Environmental Microbiology*, 70(1), 340–345.
- Mrozik, A., Piotrowska-Seget, Z., & Łabuzek, S. (2003). Bacterial degradation and bioremediation of polycyclic aromatic hydrocarbons. *Polish Journal of Environmental Studies*, 12(1), 15–25.
- Mueller, J. G., Chapman, P. J., Blattmann, B. O., & Pritchard, P. H. (1990). Isolation and characterization of a fluoranthene-utilizing strain of *Pseudomonas paucimobilis*. *Applied and Environmental Microbiology*, 56(4), 1079–1086.
- Mueller, J.G., Cerniglia, C.E., Pritchard, P.H. (1996). Bioremediation of environments contaminated by polycyclic aromatic hydrocarbons, in: *Bioremediation principles and applications*. Vol. 6 (ed. Cambridge University Press). Cambridge, UK. pp 125-194.
- Mukherjee, S., Juottonen, H., Siivonen, P., Lloret Quesada, C., Tuomi, P., Pulkkinen, P., & Yrjälä, K. (2014). Spatial patterns of microbial diversity and activity in an aged creosote-contaminated site. *The ISME Journal*, 2131–2142.
- Nayak, A. S., Sanjeev Kumar, S., Santosh Kumar, M., Anjaneya, O., & Karegoudar, T. B. (2011). A catabolic pathway for the degradation of chrysene by *Pseudoxanthomonas* sp. PNK-04. *FEMS Microbiology Letters*, 320(2), 128–134.
- Niepceron, M., Portet-Koltalo, F., Merlin, C., Motelay-Massei, A., Barray, S., & Bodilis, J. (2010). Both *Cycloclasticus* spp. and *Pseudomonas* spp. as PAH-degrading bacteria in the Seine estuary (France). *FEMS Microbiology Ecology*, 71(1), 137–47.
- Nopcharoenkul, W., Pinphanichakarn, P., & Pinyakong, O. (2011). The development of a liquid formulation of *Pseudoxanthomonas* sp. RN402 and its application in the treatment of pyrene-contaminated soil. *Journal of Applied Microbiology*, 111(1), 36–47.
- Ntougias, S., Fasseas, C., & Zervakis, G. I. (2007). *Olivibacter sitiensis* gen. nov., sp. nov., isolated from alkaline olive-oil mill wastes in the region of Sitia, Crete. *International Journal of Systematic and Evolutionary Microbiology*, 57(Pt 2), 398–404.
- Ortega-Calvo, J. J., Birman, I., & Alexander, M. (1995). Effect of varying the rate of partitioning of phenanthrene in nonaqueous-phase liquids on biodegradation in soil slurries. *Environmental Science & Technology*, 29, 2222–2225.

- Ortega-Calvo, J. J., Tejeda-Agredano, M. C., Jimenez-Sanchez, C., Congiu, E., Sungthong, R., Niqui-Arroyo, J. L., & Cantos, M. (2013). Is it possible to increase bioavailability but not environmental risk of PAHs in bioremediation? *Journal of Hazardous Materials*, 261, 733–45.
- Pasternak, G., Kołwzan, B., Bernard-Baures, G., Rybak, J., & Mroziak, A. (2012). Physiological characterization of carbazole degrading bacteria isolated from a former gasworks site. *Environment Protection Engineering*, 38(2), 121–126.
- Pathak, H., Kantharia, D., Malpani, A., & Madamwar, D. (2009). Naphthalene degradation by *Pseudomonas* sp. HOB1: in vitro studies and assessment of naphthalene degradation efficiency in simulated microcosms. *Journal of Hazardous Materials*, 166(2-3), 1466–73.
- Peng, R. H., Xiong, A. S., Xue, Y., Fu, X. Y., Gao, F., Zhao, W., Yao, Q. H. (2008, November). Microbial biodegradation of polyaromatic hydrocarbons. *FEMS Microbiology Reviews* 32(6), 927-955.
- Pothuluri, J.V. & Cerniglia, C.E. (1998). In: Bioremediation principles and practice, vol. II, Biodegradation Technology Development; Technomic Publishing Company: Lancaster, UK, 461-520.
- Poulsen, L. K., Ballard, G., & Stahl, D. A. (1993). Use of rRNA fluorescence in situ hybridization for measuring the activity of single cells in young and established biofilms. *Applied and Environmental Microbiology*, 59(5), 1354–1360.
- Rentz, J. a, Alvarez, P. J. J., & Schnoor, J. L. (2008). Benzo[a]pyrene degradation by *Sphingomonas yanoikuyae* JAR02. *Environmental Pollution (Barking, Essex : 1987)*, 151(3), 669–77.
- Rodrigues, S. M., Pereira, M. E., da Silva, E. F., Hursthouse, a S., & Duarte, a C. (2009). A review of regulatory decisions for environmental protection: part I - challenges in the implementation of national soil policies. *Environment International*, 35(1), 202–13.
- Roy, M., Khara, P., & Dutta, T. K. (2012). meta-Cleavage of hydroxynaphthoic acids in the degradation of phenanthrene by *Sphingobium* sp. strain PNB. *Microbiology (Reading, England)*, 158(Pt 3), 685–95.
- Salam, L. B., Ilori, M. O., Amund, O. O., Numata, M., Horisaki, T., & Nojiri, H. (2014). Carbazole angular dioxygenation and mineralization by bacteria isolated from hydrocarbon-contaminated tropical African soil. *Environmental Science and Pollution Research International*, 21(15), 9311–24.
- Schloss, P. D., Gevers, D., & Westcott, S. L. (2011). Reducing the effects of PCR amplification and sequencing Artifacts on 16s rRNA-based studies. *PLoS ONE*, 6(12).
- Schloss, P. D., Westcott, S. L., Ryabin, T., Hall, J. R., Hartmann, M., Hollister, E. B., Weber, C. F. (2009). Introducing mothur: Open-source, platform-independent, community-supported software for describing and comparing microbial communities. *Applied and Environmental Microbiology*, 75(23), 7537–7541.
- Schuler, L., Jouanneau, Y., Chadhain, S. M. N., Meyer, C., Pouli, M., Zylstra, G. J., Agathos, S. N. (2009). Characterization of a ring-hydroxylating dioxygenase from phenanthrene-degrading *Sphingomonas* sp. strain LH128 able to oxidize benz[a]anthracene. *Applied Microbiology and Biotechnology*, 83(3), 465–75.

- Selifonov, S. a., Grifoll, M., Eaton, R. W., & Chapman, P. J. (1996). Oxidation of naphthoaromatic and methyl-substituted aromatic compounds by naphthalene 1,2-dioxygenase. *Applied and Environmental Microbiology*, 62(2), 507–514.
- Sims, R.C. & Overcash, M.R. (1983). Fate of polynuclear aromatic compounds (PANs) in soil-plant systems. *Res. rev.* 88: 1-68.
- Singh, G. B., Gupta, S., Srivastava, S., & Gupta, N. (2011). Biodegradation of carbazole by newly isolated *Acinetobacter* spp. *Bulletin of Environmental Contamination and Toxicology*, 87(5), 522–6.
- Singleton, D. R., Jones, M. D., Richardson, S. D., & Aitken, M. D. (2013). Pyrosequence analyses of bacterial communities during simulated in situ bioremediation of polycyclic aromatic hydrocarbon-contaminated soil. *Applied Microbiology and Biotechnology*, 97(18), 8381–91.
- Singleton, D. R., Ramirez, L. G., & Aitken, M. D. (2009). Characterization of a polycyclic aromatic hydrocarbon degradation gene cluster in a phenanthrene-degrading *Acidovorax* strain. *Applied and Environmental Microbiology*, 75(9), 2613–20.
- Singleton, D. R., Richardson, S. D., & Aitken, M. D. (2011). Pyrosequence analysis of bacterial communities in aerobic bioreactors treating polycyclic aromatic hydrocarbon-contaminated soil. *Biodegradation*, 22(6), 1061–1073.
- Singleton, D. R., Sangaiah, R., Gold, A., Ball, L. M., & Aitken, M. D. (2006). Identification and quantification of uncultivated Proteobacteria associated with pyrene degradation in a bioreactor treating PAH-contaminated soil. *Environmental Microbiology*, 8(10), 1736–45.
- Soares, D., Lida, A., Fraser, M. J., Barker, J. F., & Grifoll, M. (2008). Identification of PAH-microbial metabolites in creosote contaminated soils and groundwater. In *Consoil*. Milan.
- Sohn, J. H., Kwon, K. K., Kang, J.-H., Jung, H.-B., & Kim, S.-J. (2004). *Novosphingobium pentaromativorans* sp. nov., a high-molecular-mass polycyclic aromatic hydrocarbon-degrading bacterium isolated from estuarine sediment. *International Journal of Systematic and Evolutionary Microbiology*, 54(Pt 5), 1483–7.
- Stolz, A. (2009). Molecular characteristics of xenobiotic-degrading sphingomonads. *Applied Microbiology and Biotechnology*, 81(5), 793–811.
- Stolz, A. (2014). Degradative plasmids from sphingomonads. *FEMS Microbiology Letters*, 350(1), 9–19.
- Stringfellow, W. T., & Aitken, M. D. (1995). Competitive metabolism of naphthalene, methylnaphthalenes, and fluorene by phenanthrene-degrading pseudomonads. *Applied and Environmental Microbiology*, 61(1), 357–362.
- Sun, R., Jin, J., Sun, G., Liu, Y., & Liu, Z. (2010). Screening and degrading characteristics and community structure of a high molecular weight polycyclic aromatic hydrocarbon-degrading bacterial consortium from contaminated soil. *Journal of Environmental Sciences*, 22(10), 1576–1585.
- Szabó, I., Szoboszlai, S., Kriszt, B., Háhn, J., Harkai, P., Baka, E., Tánácsics, A., Kaszab, E., Privler, Z., & Kukolya, J. (2011). *Olivibacter oleidegradans* sp. nov., a hydrocarbon-degrading bacterium

- isolated from a biofilter clean-up facility on a hydrocarbon-contaminated site. *International Journal of Systematic and Evolutionary Microbiology*, 61(Pt 12), 2861–5.
- The European Commission. (2006). *Proposal for a Directive of the European Parliament and of the council establishing a framework for the protection of soil and amending Directive 2004/35/EC*.
- The European Commission. (2007). *Environment fact sheet : soil protection — a new policy for the EU*.
- Thion, C., Cébron, A., Beguiristain, T., & Leyval, C. (2012). PAH biotransformation and sorption by *Fusarium solani* and *Arthrobacter oxydans* isolated from a polluted soil in axenic cultures and mixed co-cultures. *International Biodeterioration & Biodegradation*, 68, 28–35.
- United Nations. (2013). *World Soil Day and International Year of Soils*.
- US Sustainable Remediation Forum (SURF) (2009). Integrating sustainable principles, practices, and metrics into remediation projects. *Remediation*, 19(3), pp. 5–114.
- Van Agteren, M.H., van Keuninh, S., Janssen, D.B. (1998). *Handbook on Biodegradation and Biological Treatment of Hazardous Organic Compounds*; Kluwer Academia Publishers: Dordrecht, The Netherlands.
- Van Brummelen, T.C., van Hattum, B., van Krommetuin, T., Kalf, D.F. (1998). PAHs and related compounds: Biology, in Springer: *The Handbook of Environmental Chemistry*, vol 3, part J. Berlin, Germany. pp. 203–263
- Van Herwijnen, R., Wattiau, P., Bastiaens, L., Daal, L., Jonker, L., Springael, D., ... Parsons, J. R. (2003). Elucidation of the metabolic pathway of fluorene and cometabolic pathways of phenanthrene, fluoranthene, anthracene and dibenzothiophene by *Sphingomonas* sp. LB126. *Research in Microbiology*, 154(3), 199–206.
- Vanbroekhoven, K., Ryngaert, A., Bastiaens, L., Wattiau, P., Vancanneyt, M., Swings, J., ... Springael, D. (2004). Streptomycin as a selective agent to facilitate recovery and isolation of introduced and indigenous *Sphingomonas* from environmental samples. *Environmental Microbiology*, 6(11), 1123–36.
- Vila, J., & Grifoll, M. (2009a). Actions of *Mycobacterium* sp. strain AP1 on the saturated- and aromatic-hydrocarbon fractions of fuel oil in a marine medium. *Applied and Environmental Microbiology*, 75(19), 6232–9.
- Vila, J., López, Z., Sabaté, J., Minguillón, C., Solanas, A. M., & Grifoll, M. (2001). Identification of a novel metabolite in the degradation of pyrene by *Mycobacterium* sp. strain AP1: actions of the isolate on two- and three-ring polycyclic aromatic hydrocarbons. *Applied and Environmental Microbiology*, 67(12), 5497–505.
- Vila, J., Tauler, M., & Grifoll, M. (2015). Bacterial PAH degradation in marine and terrestrial habitats. *Current Opinion in Biotechnology*, 33, 95–102.
- Viñas, M., Sabaté, J., Espuny, M. J., & Solanas, A. M. (2005). Bacterial community dynamics and polycyclic aromatic hydrocarbon degradation during bioremediation of heavily creosote-contaminated soil. *Applied and Environmental Microbiology*, 71(11), 7008–18.

- Wang, Q., Garrity, G. M., Tiedje, J. M., & Cole, J. R. (2007). Naive Bayesian classifier for rapid assignment of rRNA sequences into the new bacterial taxonomy. *Applied and Environmental Microbiology*, 73(16), 5261–7.
- Wei, C., Bandowe, B. a. M., Han, Y., Cao, J., Zhan, C., & Wilcke, W. (2015). Polycyclic aromatic hydrocarbons (PAHs) and their derivatives (alkyl-PAHs, oxygenated-PAHs, nitrated-PAHs and azaarenes) in urban road dusts from Xi'an, Central China. *Chemosphere*, 134(June), 512–520.
- Weisburg, W. G., Barns, S. M., Pelletier, D. A., & Lane, D. J. (1991). 16S ribosomal DNA amplification for phylogenetic study. *Journal of Bacteriology*, 173(2), 697–703.
- Weissenfels, W. D., Beyer, M., & Klein, J. (1990). Degradation of phenanthrene, fluorence and fluoranthene by pure bacterial cultures. *Applied Microbiology and Biotechnology*, 32(4), 479–484.
- Wilcke, W., Kiesewetter, M., & Bandowe, B. a M. (2014). Microbial formation and degradation of oxygen-containing polycyclic aromatic hydrocarbons (OPAHs) in soil during short-term incubation. *Environmental Pollution (Barking, Essex : 1987)*, 184, 385–90.
- Wilson, S. C., & Jones, K. C. (1993). Bioremediation of soil contaminated with polynuclear aromatic hydrocarbons (PAHs): A review. *Environmental Pollution*, 81(3), 229–249.
- Wrenn, B. A., & Venosa, A. D. (1996). Selective enumeration of aromatic and aliphatic hydrocarbon degrading bacteria by a most-probable-number procedure. *Canadian Journal of Microbiology*, 42(3), 252–258.
- Wright, E. S., Yilmaz, L. S., & Noguera, D. R. (2012). DECIPHER, a search-based approach to chimera identification for 16S rRNA sequences. *Applied and Environmental Microbiology*, 78(3), 717–25.
- Yabuuchi, E., Kawamura, Y., Kosako, Y., & Ezaki, T. (1998). Emendation of genus *Achromobacter* and *Achromobacter xylosoxidans* (Yabuuchi and Yano) and proposal of *Achromobacter ruhlandii* (Packer and Vishniac) Comb. Nov., *Achromobacter piechaudii* (Kiredjian et al.) Comb. Nov., and *Achromobacter xylosoxidans* Subsp. de. *Microbiology and Immunology*, 42(6), 429–438.

CHAPTER 10

Summary (resum)

10 Summary (Resum)

10.1 Introducció

EL SÒL COM A RECURS

El sòl, generalment definit com la capa superior de l'escorça terrestre, és un sistema dinàmic que presenta unes funcions vitals per a la supervivència tant de l'ésser humà com dels ecosistemes. Proveir d'un medi físic per al desenvolupament de les activitats humanes, produir biomassa i matèries primes, albergar la biodiversitat i actuar com a embornal global de carboni són algunes d'aquestes funcions imprescindibles per la subsistència de l'espècie humana i la protecció dels ecosistemes. El sòl està considerat un recurs no renovable degut a la lentitud de la seva formació i regeneració. Mentre que la formació d'un mer centímetre de sòl pot tardar segles, la seva destrucció es pot produir molt ràpidament.

Una de les causes de destrucció del sòl és la contaminació. En l'últim informe de la Unió Europea (2014), es va identificar 342.000 emplaçaments contaminats que requerien remediació. No obstant, el mateix informe estima que fins a 2,5 milions d'emplaçaments podrien estar potencialment afectats per contaminants perillosos. Tenint en compte que només un 15% dels emplaçaments identificats foren remediats, el problema segueix creixent.

Durant l'última dècada, la remediació d'emplaçaments contaminats ha estat basada en la prevenció del risc inacceptable per la salut humana i pel medi ambient, per tal d'assegurar que reuneix les característiques pel seu posterior ús. Recentment, s'ha incorporat el concepte de sostenibilitat en la presa de decisions durant la restauració d'un sòl contaminat (Bardos et al., 2011). La remediació sostenible contempla protocols que permeten minimitzar la petjada ecològica del procés, són socialment acceptats i econòmicament factibles. La bioremediació, que aprofita les capacitats metabòliques dels microorganismes per restaurar emplaçament contaminats, és una remediació sostenible que permet recuperar les funcions ecològiques del sòl.

MARC LEGAL

Un dels motius de relatiu baix nivell d'aplicació de la (bio)remediació en els sòls contaminats és la falta d'una legislació específica que reguli les actuacions que s'han de dur a terme quan es produeix la contaminació d'un sòl. De fet, a nivell europeu no existeix una legislació sobre la protecció del sòl. El primer cop que la UE va proposar un marc i uns objectius comuns per prevenir la degradació del sòl i conservar les seves funcions va ser al 2002, en l'Estratègia Temàtica per la Protecció des Sòl (2002, 2006, i 2012).

L'estratègia inclou la instauració d'un marc legislatiu per la protecció i ús sostenible del sòl, millorar el coneixement en aquesta àrea i incrementar la conscienciació pública. La proposta per elaborar una Directiva sorgí al 2006 i era un component clau de l'estratègia, que pretenia habilitar als Estats Membres per adoptar mesures segons les seves necessitats locals i proporcionar eines per identificar diferents problemes. Després de 8 anys, els Estats Membres van ser incapaços de posar-se d'acord i la proposta de la Directiva Marc del Sòl va ser retirada.

Sota el suggeriment de la *Global Soil Partnership* de la FAO i amb el suport de la UE, al desembre del 2013, l'Assemblea General de les Nacions Unides va proclamar el 2015 com l'any internacional del sòl (en anglès, IYS) i el 5 de desembre de cada any el dia mundial del sòl (en anglès, WSD).

En l'àmbit espanyol, no va ser fins al període 1990-1995 que el Govern va dissenyar un Pla Nacional de Recuperació de Sòls Contaminats amb l'objectiu d'identificar els emplaçaments contaminats, crear una base de dades, desenvolupar una metodologia de valoració del risc, calcular el cost de les accions, proposar un programa d'acció, avaluar el costos de restauració i considerar un marc legal. Com a resultat, es va elaborar la Llei de residus 10/1998, que incloïa la definició d'àrea contaminada i de risc acceptable i la necessitat d'una llista d'activitats potencialment contaminants i un inventari d'emplaçaments contaminats. El següent pas fou l'aprovació del Reial Decret 9/2005, pel qual es van establir els nivells de referència generals (GRL) per contaminants específics com el d'hidrocarburs de petroli total (TPH, 50 ppm). Finalment, la Llei 22/2011 va ser aplicada amb l'objectiu de refinar conceptes com el de la determinació dels subjectes responsables de la contaminació, així com de les obligacions d'informació a la que queden subjectes tant els titulars de les activitats potencialment contaminants com els titulars de sòl contaminat.

SÒLS CONTAMINATS AMB HAPs

Els hidrocarburs aromàtics policíclics (HAPs) són compostos orgànics formats per 2 o més anells benzènics fusionats. Segons els número d'anells es classifiquen com a HAPs de baix pes molecular (BPM), que són els que presenten 2 o 3 anells aromàtics, o bé com a HAPs d'elevat pes molecular (EPM), que contenen més de 3 anells. La seva estructura química els confereix una gran estabilitat que es tradueix en una elevada persistència en el medi ambient. És per això que són compostos molt ubics. A més a més, presenten una elevada carcinogenicitat, que al igual que la seva recalcitrància, augmenta amb el nombre d'anells benzènics. Per totes aquestes raons, l'agència de protecció del medi ambient dels EEUU (US-EPA), va considerar 16 d'aquests HAPs com a contaminants prioritaris. A Europa, un 11% dels sòls contaminats presentaren com a compostos majoritaris els HAPs al 2011 (Agència Europea del Medi Ambient, EEA en anglès).

En emplaçaments contaminats, els HAPs es troben acompanyats d'altres compostos poliaromàtics com són els seus derivats oxidats (oxi-HAPs) i els heterocicles que poden contenir àtoms de N, S o O, com per exemple els compostos policíclics amb nitrogen (N-CAPs). Un exemple de contaminant que conté tots aquests productes és la creosota, que és un oli d'origen pirolític utilitzat històricament per la preservació de la fusta. La seva utilització va provocar la contaminació puntual de molts emplaçament arreu del món. Al 2003 la UE va prohibir la seva comercialització degut a la seva carcinogenicitat. Al ser una barreja de compostos poliaromàtics definida i discreta, la creosota es molt útil com a model per a l'estudi de la degradació dels HAPs en emplaçaments contaminats.

BIODEGRADACIÓ D'HAPs EN SÒLS

Quan els compostos orgànics entren en contacte amb una matriu complexa com és el sòl estan sotmesos a una sèrie de processos físico-químics: fotooxidació, oxidació química, biodegradació microbiana, adsorció en les partícules del sòl i lixiviació, entre d'altres. En tot cas, només de degradació microbiana permet l'eliminació completa dels compostos orgànics, transformant-los en CO₂ i H₂O. De fet, la bioremediació es serveix d'aquest procés natural per a la restauració de les funcions del sòl en emplaçaments contaminats. No obstant, la seva aplicació a sòls contaminats per HAPs està limitada per la impredictibilitat de les concentracions finals. Per millorar les tecnologies actuals és imprescindible esbrinar el funcionament les xarxes metabòliques complexes que determinen el destí final d'aquests compostos.

La biodegradació dels HAPs en sòls la duen a terme bàsicament bacteris i fongs en condicions aeròbiques. Aquest microorganismes poden aprofitar aquest substrats per treure'n carboni i energia, el que pot conduir a una eliminació completa (mineralització) o bé a una oxidació parcial provocant l'acumulació de subproductes (degradació parcial). Per altra banda, els hidrocarburs poden ser transformats de forma fortuïta per enzims inespecífics, el que no comporta un creixement bacterià i també condueix a l'acumulació de productes parcialment oxidats.

El primer pas de l'oxidació microbiana dels HAPs és catalitzada per dioxigenases dihidroxilants de l'anell (RHD, en anglès) que introdueixen dos àtoms d'oxigen en carbonis veïns formant *cis*-dihidridiols. A continuació es produeix una deshidrogenació que prepara la molècula per a un segon atac que condueix al trencament de l'anell aromàtic. Posteriorment s'alliberen compostos de 2-3 carbonis que entren en el metabolisme central. La quantificació de les RHD per PCR quantitativa serveix com a indicador del potencial degradador d'una comunitat microbiana. Cébron et al. (2008) van descriure dos jocs d'encebadors per a la detecció selectiva d'aquests enzim en Gram-negatius (GN) i Gram-positius (GP).

Es coneix un gran número de bacteris amb capacitats degradadores d'HAPs. L'aproximació clàssica per a l'estudi de vies metabòliques d'HAPs s'havia basant en la incubació de soques aïllades amb hidrocarburs individuals (Kanaly and Harayama 2010; Mallick et al. 2011). A part del gènere *Pseudomonas*, històricament conegut com a degradador d'HAPs BPM (Kazunga et al., 2001; Stringfellow & Aitken, 1995), els estudis metabòlics més recents es centren en les esfingomones, que presenten una gran versatilitat alhora d'atacar compostos diferents (Stolz, 2009). Per altra banda, els actinobacteris, amb la seva capacitat d'adhesió a superfícies hidrofòbiques, són coneguts com els grans degradadors d'HAPs EPM (Robert a Kanaly & Harayama, 2010).

Ara bé, així com els HAPs no es troben de manera individual en els emplaçament contaminats, els microorganismes tampoc viuen aïllats, sinó que formen xarxes complexes on els metabòlits produïts per unes poblacions són utilitzats com a font de carboni i energia per altres (Vila et al. 2015). Actualment, aprofitant el coneixement obtingut a partir de soques pures i amb la utilització de mètodes moleculars independents de cultiu es poden fer estudis de comunitats microbianes incubades amb barreges d'hidrocarburs que permeten investigar aquestes interaccions microbianes. La complexitat reduïda dels consorcis microbians facilita la correlació entre poblacions específiques i funcions determinades (Lafortune et al., 2009; Sun et al., 2010). Per altra banda, el desenvolupament de tècniques de seqüenciació massiva ha permès l'estudi de poblacions en mostres ambientals. Fins ara, bàsicament s'han dut a terme experiments basats en la piroseqüenciació del gen 16S ARNr que permet l'elucidació de l'estructura de la comunitat total, que pot englobar també ADN lliure o de bacteris metabòlicament inactius (Singleton et al. 2013; Singleton et al. 2011). No obstant, per poder associar funcions a poblacions específiques l'estudi de les poblacions realment actives (ARN) seria molt més adequat perquè evitaria aquest biaix. Actualment, que nosaltres coneguem, la seqüenciació massiva de transcrits del gen 16S ARNr encara no s'ha aplicat en el camp de la biodegradació.

10.2 Objectius

L'objectiu general d'aquesta Tesi és contribuir a l'elucidació dels processos microbians que tenen lloc durant la biodegradació activa d'HAPs en sòls contaminats. Això permetrà identificar els tàxons i les funcions microbianes clau, així com nous possibles analits diana, amb l'objectiu últim de millorar les tecnologies de bioremediació actuals i els seus protocols de monitorització i avaluació de riscos. Per aconseguir aquest objectiu, es va triar com a model un sòl contaminat amb creosota procedent d'un emplaçament contaminat al sud d'Espanya, que presentava una concentració d'HAP elevada i un llarg historial de contaminació, el que feia pensar que hi hauria una comunitat degradadora

d'HAPs ben establerta i altament adaptada. Es fa especial èmfasi en els HAPs EPM, ja que són els principals constituents de les concentracions residuals després d'un tractament biològic i que posen en perill l'èxit de la bioremediació. També s'investiga la formació i el destí final del oxi- i N-CAPs, generalment no contemplats en l'avaluació del risc. Dins d'aquest objectiu global, els objectius específics que es desenvoluparan en aquesta Tesi són:

- Seleccionar i caracteritzar la comunitat degradadora d'HAPs EPM del sòl contaminat mitjançant un sistema d'enriquiment utilitzant un sistema bifàsic format per medi mineral i sorra contaminada amb un NAPL de creosota biodegradada prèviament. Les poblacions claus d'aquest consorci seran identificades, en base a les seves respostes a substrats específics, perfils filogenètics, funcionals i de metabolòmica, i la seva recuperació en cultiu pur.
- Investigar els processos microbians que impulsen l'eliminació dels HAP *in situ* durant la incubació del sòl contaminat amb creosota model en condicions òptimes de biodegradació. Les cinètiques de degradació dels HAPs, oxi-HAPs i N-CAPs, juntament amb la formació i/o acumulació de possibles productes d'oxidació, es correlacionaran amb filotips clau i canvis en la comunitat. Una visió en temps real de la dinàmica de la comunitat s'obté a partir de l'anàlisi combinat dels canvis en les poblacions globals (gens) i actives (transcrits), tant des del punt de vista filogenètic (gen 16S ARNr) com funcional (gens RHD).

10.3 Resultats i discussió

BACTERIS CLAU EN LA DEGRADACIÓ D'HAPs EPM D'UN CONSORCI ENRIQUIT MITJANÇANT UN SISTEMA SORRA-LÍQUID CONTAMINAT AMB CREOSOTA ENVELLIDA

El disseny d'un sistema d'enriquiment bifàsic ha permès l'obtenció del consorci UBHP degradador d'HAPs EPM. La comunitat present en un sòl contaminat amb creosota es va enriquir mitjançant un sistema que constà d'una part líquida, medi mineral, i d'una fase sòlida, composta per sorra contaminada amb una barreja d'HAPs EPM procedents d'una creosota prèviament degradada. Aquesta barreja es va obtenir després de la incubació de creosota comercial amb la soca degradadora d'HAPs BPM *Bulkholderia* sp. F297 (Grifoll et al., 1995). La barreja resultant, que estava formada bàsicament per HAPs de 4, 5 i 6 anells aromàtics i que presentava com a productes més abundants el FT i PY, va ser utilitzada com a única font de carboni i energia en el sistema d'enriquiment. S'incubà 5 g del sòl contaminat històricament amb creosota en aquest sistema bifàsic. Cada 4 setmanes es feien ressembres en medi fresc durant 2 anys. L'estructura de les poblacions fou monitoritzada per PCR-DGGE. A partir de la segona ressembra, el perfil de DGGE del consorci es va mantenir constant demostrant que les poblacions ja s'havien estabilitzat.

Per determinar el potencial degradador del consorci obtingut, es va fer un experiment amb els mateixos cultius bifàsics utilitzats en el sistema d'enriquiment durant 12 setmanes. A temps 0, 3, 6 i 12 setmanes es van sacrificar erlenmeyers per triplicat i es va fer una anàlisi del residu orgànic per cromatografia de gasos. Els resultats (Figura 10.1) demostraren que el consorci microbià UBHP era capaç de degradar significativament compostos de 3 a 6 anells aromàtics i els seus derivats metilats de 3 i 4 anells, com per exemple el FT i PY (90%), BaA (66%) i CHY (59%). Les cinètiques dels compostos individuals mostraren un successió en la desaparició dels compostos segons la seva solubilitat en aigua. Primerament es va degradar l'HAP de tres anells PHE seguit del FT, PY i els derivat alquilats del PHE, aquests tres últims seguint cinètiques molt similars. Tot aquests compostos presentaren una baixada ràpida de la seva concentració durant les primeres tres setmanes d'incubació. Per altra banda, BaA i CHY formen una parella que presenta una cinètica de degradació lineal entre les 0 i les 6 setmanes per després estancar-se. Finalment el compostos de 5 i 6 anells es degraden lentament però de forma

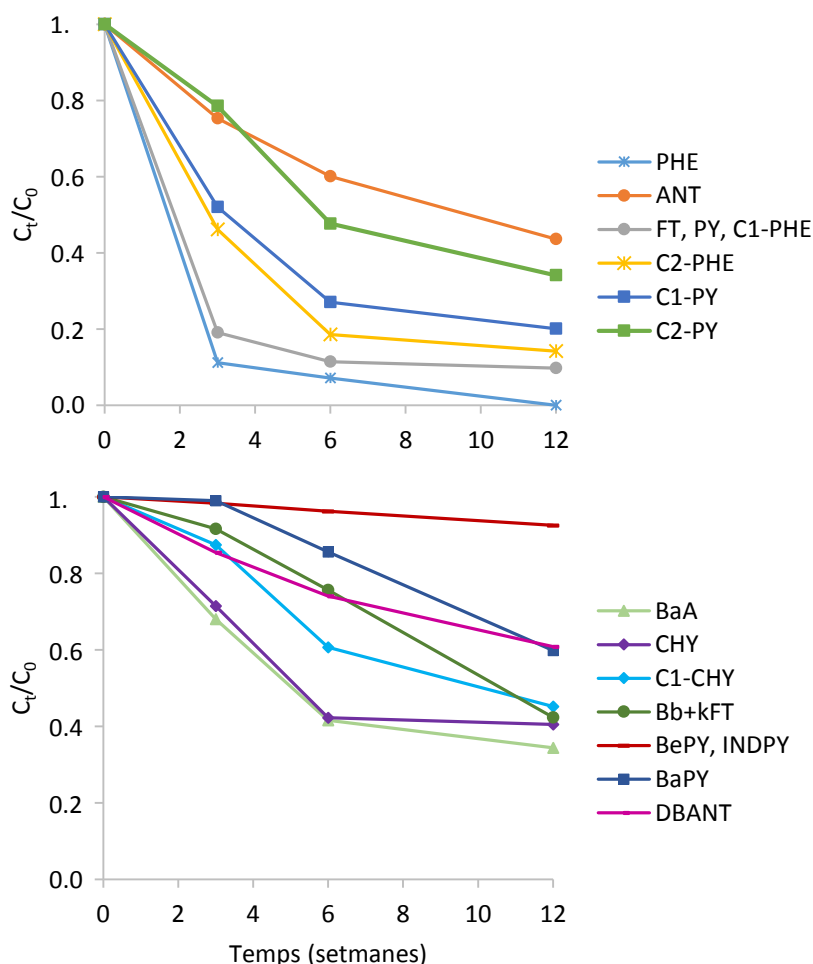


Figura 10.1. Disminució dels HAPs individuals en els cultius inoculats amb el consorci UBHP amb medi mineral i la barreja d'HAPs EPM de la creosota com a única font de carboni. Cada punt correspon a la mitjana dels triplicats. Les cinètiques del FT, PY i C1-PHE; i del BePY i INDPY es troben agrupades en una mateixa línia, ja que els valors a cada punt no van ser significativament diferents. Les barres d'error no estan representades per facilitar la lectura de les dades.

constant durant tota la incubació. L'ANT va ser l'excepció, ja que mostrà taxes de degradació baixes. Durant la degradació es van acumular una varietat de metabòlits àcids característics de la degradació de HAPs EPM per micobacteris (Figura 10.2).

Un cop confirmat l'elevat potencial degradador del consorci UBHP, es va analitzar la l'estructura d'aquesta comunitat microbiana mitjançant la combinació de varies tècniques per poder definir bé els membres que juguen un paper clau en la desaparició dels HAPs EPM. Primer de tot, es va fer una caracterització filogenètica per llibreria de clons del gen 16S ADNr i de les RHD per GN i GP. Es va incubar la comunitat amb substrats individuals (PHE, FT, PY, BaA, CHY i BaPY) per veure canvis en les poblacions i poder-les associar a una funció específica. Finalment, es van recuperar els filotips més importants en cultiu pur per confirmar el paper que jugaven en l'eliminació del HAPs EPM.

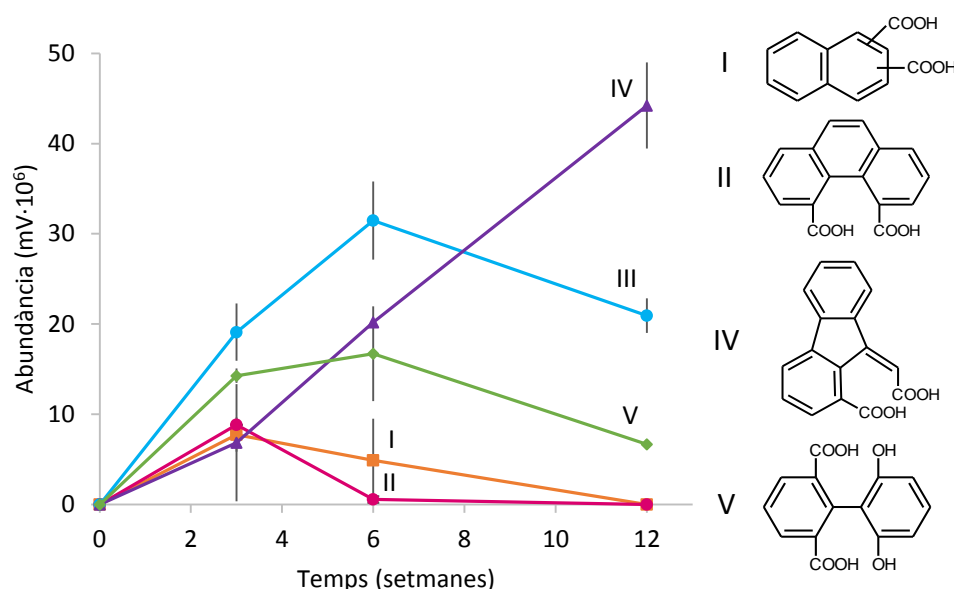


Figura 10.2. Acumulació al llarg del temps dels metabòlits més abundants identificats en els extractes àcids dels cultius del consorci UBHP amb medi mineral i i la barreja d'HAPs EPM de la creosota com a única font de carboni. Els valors d'abundància corresponen a les mitjanes de les àrees dels pics de GC-MS de cadascun dels triplicats. Les barres d'error mostren la desviació estàndard. Metabòlit I, àcid naftalè 1,2-dicarboxílic o àcid 2,3-dicarboxílic; II, àcid fenantre 4,5-dicarboxílic; III, àcid aromàtic dicarboxílic no identificat, observat prèviament durant la degradació del pirè per l'acció de micobacteris; IV, àcid Z-9(carboximetilè)9H-fluorè-1-carboxílic; V, àcid 6,6'-dihidroxi-2,2'-bifenil dicarboxílic.

El consorci UBHP incubat amb els HAPs individuals va degradar significativament i alhora va créixer amb el PHE, FT, PY i BaA (72-96%). El CHY es va degradar significativament (22%) però no va donar lloc a creixement bacterià, mentre que el BaPY no va ser atacat. Això podria indicar que la desaparició d'aquests dos HAPs depèn de la presència d'altres compostos que actuen de cosubstrats (Jones et al. 2014; Kanaly et al. 2000; Moody et al. 2004)

L'anàlisi molecular del consorci UBHP, els canvis en la comunitat en resposta a l'exposició a HAPs individuals (Figura 10.3) i l'aïllament de soques bacterianes i la seva posterior caracterització, ha permès associar inequívocament 5 gèneres a la degradació d'HAPs EPM. Aquests gèneres representen una tercera part de la comunitat segons la llibreria de clons i engloben 10 filotips diferents: *Sphingobium* i *Sphingomonas* (23%, *Alphaproteobacteria*), *Achromobacter* (4%, *Betaproteobacteria*), *Pseudomonas* (4%, *Gammaproteobacteria*) i *Mycobacterium* (menys de l'1,5%, *Actinobacteria*). Per altra banda, un 32% de la comunitat corresponia a un grup de *Gammaproteobacteria* no classificades, un filotip de les quals fou indirectament associat a la degradació de BaA i CHY. Curiosament, la seqüència del gen 16S ARNr d'aquest filotip va presentar una similitud major al 99% amb el grup de pirè 2 (PG2) descrit en un estudi de les poblacions degradadores d'HAPs en un bioreactor per ADN-SIP (Singleton et al., 2006). Finalment, un únic filotip del gènere *Terrimonas* representà un 19% de la llibreria de clons, però el seu aïllat no va demostrar capacitats degradadores al ser incubat amb el NAPL d'HAPs EPM.

L'increment en l'abundància relativa de filotips S1 i S2 de *Sphingomonadaceae* quan s'incubà el consorci amb PHE i FT i la posterior comprovació que l'aïllat *Sphingobium* S2 fou capaç d'eliminar el PHE, FT i PY del NAPL d'HAPs EPM, confirma el paper important que juga aquesta classe en la degradació d'un gran ventall d'HAPs. De fet, la seva versatilitat ha estat associada a la possessió d'enzims amb una relaxada especificitat de

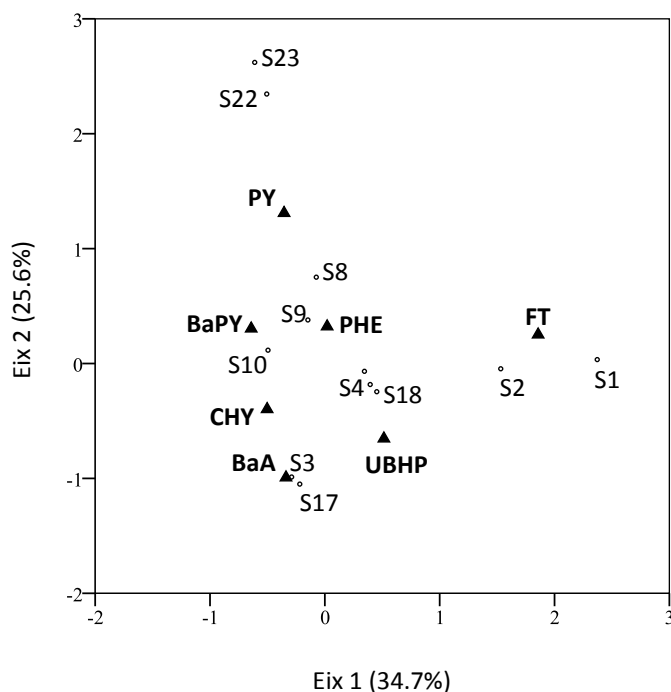


Figura 10.3. Anàlisi de correspondència de la intensitat de les bandes de cada mostra. Els dos primers eixos del gràfic expliquen el 60,3% de la variància observada. Els triangles negres representen la distribució del consorci microbià UBHP utilitzat com a inòcul (UBHP); i els triangles negres representen la distribució dels cultius amb cada un dels HAPs individuals (PHE, FT, PY, BaA, CHY, BaPY). Els cercles indiquen la distribució de les 12 bandes identificades.

substrat (Stolz, 2009) i s'han aïllat un gran número de soques amb capacitats degradadores (Kunihiro et al. 2013; Mueller et al. 1990; Roy et al. 2012; Schuler et al. 2009).

L'únic filotip detectat dins de la classe de les *Betaproteobacteria* (S8) es va identificar com *Achromobacter* i es va detectar en les DGGE de tots els substrats individuals com a una banda important. Aquest filotip també es va aconseguir aïllar en cultiu pur i també va demostrar elevats percentatges de degradació per a PHE, FT i PY quan fou incubat amb la creosota envellida. Això confirmaria la seva col·laboració amb les esfingomonas per eliminar els HAPs EPM. Tot i que membres dels betaproteobacteris han estat detectats en estudis de poblacions sotmeses a la degradació d'HAPs (M. D. Jones, Crandell, et al., 2011; Martin et al., 2012b; Viñas et al., 2005), no hi ha gaires soques degradadores aïllades (Weissenfels et al. 1990) i les seves vies metabòliques han estat escassament descrites (Kohlmeier et al., 2005).

Per altra banda, cap membre dels actinobacteris no va ser detectat en la llibreria de clons, segurament degut a que es troben en proporcions baixes respecte a la comunitat total. No obstant, la detecció de metabòlits signatura de la degradació de FT [àcid 9-Z-carboximetilè-fluorè-1-carboxílic, (López et al. 2005)] i PY [àcid 6,6'-dihidroxi-2,2'-bifenil dicarboxílic (Joaquim Vila et al., 2001)] per soques de *Mycobacterium* a l'experiment de biodegradació del consorci UBHP fa evident la importància d'aquest tàxon en la degradació d'ambdós compostos. De fet, dues soques d'aquest gènere foren aïllades i incubades amb la barreja d'HAPs EPM de la creosota i van donar elevats percentatges de biodegradació de PHE, FT i PY.

Pel que fa a l'anàlisi funcional, l'amplificació del consorci UBHP amb els encebadors descrits per Cébron et al. (2008), va donar positiu tant per GN com per GP. Les llibreries de clons dels corresponents amplicons van donar 5 seqüències úniques molt similars entre elles (95-99% en el cas de GN i 96-99% per GP) i que bàsicament amplificaren el gen *nahAc* de diferents soques de *Pseudomonas* i el gen *NidA3* de *Mycobacterium*. Les soques aïllades també foren amplificades amb aquests jocs de primers, però només les dues soques (S22 i S23) del gènere *Mycobacterium* donaren positiu. Curiosament, les dues seqüències més abundants de la llibreria de clons de cada soca tenien una similitud de 100% i corresponien a les mateixes RHD trobades en el consorci UBHP. A més a més, dues noves seqüències no detectades anteriorment en el consorci, tenien elevada similitud (93% i 99%) amb el gen *PdoA2* també de micobacteris. D'aquesta manera, es torna a confirmar el paper clau que té aquest gènere en la degradació d'HAPs EPM.

BIODEGRADACIÓ DELS HAPs I FORMACIÓ DE METABÒLITS DURANT L'ESTIMULACIÓ A ESCALA DE LABORATORI D'UN SÒL CONTAMINAT AMB CREOSOTA

Per tal d'aprofundir en el funcionament de les xarxes metabòliques que canalitzen la degradació dels HAPs *in situ*, es van seguir les cinètiques de desaparició dels HAPs i N-CAPs i les d'acumulació/degradació dels oxi-HAPs i metabòlits àcids juntament amb les dinàmiques de les poblacions degradadores corresponents. D'aquesta manera, es pretenia assignar la degradació de compostos determinats a poblacions específiques. Així, el mateix sòl utilitzat en l'enriquiment del consorci UBHP, fou barrejat (1:2) amb un sòl agrícola prèviament esterilitzat i distribuït en safates de 2,5 kg. Es van realitzar 2 tractaments per triplicat en els quals en ambdós s'ajustava la humitat al 40% de la capacitat de camp setmanalment. En un d'ells, es va afegir nitrogen i fòsfor en una proporció molar C:N:P de 300:10:1. Finalment també es van preparar 3 safates amb sòl sec com a control. El sòl amb humitat (-N), el sòl amb humitat i nutrients (+N) i el sòl sec (CTL) es van incubar durant 150 dies prenent mostres dels triplicats de cada tractament a temps 0, 7, 15, 30, 45, 60, 90, 120 i 150. Les mostres es van dividir en 3 parts: 15g per l'anàlisi química, 5g per als comptatges de degradadors i 5 g per a l'anàlisi molecular (veure capítol següent).

Mentre que en el sòl sec no es va observar una degradació significativa dels HAPs durant el període d'incubació, tant en el tractament sense nutrients com en el que sí tenia nutrients hi va haver una elevada biodegradació dels HAPs (69 i 93%, respectivament). Els HAPs BPM es van degradar més o menys per igual en els dos tractaments (90-95%), tot i que en el cas de l'addició de nutrients ho van fer de forma més ràpida. La diferència en l'extensió de la degradació va residir en els HAPs EPM, ja que mentre només es van degradar un 26% sense nutrients, l'addició de nitrogen i fòsfor va provocar un augment en el percentatge d'eliminació fins a un 87%. D'aquesta manera, es van trobar les condicions òptimes (+N) en què tots els compostos de 2, 3, 4 i 5 anells aromàtics es degradaven significativament i que, per tant, permetien estudiar les cinètiques de desaparició i correlacionar-les amb les dinàmiques de les poblacions degradadores corresponents. Així, es va triar el tractament amb nutrients per aprofundir en l'anàlisi de l'evolució de les poblacions degradadores per la tècnica del número més probable (NMP) i les cinètiques de degradació d'HAPs, oxi-HAPs, N-CAPs i metabòlits àcids.

Igual que en el cas de la degradació amb el consorci UBHP, els HAPs es van degradar de forma seqüencial i d'acord amb la seva solubilitat en aigua (Figura 10.4 i Figura 10.5). Com era d'esperar, el NAPH va ser el primer en ser eliminat amb una ràpida disminució quasi fins

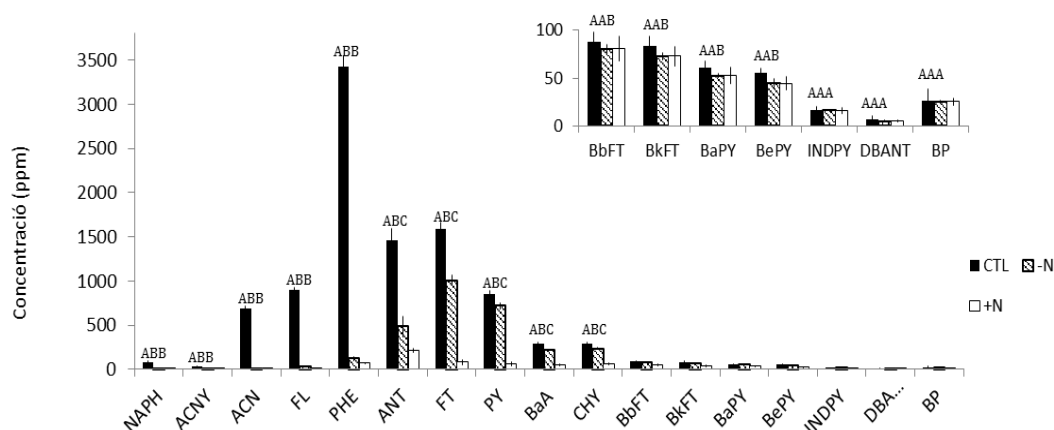


Figura 10.4. Concentracions d'HAPs a temps 150 dies del sòl control (CTL), i tractat amb (+N) i sense nutrients (-N). Lletres diferents volen dir diferències significatives entre tractaments.

a l'esgotament durant els primers 15 dies. Això va coincidir amb un increment dràstic dels degradadors de PHE (Figura 10.6), bàsicament representat pels gèneres *Pseudomonas* i *Pseudoxanthomonas*, ben coneguts com a degradadors d'HAPs EPM (Haritash & Kaushik, 2009; Pathak et al., 2009). A més, productes àcids com ara l'àcid ftàlic i l'àcid salicílic, que són productes intermedis de la via de biodegradació de NAPH, van mostrar la seva acumulació màxima durant aquest període.

El quasi esgotament de NAPH al dia 15 va desencadenar la biodegradació dels HAPs de 3 anells, que van presentar una baixada ràpida durant la segona quinzena, a excepció de l'ANT tal i com va passar també en el consorci UBHP. Al llarg d'aquest temps el creixement de les poblacions capaces de créixer en PHE es va atenuar tot i que es segueixen mantenint com la població degradadora més abundant, amb els representants trobats prèviament de *Pseudomonas* i *Pseudoxanthomonas* juntament amb membres de *Sphingobium* i *Achromobacter*. No obstant, els degradadors d'ANT i BaA van experimentar un increment ràpid, essent *Achromobacter* i *Olivibacter* els filotips més abundants. Sembla plausible que totes aquestes poblacions participaren en l'eliminació del HAPs BPM. Al llarg de la fase ràpida d'esgotament del FL, només hi va haver un petit increment inicial dels seus degradadors (menys d'un ordre de magnitud). Això suggereix que aquest HAP podria ser transformat principalment per l'acció inespecífica dels bacteris que no creixen bé a costa seva. El fluorè es cometabolitza fàcilment a 9-fluorenona per l'acció no específica de RHD del tipus naftalè (Selifonov et al., 1996). De fet, hi ha un estudi que demostra la mineralització cooperativa del fluorè per *Arthrobacter* sp. F101, produint 9-fluorenona, que després s'oxida per una soca de *Pseudomonas* que no és capaç d'atacar el FL (Casellas et al., 1998). El fet que degradadors de 9-fluorenona estan a una concentració més gran

que les de FL durant la desaparició d'aquest HAP, recolza fermament que una part important de FL passa a la seva cetona per cometabolisme. Això també és coherent amb la reducció ràpida de les concentracions inicials de 9-fluorenona. Dins de les poblacions específiques que degraden aquesta cetona destaca un membre de *Ralstonia* (*Bulkholderiaceae*).

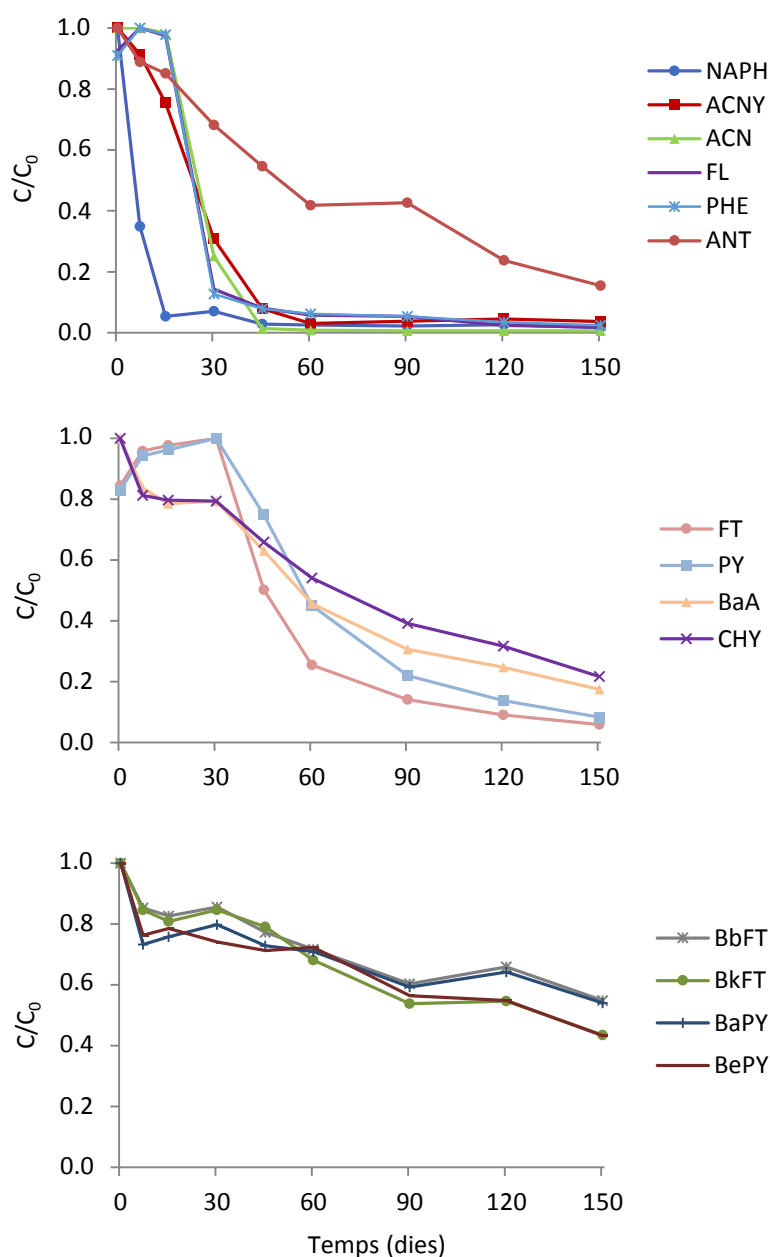


Figura 10.5. Cinètica de biodegradació dels HAPs degradats significativament durant el tractament amb nutrients (+N). Les barres d'error no estan representades per facilitar la lectura de les dades.

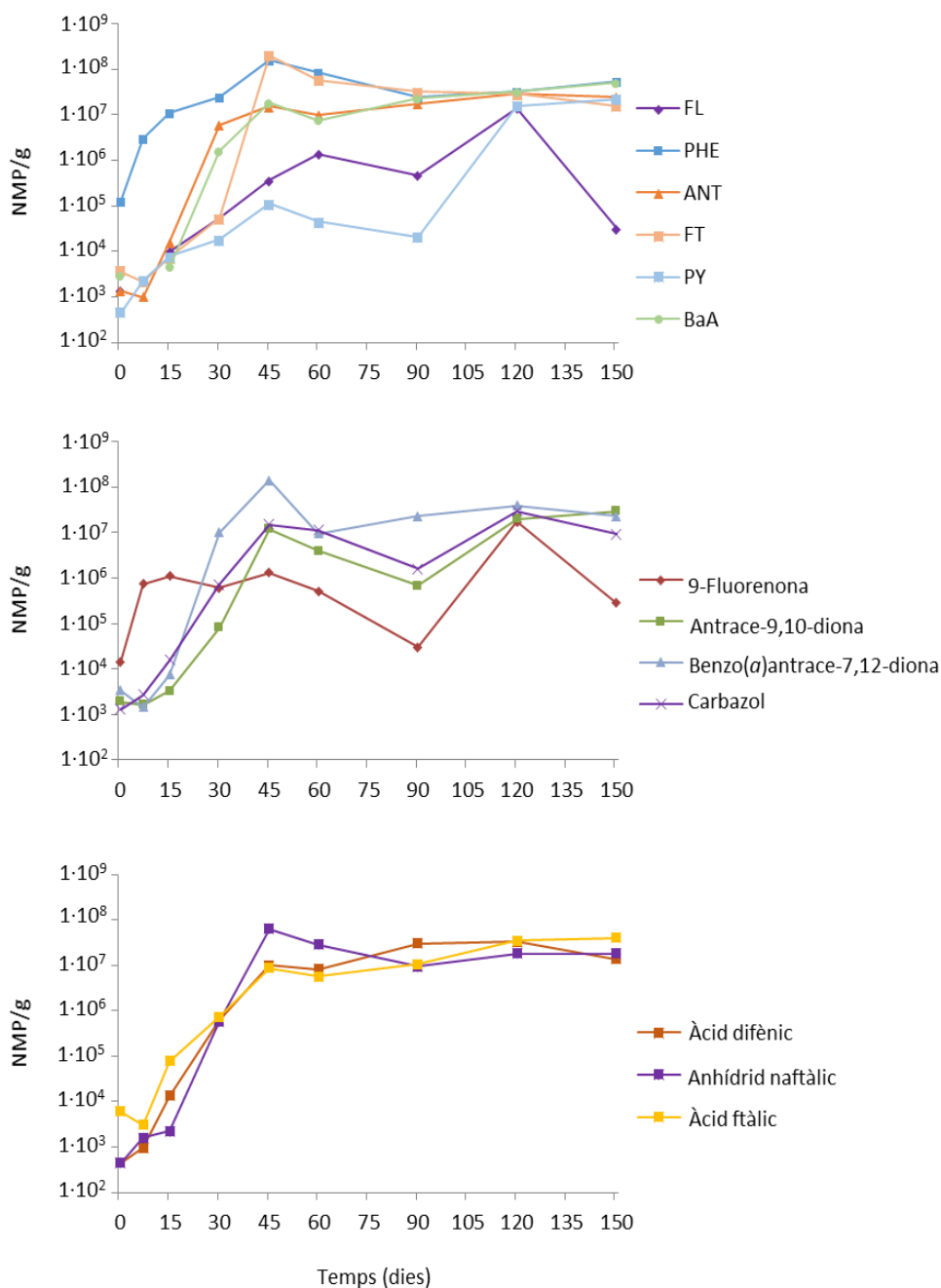


Figura 10.6. Enumeració de les poblacions degradadores dels compostos aromàtics policíclics al llarg del temps d'incubació. Les barres d'error no estan representades per facilitar la lectura de les dades.

En la bibliografia, s'ha descrit la formació i acumulació de la 9,10-antraquinona com a resultat de l'exposició d'antracè a diferents degradadors d'HAPs (Grifoll et al. 1995 and 1994). Per tant, l'alta concentració de RHD de tipus naftalè durant el primer mes també seria responsable de l'acumulació transitòria d'antraquinona. D'aquesta manera, les poblacions degradadores d'ANT no coincidiren amb les de la seva quinona. En el cas dels degradadors d'ANT les poblacions principals corresponien a *Pseudomonas*,

Achromobacter i, especialment, un membre d'*Olivibacter*, mentre que en el cas de la 9,10-antraquinona va destacar un membre específic de *Sphingobium*.

La ràpida disminució de FT coincideix amb un ràpid creixement de les poblacions degradadores d'aquest compost entre 30 i 45 dies. Per tant, està clar que els membres de *Sphingobium*, que es troben en els pous de FT més diluïts als 45 dies, juguen un paper clau en la transformació d'aquest HAP. Tenint en compte que l'esgotament de PY segueix una cinètica molt similar a la de FT, i que els microorganismes degradadors de PY romanen en concentracions baixes, és raonable suposar que els microorganismes degradadors de fluorantè van contribuir a la ràpida disminució de la concentració de pirè. Per descomptat, la identificació dels metabòlits signatura de FT i PY (pics a 45 i 60 dies) indica que els actinobacteris, encara que en concentracions més baixes, també tenen un paper clau en l'oxidació d'aquests compostos.

Com s'ha esmentat, l'increment inicial de microorganismes capaços de degradar BaA no es va correlacionar amb la seva degradació, el que suggereix que alguns microorganismes degradadors de BaA també eren capaços d'utilitzar compostos de 3 anells (Koukkou & Vandera, 2011). L'anàlisi de les poblacions es va realitzar entre 60 i 90 dies i els perfils de DGGE van mostrar com degradadors de BaA membres d'*Olivibacter*, *Achromobacter* i un representant de *Bradyrhizobiaceae* que no es trobà en altres substrats.

Desafortunadament, els degradadors de crisè no es van seguir durant l'experiment, però, d'acord amb la similitud entre la seva cinètica i la de BaA, podríem hipotetitzar que probablement foren oxidats per poblacions de bacteris similars.

CANVIS ESTRUCTURALS I QUANTITATIUS EN LA COMUNITAT MICROBIANA D'UN SÒL CONTAMINAT AMB CREOSOTA DURANT LA DEGRADACIÓ D'HAPs

Per aprofundir en la identificació de bacteris clau en la degradació d'HAPs *in situ* s'analitzaren les mostres preses en l'experiment descrit en l'apartat anterior mitjançant tècniques moleculars que permeteren descriure les dinàmiques poblacionals.

Es va procedir a l'extracció tant de l'ADN com de l'ARN totals de les mostres per triplicat al llarg del temps i pels dos tractaments (-N i +N). Els gens 16S ARNr (per bacteris total), 18S ARNr (per fongs), RHD de GN i GP i el 16S ARNr específic de *Mycobacterium* foren quantificats per qPCR tant de l'ADN com l'ADNc procedent de la retro-transcripció de l'ARN.

Aquesta és la primera vegada que la dinàmica d'una comunitat microbiana s'ha seguit durant la degradació d'HAPs en un sòl contaminat no només des del punt de vista genòmic, sinó també des del punt de vista de la transcriptòmica. Les diferències

quantitatives i qualitatives observades van demostrar la idoneïtat d'aquest enfocament metodològic combinat, ja que l'ARN permet vincular de forma més acurada funcions a poblacions específiques a través del temps. Les determinacions basades només en ADN podrien estar esbiaixades per la presència de cèl·lules amb diferents nivells d'activitat, incloent cèl·lules no viables o ADN lliure.

La disponibilitat de nutrients no va tenir un efecte sobre la concentració de la comunitat bacteriana total (16S ADN_r), ja que no van experimentar canvis substancials durant la incubació en cap dels dos tractaments (Figura 10.7). L'activitat bacteriana (16S rRNA) va augmentar durant els primers 15 dies en els dos tractaments, però, a partir de llavors l'increment amb l'addició de nutrients va ser dramàticament més alt, el que indica una limitació de nutrients. Aquests resultats són consistents amb que només hi va haver degradació d'HAPs EPM quan es va afegir nitrogen i fòsfor.

La quantificació per qPCR dels gens 18S rRNA va indicar una abundància menor de les poblacions de fongs en termes de còpies de gens · g⁻¹ de sòl, mostrant valors entre 2 i 3 ordres de magnitud inferiors als dels bacteris quan es van incubar amb addició de nutrients. No obstant això, en aquestes condicions, les poblacions de fongs no s'activaren

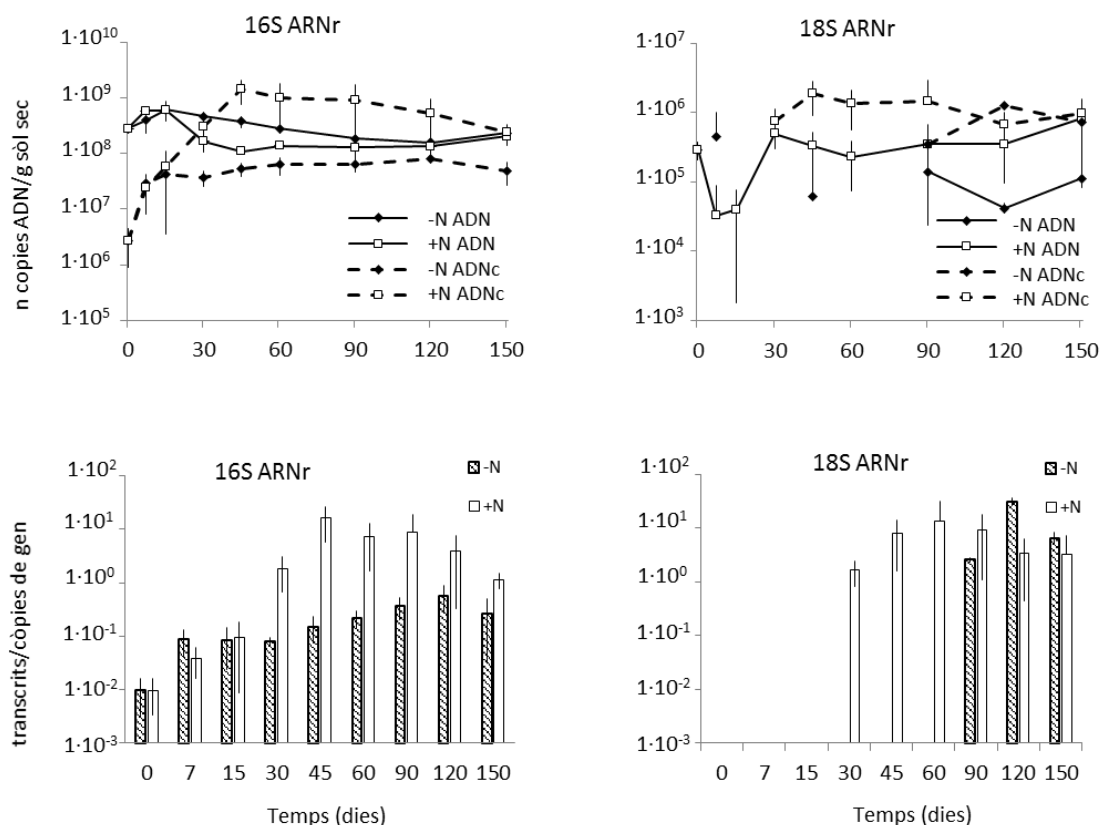


Figura 10.7. A dalt, es mostra la quantificació dels gens 16S ARNr i 18S ARNr (DNA) per qPCR i els seus transcrits (DNAc) en ambdós tractaments (-N i +N). A sota, es mostren les proporcions de transcrits/còpies dels gens 16S ARNr i 18S ARNr, respectivament. Les dades no representades al gràfic 18S ARNr corresponen a valors que es troben per sota del límit de detecció ($4.6 \cdot 10^3$ transcrits · g⁻¹ i $2 \cdot 10^3$ còpies de gen · g⁻¹).

fins després d'un mes d'incubació i es mantingueren aproximadament constants a partir de llavors. Per tant, els fongs podrien tenir un paper en la biodegradació dels HAPs EPM possiblement en col·laboració sinèrgica amb certs tàxons bacterians.

La comunitat bacteriana també va ser analitzada des d'un punt de vista funcional per quantificar específicament les poblacions degradadores de GN i GP en base a l'abundància de gens que codifiquen per RHD (Figura 10.8). En el cas de l'addició de nutrients, les dioxigenases de GN van augmentar fins a arribar a un pic màxim d'expressió als 15 dies, coincidint amb la màxima degradació del NAPH, per després mantenir-se constants fins a temps 90 i disminuir els dos últims mesos. És en aquesta última etapa que les RHD de GP augmenten arribant a un màxim d'expressió al temps 120 dies. L'afiliació taxonòmica dels respectius transcrits en aquests dos punts determinà que les RHD de GN corresponien bàsicament al gen *nahAc* de *Pseudomonas*, mentre que les de GP va mostrar elevada similitud amb els gens *NidA3*, *NidA* i *Pdo2A* de soques de *Mycobacterium*. És important destacar que, encara que les RHD de GP van presentar número de còpies de gens més baixos que els de GN durant tota la incubació amb nutrients, les RHD GP van exhibir nivells més alts d'expressió gènica que les de GN.

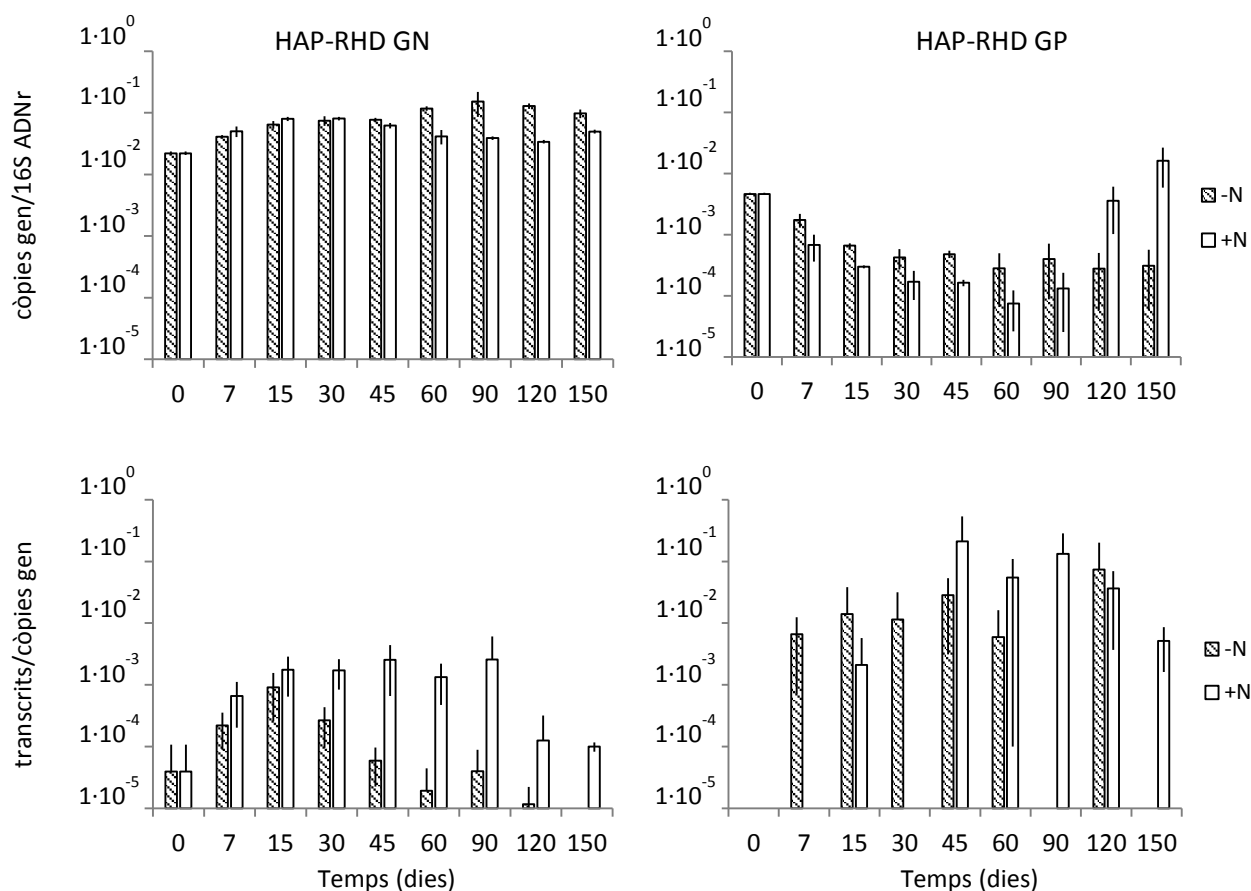


Figura 10.8. A dalt, evolució de les proporcions HAP-RHD/16S ADNr de GN i GP en ambdós tractaments (-N i +N). A baix, els transcrits d'HAP-RHD de GN i GP es representen respecte al seu número de còpies gèniques per ambdues condicions.

Curiosament, l'anàlisi per piroseqüenciació (Figura 10.9) durant de màxima expressió de GN, va mostrar que els filotips més abundants (tant en la població total com en l'activa) eren membres de *Pseudomandaceae* i *Pseudoxanthomonas*, que també és coherent amb l'anàlisi filogenètica dels transcrits de gens RHD GN i amb els taxons detectats en el NMP de capítol anterior.

La presència de membres de *Pseudoxanthomonas* s'ha trobat sovint en l'anàlisi de l'estructura de la comunitat durant la degradació d'HAPs (Louvel et al. 2011; Singleton et al 2011; Viñas et al 2005), però només unes poques soques d'aquest gènere han estat confirmades com a degradadores d'aquest compostos. Per exemple, la *Pseudoxanthomonas* sp. DMVP2 es va aïllar recentment d'un sediment i es capaç de degradar el PHE a través de la ruta de l'àcid ftàlic. Si analitzem els resultats de qPCR de transcrits de 16S rRNA juntament amb les dades de piroseqüenciació, *Pseudoxanthomonas* es va mantenir dins dels principals tàxons actius fins al dia 90, el que podria indicar el seu possible paper també en la degradació dels HAPs EPM.

A partir dels 30 dies, es van començar a degradar els HAPs EPM (veure apartat anterior). A partir d'aquest punt, es van detectar com a filotips actius importants membres de *Sphingobium*, *Achromobacter*, *Olivibacter*, *Starkeya*, *Acetobacteriaceae*, *Roseomonas*, *Rhizobiaceae* i *Methylocystaceae* que es van associar a la degradació dels HAPs de 4 i 5 anells. La majoria d'ells han estat prèviament relacionats amb la degradació de

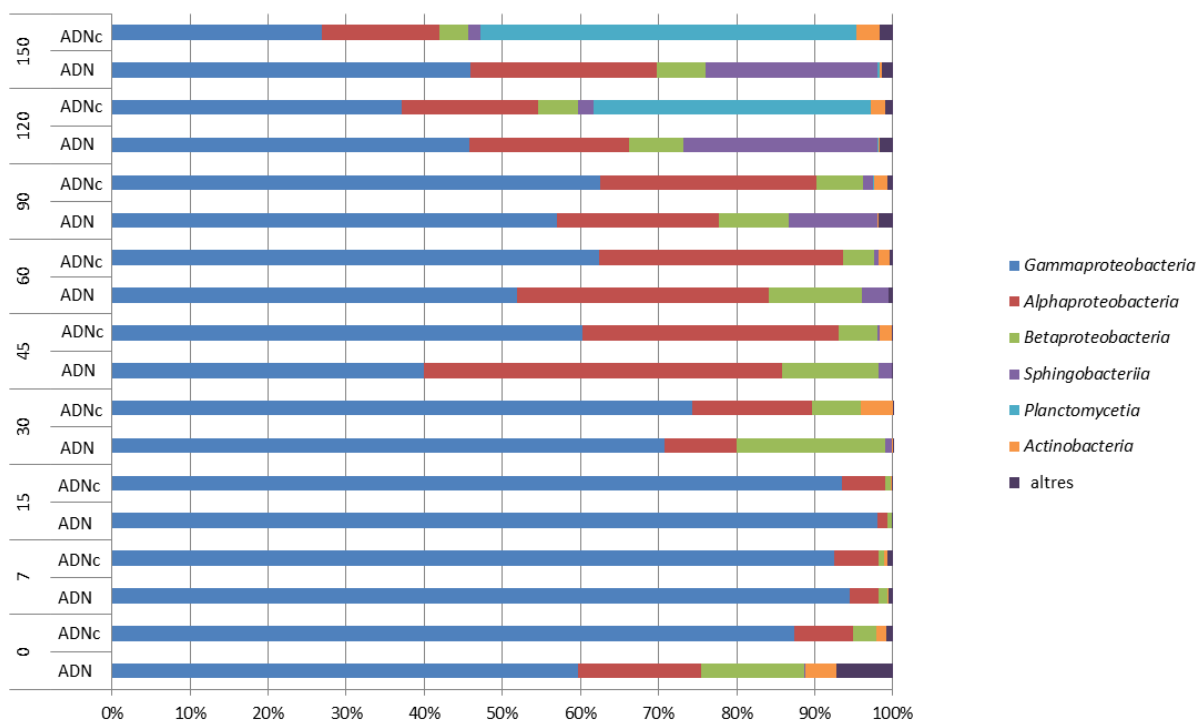


Figura 10.9. Abundància relativa de les diferents classes de la població total (ADN) i de la població activa (ADNc) en el sòl al llarg del temps d'incubació. Dins d'altres es comprenen les classes que es troben per sota del 0.5% de l'abundància relativa i les seqüències no classificades.

contaminants orgànics (Chen et al 2013; Dashti et al 2015; Viñas et al 2005), però només els dos primers són àmpliament coneguts com degradadors d'HAPs (Deng et al. 2014; Chirag et al. 2011; Kunihiro et al. 2013; Maeda et al. 2014).

La classe de degradadors d'HAPs EPM més estudiada, *Actinobacteria*, també sembla jugar un paper important en l'eliminació d'aquests compostos en el sòl estimulat amb nutrients. Els resultats obtinguts a partir de la quantificació dels transcrits de RHD de GP van indicar una activació dels bacteris degradadors Grampositius del dia 45 fins al final de la incubació, assolint un màxim a 120 dies. Alhora, durant aquest període la concentració de HAPs EPM va disminuir. Sabent que els encebadors utilitzats bàsicament amplificaren dioxigenases específiques de *Mycobacterium*, podria haver-hi un petit retard en l'activació de microorganismes degradadors de GP d'acord amb les seves taxes de creixement lent. El pic de transcrits específics de *Mycobacterium* va tenir lloc al final de l'experiment, i això podria explicar que la cinètica de degradació dels HAPs de 4 i 5 anells no aconseguís arribar a la fase asimptòtica del model del "pal d'hoquei". Durant aquest període, entre 90 i 150 dies, *Actinobacteria*, ara sense competència dels membres de més ràpid creixement de la comunitat, podria haver estat capaç de degradar la fracció residual millorant la seva biodisponibilitat, amb la seva coneguda capacitat per adherir-se a superfícies hidrofòbiques. En realitat, aquesta estratègia podria haver afavorit aquest tàxon en els últims dos mesos, quan l'activitat de tots els altres grups de bacteris es va reduir (excepte *Singulisphaera*).

Singulisphaera, un gènere del fílum *Planctomycetes* que mai s'ha relacionat amb ambients contaminats, va augmentar dramàticament la seva activitat entre 90 a 120 dies, representant al final de la incubació gairebé un 50% de la comunitat activa. En canvi, si només s'haguessin observat els resultats del 16S ADNr, aquest grup bacterià hagués passat desapercbut, ja que només representa el 0,27% de la comunitat total. Podria ser de gran interès per investigar la funció ecològica d'aquest tàxon en sòls, ja que podria estar relacionat amb la restauració de les condicions naturals del sòl, i actuar com a indicador de la millora de la qualitat del d'aquest. De fet, s'ha demostrat que l'abundància dels *Planctomycetes* és major en sòls abandonats o en sòls verges que en ambients antropitzats (Buckley et al. 2006).

10.4 Conclusions

- El desenvolupament del sistema bifàsic d'arena-en-aigua utilitzant una barreja d'HAPs d'EPM com a font de carboni ha demostrat ser efectiu per a l'obtenció d'un consorci microbià representatiu de la comunitat del sòl. Aquesta comunitat model ha permès reproduir els processos que porten a la biodegradació d'aquests hidrocarburs *in situ*.
- El consorci UBHP va dur a terme una extensa degradació dels HAPs de 4 i 5 anells. L'anàlisi exhaustiva de l'estructura i les funcions de la comunitat microbiana va permetre aprofundir en les interaccions entre poblacions, i va facilitar l'aïllament de membres rellevants de la comunitat amb capacitat degradadora d'HAPs.
- Les comunitats microbianes autòctones del sòl van respondre al tractament de bioestimulació eliminant una gran part dels HAPs (69 i 93%, respectivament, en absència i presència de nutrients). L'addició de nutrients va resultar efectiva per estimular la biodegradació dels HAPs EPM (4 i 5 anells), els N-CAPs i Oxi-HAPs.
- La ràpida degradació inicial dels HAPs de 2 i 3 anells al sòl tractat amb nutrients es va atribuir a l'elevada activitat de membres dels gèneres *Pseudomonas*, *Pseudoxanthomonas*, *Achromobacter* i *Olivibacter*. L'anàlisi funcional de la comunitat va confirmar l'expressió de diversos gens tipus *nahAc* lligats majoritàriament a pseudomonadàcies, que a més podrien tenir una acció cometabòlica sobre altres substrats.
- Les cinètiques de degradació de substrats individuals, l'anàlisi molecular de la comunitat i els perfils metabolòmics indiquen que alguns HAPs són parcialment cometabolitzats en les fases inicials de degradació, produint oxi-HAPs, especialment cetones i quinones, els quals requereixen de poblacions alternatives per a la seva posterior eliminació. En condicions no limitants, les poblacions autòctones eliminen eficientment els productes acumulats de forma transitòria, compensant de la mateixa manera la seva formació per oxidació química. Això suggereix que els oxi-HAPs podrien actuar com a nòduls en xarxes metabòliques complexes, on els subproductes d'una població podrien ser utilitzats per una altra.
- La subseqüent degradació dels HAPs de 4 anells fluorantè i pirè es va associar majoritàriament a membres de *Sphingobium*, els quals aparentment degradarien cometabòlicament el pirè de forma no productiva.

- El paper clau dels membres de *Mycobacterium* en la degradació de HAPs d'EPM en sòls es va confirmar. Aquests competirien amb els degradadors d'HAPs de BPM en la utilització de la fracció menys biodisponible de contaminant a les darreres fases de degradació. Aquest grup possiblement coopera amb altres taxons, com un grup de Gammaproteobacteries no classificades, i poblacions fúngiques.
- L'acumulació transitòria de metabòlits àcids durant la biodegradació d'HAPs i la seva posterior reutilització indica que aquests productes podrien ser utilitzats com a indicadors de biodegradació activa durant l'aplicació de tecnologies d'atenuació natural, i per monitoritzar el progrés de processos de bioremediació.
- Les poblacions totals i actives en el sòl contaminat van mostrar perfils clarament diferencials al llarg de la incubació. L'anàlisi de les dinàmiques de poblacions actives permeten una visió més acurada dels processos que tenen lloc *in situ* a temps real, permetent una associació més acurada entre les comunitats i les seves funcions.
- La detecció de gens funcionals i els seus nivells d'expressió es van mostrar útils per tal d'atribuir funcions a les diferents poblacions, fent evident l'expressió diferencial de dioxigenasses de GN (*nahAc*) i GP (majoritàriament *NidA3*) en les fases inicials i finals d'incubació, respectivament. Tot i això, la informació que es pot extreure d'aquestes anàlisis és encara limitada per la manca de disponibilitat d'uns encebadors que puguin cobrir l'àmplia diversitat de dioxigenasses del medi ambient.

CHAPTER 11

Annexes

11 Annex

Annex I. Supplementary material

Table S1. Absolute averages and standard deviations of the concentration of each PAH over the incubation of soil with nutrients.

Concentration (ppm)	T0	T7	T15	T30	T45	T60	T90	T120	T150
NAPH	272 ± 34	95 ± 47	15 ± 2	19 ± 1	8 ± 2	7 ± 4	6 ± 2	7 ± 4	5 ± 1
ACNY	40 ± 2	37 ± 1	31 ± 2	12 ± 2	3 ± 1	1 ± 0	2 ± 2	2 ± 1	2 ± 0
ACN	647 ± 36	713 ± 18	701 ± 90	179 ± 34	10 ± 2	6 ± 1	5 ± 1	5 ± 2	5 ± 1
FL	843 ± 70	911 ± 24	888 ± 143	130 ± 1	74 ± 17	53 ± 12	49 ± 10	23 ± 13	16 ± 4
PHE	2622 ± 185	2882 ± 90	2819 ± 399	366 ± 14	227 ± 29	180 ± 16	155 ± 30	100 ± 32	70 ± 3
ANT	1387 ± 356	1232 ± 137	1180 ± 312	945 ± 23	758 ± 196	581 ± 89	591 ± 196	329 ± 140	215 ± 28
FT	1228 ± 82	1394 ± 33	1420 ± 214	1453 ± 41	730 ± 49	371 ± 49	205 ± 21	132 ± 6	85 ± 29
PY	659 ± 48	748 ± 19	765 ± 122	794 ± 22	594 ± 35	358 ± 46	174 ± 13	110 ± 8	66 ± 22
BaA	278 ± 22	233 ± 20	218 ± 23	221 ± 13	175 ± 13	127 ± 15	85 ± 16	69 ± 11	48 ± 12
CHY	282 ± 21	229 ± 21	225 ± 29	224 ± 14	186 ± 13	153 ± 14	110 ± 26	89 ± 8	61 ± 14
BbFT	88 ± 8	75 ± 11	73 ± 7	75 ± 6	68 ± 6	63 ± 6	53 ± 17	58 ± 5	48 ± 13
BkFT	83 ± 7	70 ± 9	67 ± 7	70 ± 5	65 ± 10	56 ± 9	45 ± 15	45 ± 5	36 ± 10
BaPY	63 ± 6	46 ± 5	48 ± 5	51 ± 4	46 ± 5	45 ± 4	38 ± 10	41 ± 4	34 ± 9
BePY	58 ± 6	44 ± 6	45 ± 4	43 ± 3	41 ± 6	42 ± 5	33 ± 5	32 ± 3	25 ± 7
INDPY	15 ± 2	15 ± 1	14 ± 1	15 ± 1	14 ± 2	13 ± 2	10 ± 6	13 ± 2	11 ± 3
DBA	4 ± 1	6 ± 1	5 ± 0	5 ± 1	4 ± 0	4 ± 1	4 ± 1	4 ± 1	3 ± 1
BP	28 ± 3	25 ± 1	21 ± 2	23 ± 1	22 ± 2	20 ± 2	15 ± 9	18 ± 7	17 ± 4
Σ17 PAHs	8597 ± 704	8756 ± 350	8534 ± 1388	4625 ± 82	3026 ± 180	2078 ± 24	1579 ± 318	1075 ± 131	747 ± 95
LMW	5811 ± 642	5870 ± 225	5633 ± 944	1652 ± 41	1080 ± 236	827 ± 115	808 ± 234	466 ± 185	312 ± 30
HMW	2786 ± 178	2886 ± 125	2901 ± 444	2973 ± 101	1946 ± 136	1251 ± 134	772 ± 94	609 ± 55	435 ± 123

Table S2. Absolute averages and standard deviations of the concentration of each oxy-PAH over the incubation of soil with nutrients.

Concentration (ppm)	T0	T7	T15	T30	T45	T60	T90	T120	T150
9-Fluorenone	14 ± 0	15 ± 1	11 ± 1	4 ± 0	3 ± 0	2 ± 0	2 ± 0	2 ± 0	1 ± 0
Anthracene-9,10-dione	41 ± 0	47 ± 2	50 ± 5	63 ± 1	25 ± 2	13 ± 1	10 ± 1	8 ± 1	3 ± 2
4H-Cyclopenta(<i>d,e,f</i>)phenanthrenone	6 ± 0	8 ± 0	9 ± 1	52 ± 0	129 ± 5	97 ± 16	40 ± 8	19 ± 2	11 ± 2
2-Methylanthracene-9,10-dione	7 ± 1	8 ± 0	8 ± 1	9 ± 0	8 ± 1	5 ± 1	4 ± 0	3 ± 0	2 ± 0
Benzo(<i>a</i>)fluorenone	8 ± 0	10 ± 0	10 ± 1	6 ± 1	7 ± 0	5 ± 1	6 ± 0	6 ± 1	4 ± 2
Benz(<i>a</i>)anthracene-7,12-dione	2 ± 0	2 ± 0	2 ± 0	3 ± 0	4 ± 0	4 ± 1	5 ± 0	4 ± 1	3 ± 1
Naphthacene-5,12-dione	15 ± 1	16 ± 1	15 ± 2	17 ± 1	23 ± 1	21 ± 5	24 ± 1	22 ± 3	18 ± 6
Σ7 oxy-PAHs	91 ± 3	105 ± 5	105 ± 11	154 ± 4	198 ± 9	148 ± 25	90 ± 11	64 ± 8	43 ± 14

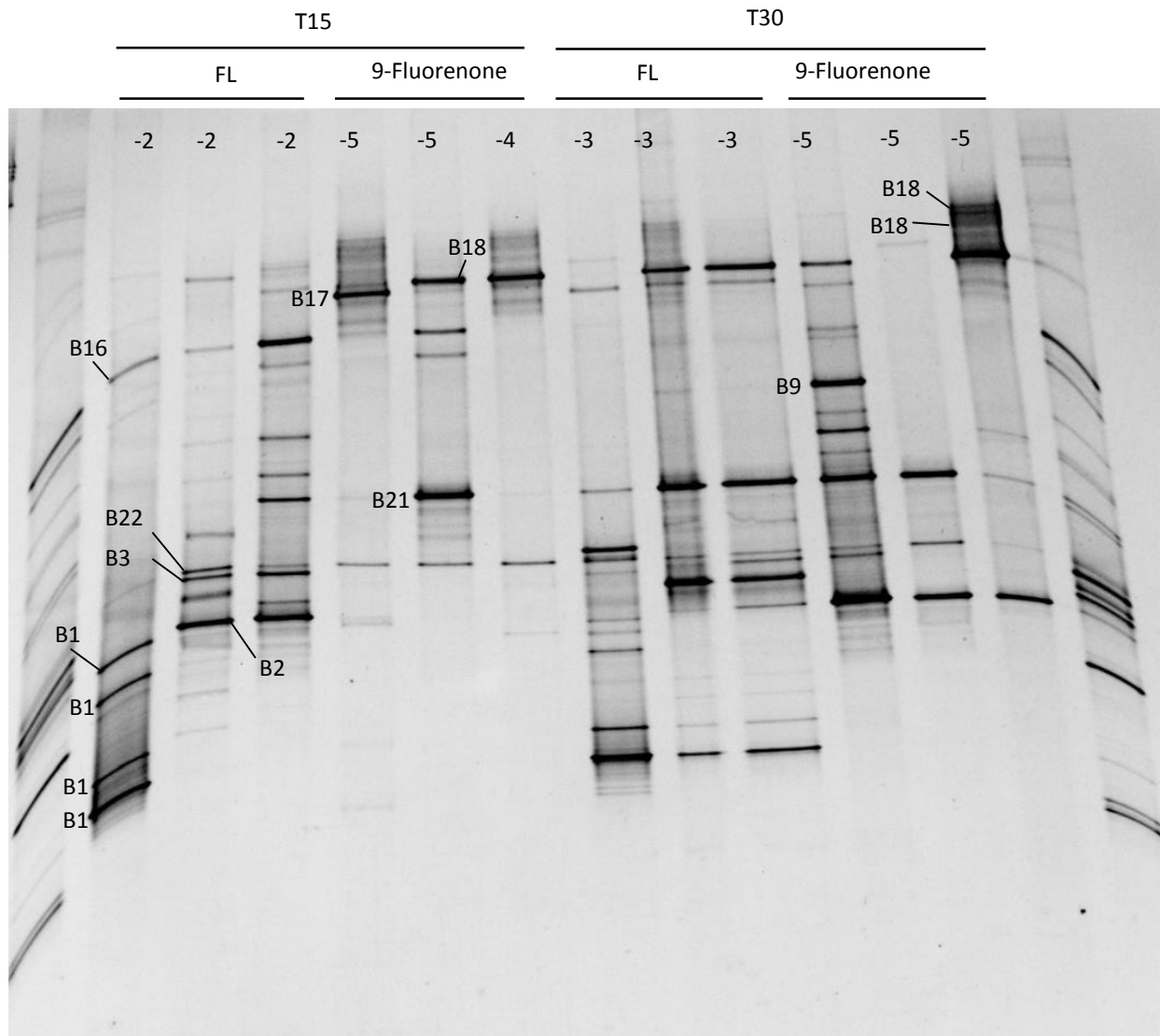
Table S3. Absolute averages and standard deviations of the concentration of each N-PAC over the incubation of soil with nutrients.

Concentration (ppm)	T0	T7	T15	T30	T45	T60	T90	T120	T150
Methylquinoline	11 ± 1	12 ± 1	9 ± 4	2 ± 0	2 ± 0	1 ± 0	1 ± 0	1 ± 0	0 ± 0
Dimethylquinoline	15 ± 3	25 ± 1	24 ± 1	22 ± 1	16 ± 1	11 ± 2	7 ± 1	3 ± 1	2 ± 1
Benzo(<i>h</i>)quinoline	11 ± 0	12 ± 0	12 ± 1	7 ± 1	10 ± 11	4 ± 2	7 ± 4	4 ± 2	3 ± 0
Acridine	113 ± 10	161 ± 5	151 ± 16	152 ± 1	157 ± 6	99 ± 16	59 ± 12	33 ± 3	20 ± 3
Methylacridine	36 ± 4	48 ± 2	45 ± 2	45 ± 0	47 ± 1	33 ± 6	21 ± 2	14 ± 2	9 ± 2
Carbazole	613 ± 138	447 ± 54	317 ± 85	269 ± 24	307 ± 90	226 ± 36	230 ± 54	123 ± 47	89 ± 23
Methylcarbazole	56 ± 3	29 ± 22	32 ± 8	16 ± 1	18 ± 4	13 ± 1	13 ± 3	7 ± 2	5 ± 0
Σ7 N-PACs	856 ± 122	734 ± 42	590 ± 24	514 ± 25	556 ± 100	389 ± 21	337 ± 70	185 ± 49	127 ± 17

Table S4. Absolute averages and Standard deviations of the enumeration of total heterotrophic populations and PAH-, oxy-PAH- and N-PAC-degrading populations throughout the treatment with nutrients.

MPN·g ⁻¹	FL	PHE	ANT	FT	PY	BaA
0	1,3E+03 ± 0,0E+00	1,3E+05 ± 5,3E+04	9,7E+02 ± 8,4E+02	3,6E+03 ± 3,9E+03	4,4E+02 ± 7,7E+02	2,8E+03 ± 2,9E+03
7	ND	3,0E+06 ± 2,5E+06	1,6E+04 ± 1,2E+04	2,1E+03 ± 1,8E+03	2,2E+03 ± 3,6E+03	ND
15	1,0E+04 ± 5,8E+03	1,1E+07 ± 8,0E+06	6,1E+06 ± 6,5E+06	7,4E+03 ± 5,4E+03	7,8E+03 ± 5,2E+03	4,4E+03 ± 1,8E+03
30	5,4E+04 ± 7,0E+04	2,5E+07 ± 8,5E+06	1,6E+07 ± 8,0E+06	5,4E+04 ± 7,0E+04	1,8E+04 ± 3,9E+03	1,6E+06 ± 4,0E+05
45	3,7E+05 ± 4,5E+05	1,6E+08 ± 3,5E+07	1,0E+07 ± 3,1E+06	2,1E+08 ± 1,4E+08	1,1E+05 ± 8,1E+04	1,8E+07 ± 1,1E+07
60	1,4E+06 ± 1,1E+06	8,6E+07 ± 5,0E+07	1,8E+07 ± 3,9E+06	5,9E+07 ± 2,8E+07	4,5E+04 ± 1,7E+04	7,7E+06 ± 2,2E+06
90	4,8E+05 ± 3,0E+05	2,5E+07 ± 8,5E+06	3,0E+07 ± 8,5E+06	3,2E+07 ± 2,2E+07	2,1E+04 ± 1,2E+04	2,3E+07 ± 1,1E+07
120	1,4E+07 ± 5,7E+06	3,3E+07 ± 2,8E+07	2,5E+07 ± 8,5E+06	2,9E+07 ± 2,1E+07	1,6E+07 ± 7,6E+06	3,2E+07 ± 2,8E+07
150	3,2E+04 ± 2,6E+03	5,6E+07 ± 6,8E+07	ND	1,6E+07 ± 1,4E+07	2,2E+07 ± 1,2E+07	5,1E+07 ± 6,0E+07

MPN·g ⁻¹	9-Fluorenone	Anthracene-9,10-dione	Benz(a)anthracene-7,12-dione	Diphenicacid	Naphthalic anhydride	Phthalic acid	Acridine	Carbazole	TSB
0	1,4E+04 ± 1,5E+04	1,9E+03 ± 1,7E+03	3,4E+03 ± 2,3E+03	4,4E+02 ± 7,7E+02	4,4E+02 ± 7,7E+02	6,1E+03 ± 5,3E+03	ND	1,3E+03 ± 8,8E+01	8,0E+06 ± 3,7E+06
7	7,4E+05 ± 3,8E+05	1,6E+03 ± 1,7E+03	1,5E+03 ± 0,0E+00	9,7E+02 ± 8,4E+02	1,6E+03 ± 1,7E+03	3,1E+03 ± 2,9E+03	ND	2,7E+03 ± 1,2E+03	5,9E+07 ± 6,7E+07
15	1,1E+06 ± 8,1E+05	3,3E+03 ± 3,2E+03	7,5E+03 ± 6,9E+03	1,4E+04 ± 6,5E+03	2,2E+03 ± 1,9E+03	7,8E+04 ± 5,1E+04	4,9E+02 ± 8,4E+02	1,6E+04 ± 1,7E+04	2,0E+08 ± 1,5E+08
30	6,0E+05 ± 1,4E+05	8,1E+04 ± 1,1E+05	1,0E+07 ± 8,9E+06	6,3E+05 ± 6,3E+05	5,8E+05 ± 3,5E+05	7,3E+05 ± 1,4E+05	ND	7,3E+05 ± 1,4E+05	9,2E+07 ± 4,1E+07
45	1,3E+06 ± 5,3E+05	1,2E+07 ± 7,1E+06	1,4E+08 ± 5,7E+07	1,0E+07 ± 8,9E+06	6,3E+07 ± 6,2E+07	8,6E+06 ± 3,3E+06	ND	1,5E+07 ± 7,6E+06	5,7E+08 ± 1,9E+08
60	5,2E+05 ± 6,1E+05	4,0E+06 ± 2,2E+06	9,6E+06 ± 9,5E+06	8,2E+06 ± 1,6E+06	2,9E+07 ± 2,1E+07	5,7E+06 ± 1,9E+06	ND	1,1E+07 ± 7,8E+06	2,3E+08 ± 1,1E+08
90	3,0E+04 ± 2,4E+03	6,9E+05 ± 4,5E+05	2,3E+07 ± 1,1E+07	3,0E+07 ± 8,5E+06	9,5E+06 ± 5,2E+06	1,0E+07 ± 9,2E+06	ND	1,6E+06 ± 8,1E+05	6,0E+08 ± 6,8E+07
120	1,7E+07 ± 1,3E+07	2,0E+07 ± 0,0E+00	4,0E+07 ± 2,2E+07	3,3E+07 ± 2,8E+07	1,8E+07 ± 3,9E+06	3,5E+07 ± 2,6E+07	1,2E+05 ± 7,7E+04	3,0E+07 ± 8,5E+06	4,0E+08 ± 2,2E+08
150	2,8E+05 ± 1,7E+05	3,0E+07 ± 8,5E+06	2,3E+07 ± 1,1E+07	1,4E+07 ± 0,0E+00	1,8E+07 ± 3,9E+06	4,0E+07 ± 2,2E+07	ND	9,3E+06 ± 6,0E+06	3,7E+09 ± 4,5E+09



Band	Prob (%)	Classification
B1	100	<i>Achromobacter</i>
B2	100	<i>Achromobacter</i>
B3	100	<i>Achromobacter</i>
B9	99	<i>Olivibacter</i>
B16	97	<i>Pseudomonas</i>
B17	100	<i>Pseudomonas</i>
B18	100	<i>Pseudomonas</i>
B21	100	<i>Pseudoxanthomonas</i>
B22	100	<i>Rashtonia</i>

Figure S11.1. DGGE profiles of the 16S rRNA gene fragments amplified from the most diluted MPN wells grown with FL and fluorenone at 15 and 30 days. The dilution factor of each well in indicated on the top of each lane. The excised bands from each profile are indicated, and their phylogenetic affiliation based on sequence analysis is shown in the accompanying table. Taxonomic affiliation was based on RDP classifier considering bootstrapping confidence scores >97%.

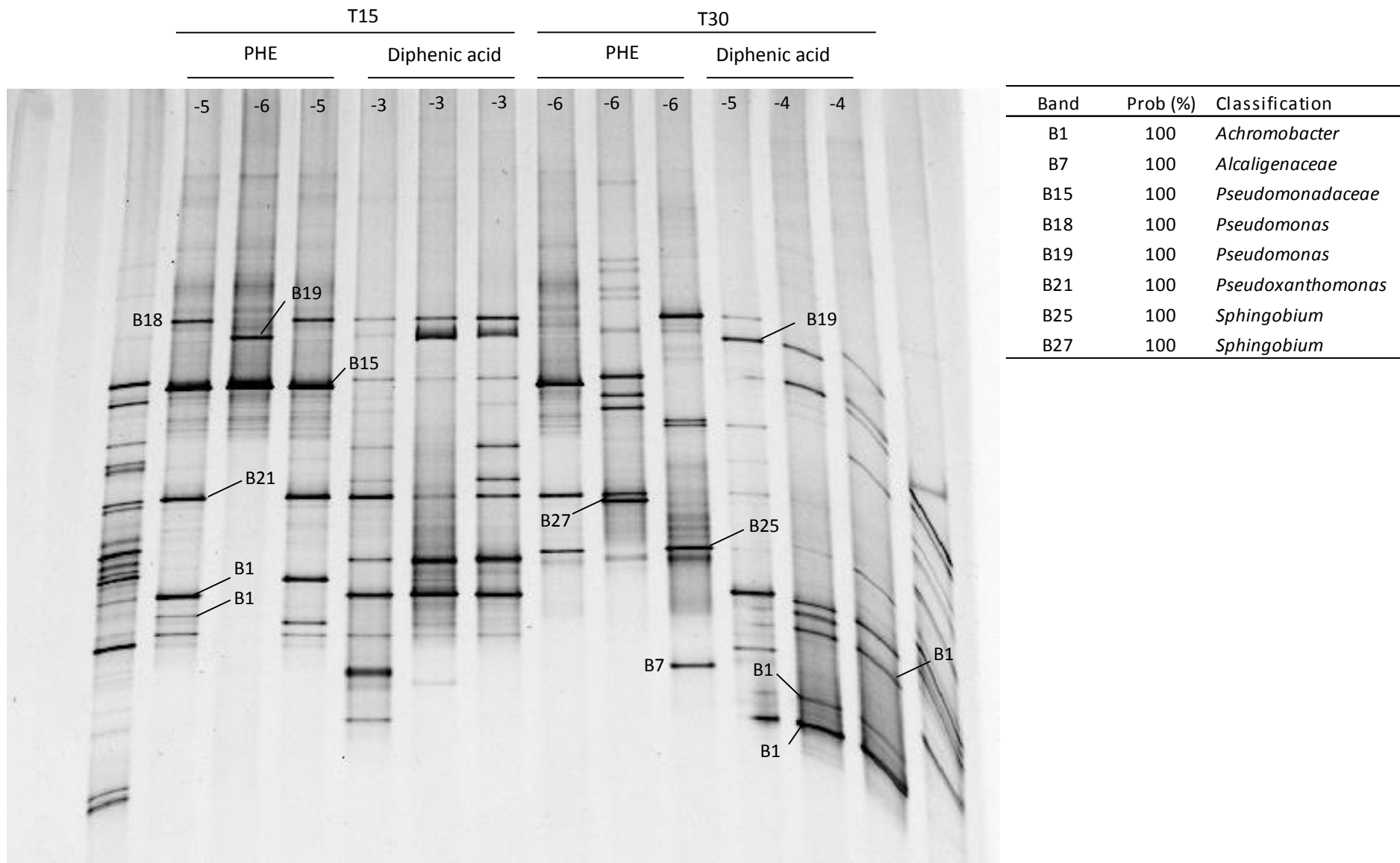


Figure S11.2. DGGE profiles of the 16S rRNA gene fragments amplified from the most diluted MPN wells grown with PHE and diphenic acid at 15 and 30 days. The dilution factor of each well is indicated on the top of each lane. The excised bands from each profile are indicated, and their phylogenetic affiliation based on sequence analysis is shown in the accompanying table. Taxonomic affiliation was based on RDP classifier considering bootstrapping confidence scores >97%.

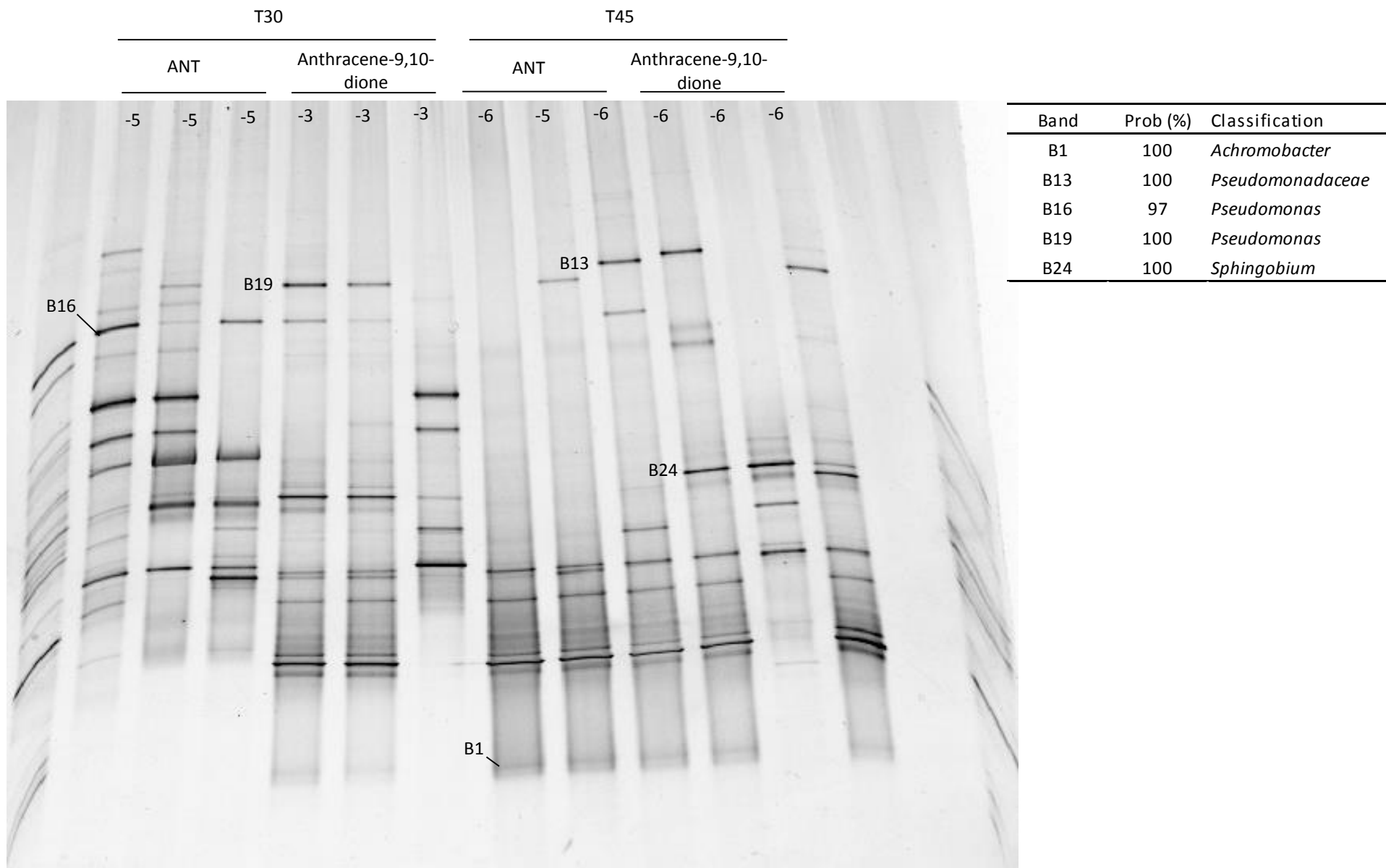
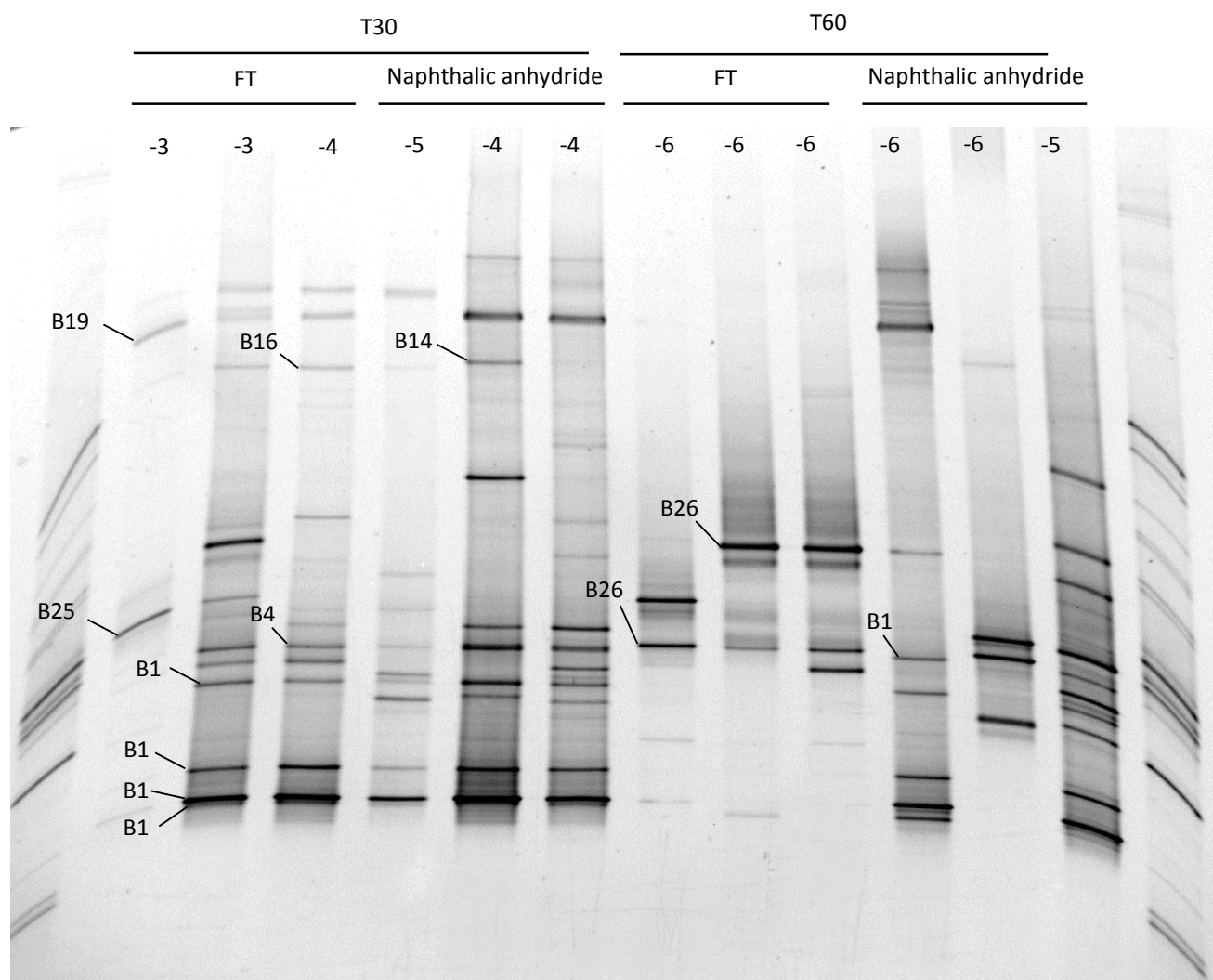


Figure S11.3. DGGE profiles of the 16S rRNA gene fragments amplified from the most diluted MPN wells grown with ANT and 9,10-anthraquinone at 30 and 45 days. The dilution factor of each well is indicated on the top of each lane. The excised bands from each profile are indicated, and their phylogenetic affiliation based on sequence analysis is shown in the accompanying table. Taxonomic affiliation was based on RDP classifier considering bootstrapping confidence scores >97%.



Band	Prob (%)	Classification
B1	100	<i>Achromobacter</i>
B4	100	<i>Achromobacter</i>
B14	100	<i>Pseudomonadaceae</i>
B16	97	<i>Pseudomonas</i>
B19	100	<i>Pseudomonas</i>
B25	100	<i>Sphingobium</i>
B26	99	<i>Sphingobium</i>

Figure S11.4. DGGE profiles of the 16S rRNA gene fragments amplified from the most diluted MPN wells grown with FT and naphthalic anhydride at 30 and 60 days. The dilution factor of each well is indicated on the top of each lane. The excised bands from each profile are indicated, and their phylogenetic affiliation based on sequence analysis is shown in the accompanying table. Taxonomic affiliation was based on RDP classifier considering bootstrapping confidence scores >97%.

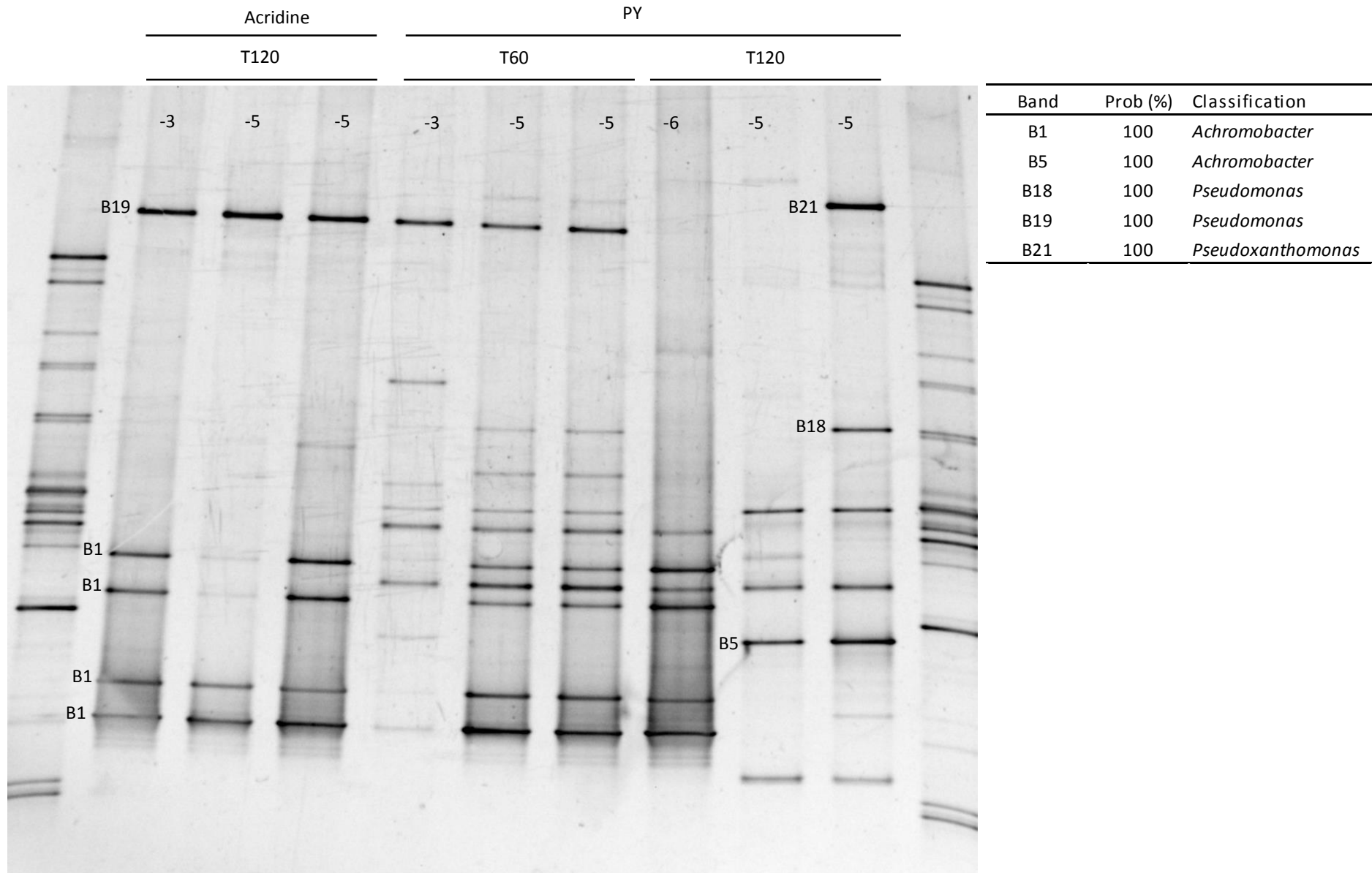


Figure S11.5. DGGE profiles of the 16S rRNA gene fragments amplified from the most diluted MPN wells grown with acridine at time 120 days and PY at 60 and 120 days. The dilution factor of each well in indicated on the top of each lane. The excised bands from each profile are indicated, and their phylogenetic affiliation based on sequence analysis is shown in the accompanying table. Taxonomic affiliation was based on RDP classifier considering bootstrapping confidence scores >97%.

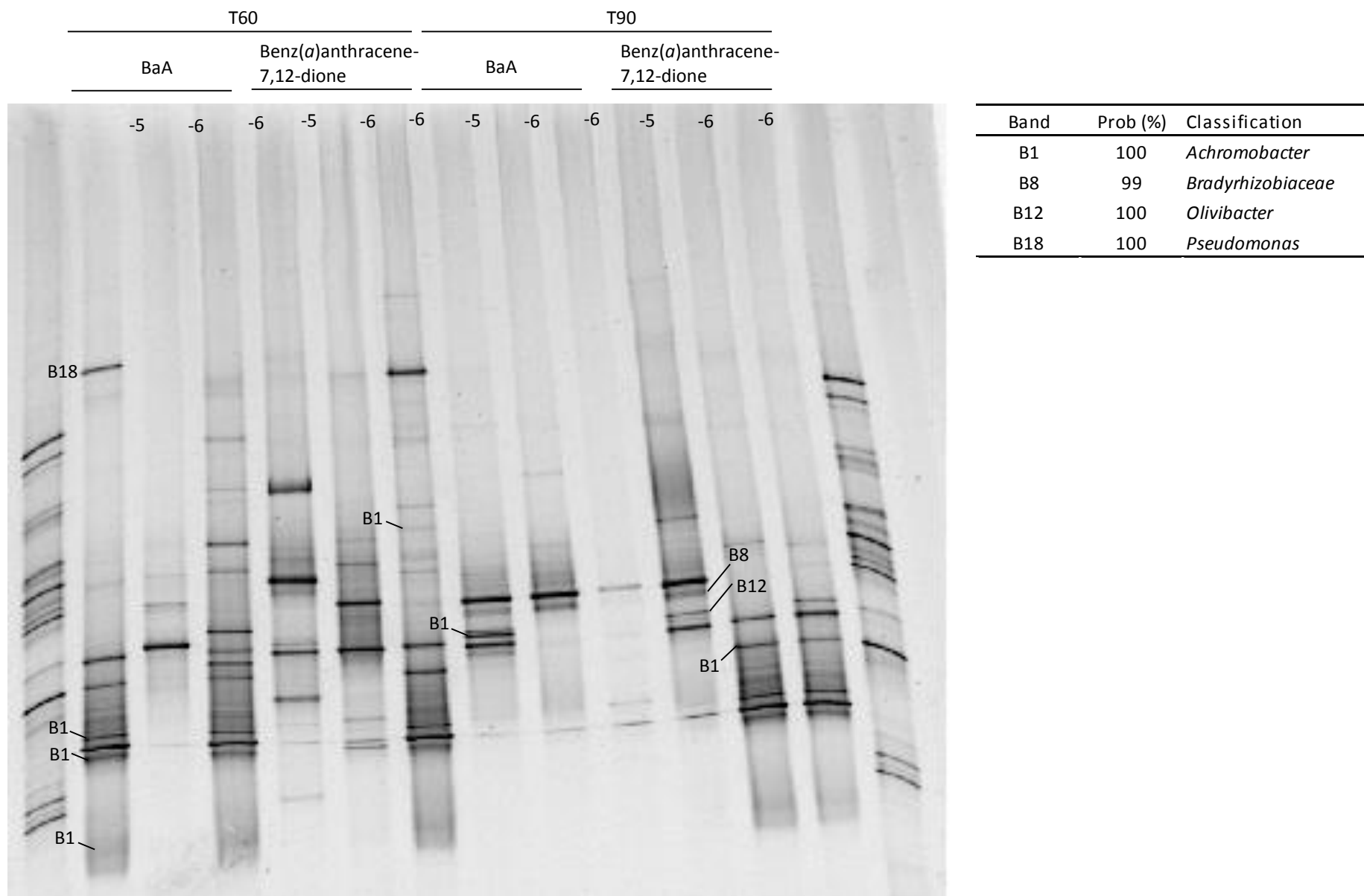
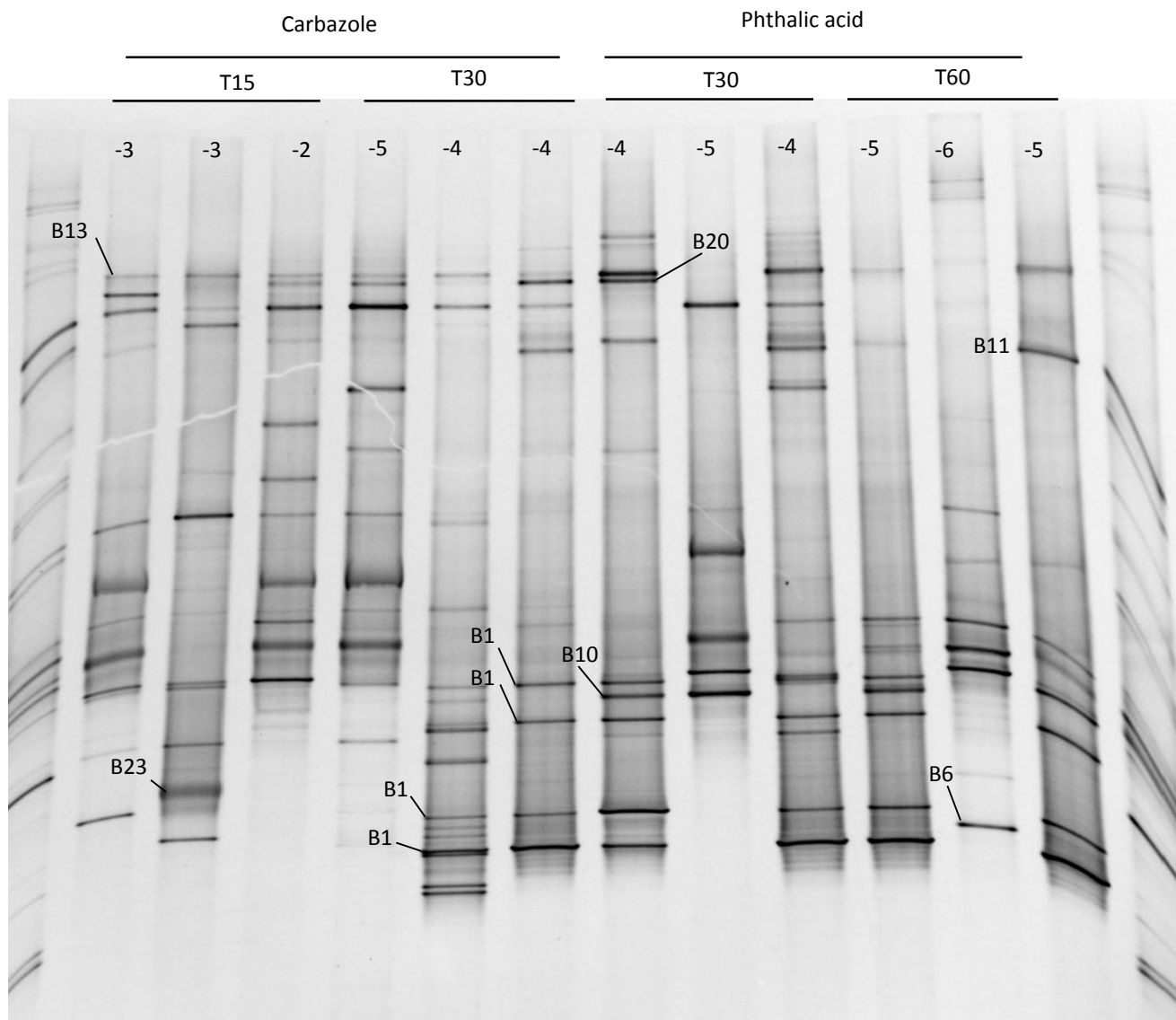


Figure S11.6. DGGE profiles of the 16S rRNA gene fragments amplified from the most diluted MPN wells grown with BaA and Benzo(a)anthracene-7,12-dione at 60 and 90 days. The dilution factor of each well in indicated on the top of each lane. The excised bands from each profile are indicated, and their phylogenetic affiliation based on sequence analysis is shown in the accompanying table. Taxonomic affiliation was based on RDP classifier considering bootstrapping confidence scores >97%.



Band	Prob (%)	Classification
B1	100	<i>Achromobacter</i>
B6	99	<i>Alcaligenaceae</i>
B10	100	<i>Olivibacter</i>
B11	99	<i>Olivibacter</i>
B13	100	<i>Pseudomonadaceae</i>
B20	97	<i>Pseudomonas</i>
B23	100	<i>Skermanella</i>

Figure S11.7. DGGE profiles of the 16S rRNA gene fragments amplified from the most diluted MPN wells grown with carbazole at 15 and 30 days and with phthalic acid at 30 and 60 days. The dilution factor of each well is indicated on the top of each lane. The excised bands from each profile are indicated, and their phylogenetic affiliation based on sequence analysis is shown in the accompanying table. Taxonomic affiliation was based on RDP classifier considering bootstrapping confidence scores >97%.

Annex II. Other publications

- Vila, J., Tauler, M. & Grifoll, M. **Bacterial PAH degradation in marine and terrestrial habitats.** *Curr. Opin. Biotechnol.* **33**, 95–102 (2015).
- Vila, J., Tauler, M., Grifoll, M., Nilsson, B., & Mundó, B. **Ensayos de tratabilidad para la bioremediación de suelos contaminados con HTF.** *Proyectos Químicos.* Octubre, 52-57 (2013).



Bacterial PAH degradation in marine and terrestrial habitats

Joaquim Vila, Margalida Tauler and Magdalena Grifoll



Cycling of pollutants is essential to preserve functional marine and terrestrial ecosystems. Progress in optimizing these natural biological processes relies on the identification of the underlying microbial actors and deciphering their interactions at molecular, cellular, community, and ecosystem level. Novel advances on PAH biodegradation are built on a progressive approach that span from pure cultures to environmental communities, illustrating the complex metabolic networks within a single cell, and their further implications in higher complexity systems. Recent analytical chemistry and molecular tools allow a deeper insight into the active microbial processes actually occurring *in situ*, identifying active functions, metabolic pathways and key players. Understanding these processes will provide new tools to assess biodegradation occurrence and, as a final outcome, predict the success of bioremediation thus reducing its uncertainties, the main drawback of this environmental biotechnology.

Addresses

Department of Microbiology, Faculty of Biology, University of Barcelona, Diagonal 643, 08028 Barcelona, Spain

Corresponding author: Grifoll, Magdalena (mgrifoll@ub.edu)
Dedicated to the memory of Professor Peter J. Chapman.

Current Opinion in Biotechnology 2015, 33:95–102

This review comes from a themed issue on **Environmental biotechnology**

Edited by Spiros N Agathos and Nico Boon

<http://dx.doi.org/10.1016/j.copbio.2015.01.006>

0958-1669/© 2015 Elsevier Ltd. All rights reserved.

Introduction

Polycyclic aromatic hydrocarbons (PAHs) are ubiquitous environmental pollutants reaching particularly high concentrations in industrial soils and oil-spill impacted marine environments. Concern about PAHs is due to their high recalcitrance and (geno) toxicity, posing a serious risk for both humans and ecosystems. Bioremediation, which exploits the natural microbially mediated degradation of organic compounds, is the most cost-effective and sustainable cleaning technology [1], causing relatively minor impact on key natural soil and marine functions. However, its application is still constrained by factors related to the unpredictable endpoint PAH concentrations, the lack of

adequate monitoring tools to guarantee the occurrence of active biodegradation processes, and the not entirely accurate risk assessment policies. To overcome these limitations, it is essential to unravel the complex metabolic networks determining the fate of PAHs *in situ*, thus allowing to move forward from the traditional ‘black box’ perspective to an actual environmental biotechnology.

Novel advances in analytical chemistry and molecular biology have gathered increasing knowledge on the different facets of microbial metabolism of hydrocarbons and their biotechnological application. This is a broad field of research involving a number of different environments, organisms, chemical compounds and, consequently, scientific disciplines. Here, we will focus on the recent developments (2010–2014) on aerobic biodegradation of PAHs by bacteria, in both marine and terrestrial environments, stressing on work performed during the last two years. Aspects that have also experienced great advance but escape the aim of this work have been reviewed elsewhere, including anaerobic biodegradation [2,3], PAH bioavailability [4], bacterial-fungal interactions [5], or biodegradation of aromatic hydrocarbons in general [6].

Unraveling *in situ* PAH metabolic networks: from pure cultures to omics

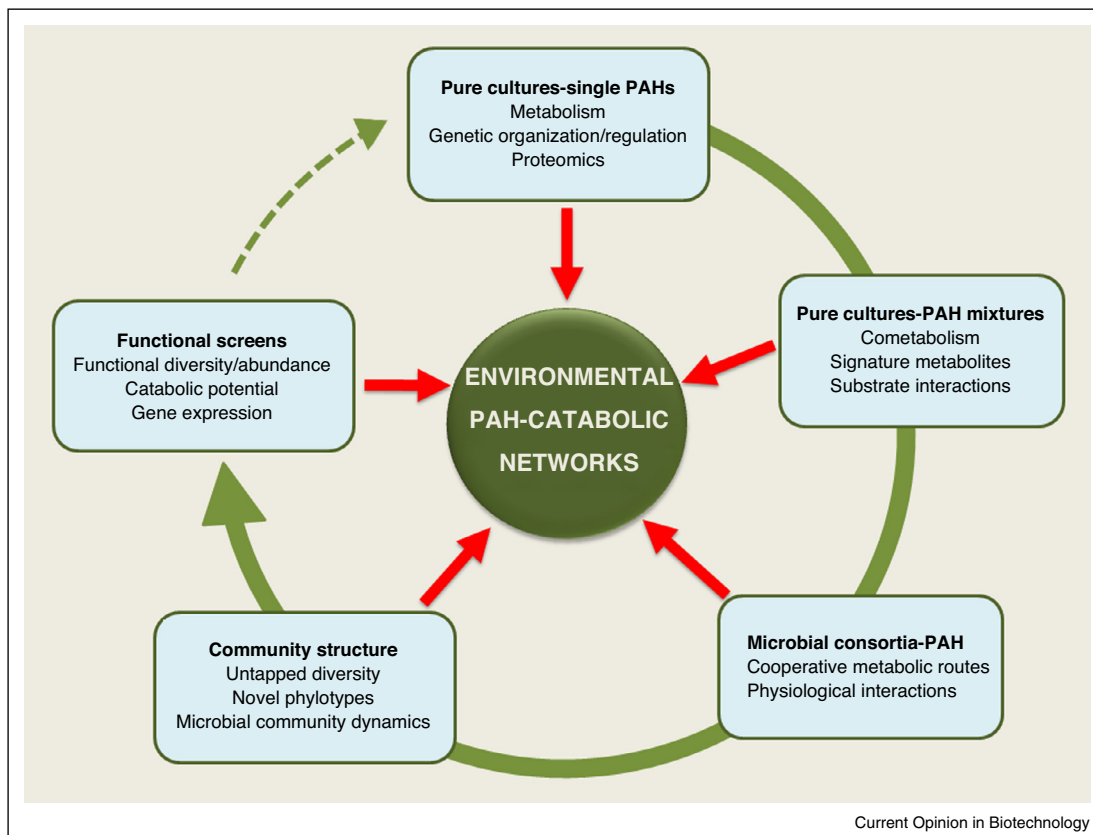
Environmental PAH biodegradation processes involve a great variety of co-occurring contaminants and are mediated by a diversity of microbes harboring different and often interconnected metabolic pathways. As depicted in Figure 1, to decipher these complex interactions, a progressive polyphasic approach is required. As a result, a flow of metabolic, genomic, transcriptomic and proteomic information is generated including:

1. Characterization of single cell PAH metabolic pathways in pure cultures.
2. Implications of cometabolic reactions in cooperative metabolic networks.
3. Discovering the guild of microorganisms responsible for PAH biodegradation.
4. Identification of functions relevant for PAH metabolism in environmental samples.
5. Integration of this information to obtain a holistic view of the *in situ* metabolic networks.

PAH catabolic networks in pure cultures

The classical approach to study PAH metabolism has been the reconstruction of pathways after identification of metabolites produced by bacteria able to use them as

Figure 1



Information flow in the complementary scientific approaches for the progressive unraveling of the terrestrial and marine microbial networks involved in PAH degradation. The integration of taxonomical and functional data from pure cultures, microbial consortia, and environmental communities after exposure to single PAHs or PAH-mixtures will permit to reconstruct the actual processes occurring in polluted sites. Insights on novel phylotypes and functions from community analysis will provide feed-back information and define targets for directed strain isolation, thus closing the circle and strengthening the information flow.

sole carbon source [7,8]. Most recent metabolic studies focus on sphingomonads and actinobacteria, especially in their ability to attack high molecular weight (HMW) compounds.

Despite their preference for low molecular weight (LMW) PAHs (i.e. phenanthrene) [9], sphingomonads show great versatility, being able to oxidize a wide range of polyaromatic substrates. This versatility relies on both the possession of several different and upregulated ring-hydroxylating dioxygenases (RHD) and the relaxed specificity of those enzymes. New contributions add on previous studies [10,11,12] in highlighting the complex network of catabolic reactions in a single cell, thus changing the perspective from the traditional linear routes to highly branched pathways. *Sphingobium* sp. KK22 grew on phenanthrene and transformed the HMW PAHs fluoranthene, benzo(*a*)anthracene and benzo(*k*)fluoranthene, initiating their oxidation in different positions [13,14]. Similarly, *Sphingobium* sp. PNB dihydroxylated phenanthrene on carbons 1,2, 3,4 or 9,10 [15]. A recent and

illustrative work on the metabolic versatility of sphingomonads shows that strain PNB, acting on a wide range of monoaromatic and polyaromatic substrates, harbors seven sets of ring-hydroxylating oxygenases (RHO) with a variety of substrate specificities that share a sole set of electron transport proteins, synthesizing in one strain earlier findings on sphingomonad RHD gene organization [16^{*}]. Similar genetic arrangements, usually involving plasmids or mobile genetic elements, were found in *Sphingobium yanoikuyae* B1, *Sphingobium* sp. P2, *Novosphingobium aromaticivorans* F199 or *Sphingomonas* sp. LH128, indicating their widespread distribution and horizontal transfer within sphingomonads [17]. A recent work demonstrated that two extradiol degradation pathways mediated by genes located in the large plasmid pLA1 and the chromosome of the marine bacterium *Novosphingobium pentaromaticivorans* US6-1, were separately induced by PAHs and monoaromatic compounds [18]. This plasticity in their catabolic networks and their short duplication times confer to sphingomonads a pronounced selective advantage towards a wide range of aromatic

pollutants, contributing to their fast response to sudden PAH pollution and nutrient supply (r-strategists).

Actinobacteria, with their ability to adhere to hydrophobic surfaces and slow growth rates, are highly adapted to the low bioavailable HMW substrates (k-strategists) [7]. Kweon *et al.* [19] demonstrated that the RHDs NidAB and NidA3B3 from the pyrene-degrading strain *Mycobacterium vanbaalenii* PYR-1, despite their relaxed specificity towards aromatic compounds, presented the highest conversion rates for pyrene and fluoranthene, respectively. These enzymes had evolved to specifically accommodate HMW PAHs in the large substrate-binding pockets of their active sites, thus satisfying spatial requirements for their efficient and regiospecific dihydroxylation. In the most exhaustive metabolic characterization of a PAH-degrading strain performed so far, these authors established an almost complete metabolic network in strain PYR-1 [20^{••}]. Combining high-throughput proteomic analyses of its response to seven aromatic substrates (phthalate, fluorene, acenaphthylene, anthracene, phenanthrene, pyrene and benzo(*a*)pyrene), with genomic and metabolic data, the authors reconstructed a comprehensive and hierarchical metabolic network (183 intermediates, 224 chemical reactions) in funnel organized modules, with a diversity of ring-cleavage and side chain processes that progressively narrow down to central metabolism, thus providing a systems-wide perspective on the biodegradation of PAHs.

Knowledge gathered from the actions of pure cultures or enzymes towards single substrates is a first and fundamental step in the progressive approach for comprehending the ecosystem networks that determine PAH fate. However, in the environment PAHs are found as complex mixtures often included in predominant aliphatic matrices (petrogenic mixtures), and degrading populations will simultaneously act on different components. The type of initial attack and extent of oxidation of one substrate will be conditioned by the presence and abundance of others, thus determining if it is channeled through productive pathways and mineralized, or partially oxidized. Dead-end products for one strain may be substrates for others. Hence, the accommodation of single cell metabolic networks to the degradation of PAH mixtures is a key issue that has been seldom addressed. When incubated with the heavy fuel oil spilled by the tanker Prestige, the pyrene-degrading strain *Mycobacterium gilvum* AP1, isolated from a polluted beach, degraded almost completely the aliphatic fraction (C12–C40), which favored an extensive degradation of 2-ring, 3-ring and 4-ring PAH families. Identification of signature metabolites indicated utilization of phenanthrene, pyrene, fluoranthene and alkyl derivatives by known assimilatory metabolic routes, while other components were co-oxidized [21]. This emphasizes the role that cometabolism may play in channeling individual PAHs

through potential cooperative networks. The real impact of these reactions is supported by recent publications on the identification of partially oxidized PAHs (oxy-PAHs) in polluted sites [22[•]].

Microbial communities reveal unknown PAH-degrading bacteria

Culture-based studies underestimate the actual diversity of natural communities and neglect potential interactions between their components. Thus, culture-independent methods have been increasingly applied to identify key microbial groups associated to PAH degradation in polluted soils and marine environments. Most widely used approaches include community structure analysis based on 16S rRNA gene-PCR amplification followed by fingerprinting (i.e. DGGE), clone libraries or tag-encoded pyrosequencing. These tools have been extensively applied to the characterization of enriched microbial consortia [23–26], or to assess structural changes in natural communities in response to PAH pollution and bioremediation processes [27–33]. This provides the taxonomical composition of the microbial community and the actual role of the identified phylotypes is presumptively assigned based on phylogenetic affiliation to previously described hydrocarbon-degrading representatives. Therefore, the function of an often substantial proportion of yet unculturable members that persist in selective enrichments or dilution-to-extinction experiments is difficult to infer. In these cases, directed isolation (i.e. custom-made media) of target phylotypes followed by thorough characterization of the new isolates could produce valuable results [34]. Stable Isotope Probing (SIP) circumvents the requirement of isolation to identify active players in specific substrate assimilation, representing a further decisive step in linking microbial populations to functions [35].

Marine environments

Massive marine oil spills are usually followed by intensification in hydrocarbon degradation research. Analyses of sand from a beach affected by the Prestige oil spill had shown high relative abundances of *Sphingomonadaceae* and *Mycobacterium* that could be associated to PAH degradation [27]. Further insight was obtained by characterization of an oil-degrading microbial consortium enriched from sand from a nearby site [26]. The link of community dynamics to depletion of specific fuel components and to single PAH exposure revealed a role in PAH utilization for the gammaproteobacteria *Methylophaga* and *Marinobacter*, and members of *Actinobacteria* [26]. The detection of a *NidA* dioxygenase gene in subcultures with pyrene identified an uncultured *Gordonia* as a key HMW PAH degrader [36]. A similar community composition was found in a beach affected by the surface oil slick from Deepwater Horizon oil spill [37,38], and an uncultured *Marinobacter* was pointed as a key phenanthrene degrader in a halophilic soil consortium [23]. The link of *Actinobacteria* to pyrene degradation in beaches [21,36] suggests a difference between

these and open sea or sediment environments, where HMW PAH degradation has been attributed to hydrocarbonoclastic gammaproteobacteria [39,40], specially *Cycloclasticus* [28,31,41].

Until now, PAH-SIP studies in marine environments have been scarce. Gutierrez *et al.* [42] investigated an algal bloom in Tampa Bay (FL) using ^{13}C -naphthalene and identified the dominant sequences in clone libraries as uncharacterized *Rhodobacteriaceae*. Their role in PAH degradation was confirmed by their selective increase (qPCR) in incubations with naphthalene and phenanthrene. Further work showed marine phytoplankton as a natural biotope for 2-ring and 3-ring PAH-degrading bacteria, producing the isolation of novel *Gammaproteobacteria* and *Bacterioidetes* PAH-degrading species [43,44]. The same authors unequivocally demonstrated that some of the dominant taxa enriched in surface waters in response to the Deepwater Horizon oil spill (i.e. the gammaproteobacteria *Alteromonas*, *Cycloclasticus* and *Colwellia*) played a key role in the degradation of 2-ring and 3-ring PAHs [45].

Soil environments

The reduced complexity of microbial consortia enriched from natural communities facilitates the correlation between specific populations and functions. Sun *et al.* [25] identified members of *Alphaproteobacteria* (*Rhizobium*) and *Betaproteobacteria* (*Hydrogenophaga*), not previously associated to PAH degradation, as the most abundant components of a pyrene-degrading consortium. More recently, Jones *et al.* [46] used substrate enrichment, co-incubation experiments and pyrosequencing to identify the genera *Cupriavidus* (*Betaproteobacteria*) and *Luteimonas* (*Gammaproteobacteria*) as the most likely related to benzo(a)pyrene cometabolism in a PAH-polluted soil. However, the most relevant studies on the identification of soil and groundwater PAH-degrading phylotypes are based on DNA-SIP [47–50]. Such methods revealed that previously neglected *Betaproteobacteria* (*Acidovorax*, *Rhodoferrax*, *Pigmentiphaga*, and *Hydrogenophaga*) may have a crucial role in the early response to PAH exposure [48,50]. In fact, a SIP directed isolation approach enabled the characterization of the PAH-degrading gene cluster from a phenanthrene-degrading *Acidovorax* strain [34]. The most comprehensive research on soil populations includes a series of studies supplying ^{13}C -labeled naphthalene, phenanthrene, anthracene, fluoranthene, pyrene or benzo(a)anthracene to soil samples from a manufactured-gas plant in North Carolina [48,49]. In addition to the relevance of *Betaproteobacteria*, the authors revealed novel and yet uncultured groups of anthracene-degrading and pyrene-degrading *Proteobacteria* [48,49,51], whose abundance and response to simulated bioremediation was demonstrated by barcoded pyrosequencing [32,33]. Further metagenomic work with a low diversity three-membered bacterial consortium, allowed the characterization of the PAH

catabolic genes of a novel *Rhodocyclaceae* belonging to the previously SIP-detected pyrene groups [52*]. Interestingly, a similar set of genes was detected in a PAH-polluted soil from France by applying a novel combination of shotgun metagenomics and DNA-SIP with ^{13}C -phenanthrene [53], thus confirming their relevance and global distribution.

Incipient research on the effect of rhizospheres on PAH biodegradation is promising. Using ^{13}C -phenanthrene and qPCR, Cébron *et al.* [47] demonstrated that root exudates favor a higher diversity and abundance of phenanthrene degraders. In a more classical approach using a weathered creosote-polluted soil, Tejada-Agredano *et al.* [54] showed that sunflower rhizosphere promotes PAH biodegradation provoking a dramatic shift in community structure and increasing the relative abundance of PAH-degrading bacteria.

New tools for functional screens

The next step in the progressive unraveling of environmental PAH biodegradation networks is the identification and quantification of key functional genes. On the basis of genomic information from isolates, a large set of primers and probes targeting ring-hydroxylating and ring-cleavage dioxygenases have been designed [55,56]. The most common approaches include gene amplification using degenerate or non-degenerate primers, and nucleic acid hybridization on functional microarrays.

RHD are classified into five clusters according to substrate preference and phylogenetic comparison of their α -subunit amino acid sequences [57]. Most PCR-mediated functional studies target the α -subunits of the two clusters specifically linked to PAH degradation in Gram-negative and Gram-positive bacteria [55]. Quantitative analyses using qPCR demonstrated changes in PAH catabolic potential of soil communities during natural attenuation [58] and in response to rhizosphere or root exudates [47,59]. Combining RHD amplification with DNA-SIP in a polluted soil, Martin *et al.* [60] demonstrated that during the degradation of ^{13}C -phenanthrene the heavy DNA included RHD gene sequences that fell into at least 5 different clusters. By cloning part of some of the detected α -subunit gene sequences in-frame in place of the catalytic domain of the RHD of *Sphingomonas* CHY-1, they elegantly determined their substrate specificity. In a comprehensive study of an oil-impacted tidal flat that identified *Alteromonas* as a key player in LMW PAH degradation, amplification was only observed with one of five sets of degenerate primers targeting naphthalene dioxygenase genes of Gram-negatives, and one specifically targeting *Alteromonas*-like RHDs [61**]. This illustrates the limitation of PCR-based approaches to cover the diversity of environmental dioxygenases, especially in marine habitats where genomic information on PAH degraders is still scarce. In fact, using an elegant

metagenomic approach (gene-targeted pyrosequencing) Iwai *et al.* [62], found a much broader sequence diversity for biphenyl dioxygenase genes than expected and, after reviewing the available RHDs primers, indicated the necessity to accurately select different sets of primers to encompass their broad diversity in environmental samples [55].

Microarrays constitute a high-throughput approach to detect thousands of genes within a single test. Targeting a variety of biogeochemical processes (including PAH-biodegradation) the most comprehensive functional gene array is GeoChip [63,64], whose most recent versions served to illustrate the potential for natural attenuation in the deep-water column [65,66] and beaches affected by the Deepwater Horizon spill [67]. A novel catabolome array (1595 50-mer probes) has been developed to evaluate the catabolic gene diversity (DNA) and expression (cDNA from retro-transcribed mRNA) of biphenyl, naphthalene and aliphatic hydrocarbon degrading communities. Its application to groundwater samples exposed to naphthalene demonstrated differences between transcriptome and overall catabolic gene composition, identifying the functions that were unequivocally active [68].

However, functional approaches are constantly being upgraded. The increasing genomic information, released from novel isolates and metagenome projects, generates a continuous requirement for the design of primers and probes targeting newly identified genes.

Recent *omic* approaches, such as shotgun metagenomics, metatranscriptomics and metaproteomics, have the potential to overcome the restrictions of directed detection methods (PCR-amplification and hybridization), but they are just starting to be applied to PAH-polluted environments. Guazzaroni *et al.* [69] used shotgun metagenomics and metaproteomics to decipher the microbial response to biostimulation and naphthalene exposure in a PAH-polluted soil from the north of Spain. Genomic analyses confirmed the presence of genes belonging to different upper PAH biodegradation pathways, those related with the gentisate pathway being the ones actively responding to naphthalene exposure according to metaproteomic profiles.

(Eco)systems biology for understanding the *in situ* PAH metabolic networks

Current molecular and analytical chemistry developments permit a systems biology approach to understand the microbial metabolic networks for PAH biodegradation *in situ*, and provide valuable tools to verify and assess biodegradation in natural attenuation and bioremediation scenarios. Studies applying such holistic analysis to unravel marine and terrestrial PAH degradation processes are still outnumbered by those focused on aliphatics and

monoaromatics [6,56,70], but they include some remarkable works.

Jin *et al.* [61] identified *Alteromonas* as a key agent in PAH removal from oil-polluted tidal flat sediments by integrating data on *in situ* PAH depletion, total and active microbial community analyses of naphthalene enrichments, strain isolation and characterization, and further *in situ* naphthalene RHD gene expression and metabolite analyses. Gentisate, detected in *Alteromonas* cultures, was identified as the main intermediate of naphthalene biodegradation *in situ*. Comparative genomics towards close relatives revealed the adaptation of the isolate to PAH biodegradation at low temperatures [71,72].

Combining functional gene microarray analyses and high-throughput 16S rRNA gene sequencing, both *in situ* and in mesocosms with PAHs, Kappell *et al.* [67] demonstrated that native populations from the Gulf of Mexico were highly efficient in PAH removal, independently of their preexposure to the Deepwater Horizon oil spill. This was attributed to continuous exposure to oil from natural seeps and accidental release from vessels.

BACTRAPs[®] combined with *in situ* protein-SIP and 16S rRNA gene pyrosequencing applied to a PAH-polluted aquifer [73] revealed the crucial role of *Burkholderiales*, *Actinomycetales* and *Rhizobiales* as active naphthalene degraders, gaining 80% of their carbon from PAH assimilation. *In situ* protein-SIP analysis of fluorene-degrading communities failed, but laboratory microcosms showed enrichment in proteins involved in the angular degradation pathway in *Actinobacteria* (*Rhodococcus*).

An interesting approach to assess *in situ* PAH degradation that would provide robust evidence for the occurrence of specific PAH transformation pathways is the detection of signature metabolites. Oxygenated PAHs (oxy-PAHs), often originating from the relaxed specificity of PAH degradation enzymes, may accumulate or act as nodes in complex food webs. The development of analytical chemistry tools is essential to ascertain their formation and further reutilization [74]. Recently, Lundstedt *et al.* [22] published the first intercomparison study of analytical methods for the simultaneous detection of PAHs and oxy-PAHs, demonstrating that in creosote polluted soils some oxy-PAHs are found at similar concentrations as their parent PAHs.

Conclusions

The understanding of the environmental networks for biodegradation of PAHs requires the integration of scientific data obtained from classical approaches, such as the characterization of pure cultures and low diversity consortia, with up-to-date high throughput screens of polluted environments. Future progress in reaching this

objective requires continuity and strengthening of several lines of research initiated in recent years:

1. Application of molecular methods to decipher the microbiomes of PAH-polluted environments is revealing an increasing number of yet uncultured players whose role remains unknown. Their directed isolation and characterization from a physiological, enzymatic and genomic point of view will provide unequivocal information on metabolic pathways and catabolic genes that will furnish the necessary feedback for completing and curating the available databases.
2. Microbial interactions, with both target pollutant-containing matrices and co-existent microbial communities, are topics that are still in their incipient phases. Analyzing low diversity consortia, by combining metabolic and genomic information, may allow identifying the succession of reactions and functions acting on the different components of the mixture.
3. Functional and phylogenetic screens applying *omic* approaches (including metabolomics), should give us the definitive insight into the processes naturally occurring in PAH-polluted environments. However, these methods are highly dependent on data integration through databases, which is one of their main bottlenecks. Despite increasing efforts on quality control of databases, most genomic data includes amplifying annotation mistakes and results from putative assignments, which is the greatest hindrance for functional and phylogenetic reconstruction.

Acknowledgements

During the writing of this manuscript, our funding included two grants (CGL2010-22068-C02-02 and CGL2013-44554-R) and a fellowship (to M.T., BES-2011-045106) from the Spanish Ministry of Economy and Competitiveness. The authors are members of the Xarxa de Referència d'R+D+I en Biotecnologia (XRB) of the Generalitat de Catalunya.

References and recommended reading

Papers of particular interest, published within the period of review, have been highlighted as:

- of special interest
 - of outstanding interest
1. Gillespie IMM, Philp JC: **Bioremediation, an environmental remediation technology for the bioeconomy**. *Trends Biotechnol* 2013, **31**:329-332.
 2. Callaghan AV: **Metabolomic investigations of anaerobic hydrocarbon-impacted environments**. *Curr Opin Biotechnol* 2013, **24**:506-515.
 3. Meckenstock RU, Mouttaki H: **Anaerobic degradation of non-substituted aromatic hydrocarbons**. *Curr Opin Biotechnol* 2011, **22**:406-414.
 4. Ortega-Calvo JJ, Tejada-Agredano MC, Jimenez-Sanchez C, Congiu E, Sungthong R, Niqui-Arroyo JL, Cantos M: **Is it possible to increase bioavailability but not environmental risk of PAHs in bioremediation?** *J Hazard Mater* 2013, **261**:733-745.
 5. Harms H, Schlosser D, Wick LY: **Untapped potential: exploiting fungi in bioremediation of hazardous chemicals**. *Nat Rev Microbiol* 2011, **9**:177-192.
 6. Jeon CO, Madsen EL: **In situ microbial metabolism of aromatic-hydrocarbon environmental pollutants**. *Curr Opin Biotechnol* 2013, **24**:474-481.
 7. Kanaly RA, Harayama S: **Advances in the field of high-molecular-weight polycyclic aromatic hydrocarbon biodegradation by bacteria**. *Microb Biotechnol* 2010, **3**:136-164.
 8. Mallick S, Chakraborty J, Dutta TK: **Role of oxygenases in guiding diverse metabolic pathways in the bacterial degradation of low-molecular-weight polycyclic aromatic hydrocarbons: a review**. *Crit Rev Microbiol* 2011, **37**:64-90.
 9. Stolz A: **Molecular characteristics of xenobiotic-degrading sphingomonads**. *Appl Microbiol Biotechnol* 2009, **81**:793-811.
 10. Demanèche S, Meyer C, Micoud J, Louwagie M, Willison JC, Jouanneau Y: **Identification and functional analysis of two aromatic-ring-hydroxylating dioxygenases from a *Sphingomonas* strain that degrades various polycyclic aromatic hydrocarbons**. *Appl Environ Microbiol* 2004, **70**:6714-6725.
 11. Pinyakong O, Habe H, Yoshida T, Nojiri H, Omori T: **Identification of three novel salicylate 1-hydroxylases involved in the phenanthrene degradation of *Sphingobium* sp. strain P2**. *Biochem Biophys Res Commun* 2003, **301**:350-357.
 12. Schuler L, Jouanneau Y, Chadhain SMN, Meyer C, Pouli M, Zylstra GJ, Hols P, Agathos SN: **Characterization of a ring-hydroxylating dioxygenase from phenanthrene-degrading *Sphingomonas* sp. strain LH128 able to oxidize benzo[a]anthracene**. *Appl Microbiol Biotechnol* 2009, **83**:465-475.
 13. Kunihiro M, Ozeki Y, Nogi Y, Hamamura N, Kanaly RA: **Benzo[a]anthracene biotransformation and production of ring fission products by *Sphingobium* sp. strain KK22**. *Appl Environ Microbiol* 2013, **79**:4410-4420.
 14. Maeda AH, Nishi S, Hatada Y, Ozeki Y, Kanaly RA: **Biotransformation of the high-molecular weight polycyclic aromatic hydrocarbon (PAH) benzo[k]fluoranthene by *Sphingobium* sp. strain KK22 and identification of new products of non-alternant PAH biodegradation by liquid chromatography electrospray ionization**. *Microb Biotechnol* 2014, **7**:114-129.
 15. Roy M, Khara P, Dutta TK: **meta-Cleavage of hydroxynaphthoic acids in the degradation of phenanthrene by *Sphingobium* sp. strain PNB**. *Microbiology* 2012, **158**:685-695.
 16. Khara P, Roy M, Chakraborty J, Ghosal D, Dutta TK: **Functional characterization of diverse ring-hydroxylating oxygenases and induction of complex aromatic catabolic gene clusters in *Sphingobium* sp. PNB**. *FEBS Open Bio* 2014, **4**:290-300.
- A very illustrative work on the metabolic versatility of sphingomonads. Shows that strain PNB, acting on monoaromatic and polyaromatic substrates, harbors seven sets of ring hydroxylating oxygenases (RHO) with different substrate specificities. Synthesizes and confirms previous findings in RHO gene organization.
17. Stolz A: **Degradative plasmids from sphingomonads**. *FEMS Microbiol Lett* 2014, **350**:9-19.
 18. Yun SH, Choi C-W, Lee S-Y, Lee YG, Kwon J, Leem SH, Chung YH, Kahng H-Y, Kim SJ, Kwon KK *et al.*: **Proteomic characterization of plasmid pLA1 for biodegradation of polycyclic aromatic hydrocarbons in the marine bacterium, *Novosphingobium pentaromativorans* US6-1**. *PLOS ONE* 2014, **9**:e90812.
 19. Kweon O, Kim S-J, Freeman JP, Song J, Baek S, Cerniglia CE: **Substrate specificity and structural characteristics of the novel Rieske nonheme iron aromatic ring-hydroxylating oxygenases NidAB and NidA3B3 from *Mycobacterium vanbaalenii* PYR-1**. *MBio* 2010, **1**:e00135-e210.
 20. Kweon O, Kim S-J, Holland RD, Chen H, Kim D-W, Gao Y, Yu L-R, Baek S, Baek D-H, Ahn H *et al.*: **Polycyclic aromatic hydrocarbon metabolic network in *Mycobacterium vanbaalenii* PYR-1**. *J Bacteriol* 2011, **193**:4326-4337.
- The most exhaustive analysis on PAH degradation metabolism at the cellular level, obtained by combining proteomic, metabolic, biochemical, physiological and genomic data. It reconstructs a comprehensive and hierarchical metabolic network in funnel organized modules, with a variety of ring-cleavage and side chain processes that progressively narrow down to central metabolism, thus providing a systems-wide perspective on the biodegradation of PAHs.

21. Vila J, Grifoll M: **Actions of *Mycobacterium* sp. strain AP1 on the saturated- and aromatic-hydrocarbon fractions of fuel oil in a marine medium.** *Appl Environ Microbiol* 2009, **75**:6232-6239.
 22. Lundstedt S, Bandowe BAM, Wilcke W, Boll E, Christensen JH, Vila J, Grifoll M, Faure P, Biache C, Lorgeoux C *et al.*: **First intercomparison study on the analysis of oxygenated polycyclic aromatic hydrocarbons (oxy-PAHs) and nitrogen heterocyclic polycyclic aromatic compounds (N-PACs) in contaminated soil.** *TrAC Trends Anal Chem* 2014, **57**:83-92.
- First intercomparison study of analytical methods for the simultaneous detection of PAH and oxy-PAHs, demonstrating that in PAH-polluted soils some oxy-PAHs are found at similar concentrations as their parent PAHs.
23. Dastgheib SMM, Amoozegar MA, Khajeh K, Shavandi M, Ventosa A: **Biodegradation of polycyclic aromatic hydrocarbons by a halophilic microbial consortium.** *Appl Microbiol Biotechnol* 2012, **95**:789-798.
 24. Lafortune I, Juteau P, Déziel E, Lépine F, Beaudet R, Villemur R: **Bacterial diversity of a consortium degrading high-molecular-weight polycyclic aromatic hydrocarbons in a two-liquid phase biosystem.** *Microb Ecol* 2009, **57**:455-468.
 25. Sun R, Jin J, Sun G, Liu Y, Liu Z: **Screening and degrading characteristics and community structure of a high molecular weight polycyclic aromatic hydrocarbon-degrading bacterial consortium from contaminated soil.** *J Environ Sci* 2010, **22**:1576-1585.
 26. Vila J, María Nieto J, Mertens J, Springael D, Grifoll M: **Microbial community structure of a heavy fuel oil-degrading marine consortium: linking microbial dynamics with polycyclic aromatic hydrocarbon utilization.** *FEMS Microbiol Ecol* 2010, **73**:349-362.
 27. Alonso-Gutiérrez J, Figueras A, Albaigés J, Jiménez N, Viñas M, Solanas AM, Novoa B: **Bacterial communities from shoreline environments (Costa da Morte, northwestern Spain) affected by the prestige oil spill.** *Appl Environ Microbiol* 2009, **75**:3407-3418.
 28. Coulon F, Chronopoulou P-M, Fahy A, Païssé S, Goñi-Urriza M, Peperzak L, Acuña Alvarez L, McKew BA, Brussaard CPD, Underwood GJC *et al.*: **Central role of dynamic tidal biofilms dominated by aerobic hydrocarbonoclastic bacteria and diatoms in the biodegradation of hydrocarbons in coastal mudflats.** *Appl Environ Microbiol* 2012, **78**:3638-3648.
 29. Lladó S, Jiménez N, Viñas M, Solanas AM: **Microbial populations related to PAH biodegradation in an aged biostimulated creosote-contaminated soil.** *Biodegradation* 2009, **20**:593-601.
 30. Lladó S, Gràcia E, Solanas AM, Viñas M: **Fungal and bacterial microbial community assessment during bioremediation assays in an aged creosote-polluted soil.** *Soil Biol Biochem* 2013, **67**:114-123.
 31. Niepceron M, Portet-Koltalo F, Merlin C, Motelay-Massei A, Barray S, Bodilis J: **Both *Cycloclasticus* spp. and *Pseudomonas* spp. as PAH-degrading bacteria in the Seine estuary (France).** *FEMS Microbiol Ecol* 2010, **71**:137-147.
 32. Singleton DR, Richardson SD, Aitken MD: **Pyrosequence analysis of bacterial communities in aerobic bioreactors treating polycyclic aromatic hydrocarbon-contaminated soil.** *Biodegradation* 2011, **22**:1061-1073.
 33. Singleton DR, Jones MD, Richardson SD, Aitken MD: **Pyrosequence analyses of bacterial communities during simulated in situ bioremediation of polycyclic aromatic hydrocarbon-contaminated soil.** *Appl Microbiol Biotechnol* 2013, **97**:8381-8391.
 34. Singleton DR, Ramirez LG, Aitken MD: **Characterization of a polycyclic aromatic hydrocarbon degradation gene cluster in a phenanthrene-degrading *Acidovorax* strain.** *Appl Environ Microbiol* 2009, **75**:2613-2620.
 35. Dumont MG, Murrell JC: **Stable isotope probing-linking microbial identity to function.** *Nat Rev Microbiol* 2005, **3**:499-504.
 36. Gallego S, Vila J, Tauler M, Nieto JM, Breugelmanns P, Springael D, Grifoll M: **Community structure and PAH ring-hydroxylating dioxygenase genes of a marine pyrene-degrading microbial consortium.** *Biodegradation* 2014, **25**:543-556.
 37. Kostka JE, Prakash O, Overholt WA, Green SJ, Freyer G, Canion A, Delgado J, Norton N, Hazen TC, Huettel M: **Hydrocarbon-degrading bacteria and the bacterial community response in Gulf of Mexico beach sands impacted by the deepwater horizon oil spill.** *Appl Environ Microbiol* 2011, **77**:7962-7974.
 38. Lamendella R, Strutt S, Borglin S, Chakraborty R, Tas N, Mason OU, Hultman J, Prestat E, Hazen TC, Jansson JK: **Assessment of the Deepwater Horizon oil spill impact on Gulf coast microbial communities.** *Front Microbiol* 2014, **5**:130.
 39. Head IM, Jones DM, Röling WFM: **Marine microorganisms make a meal of oil.** *Nat Rev Microbiol* 2006, **4**:173-182.
 40. Rodríguez-Blanco A, Vetion G, Escande M-L, Delille D, Ghiglione J-F: ***Gallaecimonas pentaromativorans* gen. nov., sp. nov., a bacterium carrying 16S rRNA gene heterogeneity and able to degrade high-molecular-mass polycyclic aromatic hydrocarbons.** *Int J Syst Evol Microbiol* 2010, **60**:504-509.
 41. Wang B, Lai Q, Cui Z, Tan T, Shao Z: **A pyrene-degrading consortium from deep-sea sediment of the West Pacific and its key member *Cycloclasticus* sp. P1.** *Environ Microbiol* 2008, **10**:1948-1963.
 42. Gutierrez T, Singleton DR, Aitken MD, Semple KT: **Stable isotope probing of an algal bloom to identify uncultivated members of the *Rhodobacteraceae* associated with low-molecular-weight polycyclic aromatic hydrocarbon degradation.** *Appl Environ Microbiol* 2011, **77**:7856-7860.
 43. Gutierrez T, Rhodes G, Mishamandani S, Berry D, Whitman WB, Nichols PD, Semple KT, Aitken MD: **Polycyclic aromatic hydrocarbon degradation of phytoplankton-associated *Arenibacter* spp. and description of *Arenibacter algicola* sp. nov., an aromatic hydrocarbon-degrading bacterium.** *Appl Environ Microbiol* 2014, **80**:618-628.
 44. Gutierrez T, Green DH, Nichols PD, Whitman WB, Semple KT, Aitken MD: ***Polycyclovorans algicola* gen. nov., sp. nov., an aromatic-hydrocarbon-degrading marine bacterium found associated with laboratory cultures of marine phytoplankton.** *Appl Environ Microbiol* 2013, **79**:205-214.
 45. Gutierrez T, Singleton DR, Berry D, Yang T, Aitken MD, Teske A: **Hydrocarbon-degrading bacteria enriched by the Deepwater Horizon oil spill identified by cultivation DNA-SIP.** *ISME J* 2013, **7**:2091-2104.
 46. Jones M, Rodgers-Vieira E: **Association of growth substrates and bacterial genera with benzo[a]pyrene mineralization in contaminated soil.** *Environ Eng Sci* 2014 <http://dx.doi.org/10.1089/ees.2014.0275>.
 47. Cébron A, Louvel B, Faure P, France-Lanord C, Chen Y, Murrell JC, Leyval C: **Root exudates modify bacterial diversity of phenanthrene degraders in PAH-polluted soil but not phenanthrene degradation rates.** *Environ Microbiol* 2011, **13**:722-736.
 48. Jones MD, Crandell DW, Singleton DR, Aitken MD: **Stable-isotope probing of the polycyclic aromatic hydrocarbon-degrading bacterial guild in a contaminated soil.** *Environ Microbiol* 2011, **13**:2623-2632.
 49. Jones MD, Singleton DR, Sun W, Aitken MD: **Multiple DNA extractions coupled with stable-isotope probing of anthracene-degrading bacteria in contaminated soil.** *Appl Environ Microbiol* 2011, **77**:2984-2991.
 50. Martin F, Torelli S, Le Paslier D, Barbance A, Martin-Laurent F, Bru D, Geremia R, Blake G, Jouanneau Y: **Betaproteobacteria dominance and diversity shifts in the bacterial community of a PAH-contaminated soil exposed to phenanthrene.** *Environ Pollut* 2012, **162**:345-353.
 51. Singleton DR, Sangaiah R, Gold A, Ball LM, Aitken MD: **Identification and quantification of uncultivated Proteobacteria associated with pyrene degradation in a bioreactor treating PAH-contaminated soil.** *Environ Microbiol* 2006, **8**:1736-1745.

52. Singleton DR, Hu J, Aitken MD: **Heterologous expression of polycyclic aromatic hydrocarbon ring-hydroxylating dioxygenase genes from a novel pyrene-degrading betaproteobacterium.** *Appl Environ Microbiol* 2012, **78**:3552-3559.
- First work characterizing PAH-degrading genes of an uncultured microorganism circumventing pure culture cultivation. In a simplified bacterial consortium, detection by metagenomic analysis and further expression of RHD genes from a predominant pyrene-degrading *Rhodocyclaceae* (previously identified by DNA-SIP) permitted to identify the actions of these enzymes on several PAHs.
53. Chemerys A, Pelletier E, Cruaud C, Martin F, Violet F, Jouanneau Y: **Characterization of novel polycyclic aromatic hydrocarbon dioxygenases from the bacterial metagenomic DNA of a contaminated soil.** *Appl Environ Microbiol* 2014, **80**:6591-6600.
54. Tejada-Agredano MC, Gallego S, Vila J, Grifoll M, Ortega-Calvo JJ, Cantos M: **Influence of the sunflower rhizosphere on the biodegradation of PAHs in soil.** *Soil Biol Biochem* 2013, **57**:830-840.
55. Iwai S, Johnson TA, Chai B, Hashsham SA, Tiedje JM: **Comparison of the specificities and efficacies of primers for aromatic dioxygenase gene analysis of environmental samples.** *Appl Environ Microbiol* 2011, **77**:3551-3557.
56. Vilchez-Vargas R, Junca H, Pieper DH: **Metabolic networks, microbial ecology and "omics" technologies: towards understanding in situ biodegradation processes.** *Environ Microbiol* 2010, **12**:3089-3104.
57. Kweon O, Kim S-J, Baek S, Chae J-C, Adjei MD, Baek D-H, Kim Y-C, Cerniglia CE: **A new classification system for bacterial Rieske non-heme iron aromatic ring-hydroxylating oxygenases.** *BMC Biochem* 2008, **9**:11.
58. DeBruyn JM, Saylor GS: **Microbial community structure and biodegradation activity of particle-associated bacteria in a coal tar contaminated creek.** *Environ Sci Technol* 2009, **43**:3047-3053.
59. Cébron A, Beguiristain T, Faure P, Norini M-P, Masfaraud J-F, Leyval C: **Influence of vegetation on the in situ bacterial community and polycyclic aromatic hydrocarbon (PAH) degraders in aged PAH-contaminated or thermal-desorption-treated soil.** *Appl Environ Microbiol* 2009, **75**:6322-6330.
60. Martin F, Malagnoux L, Violet F, Jakoncic J, Jouanneau Y: **Diversity and catalytic potential of PAH-specific ring-hydroxylating dioxygenases from a hydrocarbon-contaminated soil.** *Appl Microbiol Biotechnol* 2013, **97**:5125-5135.
61. Jin HM, Kim JM, Lee HJ, Madsen EL, Jeon CO: **Alteromonas as a key agent of polycyclic aromatic hydrocarbon biodegradation in crude oil-contaminated coastal sediment.** *Environ Sci Technol* 2012, **46**:7731-7740.
- Unequivocal identification of *Alteromonas* (*Gammaproteobacteria*) as a main player in the removal of naphthalene from crude oil-contaminated sea-tidal flat sediments, by integrating data on *in situ* PAH depletion, total and active bacterial community analysis, and isolation, with RHD gene expression and metabolite analysis.
62. Iwai S, Chai B, Sul WJ, Cole JR, Hashsham SA, Tiedje JM: **Gene-targeted-metagenomics reveals extensive diversity of aromatic dioxygenase genes in the environment.** *ISME J* 2010, **4**:279-285.
63. He Z, Deng Y, Van Nostrand JD, Tu Q, Xu M, Hemme CL, Li X, Wu L, Gentry TJ, Yin Y *et al.*: **GeoChip F 3.0 as a high-throughput tool for analyzing microbial community composition, structure functional activity.** *ISME J* 2010, **4**:1167-1179.
64. Van Nostrand JD, He Z, Zhou J: **Use of functional gene arrays for elucidating in situ biodegradation.** *Front Microbiol* 2012, **3**:339.
65. Hazen TC, Dubinsky EA, DeSantis TZ, Andersen GL, Piceno YM, Singh N, Jansson JK, Probst A, Borglin SE, Fortney JL *et al.*: **Deep-sea oil plume enriches indigenous oil-degrading bacteria.** *Science* 2010, **330**:204-208.
66. Lu Z, Deng Y, Van Nostrand JD, He Z, Voordeckers J, Zhou A, Lee Y-J, Mason OU, Dubinsky EA, Chavarria KL *et al.*: **Microbial gene functions enriched in the Deepwater Horizon deep-sea oil plume.** *ISME J* 2012, **6**:451-460.
67. Kappell AD, Wei Y, Newton RJ, Van Nostrand JD, Zhou J, McLellan SL, Hristova KR: **The polycyclic aromatic hydrocarbon degradation potential of Gulf of Mexico native coastal microbial communities after the Deepwater Horizon oil spill.** *Front Microbiol* 2014, **5**:205.
- Illustrates a potential for natural attenuation in Gulf Coast beaches independently of their previous exposure to the Deepwater Horizon spill, by showing a similar response to PAHs according to gene diversity analysis (GeoChip), bacterial community composition, and PAH degradation capacity.
68. Vilchez-Vargas R, Geffers R, Suárez-Diez M, Conte I, Waliczek A, Kaser VS, Kralova M, Junca H, Pieper DH: **Analysis of the microbial gene landscape and transcriptome for aromatic pollutants and alkane degradation using a novel internally calibrated microarray system.** *Environ Microbiol* 2013, **15**:1016-1039.
- Development of an optimized and calibrated custom array system including probes for key aromatic catabolic gene families designed from curated databases. Its application to assess the catabolic gene landscape and transcriptome of environmental samples confirmed the abundance of catabolic gene subfamilies previously detected by functional metagenomics, also revealing the presence of previously undetected catabolic groups and their expression under pollutant stress.
69. Guazzaroni M-E, Herbst F-A, Lores I, Tamames J, Peláez AI, López-Cortés N, Alcaide M, Del Pozo MV, Vieites JM, von Bergen M *et al.*: **Metaproteogenomic insights beyond bacterial response to naphthalene exposure and bio-stimulation.** *ISME J* 2013, **7**:122-136.
70. Mason OU, Hazen TC, Borglin S, Chain PSG, Dubinsky EA, Fortney JL, Han J, Holman H.-Y.N., Hultman J, Lamendella R *et al.*: **Metagenome, metatranscriptome and single-cell sequencing reveal microbial response to Deepwater Horizon oil spill.** *ISME J* 2012, **6**:1715-1727.
71. Math RK, Jin HM, Kim JM, Hahn Y, Park W, Madsen EL, Jeon CO: **Comparative genomics reveals adaptation by *Alteromonas* sp. SN2 to marine tidal-flat conditions: cold tolerance and aromatic hydrocarbon metabolism.** *PLOS ONE* 2012, **7**:e35784.
72. Jin HM, Jeong H, Moon E, Math RK, Lee K, Kim H-J, Jeon CO, Oh TK, Kim JF: **Complete genome sequence of the polycyclic aromatic hydrocarbon-degrading bacterium *Alteromonas* sp. strain SN2.** *J Bacteriol* 2011, **193**:4292-4293.
73. Herbst F-A, Bahr A, Duarte M, Pieper DH, Richnow H-H, von Bergen M, Seifert J, Bombach P: **Elucidation of in situ polycyclic aromatic hydrocarbon degradation by functional metaproteomics (protein-SIP).** *Proteomics* 2013, **13**:2910-2920.
- BACTRAPs[®] combined with *in situ* protein-SIP and 16S rRNA gene pyrosequencing identify *Burkholderiales*, *Actinomycetales* and *Rhizobiales* as crucial active naphthalene degraders in a PAH-polluted aquifer (80% of carbon gain from PAH-assimilation). Laboratory microcosms reveal proteins from the angular degradation pathway for fluorene in *Actinobacteria* (*Rhodococcus*).
74. Wilcke W, Kiesewetter M, Bandowe BM: **Microbial formation and degradation of oxygen-containing polycyclic aromatic hydrocarbons (OPAHs) in soil during short-term incubation.** *Environ Pollut* 2014, **184**:385-390.

LOS RESULTADOS OBTENIDOS DEMUESTRAN LA VIABILIDAD DEL TRATAMIENTO

Ensayos de tratabilidad para la BIORREMEDIACIÓN de suelos contaminados con HTF

Los compromisos europeos y mundiales en instalación de energías renovables, políticas de reducción de CO₂, así como la conveniencia estratégica de disminuir la dependencia energética exterior y aumentar la autonomía energética, han hecho que la energía solar se encuentre en la actualidad en una fase avanzada de investigación, desarrollo, instalación y aprovechamiento.

Por J. Vila, M. Tauler, M. Grifoll | Dpto. de Microbiología de la Facultad de Biología (Universidad de Barcelona).
J. Nilsson, B. Mundó | Litoclean.

En las plantas termosolares la energía solar se capta mediante colectores cilindro-parabólicos, que con un seguimiento solar concentran la radiación en un tubo absorbedor por el cual circula un fluido de transferencia de calor (HTF). Este fluido consiste básicamente en una mezcla de bifenilo y óxido de difenilo que se calienta hasta una temperatura de 400 °C. Al circular por una batería de tres intercambiadores (economizador, evaporador y sobrecalentador), el HTF comunica el calor que ha almacenado al agua para la generación de vapor.

La tecnología de la biorremediación

La biorremediación es una tecnología de descontaminación de suelos basada en la utilización de la capacidad biodegradadora de los microorganismos para eliminar los contaminantes del suelo, mediante

su transformación en productos inocuos o su total mineralización a CO₂ y H₂O.

Las tecnologías existentes se agrupan en dos modalidades: la biorremediación intrínseca o bioatenuación natural y la biorremediación dirigida. La primera modalidad está basada en la capacidad de las poblaciones microbianas indígenas para llevar a cabo, de forma natural y simultánea a otros procesos físico-químicos como la volatilización, una eliminación de los contaminantes. La biorremediación dirigida consiste en provocar una estimulación de la actividad microbiana degradadora, sea estimulando la actividad de los microorganismos autóctonos del propio emplazamiento (bioestimulación) o adicionando inóculos microbianos (bioaumento).

El escenario ideal es aquel en el que las poblaciones microbianas están capacitadas para utilizar los contaminantes como sustratos de crecimiento y en que las condiciones ambientales no inhiben su desarrollo. Esto supone que la metabolización del contaminante permite extraer la energía necesaria para las funciones vitales y al mismo tiempo sintetizar todos los componentes celulares necesarios para que la población microbiana vaya aumentando.

Pero, ¿qué se necesita para llevar a cabo este proceso metabólico? En el caso de los hidrocarburos y sus derivados oxidados (como el bifenilo y el óxido de difenilo), la biodegradación más eficiente es la ligada al metabolismo microbiano aeróbico, es de-

LA BIORREMEDIACIÓN
INTRÍNSECA SE BASA
EN LA CAPACIDAD
DE POBLACIONES
MICROBIANAS INDÍGENAS
PARA ELIMINAR
CONTAMINANTES

cir, una combustión. Para ello, será imprescindible el suministro de oxígeno que, en el complejo proceso metabólico celular, hará el papel de lo que denominamos aceptor terminal de electrones. La aireación será, pues, la primera estimulación que llevaremos a cabo en un proceso de biorremediación de suelo contaminado con hidrocarburos y sus derivados. En los pocos casos que se lleve a cabo un proceso anaeróbico, como podría ser en un acuífero contaminado con hidrocarburos, deberemos suministrar un aceptor terminal de electrones alternativo, como pueden ser los nitratos. Si el contaminante fuera un organoclorado, estos productos pueden actuar como aceptores de electrones en condiciones anaerobias y, en este caso, la actividad de las bacterias implicadas debe estimularse mediante la adición de materia orgánica o de un compuesto orgánico oxidable que sirva como sustrato de crecimiento. Además de obtener energía, los microorganismos deben ser capaces de multiplicarse, sintetizando nuevos componentes celulares a partir del metabolismo de los contaminantes. Los hidrocarburos y sus derivados son compuestos ricos en carbono e hidrógeno. Sin embargo, las células microbianas están constituidas por componentes como las proteínas y los ácidos nucleicos, que además de estar formados por los elementos carbono e hidrógeno, contienen nitrógeno y fósforo, entre otros. El suelo contiene nitrógeno y el fósforo en formas asimilables por los microorganismos, que los incorporan a su biomasa cuando forman nuevos individuos, pero en caso de contaminación las cantidades disponibles de estos elementos suelen ser insuficientes.

En realidad, un episodio de contaminación supone un desequilibrio del ecosistema, produciéndose un gran aporte de moléculas que contienen carbono e hidrógeno y que no va acompañado de un incremento de los otros elementos necesarios para la proliferación de las poblaciones microbianas presentes. Por lo tanto, se nos plantea otro tipo de bioestimulación: la adición de nutrientes, especialmente nitrógeno y fósforo, que deben aportarse en unas cantidades acordes con las proporciones medias celulares de C:N:P.

En todos estos escenarios la bioestimulación se refiere a las poblaciones que se encuentran en el propio suelo, las denominadas poblaciones indígenas o autóctonas. Sin embargo, en algunas ocasiones estas poblaciones o no están capacitadas para metabolizar el contaminante o están en una proporción tan baja que no responden a los bioestimulantes. En estos casos, se hace necesaria la inoculación o siembra de microorganismos previamente crecidos en el laboratorio y que pueden tener distintos orí-

genes. Cuando se utiliza esta estrategia, se habla de bioaumentación.

Importancia de los ensayos de biotratabilidad

Para que un tratamiento de biorremediación sea implementado con éxito, debe averiguarse a priori si el emplazamiento cuenta con las poblaciones microbianas degradadoras y si las condiciones son apropiadas para que éstas desarrollen su actividad, siendo necesario identificar los factores específicos que condicionan el proceso. En este proceso intervienen tres protagonistas: las poblaciones microbianas, los contaminantes y el medio contaminado.

Cada emplazamiento concreto presenta unas características propias en cuanto a factores ambientales, como disponibilidad de oxígeno, contenido en nutrientes y disponibilidad del contaminante para el ataque microbiano, entre otros. Mediante la realización de experimentos a nivel de laboratorio, denominados ensayos de tratabilidad, se pueden conocer para cada emplazamiento las características microbiológicas, edafológicas y fisicoquímicas, así como la influencia de distintos parámetros (O_2 , nutrientes, etcétera) y la capacidad que tenemos de modificarlos antes de implementar cualquier tecnología de biorremediación.



Figura 1: Acopio de suelo afectado en la planta.

Ensayos de biotratabilidad del suelo contaminado con HTF

Una rotura súbita en la tubería por la que circulaba fluido térmico (HTF) provocó un vertido sobre el terreno en una planta termosolar. Tras la retirada urgente del fluido derramado (se estima que se recuperó el 70% del producto derramado), se realizó un muestreo de suelos superficiales en la zona afectada. Se detectó presencia de fenol, benceno, bifenilo y óxido de difenilo (difenil éter o óxido de bifenilo), y se procedió a retirar dichos suelos, acopiándolos sobre lámina de polietileno para su posterior tratamiento, gestionándose en vertedero de residuos peligrosos únicamente los más afectados. Ver figura 1, "Acopio de suelo afectado en la planta".

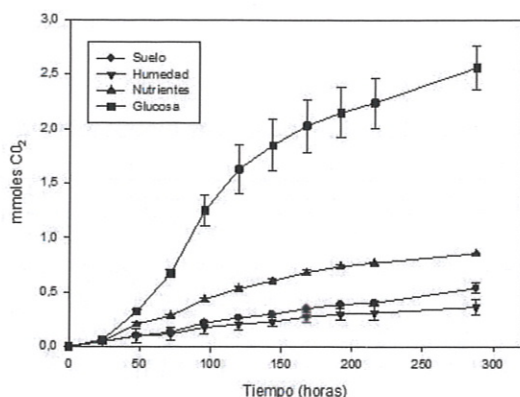


Figura 2: Actividad microbiana medida como cantidad de CO₂ producido (respirometría) al incubar el suelo en distintas condiciones.

Tanto el bifenilo como el óxido de difenilo presentan un bajo potencial de movilidad en el suelo. En presencia de las poblaciones microbianas apropiadas, el primero puede degradarse con una relativa facilidad, mientras que el óxido de difenilo se degrada más lentamente. Teniendo en cuenta el volumen de suelo a tratar y la disponibilidad de espacio en el emplazamiento, se estimó la implantación y operación de una biopila como técnica apropiada.

A continuación se describirán los ensayos realizados. Durante la segunda mitad del año 2012 la empresa Litoclean y el Departamento de Microbiología de la Universidad de Barcelona realizaron una serie de ensayos de biotratabilidad del suelo afectado para determinar la viabilidad de una estrategia de biorremediación para su descontaminación. Los ensayos se realizaron a dos niveles: el nivel 1, ensayos rápidos de factibilidad y de biodegradabilidad en microcosmos con suspensiones acuosas de suelo (*slurries*), y nivel 2, ensayos de biodegradabilidad en estado sólido.

Ensayos rápidos de factibilidad y de biodegradabilidad con *slurries*

La finalidad del primer nivel era determinar en un plazo de tiempo relativamente corto (dos semanas) si el suelo poseía una microbiota apropiada para la biodegradación del contaminante, y si existían limitaciones para su estimulación hasta conseguir la eliminación o reducción de los contaminantes a niveles deseados. Paralelamente, se pretendía

desarrollar un inóculo microbiano a partir de poblaciones autóctonas para su utilización en el caso de que fuera necesario un bioaumentación.

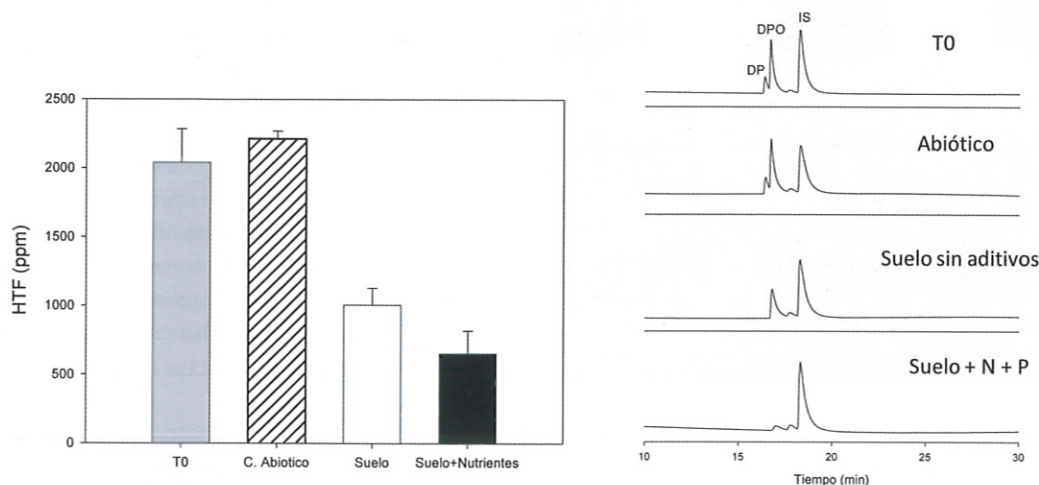
En primer lugar se llevó a cabo un análisis microbiológico consistente en el recuento de las poblaciones total heterótrofa (microorganismos capaces de crecer con materia orgánica en condiciones aerobias) y de degradadores de HTF (capaces de crecer utilizando el HTF como sustrato). Los resultados obtenidos mostraron una microbiota heterótrofa de aproximadamente 4×10^3 microorganismos por gramo de suelo, mientras que los degradadores estaban alrededor de 1×10^3 . Por lo tanto, las poblaciones microbianas no eran muy altas, pero estaban enriquecidas en degradadores de HTF.

A continuación se llevó a cabo un ensayo de respirometría en el que se realizó un seguimiento de la actividad microbiana en muestras del suelo afectado por HTF, incubadas en distintas condiciones durante un periodo de 12 días (288 horas). Las condiciones fueron: suelo tamizado sin modificar, suelo con una humedad ajustada al 40% de la capacidad de campo, suelo con nutrientes (nitrógeno, fósforo) y suelo con nutrientes y glucosa como fuente de carbono fácilmente asimilable. Ver figura 2, "Actividad microbiana medida como cantidad de CO₂ producido (respirometría) al incubar el suelo en distintas condiciones".

Los resultados mostraron que al suministrar una fuente de carbono fácilmente asimilable (glucosa) incrementaba rápidamente la actividad, indicando que en el suelo no existen factores inhibidores de la actividad microbiana. La estimulación solo con nutrientes fue menor, lo que sugería que para la degradación de los contaminantes sería apropiado adicionar un cosustrato o inóculo especializado. Estos resultados son consistentes con los obtenidos en el recuento de microorganismos.

Para determinar de forma rápida la capacidad de las poblaciones microbianas para degradar o reducir satisfactoriamente las concentraciones de HTF en condiciones de laboratorio, se llevaron a cabo ensayos rápidos de degradación con microcosmos de suelo en suspensión acuosa (*slurry*). Los ensayos se realizaron con y sin la adición de nutrientes, y como control para evaluar las pérdidas abióticas se incluyeron microcosmos en los que se habían eliminado las poblaciones microbianas. Los análisis por cromatografía de gases mostraron que, tras diez días de incubación en condiciones aeróbicas y 25 °C, no se produjeron pérdidas abióticas significativas del contaminante. La concentración de HTF se redujo un 54% en los microcosmos a los que se aplicó aireación, y un 71% en los que se aplicó aireación y nutrientes. Ver figuras

LA BIORREMEDIACIÓN DIRIGIDA CONSISTE EN PROVOCAR UNA ESTIMULACIÓN DE LA ACTIVIDAD MICROBIANA DEGRADADORA



Figuras 3 y 4: A la izquierda, reducción en la concentración de HTF en microcosmos de suspensiones de suelo en agua incubados con aireación (suelo) y con aireación y adición de nutrientes (suelo+nutrientes). A la derecha, cromatogramas mostrando los picos de difenilo (DP) y difeniléter (DPO). IS corresponde al estándar interno añadido a los microcosmos antes de la extracción.

DEBE CONOCERSE SI EL EMPLAZAMIENTO CUENTA CON POBLACIONES MICROBIANAS DEGRADADORAS Y SI LAS CONDICIONES PARA QUE DESARROLLEN SU ACTIVIDAD SON APROPIADAS

3 y 4: "A la izquierda, reducción en la concentración de HTF en microcosmos de suspensiones de suelo en agua incubados con aireación (suelo) y con aireación y adición de nutrientes (suelo+nutrientes). A la derecha, cromatogramas mostrando los picos de difenilo (DP) y difeniléter (DPO). IS corresponde al estándar interno añadido a los microcosmos antes de la extracción". En conclusión, el suelo posee una población microbiana capaz de reducir de forma importante la concentración de HTF del suelo. Esta actividad degradadora de HTF se estimula mediante la adición de humedad y nutrientes al suelo y suministrando aireación adecuada.

Ensayos de biodegradabilidad en estado sólido

Los resultados obtenidos permitieron pasar al segundo nivel de ensayos en los que se pretendía evaluar la viabilidad de un tratamiento en fase sólida, así como identificar las enmiendas que proporcionan mejores resultados en estas condiciones.

La manipulación del suelo en la fase previa reveló su naturaleza altamente arcillosa y por tanto su poca porosidad, lo que recomendaba realizar el tratamiento con poca humedad y ensayar la adición de un agente esponjante. Con ello, se conseguiría asegurar la aireación del suelo. Los ensayos de respirometría se habían realizado con una humedad del 40% de la capacidad de campo y no se habían observado diferencias significativas entre el suelo seco y el húmedo, por lo que en los tratamientos en estado sólido se decidió reducir esta humedad al 20%.

El hecho de que en los ensayos en slurry no se llegara al 100% de la degradación de HTF podía deberse a la baja concentración de la microbiota en el suelo contaminado. Se optó por incluir en los ensayos en fase sólida la amplificación de microbiota mediante dos estrategias distintas: biogmagnificación mediante la adición de un inóculo obtenido del propio suelo o la adición de una fuente de carbono alternativa (bioestimulante vegetal). Otra causa que explicaría que no se hubiera degradado completamente el HTF podría ser que una parte del mismo se encontrara adsorbido al suelo (poco biodisponible), lo que recomendaba incluir en el ensayo un fertilizante con capacidad surfactante. Uno de los más utilizados en biorremediación es la formulación oleofílica S200.

Por lo tanto, se pusieron a punto distintos microcosmos de suelo a los que se adicionó: nutrientes, un inóculo microbiano autóctono desarrollado en el laboratorio, un agente esponjante (paja triturada), un bioestimulante vegetal y un surfactante utilizado habitualmente en biorremediación. Como control se incubó el suelo sin aditivos ni humedad (suelo seco). El inóculo microbiano se había cultivado en



Figura 5: Microcosmos de suelo en estado sólido correspondientes a algunos de los tratamientos ensayados.

tuvo un efecto adicional. La inoculación incrementó la población microbiana degradadora diez veces más que los nutrientes. El tensioactivo S200, que ha demostrado su efecto en vertidos marinos y se utiliza también en la biorremediación de suelos, en el caso que nos ocupa no mostró un efecto adicional al de los nutrientes en cuanto a las poblaciones degradadoras. El mayor efecto se observó en el tratamiento con bioestimulante vegetal, donde las poblaciones aumentaron en cinco órdenes de magnitud respecto al control. En cuanto a la reducción de las concentraciones de bifenilo y difeléter, los efectos de los distintos

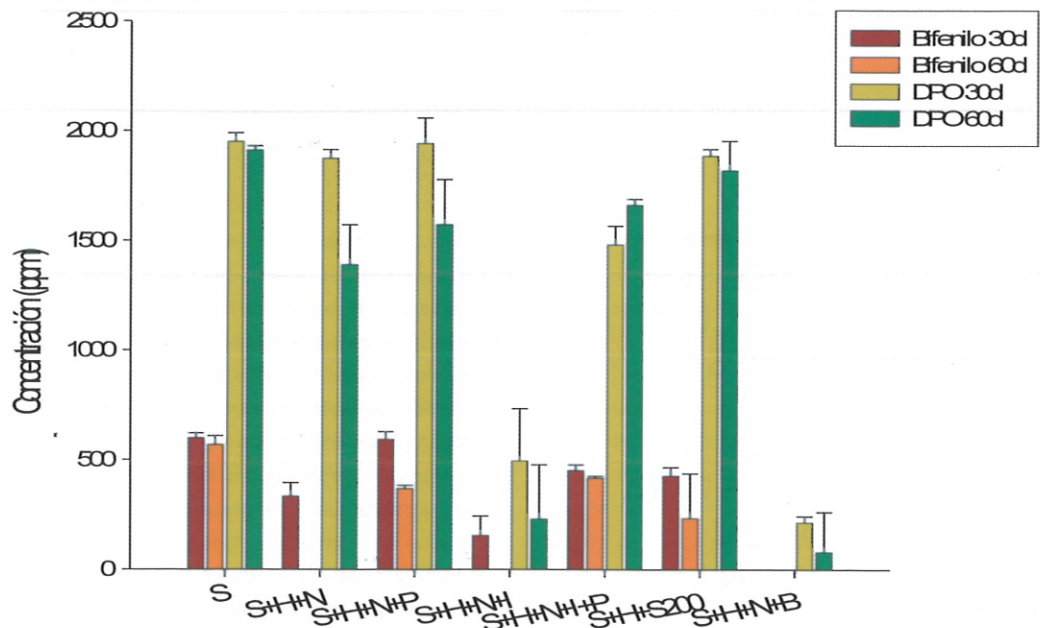


Figura 6: Concentración residual de bifenilo y óxido de difenilo (DPO) en los microcosmos de suelo incubados a 30 y 60 días. S corresponde al suelo seco, tomado como control no tratado, S+H+N al suelo con humedad al 20% de la capacidad de campo y nutrientes, S+H+N+P a suelo con humedad, nutrientes y paja triturada, S+H+N+I a suelo con humedad, nutrientes e inóculo autóctono, S+H+N+I+P a suelo con humedad, nutrientes, inóculo autóctono y paja, S+H+S200 a suelo con humedad y el tensioactivo comercial S200 y S+H+N+B a suelo con humedad, nutrientes y el bioestimulante vegetal.

el laboratorio y contenía poblaciones seleccionadas del propio suelo contaminado. Ver figura 5, "Microcosmos de suelo en estado sólido correspondientes a algunos de los tratamientos ensayados".

Los microcosmos de suelo se incubaron a temperatura ambiente y se analizaron a tiempo 0, 30 días y 60 días, tanto desde el punto de vista microbiológico como químico.

Todos los tratamientos estimularon el crecimiento de las poblaciones microbianas tanto heterótrofas como degradadoras de HTF. El incremento se produjo sobre todo durante los 30 días iniciales para después mantenerse aproximadamente constantes y viables hasta el fin de la incubación. La adición de nutrientes y humedad aumentó las poblaciones degradadoras en tres órdenes de magnitud. El agente esponjante no

tratamientos fueron consistentes con los observados en las poblaciones degradadoras. El control de suelo seco se mantuvo sin cambios apreciables, mientras que todos los tratamientos causaron una eliminación significativa de dichos compuestos. Tal y como se había anticipado, la mera adición de nutrientes no fue suficiente para la eliminación de difenil éter, contaminante más persistente que el bifenilo. El tratamiento con paja, a pesar de haber estimulado la población en general, no mostró un mejor efecto, lo que se debe sin duda a que ésta es utilizada como fuente de carbono alternativa por los microorganismos, causando una inhibición en la degradación, tanto en ausencia como en presencia del inóculo degradador autóctono. Los resultados más positivos se consiguieron con el

inóculo autóctono y con el bioestimulante vegetal, que redujeron considerablemente las concentraciones a los 30 días, y posteriormente prolongaron su efecto hasta los 60. El efecto más dramático en estas condiciones lo produjo el bioestimulante vegetal, eliminando por completo el bifenilo a los 30 días y causando una reducción del 90% del difenil éter a los 30 días y del 96% (hasta 79 ppms) al final del tratamiento. Ver figura 6, "Concentración residual de bifenilo y óxido de difenilo (DPO) en los microcosmos de suelo incubados a 30 y 60 días".

Conclusiones

Los resultados obtenidos demuestran la viabilidad del tratamiento del suelo afectado por HTF mediante biorremediación. La bioestimulación con nutrientes no es suficiente para la eliminación de difenil éter, sustancia más persistente que el bifenilo.

El tratamiento con agente esponjante estimula el crecimiento de las poblaciones microbianas, pero no causa una mayor reducción de la concentración de contaminantes. Ello se atribuye a que este agente compite con el contaminante como sustrato de crecimiento para las poblaciones degradadoras.

Los mejores resultados se consiguen con el inóculo autóctono y con el bioestimulante vegetal, que reducen considerablemente las concentraciones a los 30 días y después las continúan reduciendo hasta los 60. El resultado más efectivo lo produce el bioestimulante vegetal, eliminando por completo el bifenilo a los 30 días y causando una reducción del 90% del difenil éter a los 30 días y del 96% al final del tratamiento.

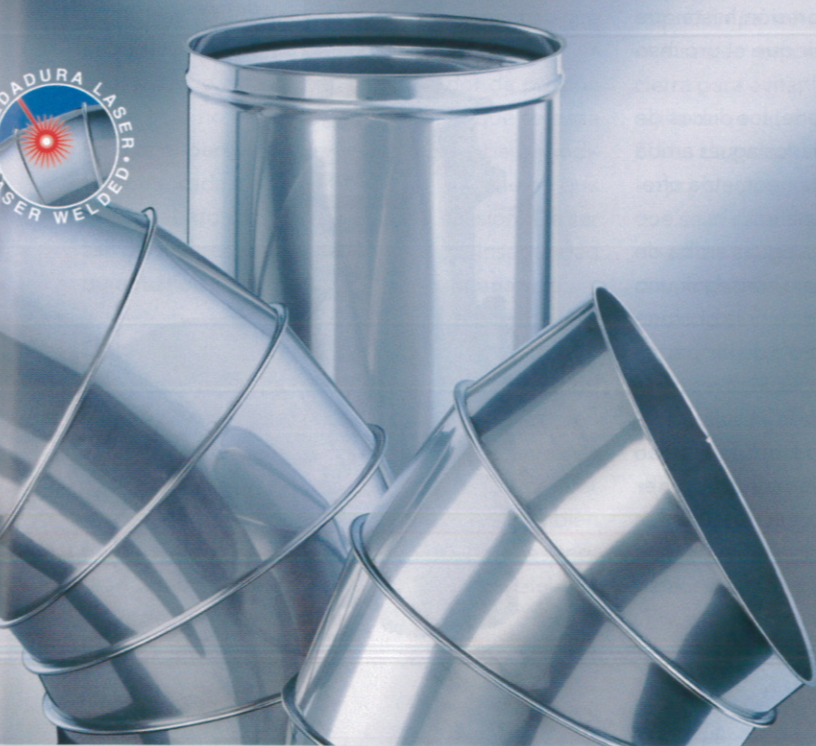
Dados los resultados obtenidos deberían implantarse estas condiciones a escala de campo para el tratamiento de los suelos contaminados. El establecimiento de dichas condiciones en campo podría realizarse mediante biopilas dinámicas o estáticas.

Las biopilas dinámicas implicarían el volteo periódico de los suelos combinado con la adición de agua, nutrientes y, en el caso que nos ocupa, inóculo autóctono y/o bioestimulante vegetal.

Las biopilas estáticas, por el contrario, se acondicionarían adecuadamente para establecer las condiciones idóneas antes de cubrirla. En este caso la aireación sería forzada y debería asegurarse una buena homogenización del suelo a tratar previa a la construcción de la biopila. ●

ROSTUBOS®

Sistemas de tubería modular



www.rostubos.com